5. Model Calibration

The LMB model is very large (in excess of 2 million cells that cover parts of four states) and simulates the transient response of multiple aquifers to multiple pumping centers. It also simulates the exchange of groundwater between a dense surface-water network and notably heterogeneous glacial deposits underlain by a series of overlapping bedrock units dipping from the Wisconsin Arch into the saline Michigan Basin. These elements complicate the calibration process, which involves updating the initial estimates for a large number of input values in order to improve the match between simulated groundwater levels and flows and corresponding field observations, called *targets*. Multiple strategies are employed to enhance the calibration process and make it tractable for *parameter estimation* through the use of nonlinear regression techniques to adjust model inputs as a function of target outputs; in this study, parameter estimation was done by use of the code PEST (Doherty, 2008a). The strategies include linearization of the flow equation, grouping of input blocks into parameter zones subject to a single multiplier, assembly of diverse predevelopment and postdevelopment target types, filtering of targets, adjustment of target weights, special regression methods such as singular value decomposition, and focused use of pilot points to fully extract information from available targets and thereby allow more variation of crucial parameters. In the end, the calibration process not only improves the fit between measured and simulated targets but also adds insight into the major controls on the flow system through identification of parameter groups to which model results are most sensitive.

5.1 Linearization of Flow Equation

The original calibration strategy involved a version of the LMB model that included unconfined aquifers in areas where the water table is below the top of the model layer. Unconfined conditions typically occur in layer 1 but can also occur in layers 2 and below in areas where the stage elevations of surface-water features are below the bottom of the top layer. Finally, partially saturated conditions occur where drawdown from pumping deep wells creates unconfined conditions within deep confined aquifers. This pumping causes the upper part of the flow system to detach from the lower in the form of an unsaturated zone between the two and the formation of a second water table at depth.[20]

When the LMB model is simulated in confined mode, the original transmissivites and storage parameters (as well as pumping rates) assigned to cells still pertain even if dewatering has occurred and the head associated with the dewatered cell has fallen below the layer top (in which case the cell is implicitly a water-table cell) or below the layer bottom (in which case the cell is implicitly dry, although in confined mode it remains part of the model solution). The transmissivity is still calculated as a function of the total cell thickness, and the storage change is still calculated as a function of specific storage.

When the LMB model is simulated in unconfined mode, then, for unconfined aquifers, the transmissivity is calculated from the saturated thickness of the aquifer rather than the total thickness. In addition, storage is controlled by the specific yield rather than by specific storage. When transient simulations are run with the unconfined version of the LMB model, any changes from confined to unconfined conditions are accounted for by SEAWAT, which recomputes the transmissivity and storage parameters during the model-solution iteration. These changes have two effects: (1) the flow equation is no longer linear in the sense that model parameters (transmissivity and storage) are now dependent on simulated water levels, and (2) in areas where simulated water levels decline below the bottom of the unconfined aquifer, the model solution produces “dry cells” with zero saturated thickness. The latter phenomenon can be important because some of the wells in the dry cells are removed from the numerical solution and, as a result, pumping that is associated with these areas is not represented. The conversion from confined to unconfined conditions potentially poses several problems for automated calibration of the LMB model through nonlinear regresssion. A transient simulation can produce dry cells in any time step, which means that some cells containing calibration targets and pumping wells could be omitted from the numerical solution during the exploration of the parameter space. A second consideration is that the accuracy of the simulation of the vertical flow field is affected by the continuity of saturated conditions. It is possible for the MODFLOW-2000/SEAWAT-2000 codes in unconfined mode to simulate discontinuous saturated conditions at depth when a dewatered zone overlies a deep water table. The dewatered zone can be represented by a single *partially saturated* cell that contains a water table, or it can correspond to one or more inactive cells (that is, unsaturated or dry cells) stacked vertically above a deeper cell that is partially or fully saturated. Under partially saturated conditions, the code transfers water between the overlying cell and the saturated

[20] Field evidence for dewatering in deep aquifers west of Lake Michigan is provided below in section 7.1, along with modeling results in line with the field evidence.

part of a partially saturated cell by using a simplified algorithm that modifies the vertical gradient but does not take account of the unsaturated properties of the dewatered zone. When a cell is inactive, the code allows no exchange at all between the inactive cell and vertically or horizontally adjacent cells (McDonald and Harbaugh, 1988).[21] In the present study, areas with multiple water tables are present but limited in extent *and* concentrated around major deep pumping centers. (For fuller analysis of deep water-table conditions and the effect on confined and unconfined model results, see section 7.)

An additional disadvantage of an unconfined simulation is the tradeoff between runtimes (the time needed to solve the model across stress periods) and the solution-convergence criteria, which determine the number of iterations within the time step to obtain a solution deemed sufficiently accurate. The PCG2 solver applied to the LMB model applies two convergence criteria: one to limit the maximum head change that can occur in any cell between iterations within a time step, and one to impose a maximum change in the flux passing through the cell. The more restrictive these criteria are, the longer the runtime but the smaller the global water-budget error arising from an imbalance between flows into and out of the model domain for any time step. Criteria are normally set to insure that the global water-budget error (calculated for SEAWAT-2000 in terms of mass rather than volumetric flux) is less than 1 percent for any time step, and, preferably, less than 0.1 percent. For an unconfined solution, the criteria necessary to meet the 0.1-percent water-budget error yield a runtime on the order of 11 hours on a 2008 model IBM personal computer. A confined run with the same initial input solves in less than 2 hours. Finally, the most serious difficulty arising from using the unconfined solution for parameter estimation stems from relatively large degradation in the differentiability of the problem. Nonlinear regression methods commonly rely on tracking the effect of small perturbations of parameter values to changes in model outputs, in this case simulated head or flux values associated with calibration targets (Doherty, 2008a). The ratio of the latter to the former defines a matrix of observation to parameter derivatives (called the "Jacobian" or sensitivity matrix), a matrix whose size is the number of parameters multipled by the number of observations. Sensitivity information contained in the Jacobian matrix guides the search for updated and improved input values and better model fit. The method is most robust when the derivatives calculated by perturbation are largely independent of the exact size of the perturbation. This robust condition is demonstrated when a graph of parameter perturbation increments versus target value yields a trend that approximates a straight line.

The parameter estimation code PEST contains a useful utility (called JACTEST; see Doherty, 2008b) that allows the behavior of derivatives to be tested and the results graphed for selected parameters and targets. For the LMB model, the tests indicate that the linearity of the derivatives is strongly influenced by both the size of convergence criteria and whether the model was run under unconfined or confined conditions. An example is the drawdown simulated at six observation wells produced by perturbations of the vertical hydraulic conductivity of the Maquoketa shale unit below the Southeastern Wisconsin subregion of the model (SE_WI, fig. 44). For an unconfined model with relatively larger (looser) convergence criteria (though one that still produces an acceptable mass water-budget error between 0.1 and 1 percent), the simulated model outputs resulting from successively increasing small perturbations are irregular, without an obvious single trend or slope (fig. 44). Such results are representative of highly nonlinear derivatives—derivatives that can confound nonlinear regression methods. For a confined model with smaller (tight) convergence criteria (tolerances reduced by about 20 times, producing water-budget errors on the order of 0.1 percent), the relation is generally linear (fig. 44). This analysis can be further extended by separating out effects of convergence criteria and unconfined/confined model and quantifying the linearity of the slope by means of a R^2 term arising from applying standard linear regression to the JACTEST graphs, where a R^2 of 1.0 indicates a perfectly linear response. By using a larger number of targets (189) linked to the Maquoketa K_v parameter, median R^2 values were about 0.10 for both unconfined and confined models with larger (looser) PCG2 convergence criteria, indicating nonlinear behavior and inaccurate derivatives in the inversion routines. For the unconfined model with tight convergence criteria, the linearity improved modestly (median R^2 equal to 0.38). It is likely that the persistent nonlinearity (deviation from 1.0) is related to trouble obtaining accurate saturated thicknesses and to the development of desaturated conditions under confined aquifers in later stress periods. For the confined model with small (tight) convergence criteria, the R^2 improves to 0.96, indicating fairly linear behavior and appreciably more reliable derivatives.

[21] In **unconfined mode** the MODFLOW-2000/SEAWAT-2000 codes calculate the downward flow between a fully saturated cell in an overlying layer and a partially saturated cell (that is, one containing a water table) in an underlying layer as the product of the vertical conductance between the layers (fixed by the model input) and a head difference equated with the difference between the head in the overlying cell and the overlying cell's bottom elevation. When a cell is simulated as completely dry in unconfined mode and is, therefore, inactive, no vertical exchange occurs across it. When a layer in MODFLOW-2000/SEAWAT-2000 is restricted to confined model, desaturation of cells is not simulated, and all cells are assumed to be fully saturated throughout the simulation. A simulated water level may be within the cell, above the cell top, or below the cell bottom. The vertical flow between a cell in a confined and an overlying cell is determined by the heads in the two cells and the vertical conductance between the cells. Although a cell in a confined mode layer cannot be desaturated from the standpoint of the flow equation, it is also true that if the water level is below the cell top, then the the confined solution is implying that the cell is either partially dewatered (water level between the top and bottom of the cell) or fully dewatered (water level below the bottom of the cell).

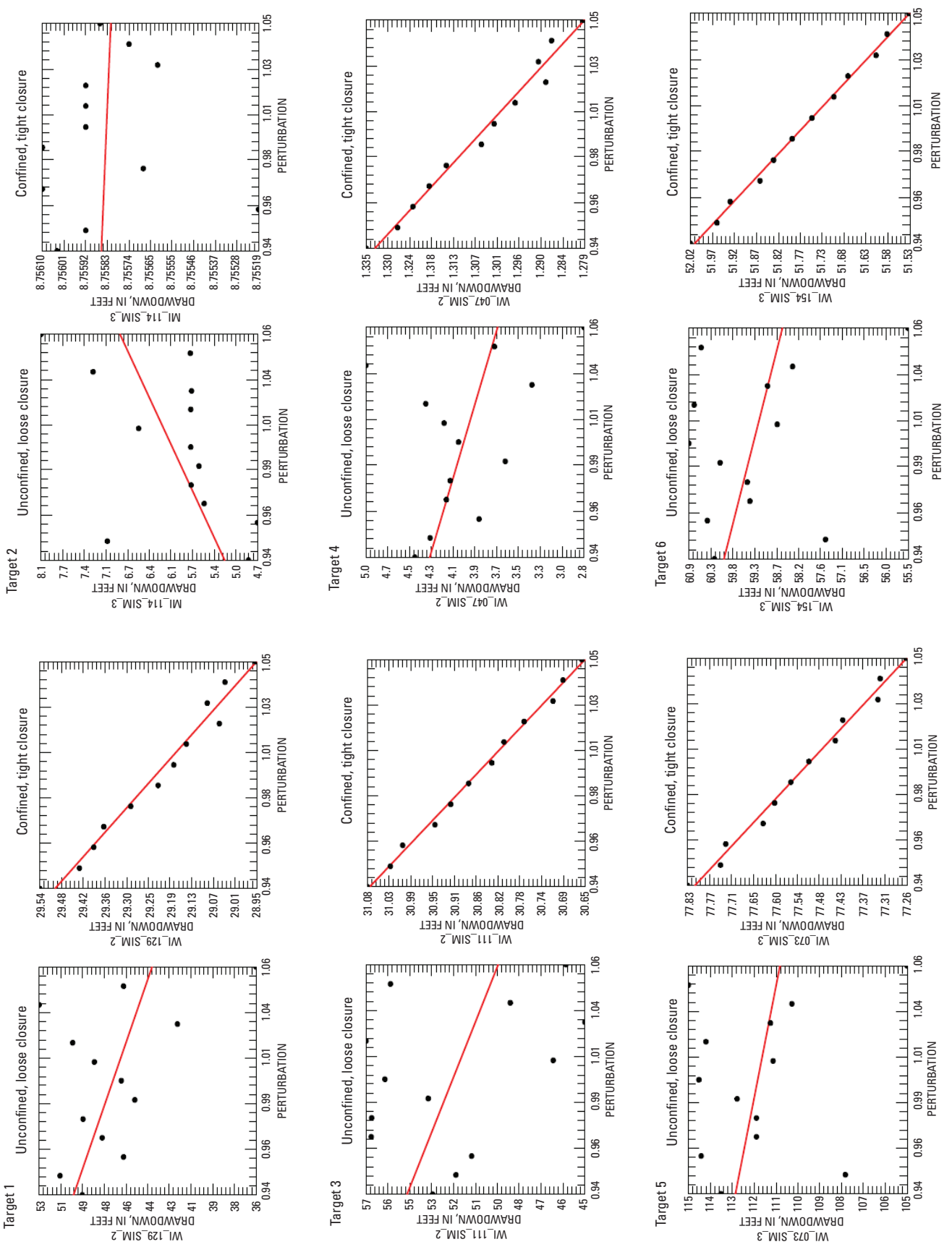

Figure 44. Sample plots of Jacobean derivatives for vertical hydraulic conductivity in the Maquoketa confining unit.

Though responding more linearly to parameter perturbation, the confined version of the LMB also must approximate actual water levels and responses to stresses measured in the groundwater flow system. Therefore, actual deviations from confined conditions were accounted for by modifying a subset of the confined model input, those involving transmissivity and storage. It is fairly easy to approximate the effect of partially (or wholly) desaturated layers on transmissivity as input into the adjusted confined model, and solutions of the unconfined simulation and confined simulation with adjusted parameters did not differ dramatically at initial or final optimal parameter values. The agreement in solutions is especially close for the water-table surface, owing to the effect of locally pinning or "stapling" of heads near head-dependent boundaries representing surface-water features (see section 3). Thus, it is possible to convert the transmissivity in cells that go dry to an extremely low value to simulate inactive conditions, and, in cells only partly saturated, to reduce the full-thickness transmissivity by the difference in saturated thickness in order to simulate water-table conditions. Both conversions are made by means of changes to the K_h cell value: in the case of dry cells it is reduced to 1 E−5 ft/d; in the case of water-table cells the initial value is multiplied by the ratio of the saturated thickness to the total thickness. The calculation is made for the minimum saturated thickness recorded for the initial simulation at the end of any stress period. The revised K_h value is used in parameter estimation for the adjusted confined version of the model, where it is then subject to decrease or increase during calibration.

The treatment of the storage parameter in the adjusted confined model is generally similar to the treatment of transmissivity in the case of dry or water-table cells. For a dry cell the storage parameter should be effectively zero, whereas for a water-table cell it should be proportional to the specific yield (S_y). The confined version of the LMB model does not have the option for unconfined cells of substituting S_y directly for the product of specific storage (S_s) and cell thickness because in confined mode the MODFLOW code permits the application of only one type of storage term. However, the S_s term can be adjusted so that its product with cell thickness approximates the value of S_y and, thereby, provide a more realistic treatment of storage release in cells which contain a water table. Accordingly, construction of the confined version of the LMB model entails setting S_s to 1 E−10 for dry cells and setting S_s to the value of S_y divided by saturated thickness (to yield an effective S_s parameter) for water-table cells. A special difficulty arises in the transition case when drawdown around wells causes desaturation of deep cells and formation of stacked water tables within a given stress period. Because of the relatively coarse time discretization, it is not clear which storage parameter is most representative for the deep layer during the transition—the original S_s value proper for the original confined conditions or the S_y value proper for the eventual water-table conditions. (Note that the input to MODFLOW-2000/SEAWAT-2000 does not allow either the hydraulic conductivity or storage input to change in time.) Unlike the case of transmissivity, where the water-table condition typically produces a fraction of the original horizontal hydraulic conductivity with an expected value in the neighborhood of 0.5, the transition from a fully saturated to partly saturated condition produces a dramatic increase in the storage capability on the scale of several orders of magnitude.

To handle the possibility of this nonlinear behavior, the algorithm to convert storage in the adjusted confined model contains two steps. For the steady-state solution corresponding to predevelopment conditions, no deep dewatered zones overlying deep water tables are present because no deep wells are pumping to induce unconfined conditions. Accordingly, the initial steady-state solution can be applied to the uppermost water-table cell at a row/column location to convert specific yield to specific storage as a function of the degree (or absence) of saturation. The second step applies to cells in layers 2–20 that desaturate after the first steady-state stress period when pumping is active. An initial rough approximation is used to estimate the combined specific storage term—it is set to twice the geometric mean of the initial S_y and S_s assigned to the cell. Initial comparison simulations showed that this compromise value serves to roughly approximate the storage release behavior of the direct unconfined solution. However, the inevitable result of using a geometric mean is the introduction of some error by causing the storage release to be overestimated in the adjusted confined model version before the water-table condition occurs in a deep cell and to be underestimated after they occur.

The scaling of K_h and S_s as a function of unconfined or dry conditions to mimic unconfined conditions in confined mode was done once at the beginning of the calibration process by using the solution obtained with initial parameter values. In principle, the scaling should be updated during intermediate solutions when parameters are updated during calibration, but this refinement was not made on the assumption that the saturated thickness of cells does not change appreciably as parameters are updated and that the initial scaling is adequate to reliably capture the effect of partial saturation on groundwater flow.

The need for these simplifications notwithstanding, the adjusted confined version of the model is superior to the unconfined model for parameter estimation because it inherently keeps all targets and pumping wells active and its linearity promotes numerical stability, shortens runtimes, and preserves the integrity of the derivatives (high linearity of the Jacobian matrix). Nonetheless, it is prudent to compare the calibration and findings of the confined model to those obtained with the unconfined model to assess the effects of the simplification. To that end, two calibration processes were followed: one for the confined version of the model adjusted

as described to approximate unconfined conditions, and one for the original unconfined version. The first calibration is presented in this section of the report, and its findings with respect to water levels and fluxes are presented in section 6. Both the calibration and results of the second, unconfined version are presented in section 7, which is devoted to alternative models.

5.2 Calibration Parameters

Some model parameters—for example, the K_h and K_v of the QRNR system, the conductance of RIV cells, and recharge—vary across layers or across stress periods on a cell-by-cell basis. Other inputs—for example, the K_h and K_v of the bedrock aquifers and the K assigned lakebed of Lake Michigan—vary within each layer on a block basis. Still other inputs—for example, storage terms—vary by layer or by groups of layers. It is not practical given the number of parameters, nor even desirable given the limited number of informative calibration targets, to attempt to adjust every input value. Rather, it is necessary to group inputs in ways representative of the system and in a way that obtains a unique set of optimal parameters. In this work, grouping was accomplished by estimating a single multiplier that scales initial values of a particular parameter for a specified collection of cells grouped into a zone. The multipliers applied to zones are adjusted during the calibration and are applied to all values in the zone, thus maintaining the original relative nodal differences present in initial parameter values. By way of example, a single recharge multiplier is applied to the recharge array; thus, the array can be thought of as a single zone that incorporates the highest active cell at every row/column location. A second example involves K_h and K_v of the glacial sediments: six multipliers are estimated for each of the six glacial categories (zones), which are distributed over three model layers. A single multiplier is also applied to the vertical anisotropy (K_h/K_v) in each glacial category[22] and to all the conductance terms accompanying RIV cells in each glacial category, resulting in 12 more parameter-estimation multipliers that are applied within these same six zones. A final example is the most complicated. In the case of the bedrock hydraulic conductivity, K_h and K_v input is grouped according to the grouping described in appendix 4. A zone multiplier varied in parameter estimation can correspond to a single block in a layer that incorporates a single initial value, or it can correspond to multiple blocks in a layer that incorporates multiple initial values. Two rules were developed to assign multipliers to bedrock hydraulic conductivity: (1) no bedrock layer can contain more than nine K_h or nine K_v zones (to reduce the total number of parameters estimated but still maintain calibration flexibility), and (2) zones primarily combine blocks by geographic contiguity and secondarily combine blocks with similar values. As always, a single parameter is estimated during the calibration process that serves to multiply the initial bedrock K values assigned all the cells in the corresponding zone.

The foregoing discussion requires one qualification. Not all zones are subject to an estimated multiplier in the form of a calibration parameter. In some cases, the initial value in a zone is left unchanged either because the flow component is not appreciable and thus is insensitive (K_h in confining units the bed of Lake Michigan) or because values were estimated implicitly through estimation of an associated parameter (K_v in aquifer units estimated indirectly as a ratio of the estimated K_h value). The total number of zones corresponding to unestimated parameters is 38; they are listed and characterized in terms of initial input values in appendix 5, table A5−1. The remaining 165 zones subject to parameter estimation are listed and described in appendix 5, table A5–2. Estimated parameters include recharge (1 parameter), Quaternary sediment K_h (QRNR, 6 parameters), Quaternary sediment vertical anisotropy (QRNR, 6 parameters), lakebed of Lake Michigan K_v (1 parameter), K_h for bedrock layers (81 parameters), K_v for bedrock layers (53 parameters), RIV conductance (7 parameters), and storage terms (5 parameters in the confined model or 10 parameters in the unconfined model). For calibration with the confined version of the LMB model, five S_s parameters that represent both confined and unconfined conditions are estimated, whereas for the unconfined version of the LMB model, five S_s and five S_y parameters are estimated. The configuration of K_h zones and a statistical summary of initial values is shown for nine (mostly aquifer) layers in appendix 6*A*; the pattern of K_v zones with accompanying statistical summaries is shown for nine (mostly confining unit) layers in appendix 6*B*. One set of inputs is estimated on a cell-by-cell rather than zonal basis—the K_v of the Maquoketa hydrogeologic unit in two subregions, Southeastern Wisconsin and Northeastern Illinois (SE_WI and NE_ILL). The use of pilot points in this context is discussed later in this section.

5.3 Calibration Targets

Diverse types of calibration targets can enhance the parameter-estimation process. The most common type of target for groundwater-flow-model calibration is water-level data derived from well measurements or contour maps. Water-level data provide information on the configuration of the water-table surface and of water-level surfaces corresponding to elevations below the water table, which, in turn, helps to

[22] The K_v of the unconsolidated deposits, initialized as 1/20 the value of K_h and therefore, like K_h, varying on a cell-by-cell basis, is not estimated directly but indirectly by means of the vertical anisotropy ratio. The six anisotropy multipliers are estimated with the benefit of the *updated* K_h values from an earlier sweep of the inversion algorithm; the new anisotropy ratios for each zone are then applied to the updated K_h arrays, and this procedure results in updated values of K_v that again vary cell by cell.

estimate horizontal hydraulic conductivity, recharge, and, to a lesser extent, the RIV conductance values. However, K_h and recharge values often correlate because, in principle, increases in one can be offset by increases in the other, thus resulting in a similar simulated head (see Haitjema, 1995). Moreover, either term can be adjusted to handle the degree of water-level mounding resulting from grid discretization (Feinstein and others, 2003; see also "Target Filtering," section 5.3.2). The addition of base-flow targets, which sum the groundwater contribution upgradient from the streamgage where flow is measured, can constrain the estimation of recharge, which in turn can help constrain estimation of hydraulic conductivity and storage (Poeter and Hill, 1997; Hill and Tiedeman, 2007). Vertical-head-gradient targets from nested shallow and deep wells and packer intervals in a same well also facilitate estimation of vertical hydraulic conductivity, and head changes over time (drawdown and recovery) also can constrain storage estimates. Finally, distribution of calibration targets in time and space can also be important for identifying unique optimal values. In the LMB model calibration, targets from both predevelopment and postdevelopment periods were included and were spread over every model subregion, where possible. Like most regional models, the LMB model is characterized by a large cell size. Thus, it is worth noting that an algorithm was employed to interpolate values spatially between cell centers (so that the exact location of a target was honored) and temporally between model stress periods (so that the timing of the measurement was respected).

5.3.1 Target Composition

The sets of targets applied to the calibration of the confined version of the LMB model are listed in table 11*A*, along with the number of targets in each set and other information pertaining to their role in the parameter-estimation process. The targets include representative water levels, base flow, vertical head gradients, and drawdown and recovery differences. Some sets are linked to the pre-1940 period and some to the post-1940 period. Many target types are divided into geographic subsets. Figure 45 presents the spatial coverage as well as the data sources for

(a) USGS network wells, household wells, and contour-derived targets, serving as *predevelopment* and *early postdevelopment* (1860–1940) water-level targets;

(b) USGS network wells, serving as *postdevelopment* (1940–present) water-level targets;

(c) USGS network wells, as well as RASA packer tests from the early 1980s, serving as vertical-head-gradient targets;

(d) multiple observations from USGS network wells and differences computed between contour maps at different times, serving as head-change (drawdown and recovery) targets;

(e) USGS streamgages, serving as base-flow targets; and

(f) household wells, serving as *postdevelopment* water-level targets.

Several target sets merit special attention. In general, it is possible to identify the unit(s) penetrated by USGS network wells and by household wells on the basis of the wells' geologic logs. Where multiple units are penetrated, depth information in the log is juxtaposed with land-surface data and stratigraphic layering used to construct the LMB model layers for the cell corresponding to the well location. In this cell, the water level is assigned to the thickest aquifer unit penetrated by the well, where the thickest unit is used as a surrogate for the most transmissive unit encompassed. When unit information is missing, the total depth of the well, in conjunction with the model layering, is used alone to identify the target layer.

Mapped predevelopment and postdevelopment head contours for the C-O aquifer system are composite heads that reflect conditions in the multiple units extending from the Sinnipee (SNNP) aquifer (layer 14) to the Mount Simon (MTSM) aquifer (layer 19 or layer 20). Where flow is not strictly horizontal, the contours are assumed to reflect average head conditions in the aquifer system. For the purposes of calibration of the LMB model, the targets derived from these contour maps are assigned to a single intermediate layer in the C-O aquifer system corresponding to the Prairie du Chien-Franconian (PCFR) aquifer (layer 16).

Postdevelopment water-level targets that correspond to household wells were not used (not given weight) in the parameter estimation process on account of their shallowness and the inability of LMB model cell size to simulate the actual groundwater-surface water interaction in the basin. However, residuals for 50,000 measurements in the model nearfield were computed and qualitatively evaluated as a check on calibration.

Results from multiple base-flow estimation methods were tested for this study, but the regression base-flow method of Gebert and others (2007) was selected to generate the 62 base-flow targets. Appendix 7 describes the selected regression equations, which estimate base flow as a function of coefficients and exponents computed from (1) the amount of streamflow under low-flow conditions and (2) the upstream basin area. The Gebert method equates the low-flow term in the regression with the flow exceeded 90 percent of the time (the Q_{90} value) at a streamgage location for a given period of record. Appendix 7 also contains a table with the names of the 62 streamgages (referenced to locations in fig. 45*E* and grouped by model subregion). Each gage is accompanied by its upstream basin area, duration of record, the base-flow estimate based on the Gebert equations, base-flow estimates derived from five other base-flow estimation methods, and comparison of the Gebert-method results to the Q_{50}, Q_{75}, and Q_{90} values from the stream's flow-duration curve. Summary statistics for basin area, duration of record, and base-flow comparisons are compiled at the foot of the table.

Table 11. Calibration target sets and target groups for model calibration.

11*A*. Confined conditions.

Target set	Number of observations	Individual (observation weight)^2	Weighted sum of squares of calibrated residuals (feet squared)	Percent contribution to weighted sum of squares of residuals	
Target subset				By subset	By set
"Predevelopment"—before 1940					**22.8**
USGS network water levels	11	1	6,776	1.45	
Driller-log water levels	51	0.25	4,826	1.03	
Wisconsin Cambrian-Ordovician head contours	233	.04	30,995	6.62	
Michigan Pennsylvanian head contours	115	.04	20,183	4.31	
Michigan Marshall head contours	103	.04	20,810	4.44	
Indiana miscellaneous water levels	19	.16	4,712	1.01	
Illinois Cambrian-Ordovician head contours	231	.04	18,422	3.93	
USGS network wells—"historical" water levels					**40.0**
Southern Lower Peninsula, Michigan	1,761	.01–.04	18,032	3.85	
Northern Lower Peninsula, Michigan	272	.01	11,727	2.51	
Upper Peninsula, Michigan	426	.01–.04	1,565	.33	
Northeastern Wisconsin	1,964	.01–.04	75,631	16.16	
Southeastern Wisconsin	1,149	.01–.04	58,905	12.62	
Northern Indiana	294	.01	1,709	.37	
Farfield	2422	.0025–.01	19,685	4.20	
Northeastern Illinois Cambrian-Ordovician					**4.3**
2000 water-level contours	248	.01	7,434	1.59	
Drawdown, 1864–2000 contours	248	.01	6,398	1.37	
Recovery, 1980–2000 contours	267	.0025–.01	6,133	1.31	
Decadal head changes in USGS network wells					**21.1**
Southern Lower Peninsula, Michigan	1	49	530	.11	
Northeastern Wisconsin	22	1–4	38,359	8.19	
Southeastern Wisconsin	40	1	59,875	12.79	
Vertical head differences					**4.9**
USGS network wells	41	.25–4	10,231	2.19	
USGS RASA packer tests in early 1980s	31	4	12,763	2.73	
Base-flow targets at USGS streamgages in 2000					**6.9**
Southern Lower Peninsula, Michigan	17	3.60E−11	7,582	1.62	
Northern Lower Peninsula, Michigan	11	3.60E−11	4,846	1.04	
Upper Peninsula, Michigan	9	3.60E−11	3,455	.73	
Northeastern Wisconsin	12	3.60E−11	6,138	1.31	
Southeastern Wisconsin	4	3.60E−11	2,864	.61	
Northern Indiana	3	3.60E−11	676	.14	
Northeastern Illinois	6	3.60E−11	6,749	1.44	
Total	**10,011**		**468,011**	**100.00**	**100.0**

Table 11. Calibration target sets and target groups for model calibration.—Continued

11*B*. Unconfined conditions.

Target set	Number of observations	Individual (observation weight)^2	Weighted sum of squares of calibrated residuals (feet squared)	Percent contribution to weighted sum of squares	
Target subset				**By subset**	**By set**
"Predevelopment"—before 1940					**23.2**
USGS network water levels	11	1	6,847	1.48	
Driller-log water levels	51	0.25	5,097	1.10	
Wisconsin Cambrian-Ordovician head contours	233	.04	31,071	6.72	
Michigan Pennsylvanian head contours	115	.04	21,129	4.57	
Michigan Marshall head contour	103	.04	20,616	4.46	
Indiana miscellaneous water levels	19	.16	4,837	1.05	
Illinois Cambrian-Ordovician head contours	231	.04	17,941	3.88	
USGS network wells—"historical" water levels					**40.6**
Southern Lower Peninsula, Michigan	1,761	.01–.04	18,840	4.07	
Northern Lower Peninsula, Michigan	272	.01	13,309	2.88	
Upper Peninsula, Michigan	426	.01–.04	1,506	.33	
Northeastern Wisconsin	1,964	.01–.04	76,691	16.58	
Southeastern Wisconsin	1,149	.01–.04	55,868	12.08	
Northern Indiana	294	.01	1,849	.40	
Farfield	2,422	.0025–.01	19,862	4.29	
Northeastern Illinois Cambrian-Ordovician					**5.7**
2000 water-level contours	248	.01	8,640	1.87	
Drawdown, 1864–2000 contours	248	.01	9,103	1.97	
Recovery, 1980–2000 contours	267	.0025–.01	8,658	1.87	
Decadal head changes in USGS network wells					**17.5**
Southern Lower Peninsula, Michigan	1	49	543	.12	
Northeastern Wisconsin	22	1–4	32,373	7.00	
Southeastern Wisconsin	40	1	48,056	10.39	
Vertical head differences					**6.3**
USGS network wells	41	.25–4	13,460	2.91	
USGS RASA packer tests in early 1980s	31	4	15,831	3.42	
Base-flow targets at USGS streamgages in 2000					**6.6**
Southern Lower Peninsula, Michigan	17	3.60E−11	7,265	1.57	
Northern Lower Peninsula, Michigan	11	3.60E−11	4,241	.92	
Upper Peninsula, Michigan	9	3.60E−11	3,751	.81	
Northeastern Wisconsin	12	3.60E−11	5,568	1.20	
Southeastern Wisconsin	4	3.60E−11	2,488	.54	
Northern Indiana	3	3.60E−11	895	.19	
Northeastern Illinois	6	3.60E−11	6,327	1.37	
Total	**10,011**		**462,662**	**100.00**	**100.0**

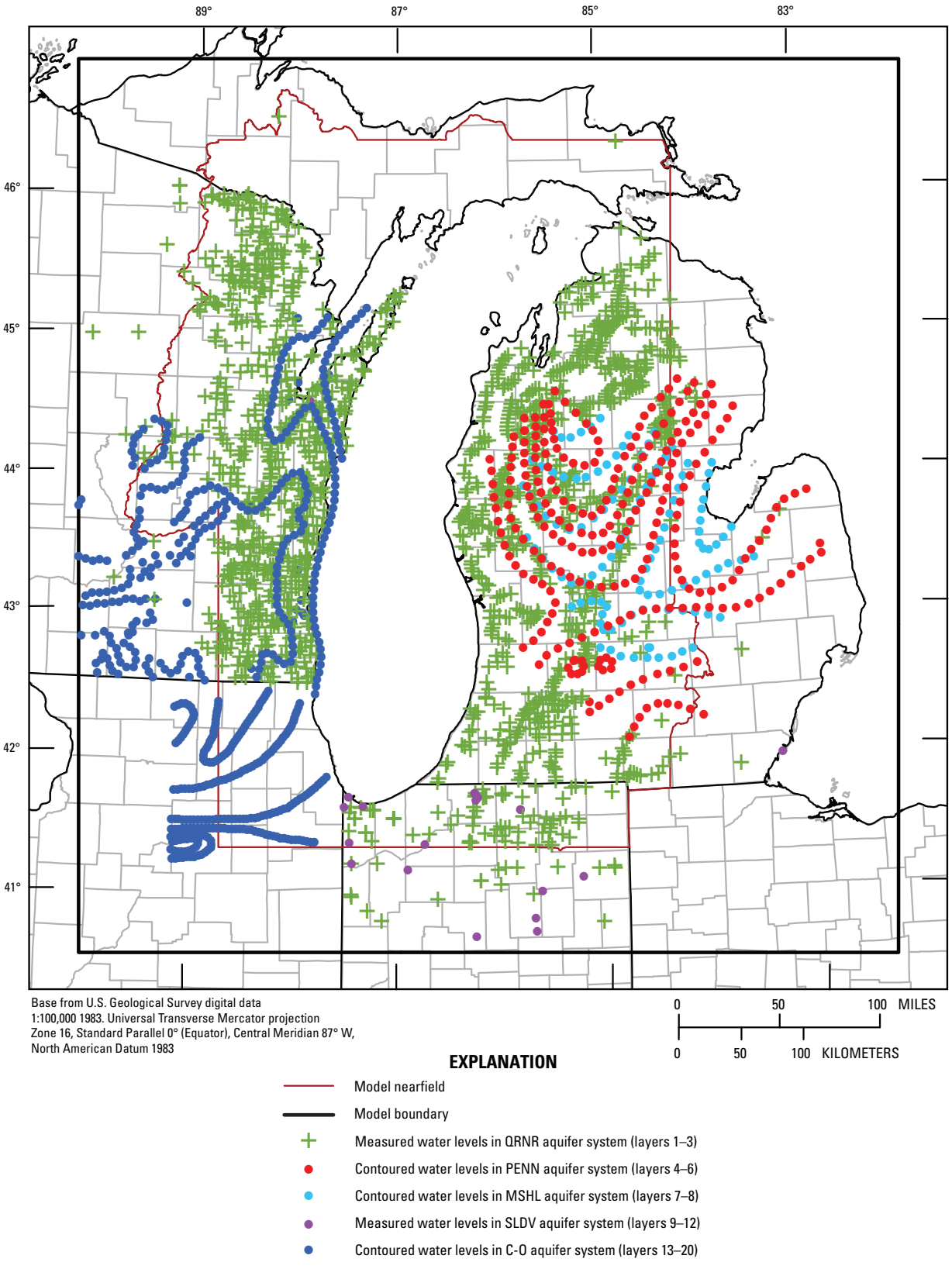

Figure 45*A*. Spatial distribution of calibration targets: USGS network wells, household wells, and contour-derived targets, providing predevelopment water-level targets (Sources: U.S. Geological Survey, National Water Information System, *http://waterdata.usgs.gov/nwis*; Arihood, 2009; Barton and others, 1996; Weidman and Schultz, 1915; Capps, 1910; Visocky and others, 1985; Mandle and Kontis, 1992).

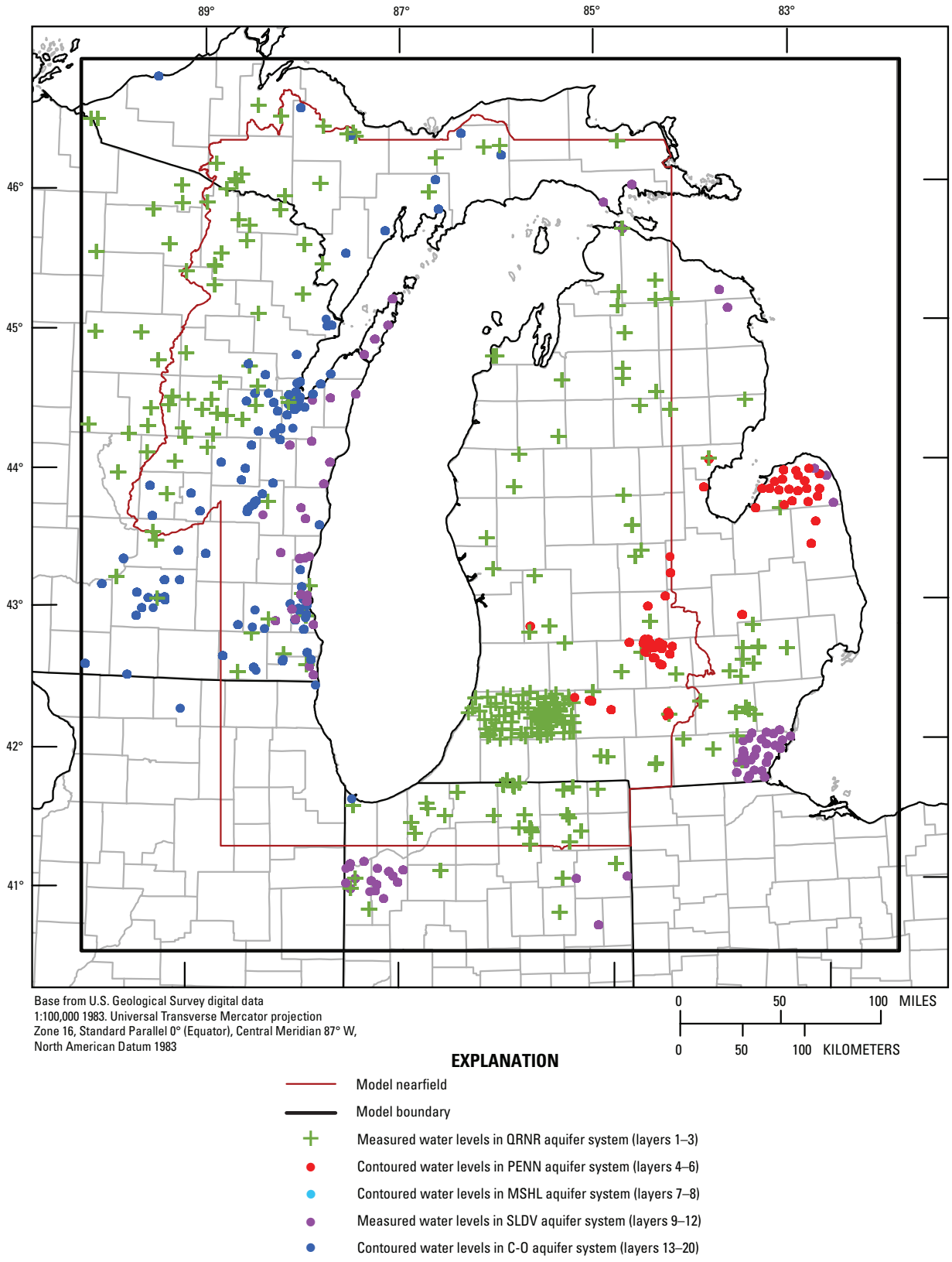

Figure 45*B*. Spatial distribution of calibration targets: USGS network wells, providing postdevelopment water-level targets (Source: U.S. Geological Survey, National Water Information System, *http://waterdata.usgs.gov/nwis*).

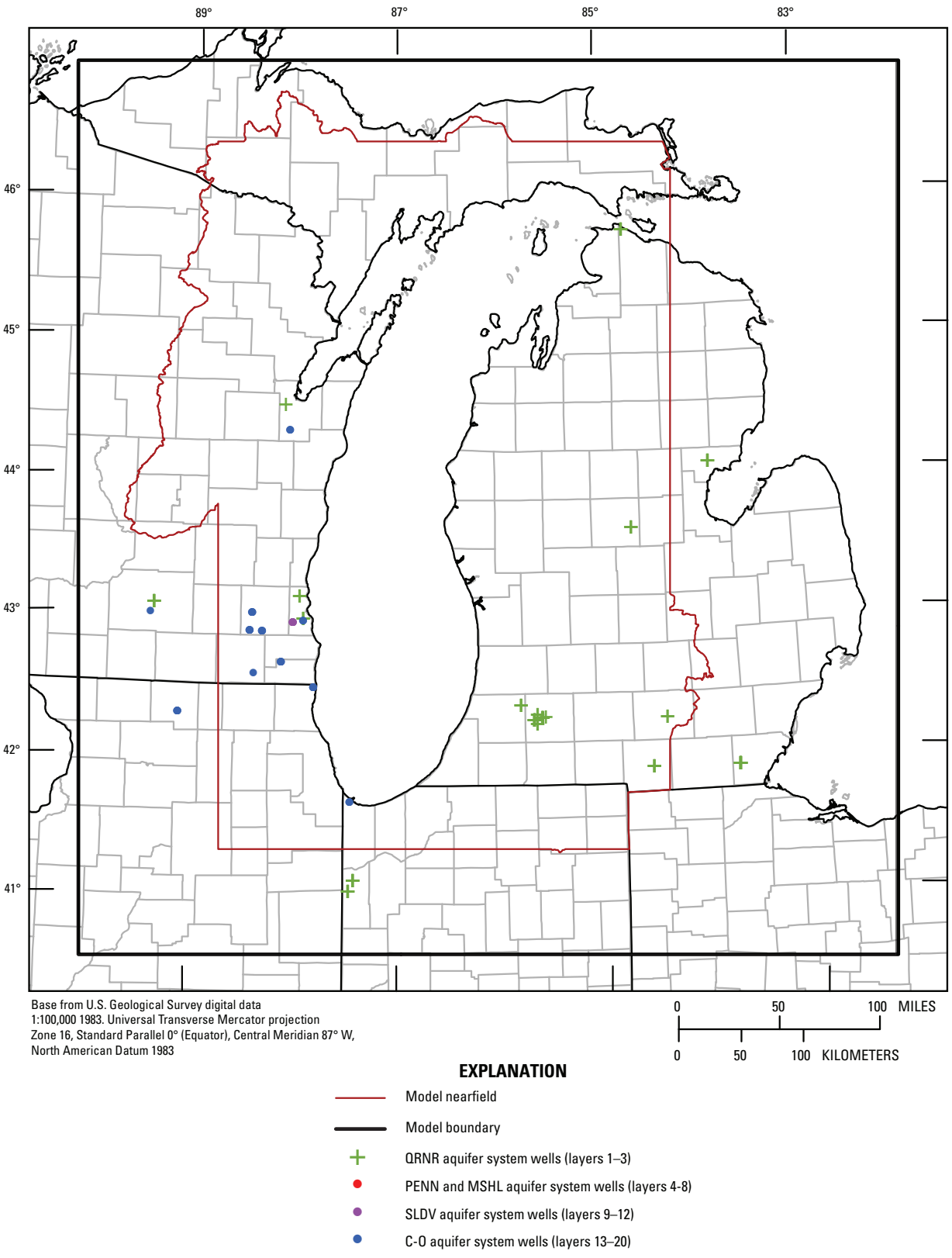

Figure 45*C*. Spatial distribution of calibration targets: USGS network wells as well as RASA packer tests from the early 1980s, providing vertical-head-difference calibration targets (Sources: U.S. Geological Survey, National Water Information System, *http://waterdata.usgs.gov/nwis*; Young, 1992; Nicholas and others, 1987).

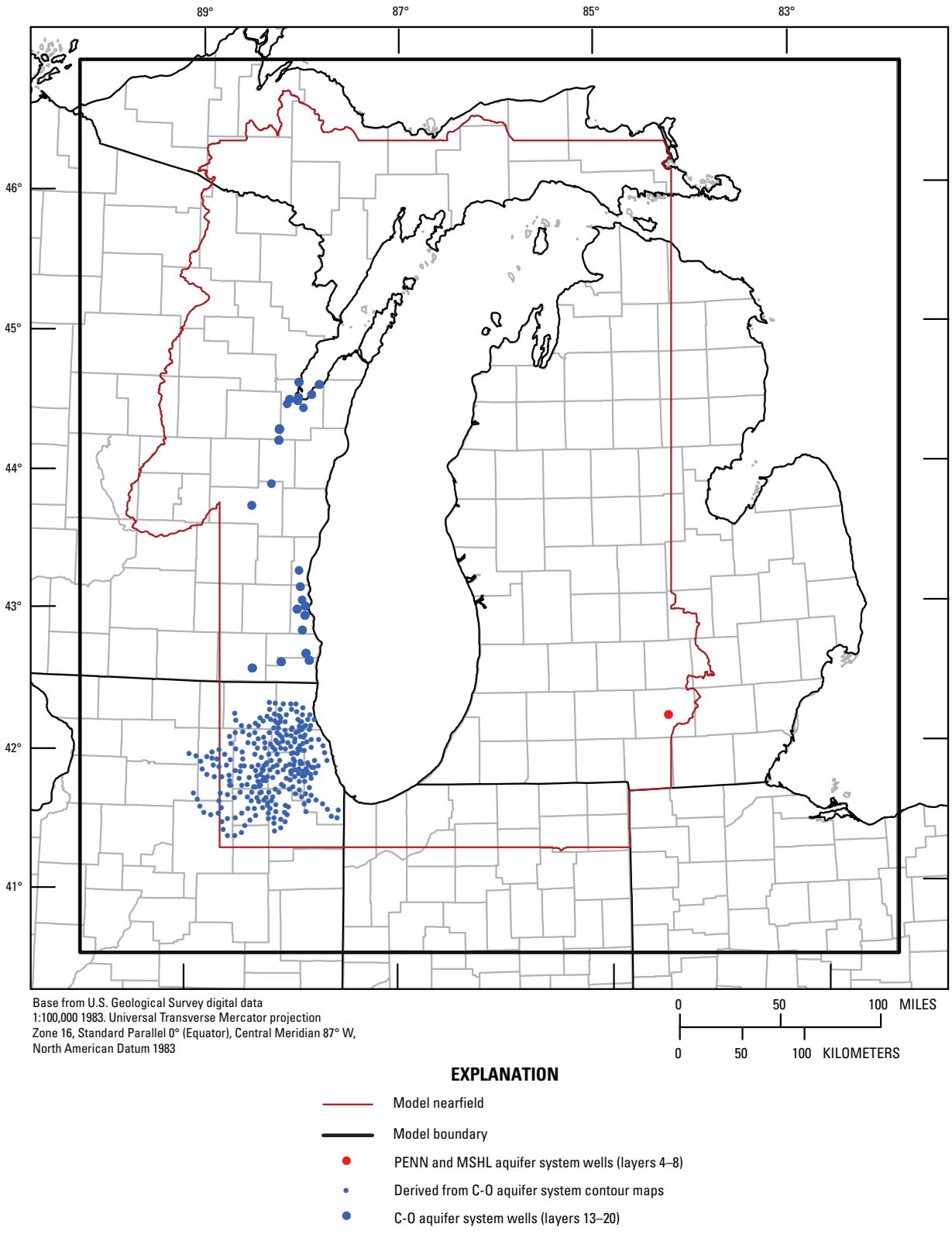

Figure 45*D*. Spatial distribution of calibration targets: Multiple readings from USGS network wells supplemented by targets based on differences between contour maps over time, providing head change (drawdown and drawup) targets (Sources: U.S. Geological Survey, National Water Information System, *http://waterdata.usgs.gov/nwis*; Visocky and others, 1985; Burch, 2002).

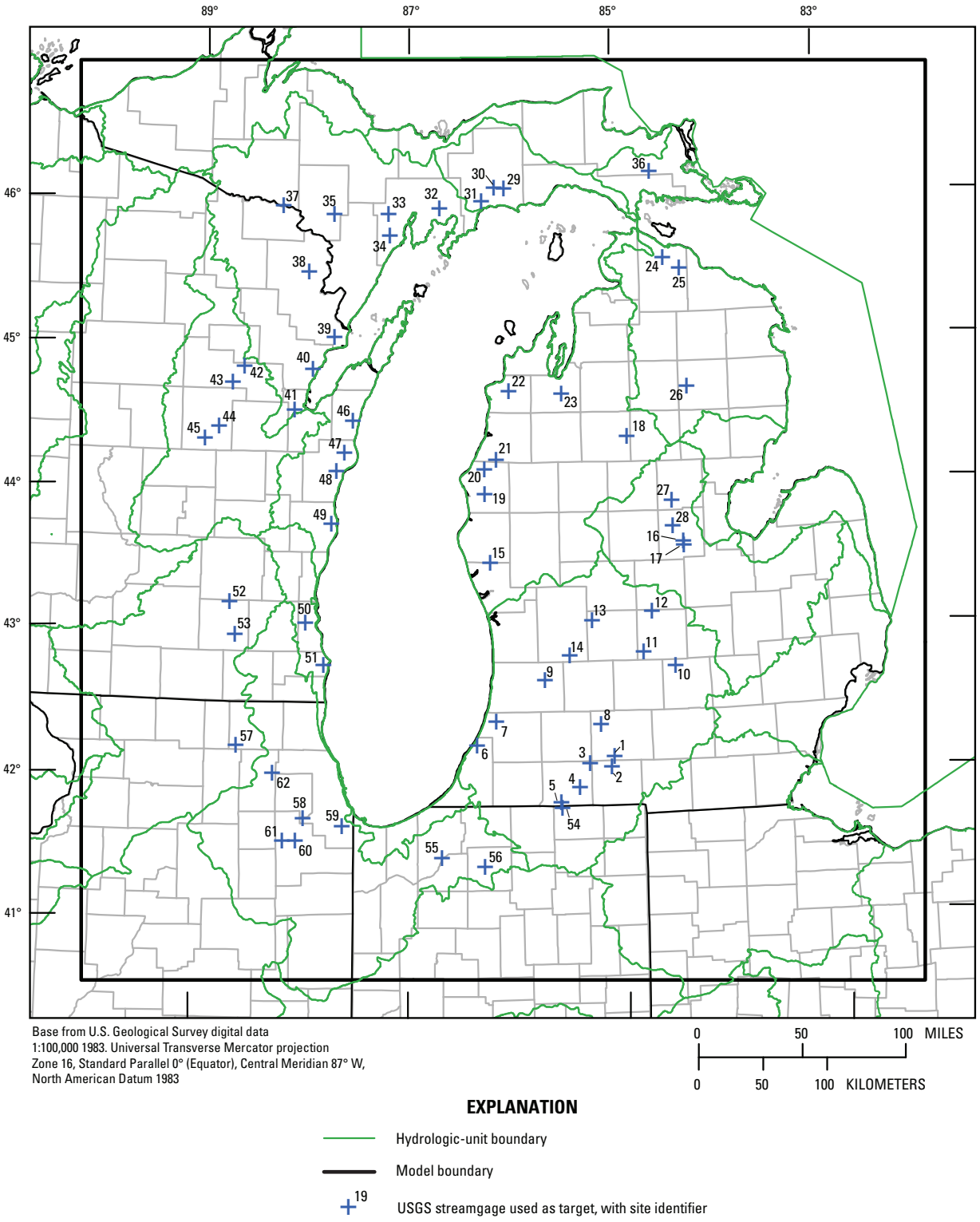

Figure 45*E*. Spatial distribution of calibration targets: USGS streamgages, providing base-flow calibration targets (Source: U.S. Geological Survey, National Water Information System, *http://waterdata.usgs.gov/nwis*).

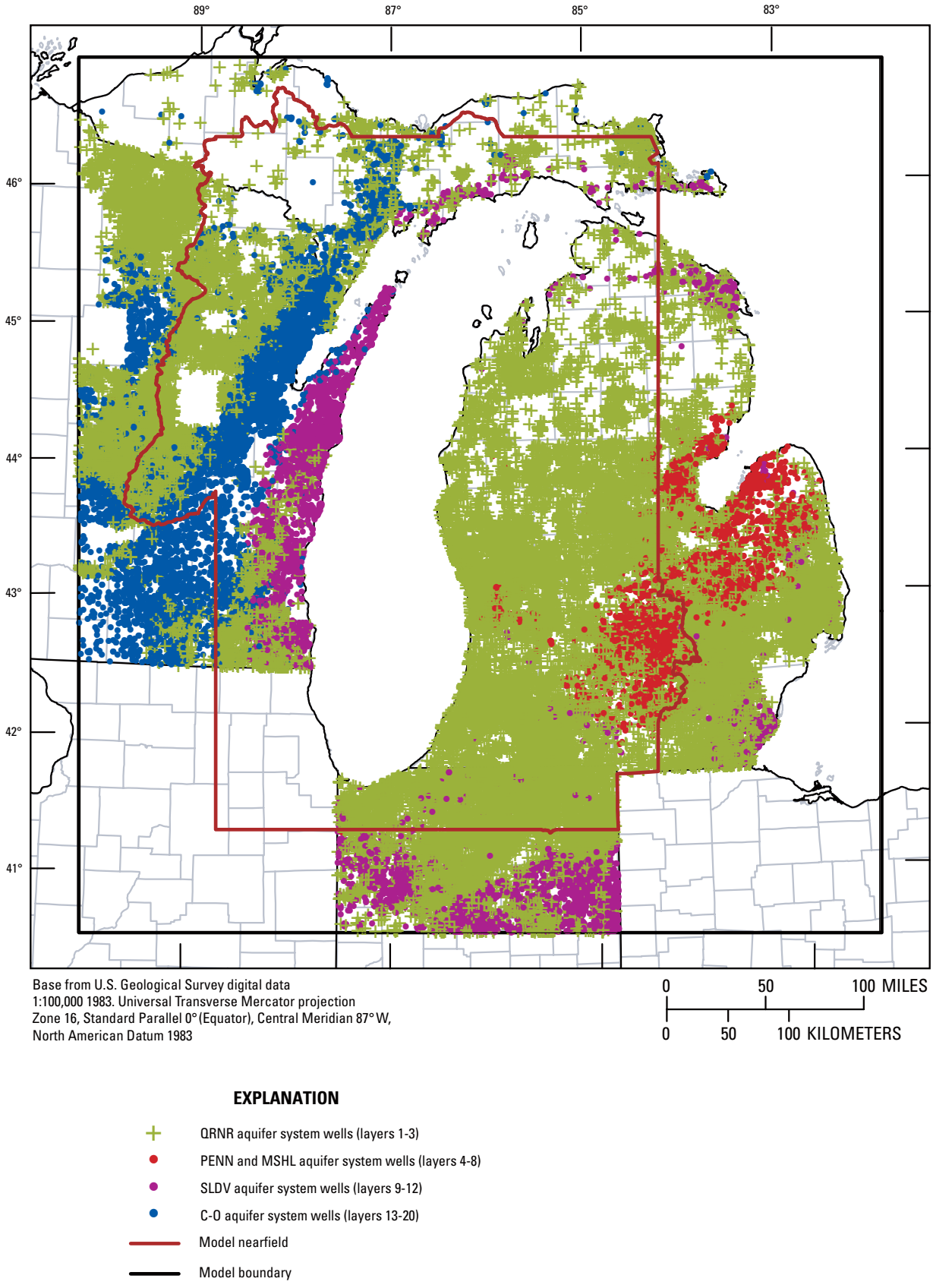

Figure 45*F*. Spatial distribution of calibration targets: household wells, providing postdevelopment water-level targets (Arihood, 2009).

The summary statistics for the 62 streamgage locations suggest that base-flow discharges estimated with the Gebert method are similar to those estimated with other methods. It is also informative to compare base-flow discharges to streamflow exeedances to obtain an idea of what fraction of the annual average streamflow is attributable to base flow. The base-flow discharges are typically less than Q_{50} and greater than Q_{75}, implying that on average the base flow is between streamflow discharges that are exceeded one-quarter and one-half of the time on an annual basis. The relation of base flow to streamflow exceedances varies by subregion and is influenced by the texture of unconsolidated deposits in different parts of the model. For example, in the Northern Lower Peninsula of Michigan (NLP_MI) where material is predominantly sandy, the base-flow discharge is generally close to the Q_{50} discharge rate, whereas in Northeastern Illinois (NE_ILL) where the material is generally fine grained, it is generally substantially less than the Q_{50} rate. In areas underlain by outwash, it is likely that recharge rates are high, yielding high discharges for base flow; in areas underlain by clayey till, recharge is less because more precipitation is diverted through overland runoff, resulting in less base flow.

The 62 base-flow targets provide information for many areas of the model nearfield and are distributed fairly evenly across subregions. (See colored stream and water bodies in figs. 28*A* and *B*). The entire surface-water network captured by nodes upgradient from a streamgage is assumed to contribute to the estimated base flow. However, surface-water network may not always be completely integrated and routed to the streamgage. For example, isolated wetlands can lose groundwater discharge to evapotranspiration rather than transport to an outlet stream. Consequently, the targets used in model calibration may overestimate base flow, and the parameter estimation may reduce the multiplier on recharge to compensate. As discussed in the section 8 ("Model Limitations"), this artifact is only one of several probably small and possibly offsetting interferences that affect the estimation of recharge.

Estimates of direct discharge of groundwater to Lake Michigan were not included in model calibration given their uncertainty. Direct discharge has been estimated from several field studies and models that have reported a wide and uncertain range of results (for example, see Grannemann and Weaver, 1998). Neff and Nicholas (2005) estimate that the whole-lake direct-discharge estimates for the Great Lakes range between 0.5 and 2.0 ft^3/s per mile of shoreline. The results of the calibrated model are qualitatively compared to this target range in section 6 ("Model Results") and section 7 ("Alternative Models and Model Sensitivity").

5.3.2 Target Filtering

Two calibration issues arise from the abundance of surface-water features in the Lake Michigan Basin and the relatively coarse discretization used to define the model grid. First, many shallow water-level targets correspond to RIV cells and, therefore, are too constrained by the influence of the head-dependent boundary to be useful for calibration; consequently, they are summarily filtered or removed from the targets used for parameter estimation and do *not* appear in table 11*A* or figure 45. Second, these surface-water features can act as model boundaries, thus limiting the model's ability to accurately simulate the transient response of the water table to pumping from shallow wells. In parts of the model domain (notably Michigan and Indiana), almost all the pumping is from the Quaternary (QRNR) aquifer or shallow unconfined bedrock aquifers (see table 9*B*). Because the model cannot simulate the groundwater/surface-water interaction with a meaningful resolution, it returns a poor match to observed drawdown produced by shallow pumping in these areas. Moreover, inclusion of these shallow drawdown targets in the calibration process obfuscates information available from targets that can be properly simulated given the model resolution (for example, drawdown targets in the confined bedrock aquifers), thereby undermining parameter estimation. For this reason, all the shallow drawdown targets also were removed from the target list and do *not* appear in table 11*A* or figure 45. Finally, water-level targets derived from contour maps are omitted in areas where the contours cross saline water. This filtering affects some targets derived from predevelopment contours in the Marshall Aquifer (MSHL) unit and, to a lesser extent, predevelopment and postdevelopment contours in the Cambrian-Ordovician (C-O) aquifer system in northeastern Illinois. Targets are restricted to freshwater areas because extremely few measurements of water levels in the Michigan Basin have been collected in brackish water (defined here as those with concentrations between 10,000 mg/L and 100,000 mg/L) or brines (defined here as those with concentrations greater than 100,000 mg/L).

5.3.3 Target Weights and Bounds

The parameter-estimation program PEST uses algorithms to modify parameter values so as to minimize the objective function; that is, the sum of squares of the weighted target residuals.[23] The modeler-assigned target weights are a primary mechanism for translating the modeler's relative ranking of target fit used to assess calibration quality; consequently, the weights are important for guiding the search for optimal parameters. For this study, target weights were selected to balance the contribution to the objective function among the different target types so that information contained in targets can influence the inversion regardless of the small number of targets contained in that target type.

The weights for each target carry units that, when multiplied by the residuals, yield dimensionless weighted residuals. In the calibration process the targets and residuals corresponding to water levels, change in water levels, vertical difference between water levels, or water levels derived from contour maps carry units of *feet*; therefore, their weight units are ft^{-1}.

[23] The target residual is equal to the measured value minus the simulated value at the target location for the appropriate model time step.

The targets corresponding to base-flow estimates in the calibration process carry units of *cubic feet per day* (ft^3-day^{-1}); therefore, their weight units are day-ft^{-3}. Water-level measurements obtained largely from the USGS monitoring-well networks are plentiful, and many targets are available. However, the value of individual measurements to improving model fit is highly variable because the model results are insensitive to some observations. In this study, the most value belongs to the relatively small number of measurements that allow for matching predevelopment conditions, for determining aquifer responses to pumping, and for properly simulating vertical gradients. These select head targets, in addition to base-flow targets (that break the correlation between hydraulic conductivity and recharge), were deemed important for constraining the parameter estimation. By adjusting an observations' weight, it is possible to avoid having the inversion routine "chase noise" (obtain slightly better fits at unimportant targets at the expense of fitting important targets). The final roster of weights for the confined version of the LMB model (column 3 in table 11*A*) ensures that all the target types ultimately contribute at least 4 percent to the objective function that drives the parameter-estimation process (column 6 in table 11*A*).

Another important modeler-specified constraint on the PEST parameter estimation is the presence of upper and lower parameter bounds that limit the range of potential values. The range used in this study was informed in part by the coarse grid spacing (5,000 ft on a side in the model nearfield) necessitated by the extent of the regional model. As discussed in section 3 (and also section 8, which is devoted to model limitations), the large cells require a compromise between a version of the model that incorporates the entire surface-water network, including first-order streams, and largely fixes the water table prior to simulation and, alternatively, a version that inserts only major surface-water features and is liable to distort the value of model input in order to control excessive water-table mounding. Because some groundwater-discharge features are absent in the compromise configuration, the inversion routines tend to raise the shallow horizontal hydraulic conductivity of the unconsolidated and shallow bedrock units higher than evidence indicates in order to match the degree of observed water-table mounding in between surface-water bodies. By bounding the maximum value of K_h for these parameters at levels only somewhat higher than initial values, one can generate reasonable values for these inputs while achieving most of the reduction in the objective function potentially obtainable given the model discretization. The parameters affected by this strategy include the multipliers for the K_h of the six glacial categories and also some multipliers assigned K_h zones of the Silurian-Devonian (SLDV) bedrock unit, which subcrops west of Lake Michigan. For these parameters, the upper bounds lead to final values that are less than 10 times the initial values (lower bounds are less than 0.1 times the initial value). For all other parameters in the adjusted confined model calibration, the upper and lower bounds are set to 10 times and 0.1 times, respectively. Appendix 5, table A5–2, tabulates the bounds for each of the 160 parameters estimated for the confined model calibration.

5.4 Regularized Inversion Techniques

Unique calibration of the large and complex LMB model is tractable only if the parameter estimation process operates on an input structure that simplifies the complexity of the natural world. As explained previously, the simplification involves grouping input variables into a restricted number of multiplying parameters applied to zones of cells. The zones group either areas with cell-by-cell variation or areas with block variation. Zonation of inputs is a common simple form of "regularization" applied during model construction and calibration (Hunt and others, 2007). However, there are other forms of regularization that can facilitate the inversion process. These other forms can be particularly important when, as in this study, the combined number of parameters (even after zonation) cannot be uniquely estimated. Moreover, for a complex model it can be important to use inversion methods that minimize the number of times the Jacobian matrix—consisting of derivatives for each calibration target relative to each estimated parameter—is recalculated in the effort to identify the objective function minimum.

The LMB model calibration is notable for its use of the sophisticated regularized inversion tools available in the parameter-estimation computer code PEST (Doherty, 2008a; Doherty and Hunt, in press). Specifically, the calibration approach used here differs from traditional nonlinear regression parameter estimation in its use of (1) pilot points (Doherty, 2003; Doherty and others, in press), in addition to a traditional parameter zone approach in one area of the model; (2) Tikhonov regularization (Tikhonov, 1963a, 1963b; Doherty, 2003; Fienen and others, 2009); and (3) hybrid singular value decomposition (Tonkin and Doherty, 2005; Hunt and others, 2007; Doherty and Hunt, in press), also referred to as SVD-Assist (SVDA) by Doherty (2008a). Application of these advanced tools not only enhanced the calibration of the complex LMB model but also helped demonstrate the utility of innovative methods, a goal of the broader pilot-study design.

5.4.1 Pilot Points

During calibration, it became apparent that one important area of the regional model—the SE_WI and NE_ILL pumping centers—was parameterized by using zones that were too large to accurately simulate local water levels and vertical gradients. The leakage of water from the shallow flow system to underlying confined aquifers of the deep pumping centers is controlled in large measure by the resistance posed by the Maquoketa confining unit. Thus, rather than employ large blocks of homogeneous values to characterize the hydraulic conductivity of the bedrock, as done elsewhere in the model domain, the vertical hydraulic conductivity of the Maquoketa

confining unit in this part of the model is simulated by means of pilot points as a way to constrain cell-by-cell variation of the K_v value within this area of the model domain. Kriging (a geostatistical algorithm) is used to interpolate values estimated at the 78 pilot-point locations (fig. 46) to the other cells in the unit. The pilot points are used to characterize conditions in two zones, one representing a subcrop area where the Maquoketa is subject to enhanced weathering, and a second to the east where the unit is overlain by SLDV. The method is "regularized" by using a preferred homogeneity condition, by which one attempts to minimize variation between values at pilot points within each zone by penalizing deviations from "smoothness." Regularization and interpolation between pilot points are limited to cells within their respective zones, and this restriction conforms to the geologic conceptualization of the two zones. This approach facilitates geologic continuity where it is believed to exist but still allows heterogeneity to be expressed within zones as informed by the observations of water-level, vertical gradient, and head-change targets. In sum, the pilot point approach allows the use of "soft" knowledge (based on geologic zonation) that it is not "hardwired" to one fixed parameter value over the entire zone as in a traditional calibration approach. The ability of observed data to inform the parameterization is enhanced by an appreciable number of representative targets that pertain to the parameter used for a pilot-point representation. Thus, in this study, pilot points and related regularization were restricted to evaluating the Maquoketa K_v in two subregions where vertical head and gradient targets are plentiful and where the calibration proves highly sensitive to its values. (See discussion of model fit below.)

5.4.2 Tikhonov Regularization

A groundwater-flow model with many parameters is commonly affected by parameter insensitivity and correlation, which in turn lead to solution non-uniqueness and an ill-posed inverse problem. Two forms of Tikhonov regularization were used to counter these problems in the LMB model: preferred value and preferred homogeneity (Tikhonov 1963a, b). Preferred value regularization was applied to non-pilot-point parameters such as the hydraulic conductivity in zones, anisotropy, storage, and river-conductance parameters. The preferred values were set at the initial parameter values that resulted from previous modeling in the basin (for example, Krohelski, 1986; Mandle and Kontis, 1992; Young, 1992; Arihood and Basch, 1994; Conlon, 1998; Eberts and George, 2000; Krohelski and others, 2000; Reeves and others, 2004; Luukkonen and others, 2004; Feinstein, Eaton, and others, 2005; Meyer and others, 2009). As discussed above, preferred homogeneity regularization was specified for the pilot points within each weathering zone; thus, homogeneity was preferred within a weathering zone, but the preferred condition was not expressed across zones. Finally, the compromise between model fit and the preferred conditions was initially weighted in favor of model fit and later weighted to favor the preferred condition (PEST variable PHIMLIM— Doherty 2003; 2008a; and Fienen and others, 2009).

5.4.3 Singular Value Decomposition

In addition to the Tikhonov regularization, subspace methods were also employed through hybrid singular value decomposition (SVD) (see Tonkin and Doherty, 2005). SVD uses the Jacobian matrix to divide the full parameter space (as defined by all the original or "base" parameters) into linear combinations of base parameters (hereafter referred to as "superparameters") from those parameters that cannot be estimated by using the available targets due to parameter insensitivity or correlation; only the former are included in the parameter-estimation process. As discussed in Doherty and Hunt (in press), SVD can be relentless in pursuit of a best fit even at the expense of realism, which can result in unreasonable and extreme parameter values considered optimal because of small improvements in fit. Tikhonov regularization and specification of parameter bounds were used to balance model fit with parameter reasonableness.

In this pilot application, the Jacobian matrix (containing the 238 original, or "base," parameters for the confined model: 160 zone multipliers plus 78 pilot points) was reconfigured to define 40 superparameters used for model calibration. The estimation of 40 superparameters was found to be a stable process over the range of values evaluated during the parameter estimation (as indicated by a matrix condition number less than 1 E6 for all parameter-estimation iterations; see Doherty and Hunt, in press, for more information). The parameter-estimation problem was run on an 80-processor modeling array by using Parallel PEST (Doherty 2008a), facilitating runtime reductions of two orders of magnitude in the parameter-estimation operation.

5.4.4 Integrity of Derivatives

Beyond its use of sophisticated regularized inversion tools for parameter estimation, the LMB pilot application is also notable for its employment of new tools for assessing the quality of the model for nonlinear-regression parameter-estimation techniques. As described previously, nonlinear regression is based on the expectation that the derivative of the change in parameter value to the change in observation is a smooth function. However, the number of significant figures carried through the computations, the tightness of solver solution-convergence criteria, solution thresholds such as those involving dry nodes, and nonlinearities such as those generated by fluctuations in saturated thickness can degrade the smoothness of this function by introducing granularity in the derivatives. Granularity can be expressed as jumps, thresholds, and other irregularities in the derivative, often manifesting itself as a seemingly random variation of the observed quantity to regular changes in the parameter value. Regardless of the form, granularity decreases the signal-to-noise ratio of the target-to-parameter sensitivity information contained in the Jacobian matrix; if sufficiently degraded, the Jacobian matrix can become so noisy that the quality of the parameter upgrade calculated from that Jacobian matrix could be compromised.

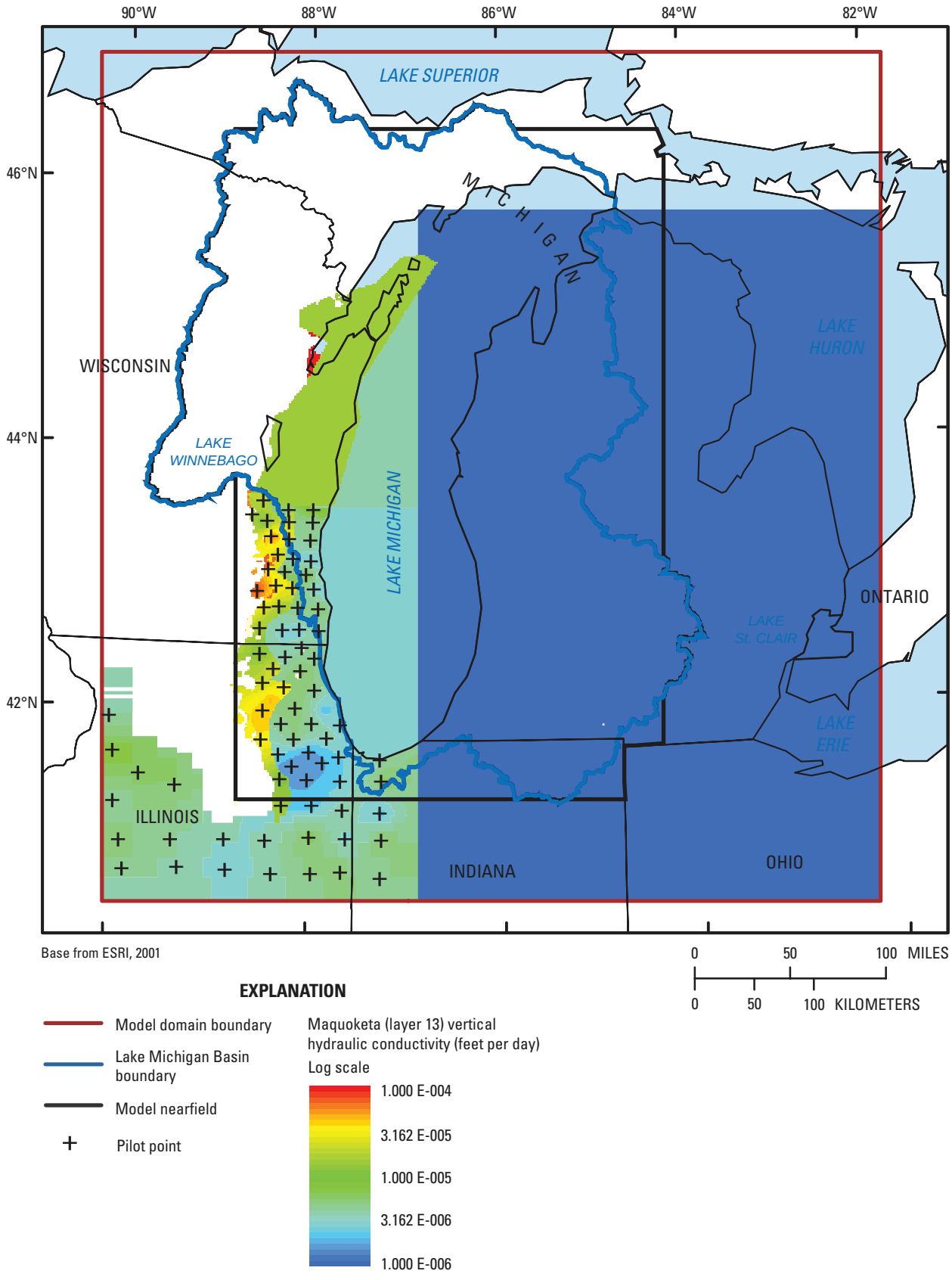

Figure 46. Pilot point locations and calibration results for vertical hydraulic conductivity of the Maquoketa confining unit.

As discussed previously in this report and also by Feinstein and others (2008), the unconfined SEAWAT model exhibited appreciable granularity, so most parameter estimation was done on the confined case where the granularity was reduced.[24]

5.5 Calibration Results

In the following subsections, the results of the calibration process are evaluated in terms of (1) improvements in the model fit between the measured and simulated targets and (2) plausibility of parameter values estimated from the calibration process.

5.5.1 Model Fit

The initial model input for the confined version of the LMB model yielded a value for the sum of squares of weighted residuals—the objective function measuring overall model error—equal to 9.43 E5. After five iterations of nonlinear regression, the model error was approximately halved, to a value of 4.68 E5. Additional iterations result in very small reduction of the model error at the expense of having more parameter estimates approach unreasonable and extreme values. The final calibrated confined version of the LMB model was chosen before the extreme values dominated, and it is called SLMB-C (SEAWAT-LMB-confined). Table 11*A* records the contribution of each target type and the total objective function for SLMB-C. Table 12 lists summary calibration statistics across head target subsets for SLMB-C.[25] The first statistic, mean error (*ME*) is a measure of bias; that is, the tendency of the simulated targets values to be less than measured values (positive *ME*) or greater than measured values (negative *ME*). It is computed as the average of the weighted residuals in a target subset. The second statistic, mean absolute error (*MAE*), is computed as the average of the *absolute values* of the weighted residuals in a target subset and is always positive. For the targets related to water levels or differences in water levels, the *ME* across target subsets for SLMB-C ranges from about −21 to +16 ft; the *MAE* ranges from about 1 to 50 ft.

Two different calibration statistics are computed for the base-flow targets to account for the different scale of units associated with these observations (typically 1 E7 ft^3/d). The *ME* is computed as the average ratio of the measured to simulated target flows, and the *MAE* is the average of the absolute value of the flow ratios. The *ME* (1.07) indicates that the simulated flux is, on average, 7 percent smaller than the estimated base-flow targets, and the *MAE* (1.25) indicates an average error of about 25 percent.

The model fit for each target subset in the confined SLMB-C model is displayed visually in appendix 8 by means of scatterplots that show model error and the degree of bias about the 1:1 line. Most plots show close agreement over the entire range of targets in the subset; but a few (for example, the plot for predevelopment water levels in the Marshall unit (MSHL)) show some bias and large residuals over part of the range, indicating that the model could be improved in those areas with a different conceptualization. Plots for the target subsets involving drawdown, recovery, and vertical gradient targets indicate the SLMB-C model reasonably reproduces the formation of cones of depression around deep pumping centers, as well as the recovery of water levels in deep aquifers in the northeastern Illinois area after communities there shifted to a Lake Michigan water source. Vertical gradients measured in packer tests and between nested USGS network wells also are well reproduced. The base-flow residuals are plotted on a log scale and show that, in general, the model preserves the relative rank of observed fluxes estimated at streamgages. Finally, the qualitative comparison between the water levels observed in household wells and the water levels simulated at those locations shows reasonable agreement over the entire range of values, indicative of a consistently close average match across model subregions.

In order to gain additional insight into the quality of the calibration of the SLMB-C model, a subset of the calibration targets was selected for additional analysis. The subset incorporated all water-level measurements, both predvelopment and postdevelopment, that contributed to the calibration process—a total of 8,350 targets. The *ME* for the subset was −1.97 ft and the *MAE*, 25.21 ft. An additional statistic, equal to the square root of the average of the squared residuals of the targets and called the root mean squared error (Anderson and Woessner, 1992), is more sensitive to outlier values than is the *MAE*. For the ensemble of measured head targets (unweighted), the root mean squared error was 36.78 ft. This statistic is often compared to the range of measurements as a general way of indicating agreement between measured and simulated values. The smaller the ratio, the better the overall model fit. For the SLMB-C model, measured water-level altitudes vary between 195 and 1,650.7 ft, yielding a ratio of 0.025. This value is well below the 0.100 threshold for the ratio commonly posited to indicate a good fit (Spitz and Moreno, 1996).

[24] In cases where granularity cannot be addressed within the model itself, global search methods within PEST such as shuffle-complex evolution (Duan and others 1992; 1993) or covariance matrix adaptation evolution scheme methods (Hansen and Ostermeier, 2001; Hansen and others, 2003) can be used in place of nonlinear regression methods. However, these nonregression methods were not needed in the LMB model application.

[25] The comparison in table 12 between the results for SLMB-C and those for the unconfined calibratred model, SLMB-U, are discussed in section 7.

Table 12. Confined and unconfined model calibration statistics for weighted targets and for driller-log targets.

[Arrows indicate which version of the model performed better in terms of calibration statistics. Double arrow indicates large discrepancy]

Target subset	Confined model (SLMB_C)			Unconfined model (SLMB_U)		
	Mean error	Mean absolute error		Mean error	Mean absolute error	
Predevelopment USGS network water levels (pre-1940)	−5.36	14.94	<==	−5.89	15.13	
Predevelopment driller-log water levels (pre-1940)	.01	14.09	<==	−.78	14.60	
Predevelopment Wisconsin Cambrian-Ordovician head contours	−19.97	41.26	<==	−20.03	41.49	
Predevelopment Michigan Pennsylvanian head contours	−8.56	49.91	<==	−9.41	50.64	
Predevelopment Michigan Marshall head contours	9.07	44.52		7.92	43.92	<==
Predevelopment Indiana miscellaneous water levels (pre-1940)	−11.24	22.99	<==	−13.11	23.80	
Predevelopment Illinois Cambrian-Ordovician head contours	4.63	31.07		5.79	29.96	<==
2000 Illinois Cambrian-Ordovician head contours	−3.27	29.98	<== <==	−17.69	34.84	
1864–2000 Illinois Cambrain-Ordovician drawdown contours	14.82	41.66	<== <==	30.00	47.40	
Base flow	1.07	1.25		1.05	1.24	<==
Vertical head difference—USGS network	9.74	11.03	<== <==	6.91	14.96	
Vertical head difference—USGS RASA packer tests	−1.64	7.80	<==	3.34	8.95	
Southern Lower Peninsula, Mich., network water levels (post-1940)	−13.74	20.83	<==	−14.74	21.40	
Northern Lower Peninsula, Mich., network water levels (post-1940)	−21.46	37.71	<== <==	−28.23	41.20	
Upper Peninsula, Mich., network water levels (post-1940)	3.91	11.20		2.54	11.09	<==
Northeast Wisconsin network water levels (post-1940)	−1.79	31.49	<==	−.18	31.56	
Southeast Wisconsin network water levels (post-1940)	−12.81	35.60		−12.09	34.66	<==
Northern Indiana network water levels (post-1940)	−8.84	15.02	<==	−9.70	15.33	
Farfield network water levels (post-1940)	11.37	22.48	<==	11.73	22.60	
Decadal head changes in USGS network wells	−14.60	25.67		−12.39	22.40	<== <==
1980–2000 recovery in Illinois Cambrian-Ordovician head contours	15.57	37.32	<== <==	−28.07	44.25	
Water levels from nearfield driller logs for all time periods*	11.30	19.81		10.13	19.09	<==

* The post-1940 driller logs were assigned zero weight in the parameter inversion.

5.5.2 Estimated Parameter Values

Parameter estimation of the SLMB-C model (1) resulted in some optimal parameter values very close to their initial values (signified by a multiplier close to 1.0), (2) changed most inputs by a moderate amount, and (3) drove a few parameters to the bounds set as user-specified constraint. Appendix 5, table A5–2, tabulates the parameter multiplier for each estimated parameter. Multipliers less than 0.5 and greater than 2.0 are annotated, as are multipliers that are equal to an upper or lower bound. The following calibration results for the confined SLMB-C model are notable:

- The recharge multiplier was constrained when using the most complete dataset—that constructed from measurements from recent conditions corresponding to year 2000; thus, the optimal multiplier of 1.048 is derived from conditions in the final model stress periods (1991 to 2005). This same multiplier is then applied to every cell in the model and to every time step. Thus, the relative distribution of recharge through time and space is unchanged, but all values are increased by about 5 percent relative to the initial recharge arrays generated by the soil-water-balance (SWB) model and shown in figures 30 and 31.
- Storage parameter multipliers (ranging from 0.697 to 1.69) and RIV conductance multipliers (ranging from 0.96 to 1.52) deviate modestly from 1, indicative of relatively small changes to initial storage and conductance inputs compared to changes in hydraulic conductivity discussed below.
- The pilot point cell-by-cell variation in the K_v assigned the Maquoketa (MAQU) confining unit in the SE_WI and NE_ILL subregions (fig. 46) was characterized by overall values consistent with the geologic conceptualization. In the weathered zone at the western fringe, the geometric mean of the updated cell K_v values is 2.61 E−5 ft/d. To the east, where the MAQU does not subcrop and is not weathered to the same degree, the geometric mean of values is lower (6.30 E−6 ft/d). Although the average change from initial values (2.0 E−5 ft/d and 5.85 E−6 ft/d, respectively) is small, the cell-by-cell variation in this parameter is important in reducing the magnitude of the objective function and improving calibration. In particular, the focused use of pilot points allowed a much improved fit to the high-quality targets associated with the RASA packer-test water-level data and, thereby, allowed the model to simulate more closely the gradients controlling vertical leakage within the deep part of the flow system in the SE_WI, NE_ILL and N_IND subregions.
- The following multiplier parameters hit the upper bounds imposed as constraints on the parameter estimation: K_h for clayey till (5.0), K_h for loamy till (2.70), K_h for sandy till (1.73), and K_h for the Silurian-Devonian unit (SLDV) in zone 2 of layer 10 (2.0). In each case, it is likely that horizontal hydraulic conductivities above the bounds (and also above reasonable values for the deposits in question) would lower simulated water-table elevations and reduce the reported model error. This model error could also be reduced by decreasing the model grid spacing to enable better representation of the surface-water network, as discussed previously.
- The following multiplier parameters hit their lower bounds: K_h for the Prairie du Chien-Franconia unit (PCFR) in zones 2 and 6 of layer 16 (0.1) and K_h for the Mount Simon unit (MTSM) in zones 5 and 6 of layer 19 (0.1).
- Out of the 160 parameter multipliers estimated in the SLMB-C calibration, 24 are greater than 2.0 (maximum=6.9 for a K_h MTSM zone in layer 19) and 15 are less than 0.5 (minimum=0.10 for bedrock parameters that hit their lower bounds).

The spatial distribution of calibrated horizontal hydraulic conductivities given the optimal parameter multipliers are shown for layer 1 in figure 47 and for selected layers (upper, middle, and lower QRNR, PEN1, MSHL, upper SLDV, STPT, IRGA, and upper MTSM) in appendix 6*A*. Given the optimal multipliers, the spatial distribution of the calibrated vertical hydraulic conductivities are shown for selected layers (upper, middle, and lower QRNR, PEN2, MICH, DVMS, middle SLDV, MAQU, EACL) in appendix 6*B*. The initial values of hydraulic conductivity are compared to the optimized values in three ways:

1. Comparison of figure 39 to figure 47 shows that the calibration process yielded generally higher hydraulic conductivity values for the upper QRNR deposits in layer 1.

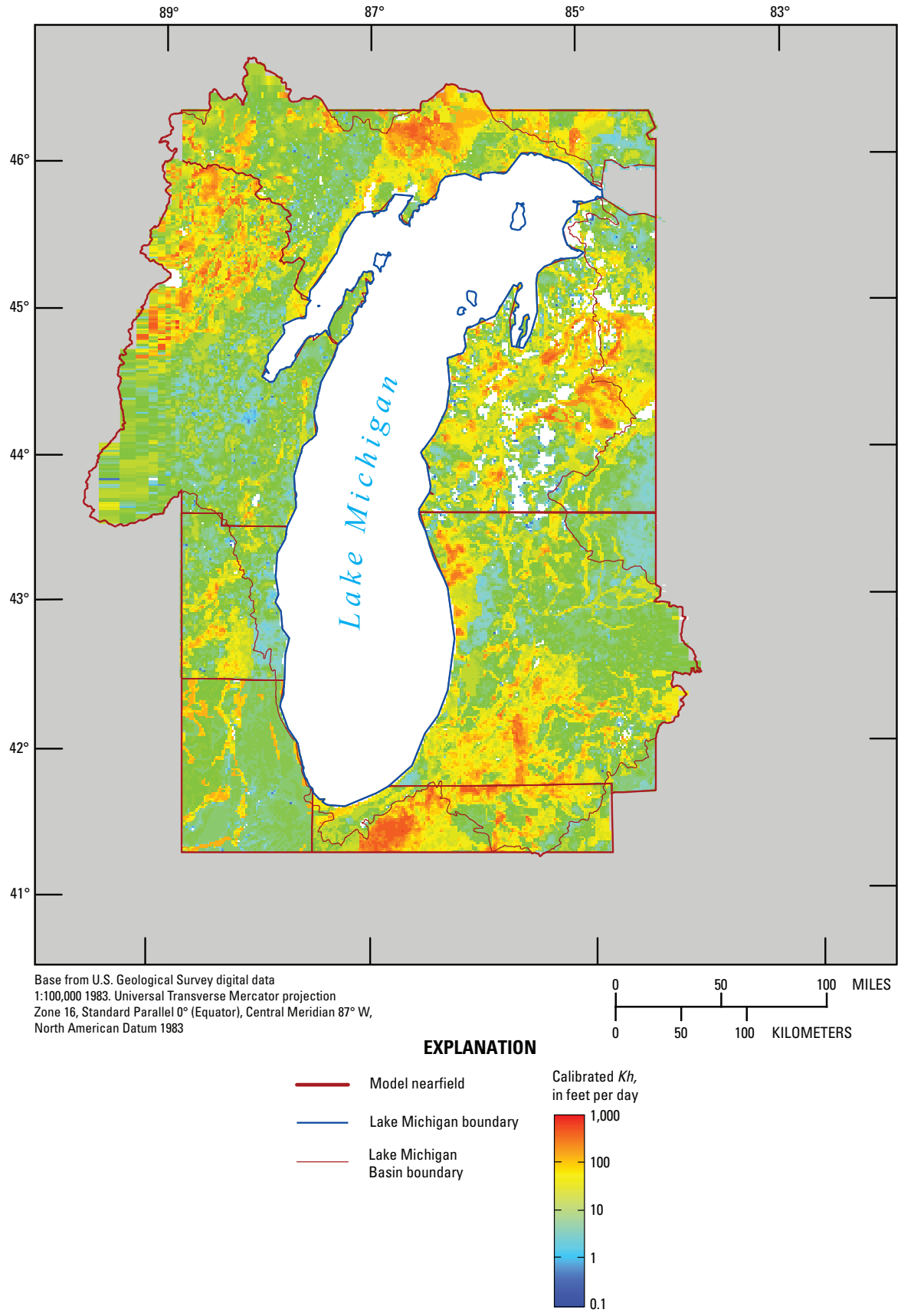

Figure 47. Calibrated horizontal hydraulic conductivity distribution in nearfield area of model layer 1.

2. In appendix 9, the average and geometric mean of thickness-weighted horizontal hydraulic conductivity for aquifer systems is compared for the initial and calibrated SLMB-C input. The calculation is restricted to the inland parts of the nearfield; that is, the seven model subregions.[26] Inspection of the results shows that the average and geometric mean values for the QRNR aquifer system uniformly increase across subregions as a result of calibration. The initial geometric mean values range between 2.5 and 21.0 ft/d by subregion, whereas the calibrated geometric mean values range between 8.0 and 34.1 ft/d. The biggest relative change occurs in NE_ILL; the large increase there can be attributed to the 5.0 calibration multiplier applied to its dominant glacial category, clayey till. The remaining bedrock aquifer systems show less dramatic and systematic changes from initial to calibrated average and geometric mean values. The calibrated K_h values are on average higher for the PENN and MSHL aquifer systems (between 4 and 14 ft/d by subregion) than for the SLDV and C-O aquifer systems (between 0.5 and 3.8 ft/d by subregion).

3. The spatial distributions of initial transmissivity by aquifer system (figs. 41*A*–*E*) can be compared to the distributions of calibrated transmissivity (figs. 48*A*–*E*, starting on p. 142). The higher calibrated *K* input values noted after calibration for the Quaternary (QRNR) sediments are reflected in higher calibrated transmissivities. Other aquifer systems show more muted changes between distributions of initial and calibrated values and generally maintain the pattern of low- and high-transmissivity areas initially imposed as a result of the geologic conceptualization. The calibrated transmissivities are generally highest for the QRNR aquifer system (fig. 48*A*); the bedrock systems, where present, all display bulk transmissivity values roughly similar in magnitude (figs. 48*B*–*E*).

4. The distribution of initial K_v in confining units (fig. 42) can be compared to the distribution of calibrated K_v (fig. 49). Both increases and decreases are evident in the sample cross section, with the biggest relative changes due to calibration occurring in the Salina Group within the SLDV (layer 11), the PCFR unit (layer 16), and the EACL unit (layer 18).

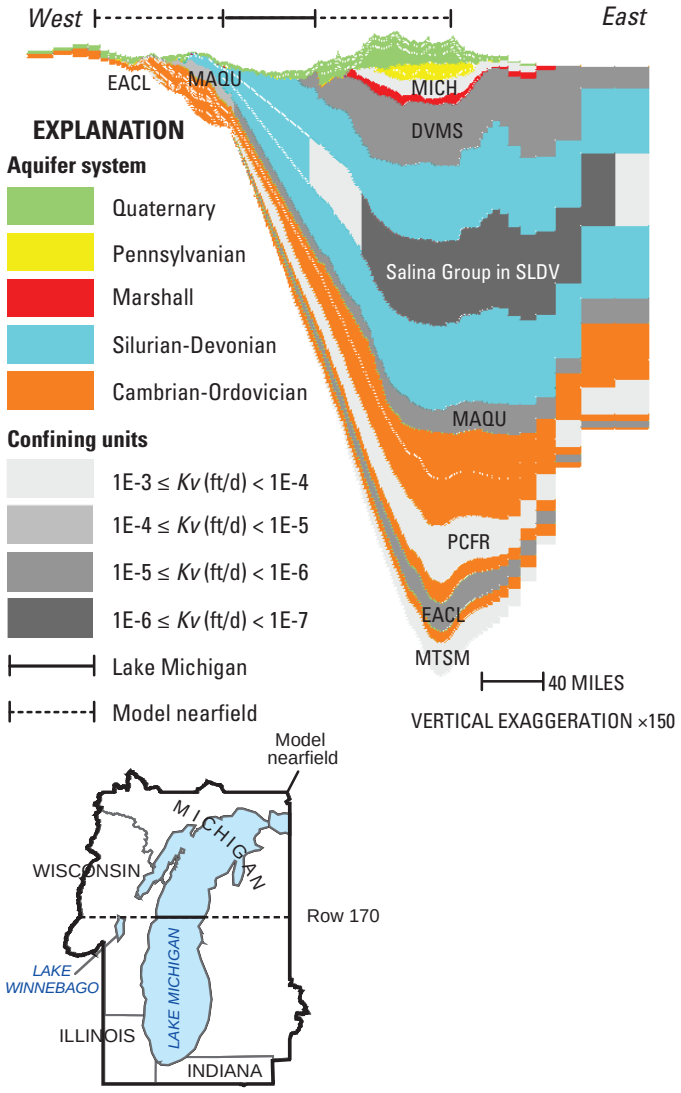

Figure 49. Calibrated vertical hydraulic conducitivity values for major confining units, row 170.

[26] For example, the average thickness-weighted K_h for the QRNR system is calculated by summing the weighted K_h assigned to each subregion cell for layers 1, 2, and 3, where weights are proportional to the thickness of the cell, and then dividing the total by the number of cells. The geometric-mean calculation sums the logs of the thickness-weighted values, divides the total by the number of cells, and then applies the antilog. The average and geometric mean calculations effectively weight the *K* values by the *saturated* thicknesses used in the confined version of the LMB model.

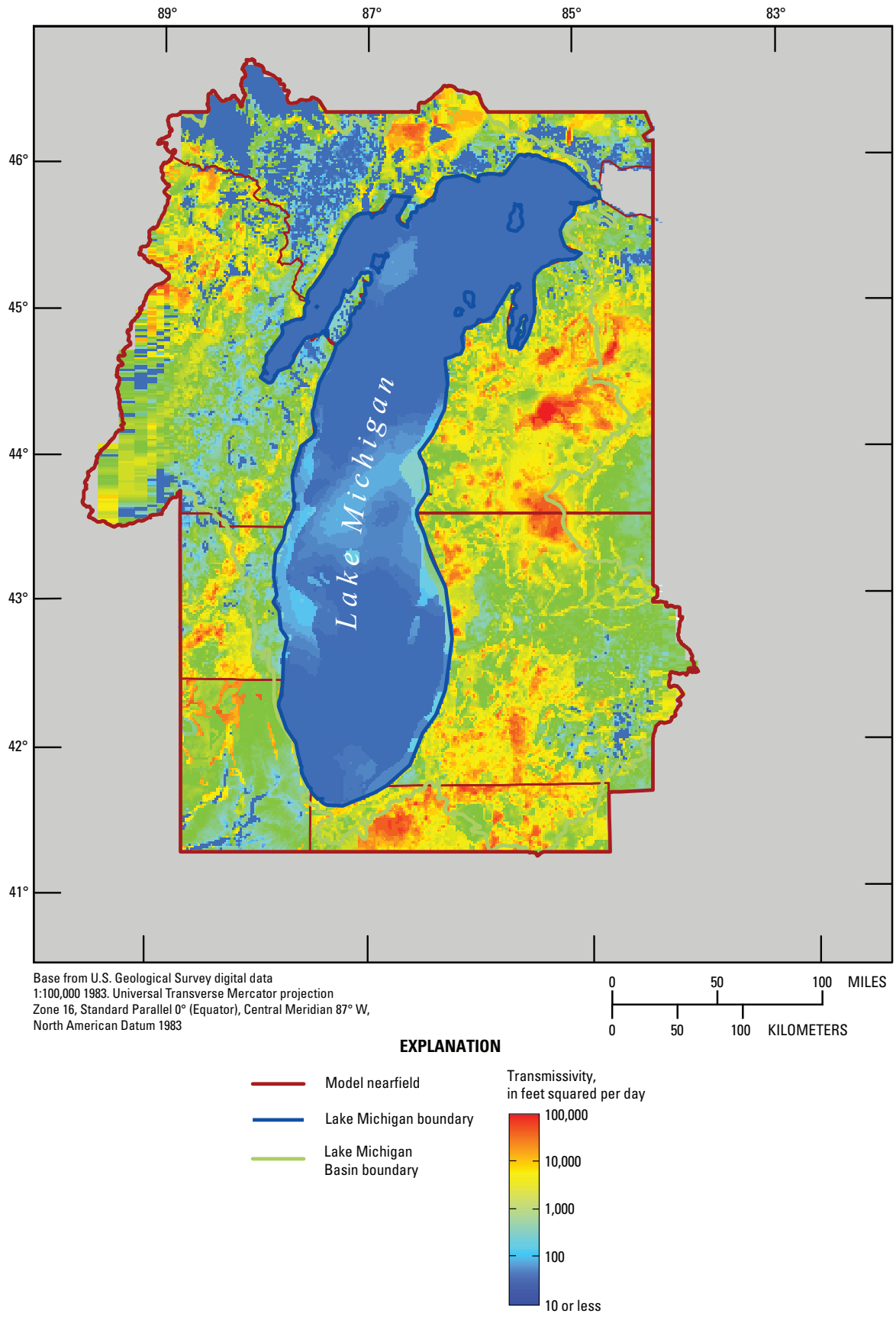

Figure 48*A*. Calibrated transmissivity distribution in aquifer system QRNR.

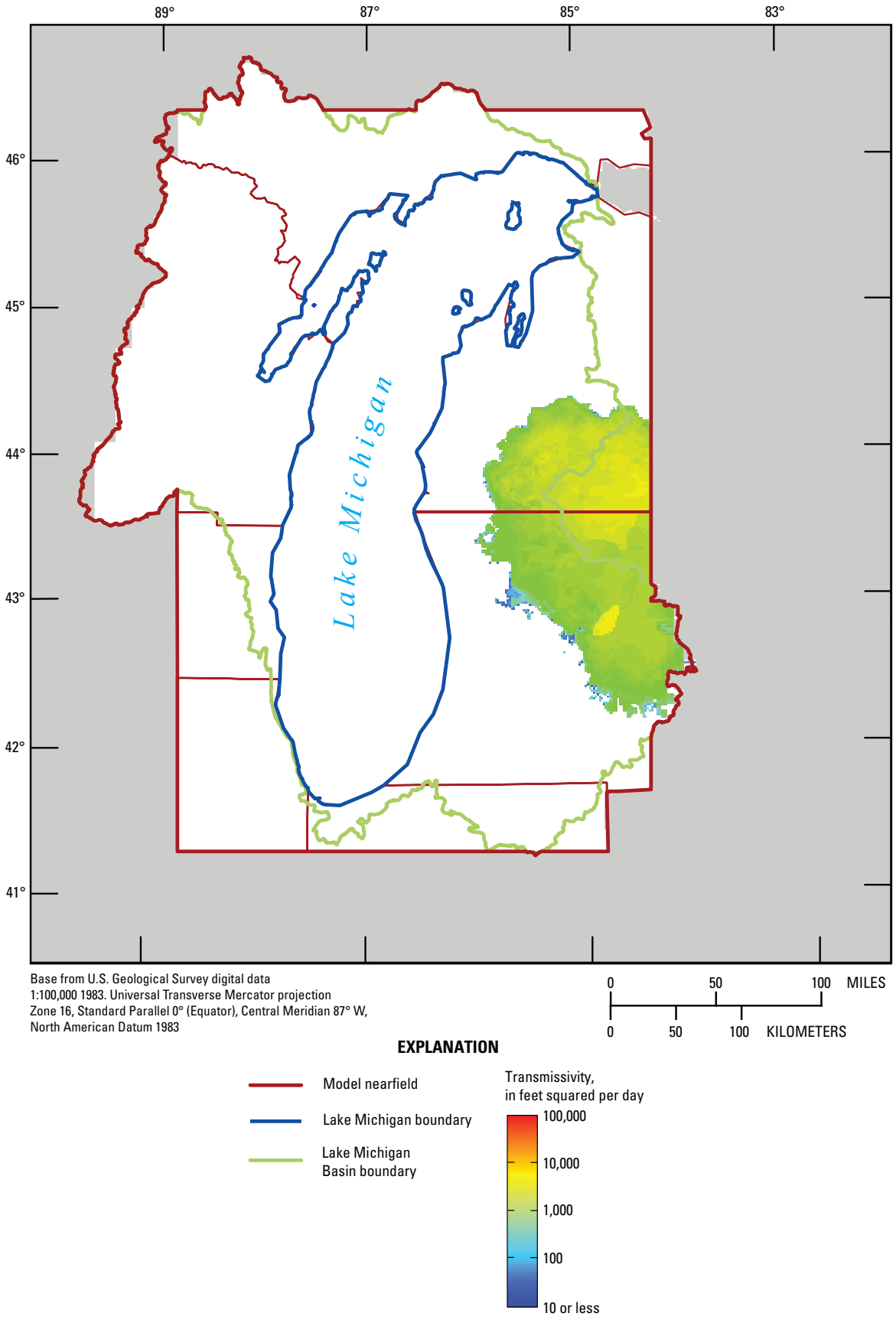

Figure 48*B*. Calibrated transmissivity distribution in aquifer system PENN.

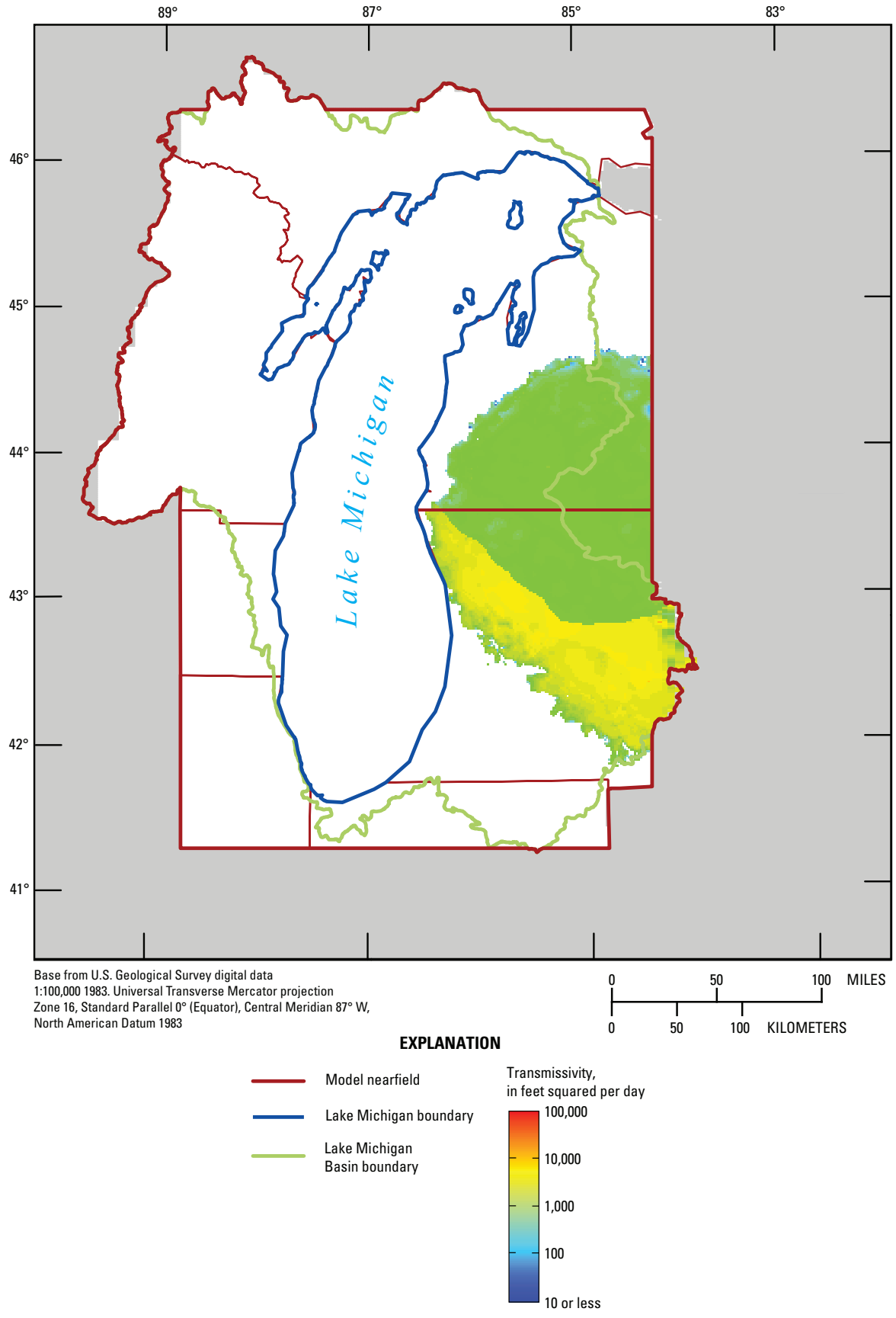

Figure 48*C*. Calibrated transmissivity distribution in aquifer system MSHL.

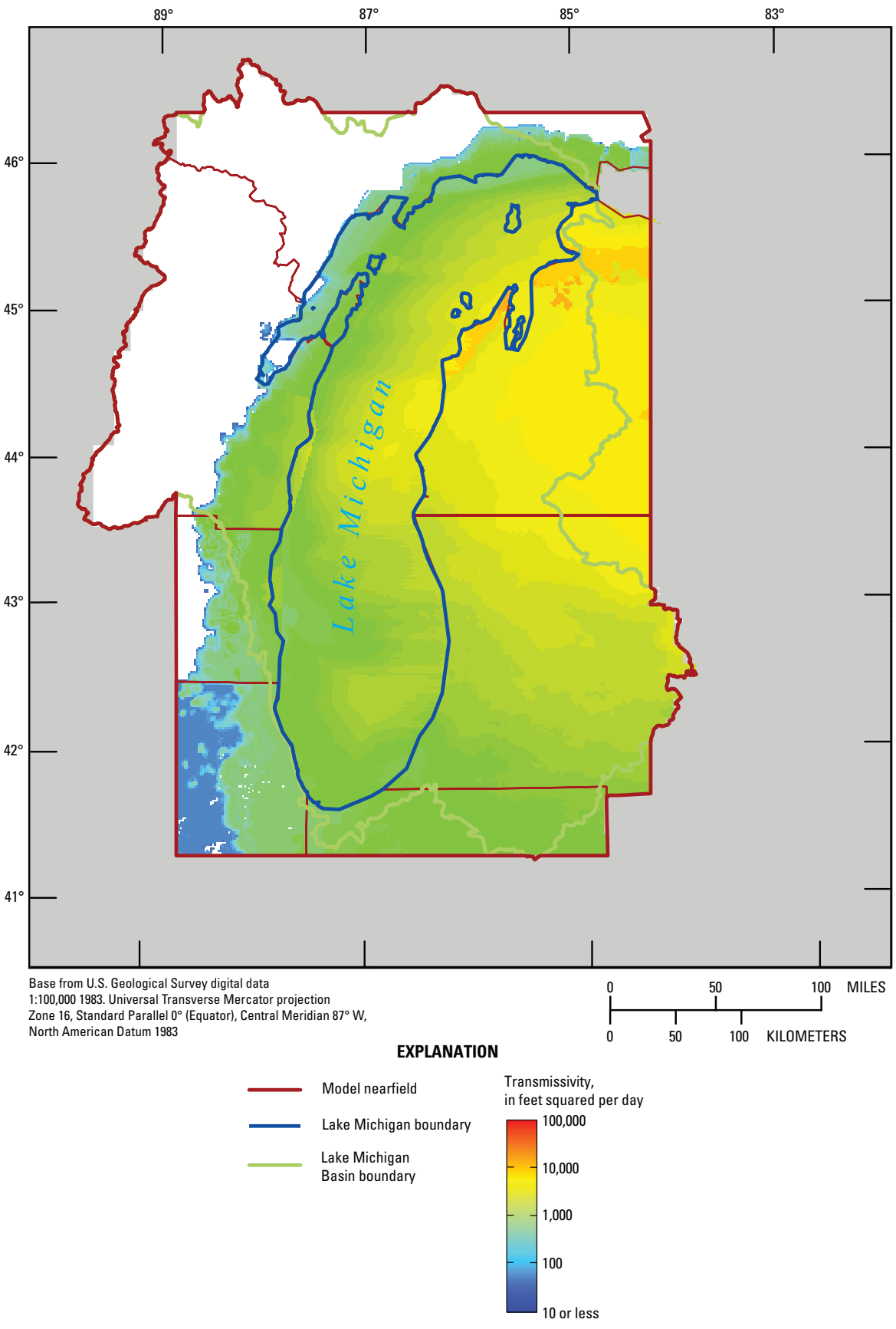

Figure 48*D*. Calibrated transmissivity distribution in aquifer system SLDV.

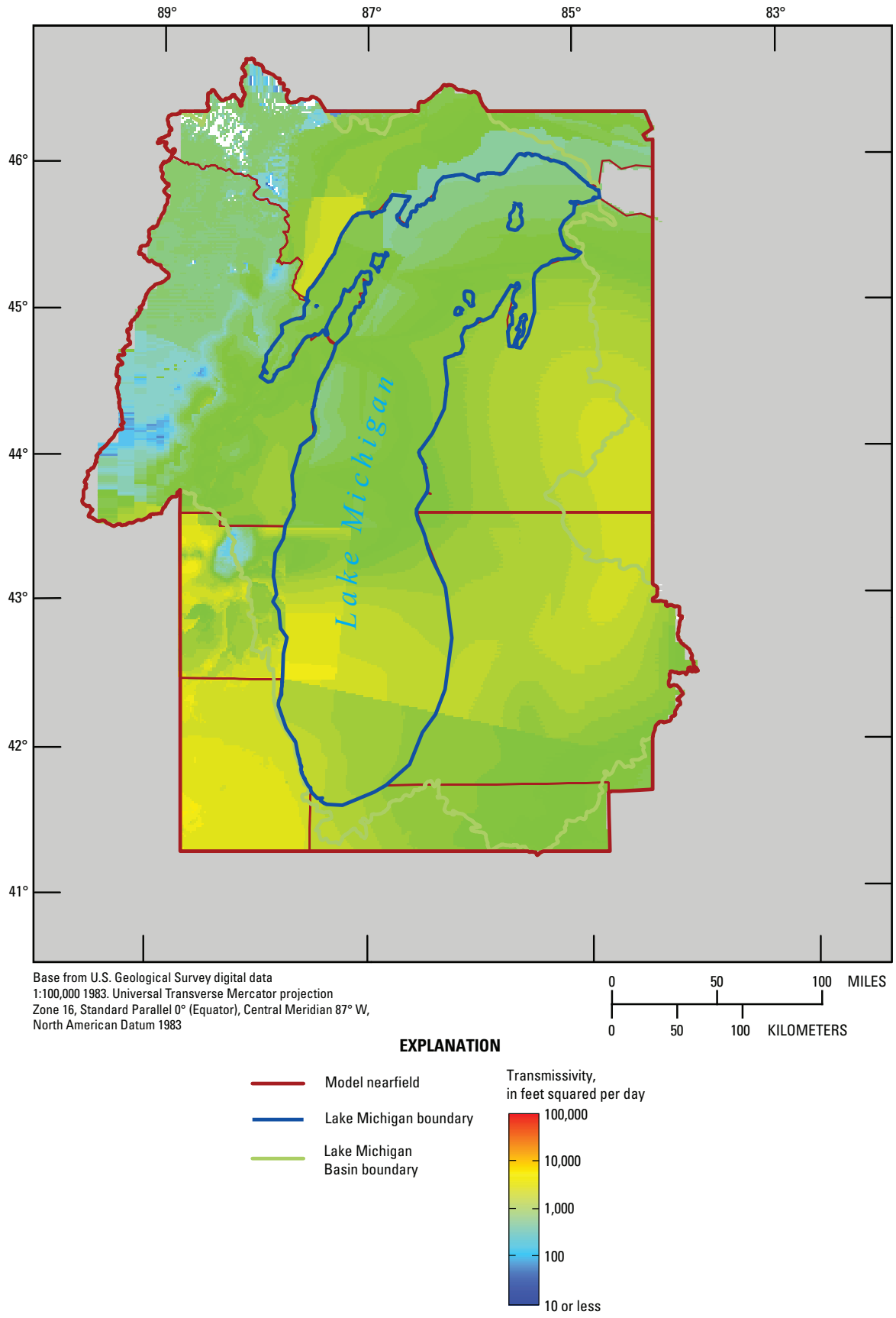

Figure 48*E*. Calibrated transmissivity distribution in aquifer system C-O.

5.6 Parameter Sensitivity

Parameter estimation generates output that ranks the sensitivity of the weighted ensemble of simulated target values to perturbations in individual parameter values. It is convenient to group the individual parameter values by "composite sensitivity," a measure of the sum of all observation sensitivity reported for each parameter. This measure provides a visualization of information content in the dataset for the parameters included in the calibration.

The model input is divided into 14 parameter groups, which include between 1 and 78 individual parameters (the largest group being the set of pilot points for the Maquoketa K_v in the SE_WI and NE_ILL subregions). The groups are ranked by the composite sensitivity across the individual parameters and the sum of composite sensitivity (table 13*A*). The two rankings are in some respects quite different. Whereas the sensitivity of the single parameter in the recharge group is relatively quite high, the larger number of individual parameters in other groups renders them collectively more important to the calibration process. About 60 percent of the summed composite sensitivity is attributable to three parameter groups associated with the C-O aquifer system. The remaining sensitivity is distributed roughly equally among K_h and K_v parameter groups of other aquifer systems, plus RIV conductance, storage, and recharge parameter groups.

Consolidation of the base parameters into eight parameter groups further illustrates the pronounced sensitivity of the SLMB-C calibration to the *K* parameters for the C-O aquifer system compared to the sensitivity toward other types of inputs (fig. 50). Part of this difference is due to the high number of water-level, vertical-head-difference, and time-dependent head-change targets in the C-O system, and part is due to the dramatic effect deep pumping west of Lake Michigan has had on the groundwater-flow system (see section 6, "Model Results"). Shallow-aquifer parameters as a whole tend to be less important than deep-aquifer parameters because the water-table solution in the regional model is constrained by head-dependent boundaries in the form of RIV cells. These constraints particularly affect the ability of the calibration process to inform the estimation of the specific yield of unconfined aquifers (as illustrated by low composite sensitivity). The relative weakness of recharge in guiding the calibration process can be attributed, at least somewhat, to the relatively small weights assigned to the base-flow targets and, by extension, the comparatively modest contribution of these targets to the final objective function. The decision to limit the importance of recharge via weighting was imposed on the calibration process because the base-flow targets used to calibrate recharge in the SLM-C groundwater-flow model were also used to calibrate the SWB recharge model that created the recharge array (see last section of appendix 7).

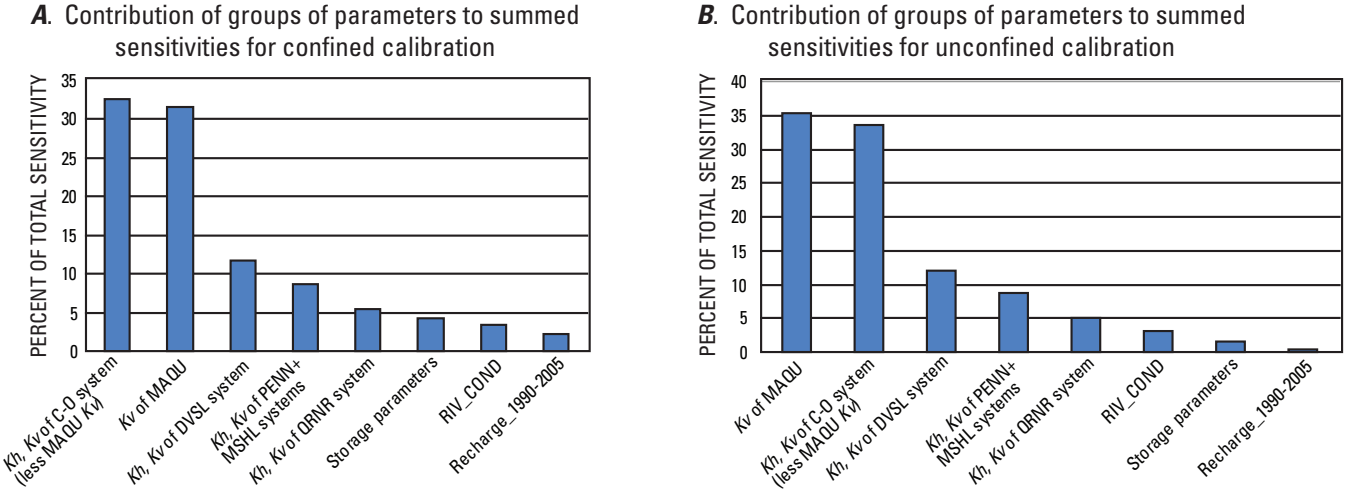

Figure 50. Composite sensitivities of calibration targets to eight parameter groups for *A*, confined (SLMB-C) calibration and *B*, unconfined (SLMB-U) calibration.

Table 13*A*. Composite sensitivities by parameter groups for confined calibration (SLMB-C).

[The 238 estimated parameters (including 78 pilot points) are divided into 14 groups. See appendix 5, table A5–2 for groupings]

Sorted by number of parameters in group		Sorted by average composite sensitivity in group		Sorted by sum of composite sensitivities in group		Percent of sum
Kv_MAQU-pilot_points	78	Ss_C-O	0.115	Kv_MAQU-pilot_points	1.43	29.47
Kh_C-O	46	Recharge_1991-2005	.108	Kh_C-O	.95	19.56
Kv_C-O	30	Kh_QRNR	.025	Kv_C-O	.63	13.11
Kh_SLDV	21	Ss_QRNR-PENN-MSHL-SLDV	.024	Kh_SLDV	.37	7.75
Kh_PENN-MSHL	14	RIV_COND	.023	Kh_PENN-MSHL	.27	5.52
Kv_SLDV	11	Kv_PENN-MSHL	.022	Kv_SLDV	.19	3.99
Kv/Kh_QRNR	7	Kv_C-O	.021	RIV_COND	.16	3.39
RIV_COND	7	Kh_C-O	.021	Kv_PENN-MSHL	.15	3.19
Kv_PENN-MSHL	7	Kv_MAQU-zone	.020	Kh_QRNR	.15	3.06
Kh_QRNR	6	Kh_PENN-MSHL	.019	Ss_C-O	.11	2.37
Kv_MAQU-zone	5	Kv_MAQU-pilot_points	.018	Kv/Kh_QRNR	.11	2.33
Ss_QRNR-PENN-MSHL-SLDV	4	Kv_SLDV	.018	Recharge_1991-2005	.11	2.23
Ss_C-O	1	Kh_SLDV	.018	Kv_MAQU-zone	.10	2.06
Recharge_1991-2005	1	Kv/Kh_QRNR	.016	Ss_QRNR-PENN-MSHL-SLDV	.09	1.95
Total number	**238**			**Total composite sensitivity**	**4.84**	**100.00**

Table 13*B*. Composite sensitivities by parameter groups for unconfined calibration (SLMB-U).

[The 243 estimated parameters (including 78 pilot points) are divided into 16 groups. See appendix 5, table A5–2 for groupings.]

Sorted by number of parameters in group		Sorted by average composite sensitivity in group		Sorted by sum of composite sensitivities in group		Percent of sum
Kv_MAQU-pilot points	78	Kv_PENN-MSHL	0.108	Kv_MAQU-pilot_points	7.45	33.35
Kh_C-O	46	Recharge_1991-2005	.107	Kh_C-O	4.37	19.56
Kv_C-O	30	Kv_C-O	.105	Kv_C-O	3.15	14.07
Kh_SLDV	21	RIV_COND	.096	Kh_SLDV	1.89	8.44
Kh_PENN-MSHL	14	Kv_MAQU-pilot_ points	.096	Kh_PENN-MSHL	1.22	5.44
Kv_SLDV	11	Kh_C-O	.095	Kv_SLDV	.81	3.62
Kv/Kh_QRNR	7	Kh_QRNR	.095	Kv_PENN-MSHL	.76	3.39
RIV_COND	7	Kv_MAQU-zone	.092	RIV_COND	.67	3.02
Kv_PENN-MSHL	7	Kh_SLDV	.090	Kh_QRNR	.57	2.54
Kh_QRNR	6	Kh_PENN-MSHL	.087	Kv/Kh_QRNR	.56	2.49
Kv_MAQU-zone	5	Kv/Kh_QRNR	.080	Kv_MAQU-zone	.46	2.06
Ss_QRNR-PENN-MSHL-SLDV	4	Kv_SLDV	.074	Sy_QRNR-PENN-MSHL-SLDV	.13	.56
Ss_C-O	4	Ss_C-O	.055	Ss_QRNR-PENN-MSHL-SLDV	.12	.54
Sy_QRNR-PENN-MSHL-SLDV	1	Sy_C-O	.044	Recharge_1991-2005	.11	.48
Sy_C-O	1	Sy_QRNR-PENN-MSHL-SLDV	.031	Ss_C-O	.05	.25
Recharge_1991-2005	1	Ss_QRNR-PENN-MSHL-SLDV	.030	Sy_C-O	.04	.19
Total number	**243**			**Total composite sensitivity**	**22.35**	**100.00**

6. Model Results

Quantitative results from the calibrated SLMB-C model provide a portrait of the groundwater resource in the Lake Michigan Basin and its evolution through space and time. Some results provide an overview of the resource's status at the regional scale:

- Water levels and drawdown by aquifer system
- Relative strengths of sources and sinks in the groundwater budget
- Change through time of groundwater flow rates and patterns

Other indicators address questions pertinent to protecting the long-term sustainability of the water supply:

- Sources of water to shallow and deep wells
- Shifting groundwater divides between the Lake Michigan Basin and surrounding basins
- Groundwater interactions with Lake Michigan

All these model findings, based on the calibrated confined model SLMB-C, reflect the changes introduced by two time-dependent stresses: variable recharge and pumping.

6.1 Water Levels and Drawdown

The LMB model simulates water levels in QRNR and bedrock units for both the fresh and saline parts of the model domain. However, only the results for the freshwater part indicate the lateral direction of flow in each unit as a function of the water-level gradients. The interpretation of water levels and of the direction of flow in the saline part of the model is complicated by the influence of density on head elevations and head gradients (Christian Langevin, U.S. Geological Survey, oral commun., April 4, 2008). For this reason, predevelopment (pre-1864) water levels (fig. 51) are presented only where salinity is less than 10,000 mg/L, a common threshold for distinguishing freshwater from saline water. The predevelopment water table is shown regardless of the layer it occupies (fig. 51*A*), although typically the water table is at the top of the hydrogeologic system in the QRNR aquifer system, in model layer 1. Other plots show predevelopment water levels for layers within each bedrock aquifer system: the PENN system is represented by layer 5 (fig. 51*B*), the MSHL system by layer 8 (fig. 51*C*), the SLDV system by layer 10 (fig. 51*D*), and the C-O by the IRGA unit in layer 17 (fig. 51*E*).

The configuration of the predevelopment water table tends to be a subdued reflection of the land surface (as can be seen by comparing fig. 51*A* to fig. 6). The presence of major discharge areas is evident along river valleys, where the water table occurs at low elevations. Predevelopment water levels in bedrock units also reflect land-surface topography. However, it is possible to detect vertical head differences within the groundwater flow system that influence flow. For example, comparison of the simulated water table (fig. 51*A*) to simulated head conditions in the C-O (fig. 51*E*) indicates that deep water levels, which are lower than shallow water level in the western parts of NE_WI, SE_WI, and NE_ILL, become higher than shallow levels in the vicinity of Lake Michigan. This pattern defines a regional flow system characterized by recharge areas to the west (where water leaks to deep layers) neighboring discharge areas to the east (where water eventually circulates back upward and flows toward Lake Michigan). The first wells installed in the Cambrian-Ordovician rocks around Chicago and Milwaukee encountered artesian (flowing) conditions, with water levels in the deep confined aquifer registering more than 100 ft above land surface in some locations (Weidman and Schultz, 1915). The model reproduces this condition for the predevelopment stress period and suggests that artesian conditions continued in the early postdevelopment stress periods at the beginning of the 20th century.

Pumping has perturbed parts of the predevelopment regional flow system. Simulated drawdown at the water table is hardly detectable for any stress period, largely because the proximity of surface water restricts the effects of wells to a radius smaller than the 5,000-ft spacing of the regional grid. In bedrock layers and particularly in confined parts of the flow system, however, drawdown is substantial in both freshwater and saline areas.[27] Inspection of the simulated head change between predevelopment and 2005 along four east-west cross sections (fig. 52) demonstrates the regional extent of the drawdown cones. Sections along rows 260 (fig. 52*C*) and 350 (fig. 52*D*) show clearly that well withdrawals from centers west of Lake Michigan influence simulated conditions under Lake Michigan and to the east.

The pumping centers east of Lake Michigan caused much less drawdown than the centers to the west of the lake. Both the extent and depth of drawdowns attributable to pumping in the MSHL aquifer system (figs. 53*A*–*C*; scale from 1 to 100 ft of drawdown) are smaller than those attributable to pumping in the C-O aquifer system (figs. 54*A*–*C*; scale from 10 to 1,000 ft of drawdown).

[27] The representation of drawdown, as opposed to water levels, is not affected by variable density. It is therefore useful to map the drawdown results continuously from pumping centers through areas of brackish groundwater as far as the brines within the Michigan Basin.

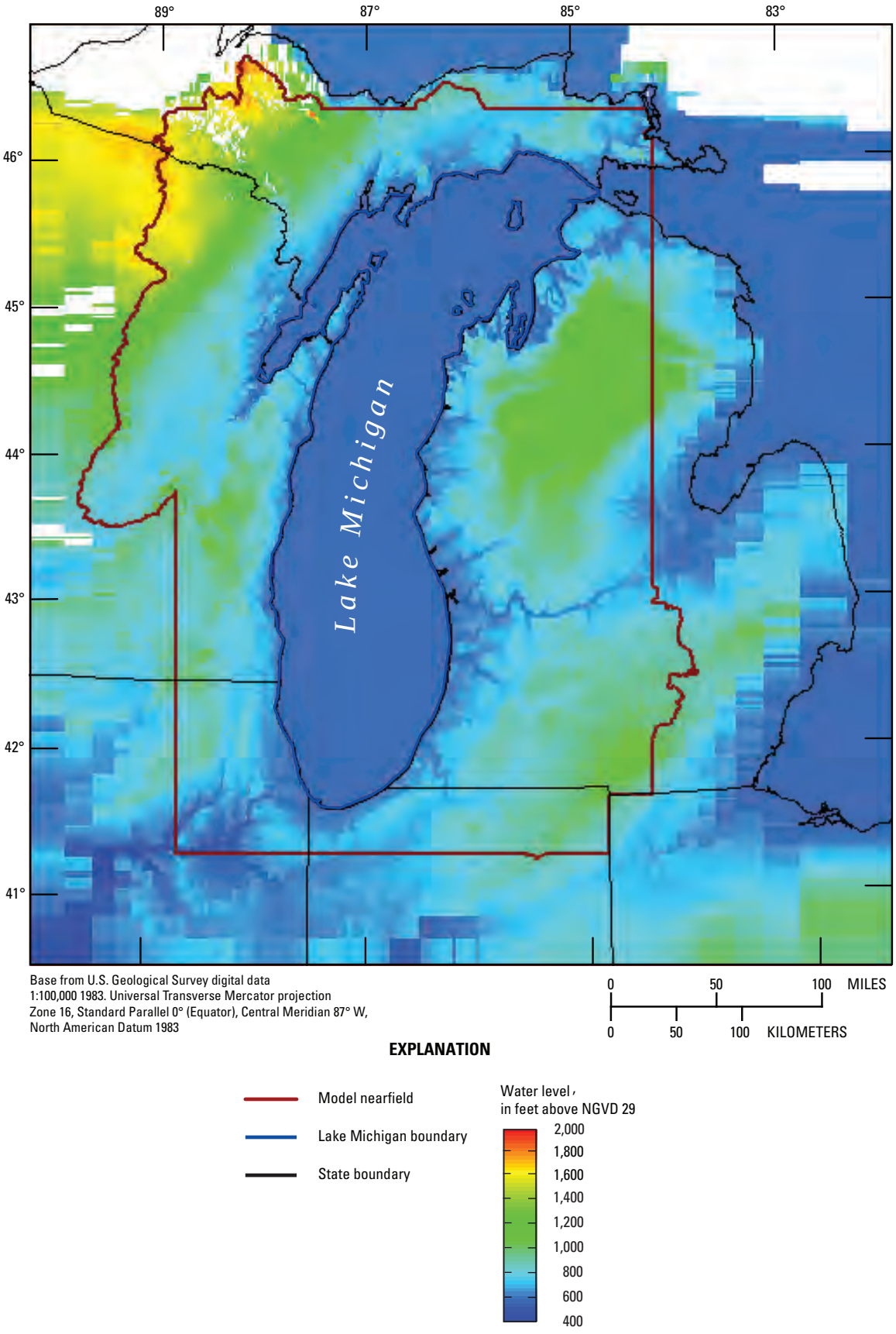

Figure 51*A*. Simulated predevelopment water levels for QRNR aquifer system.

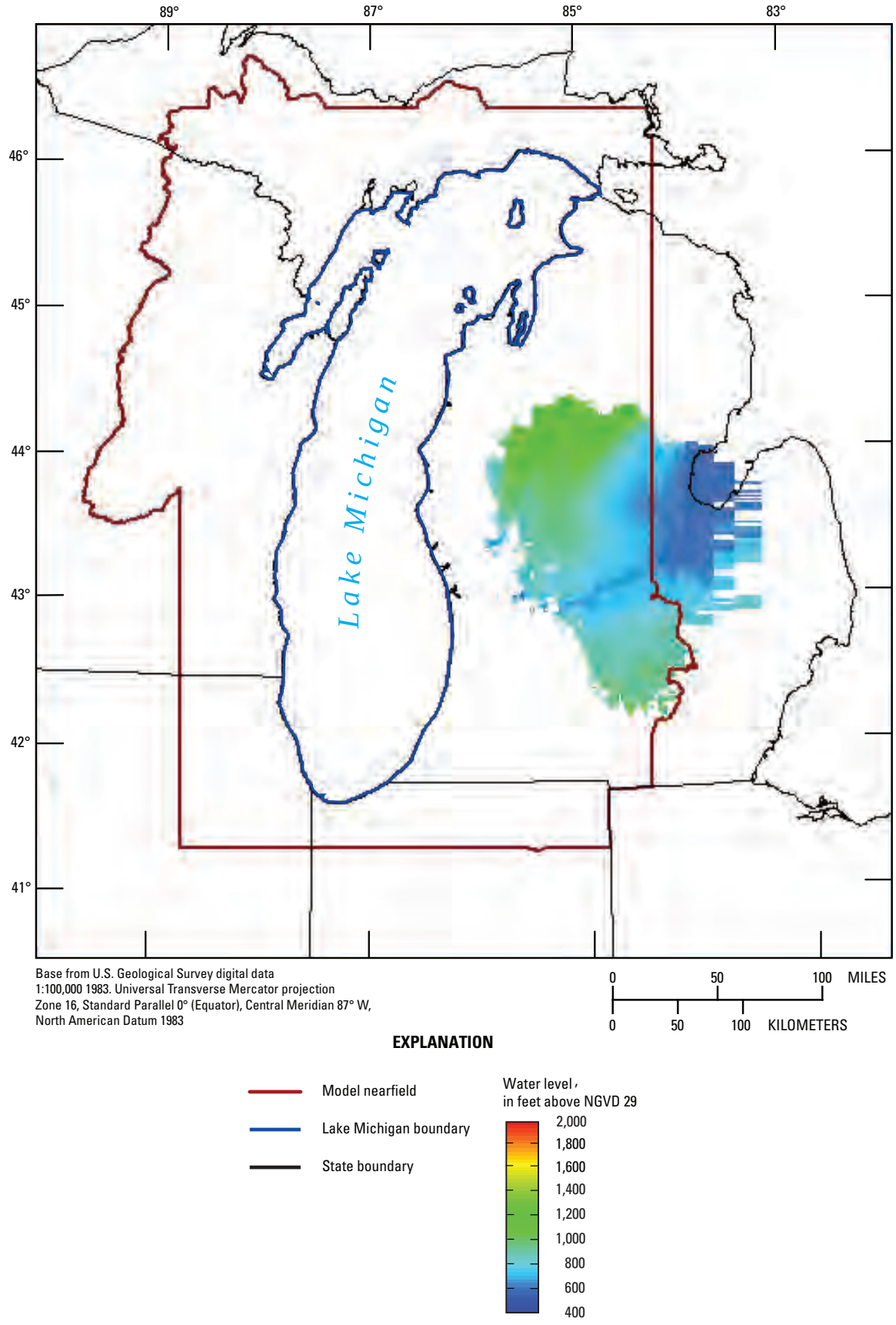

Figure 51*B*. Simulated predevelopment water levels for PENN aquifer system.

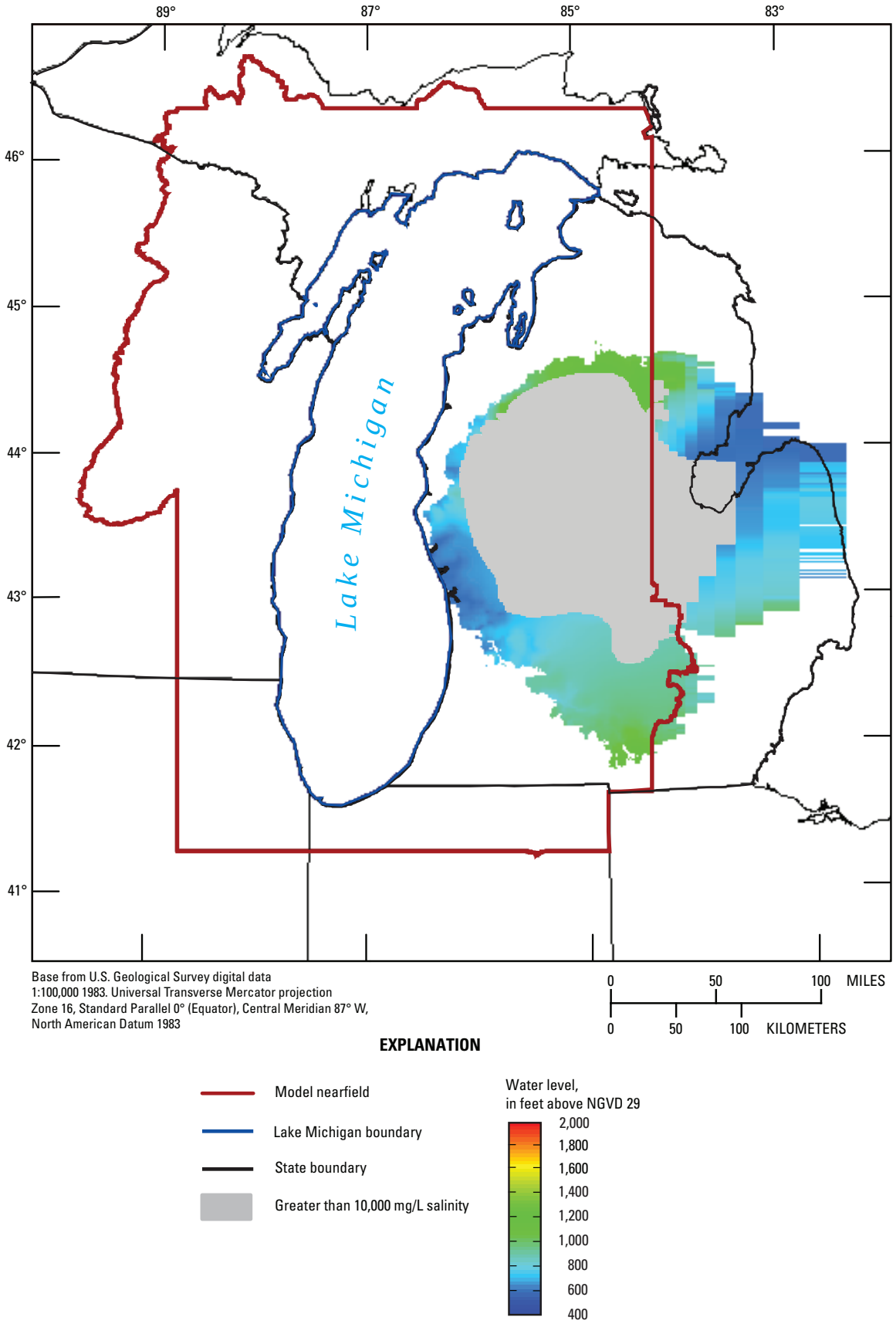

Figure 51*C*. Simulated predevelopment water levels for MSHL aquifer system.

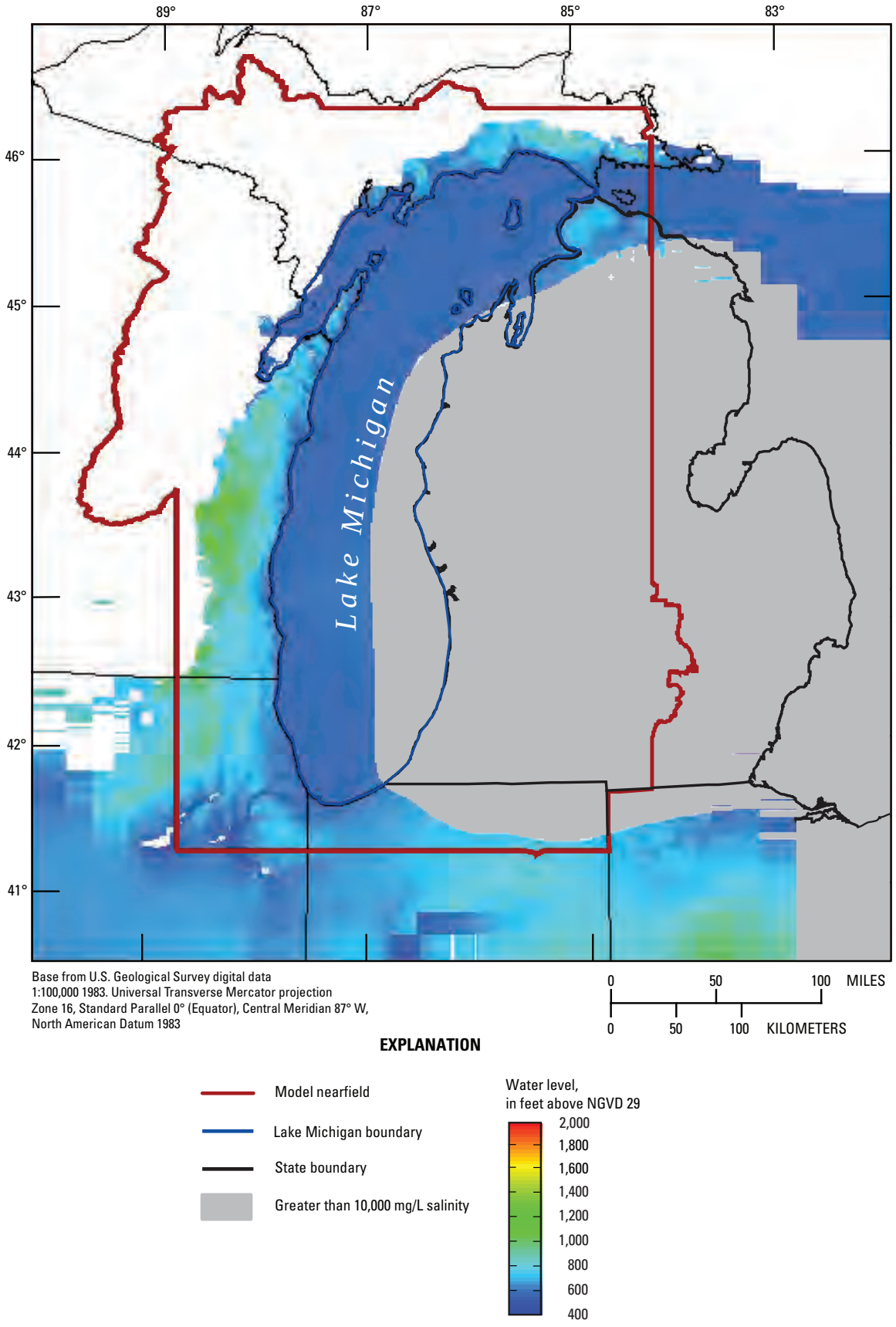

Figure 51*D*. Simulated predevelopment water levels for SLDV aquifer system.

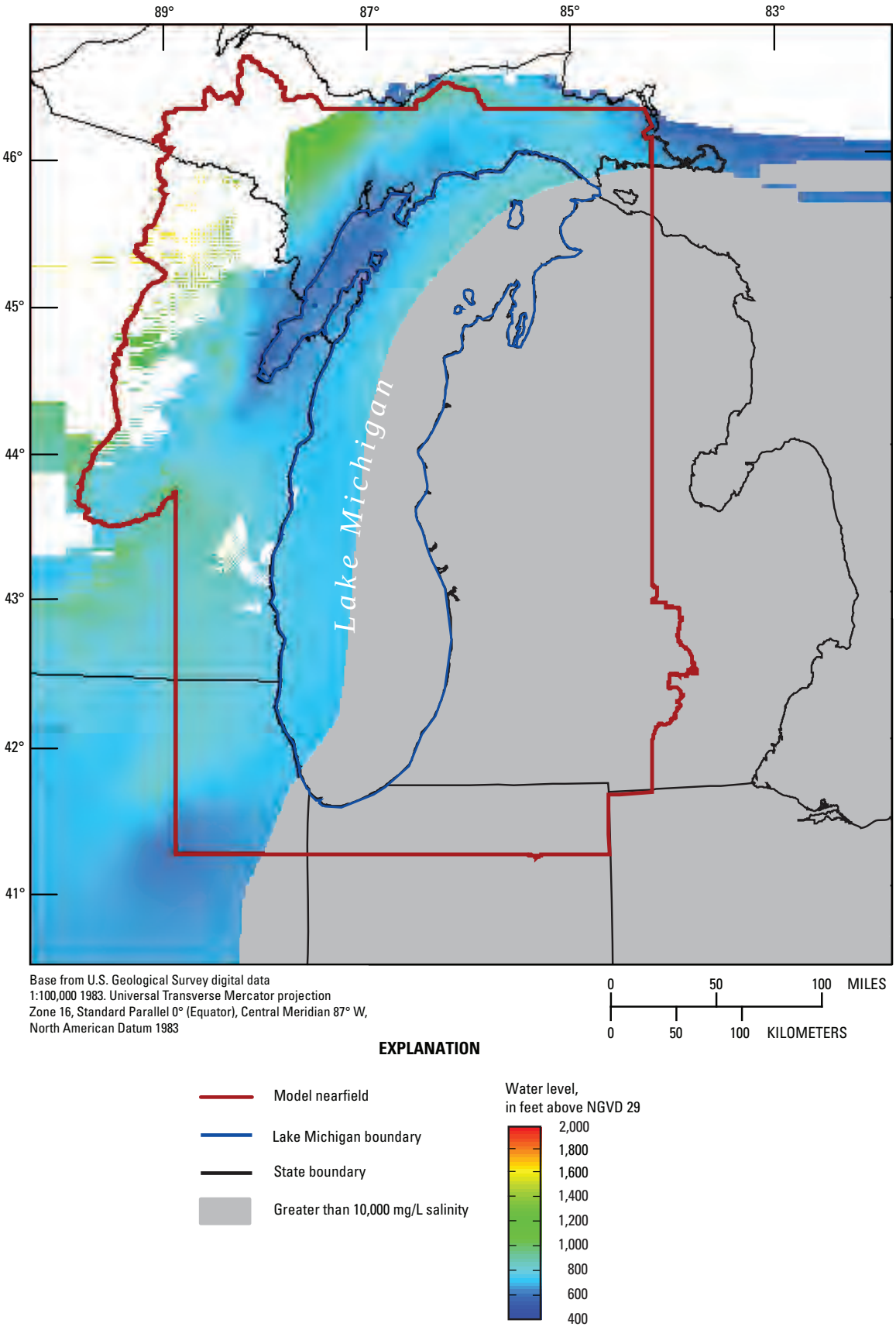

Figure 51*E*. Simulated predevelopment water levels for C-O aquifer system.

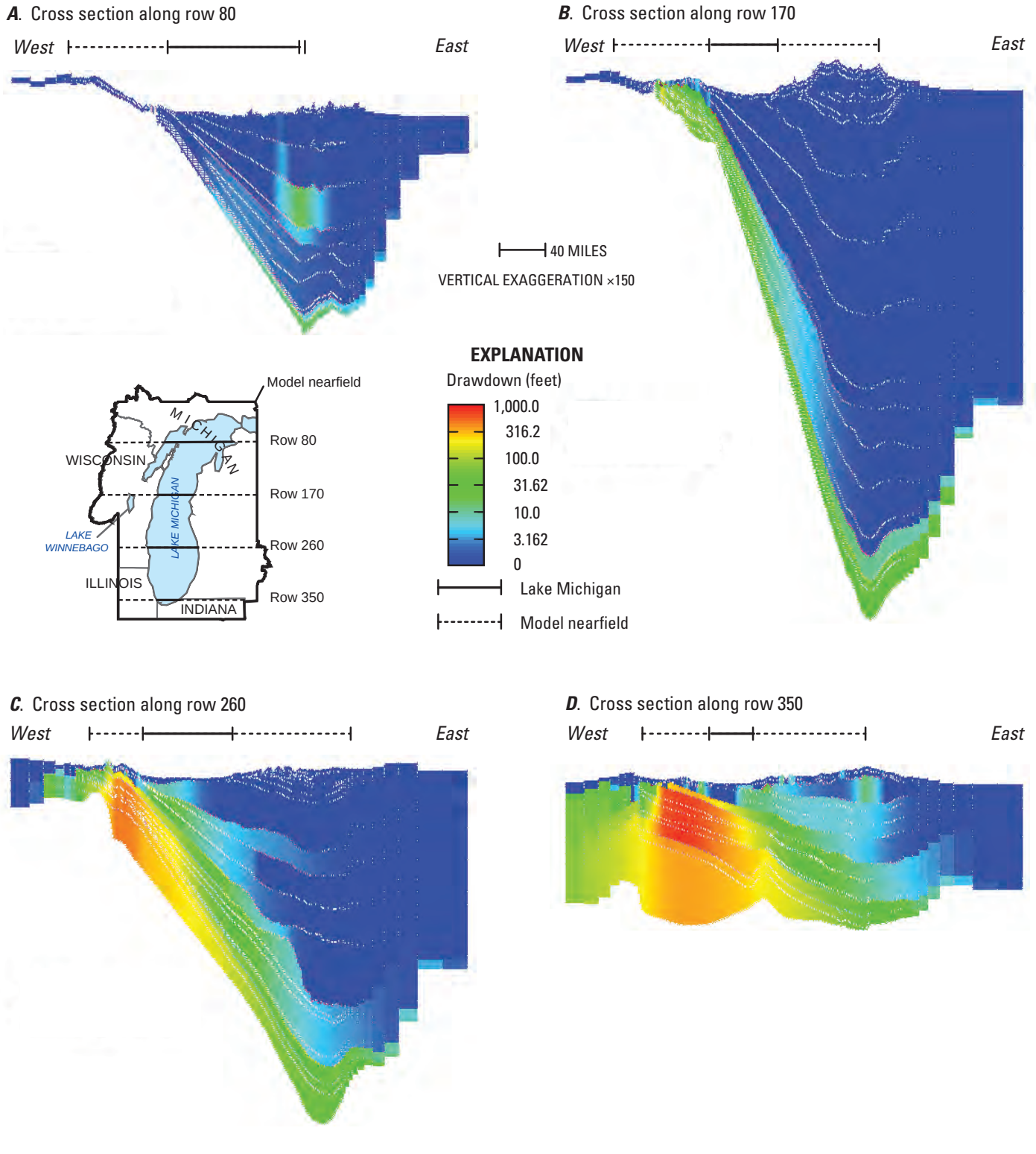

Figure 52. Simulated drawdown in 2005 along selected west/east cross sections.

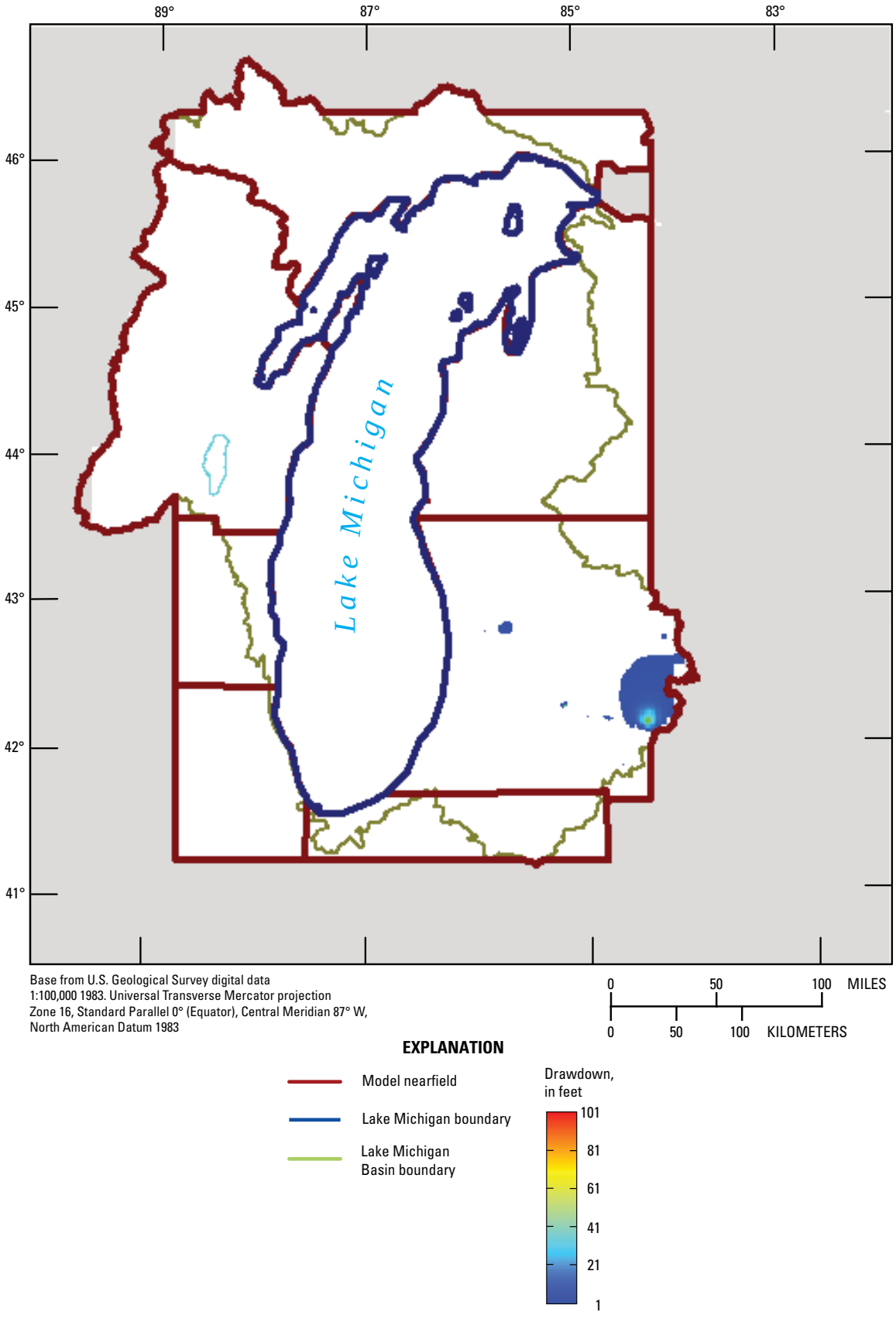

Figure 53*A*. Simulated drawdown in Marshall aquifer, 1950.

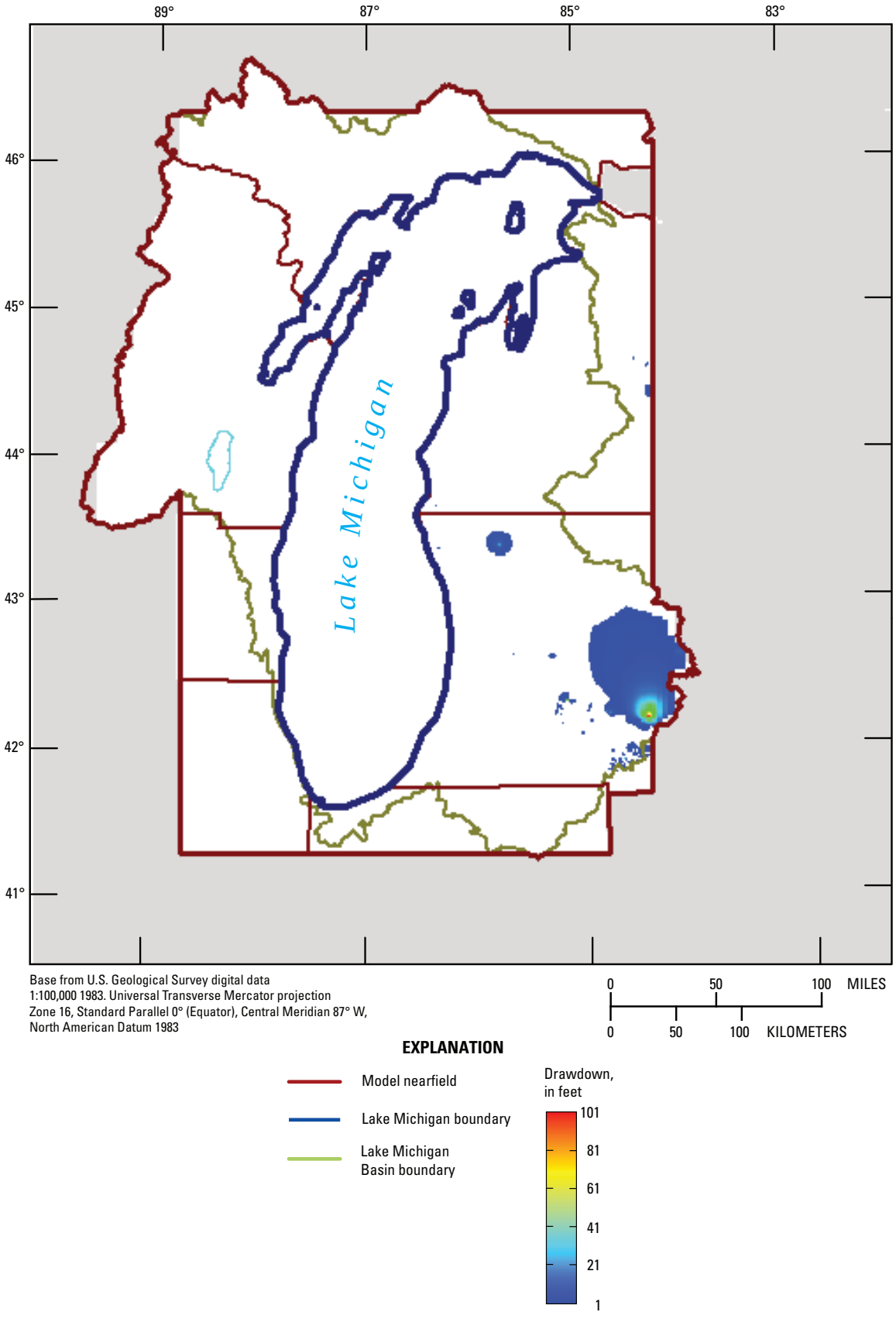

Figure 53*B*. Simulated drawdown in Marshall aquifer, 1980.

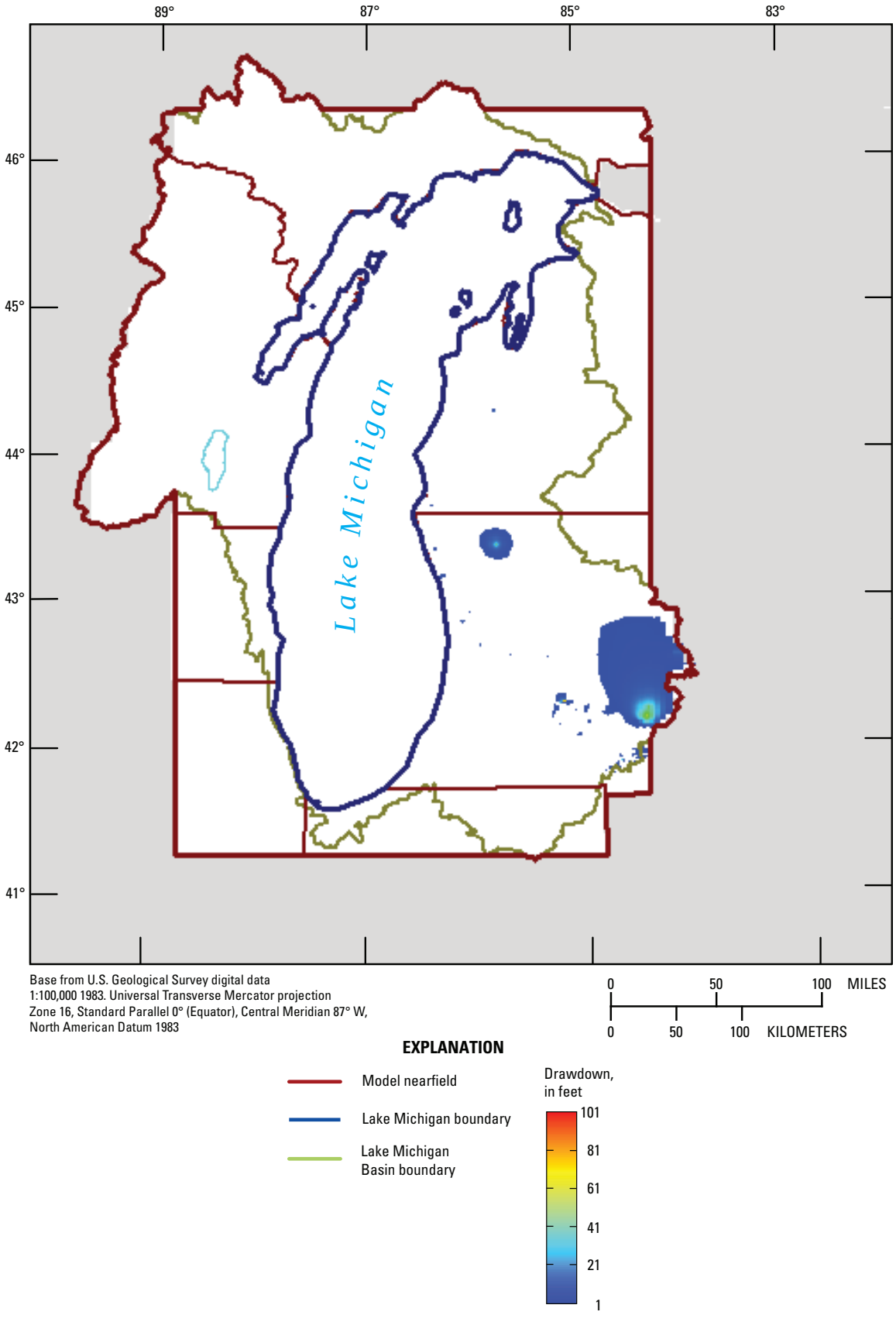

Figure 53*C*. Simulated drawdown in Marshall aquifer, 2005.

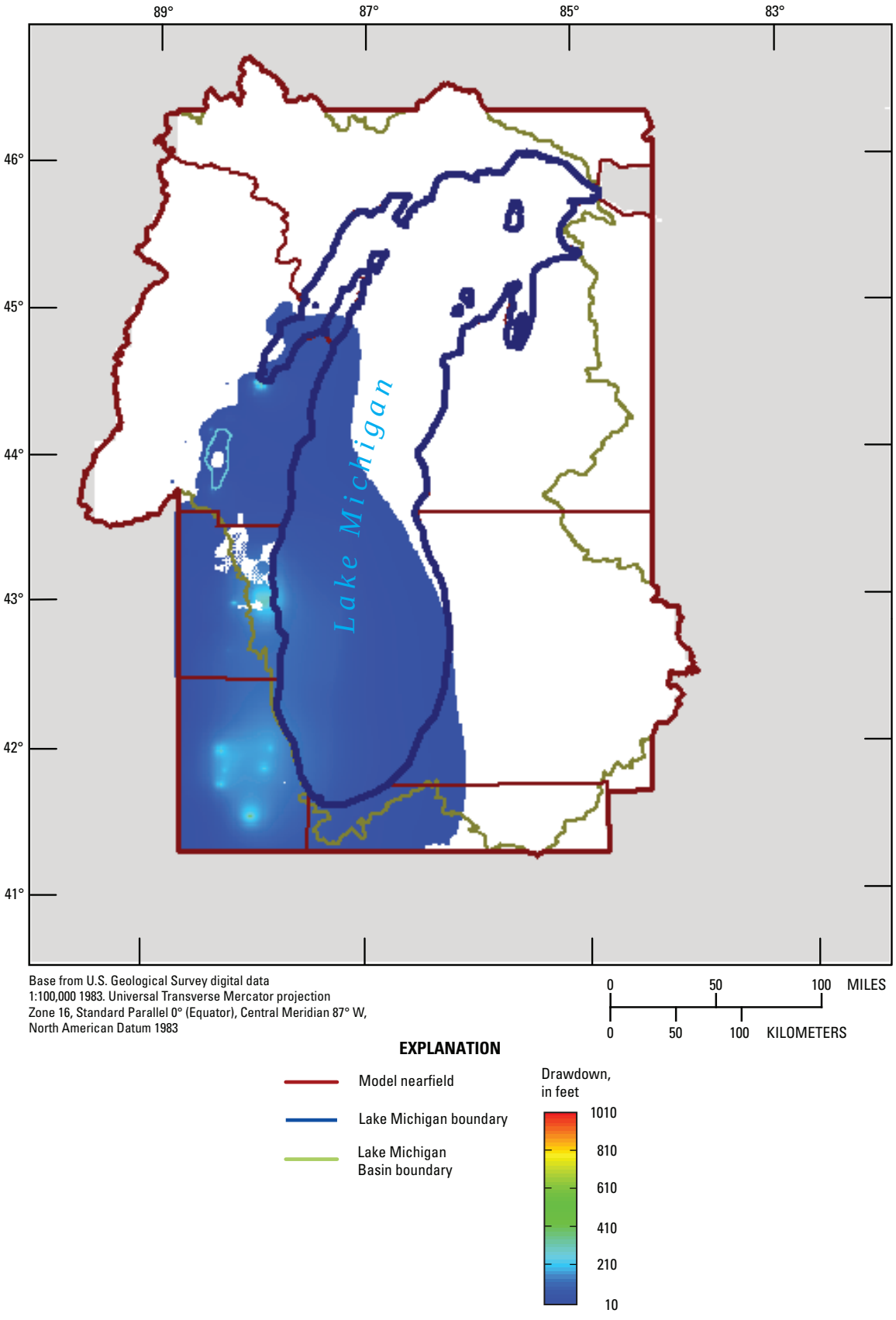

Figure 54*A*. Simulated drawdown in Ironton-Galesville aquifer, 1950.

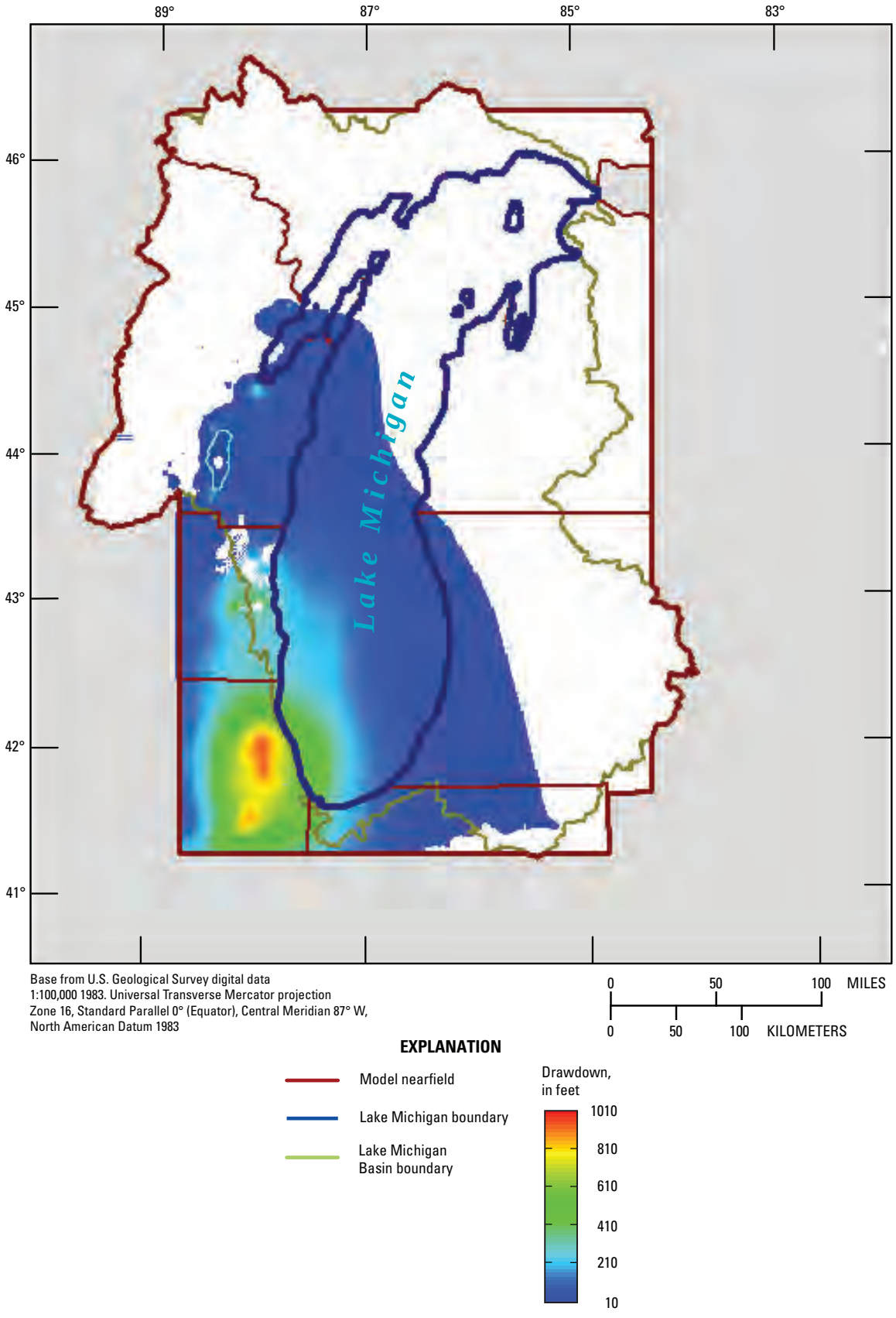

Figure 54*B*. Simulated drawdown in Ironton-Galesville aquifer, 1980.

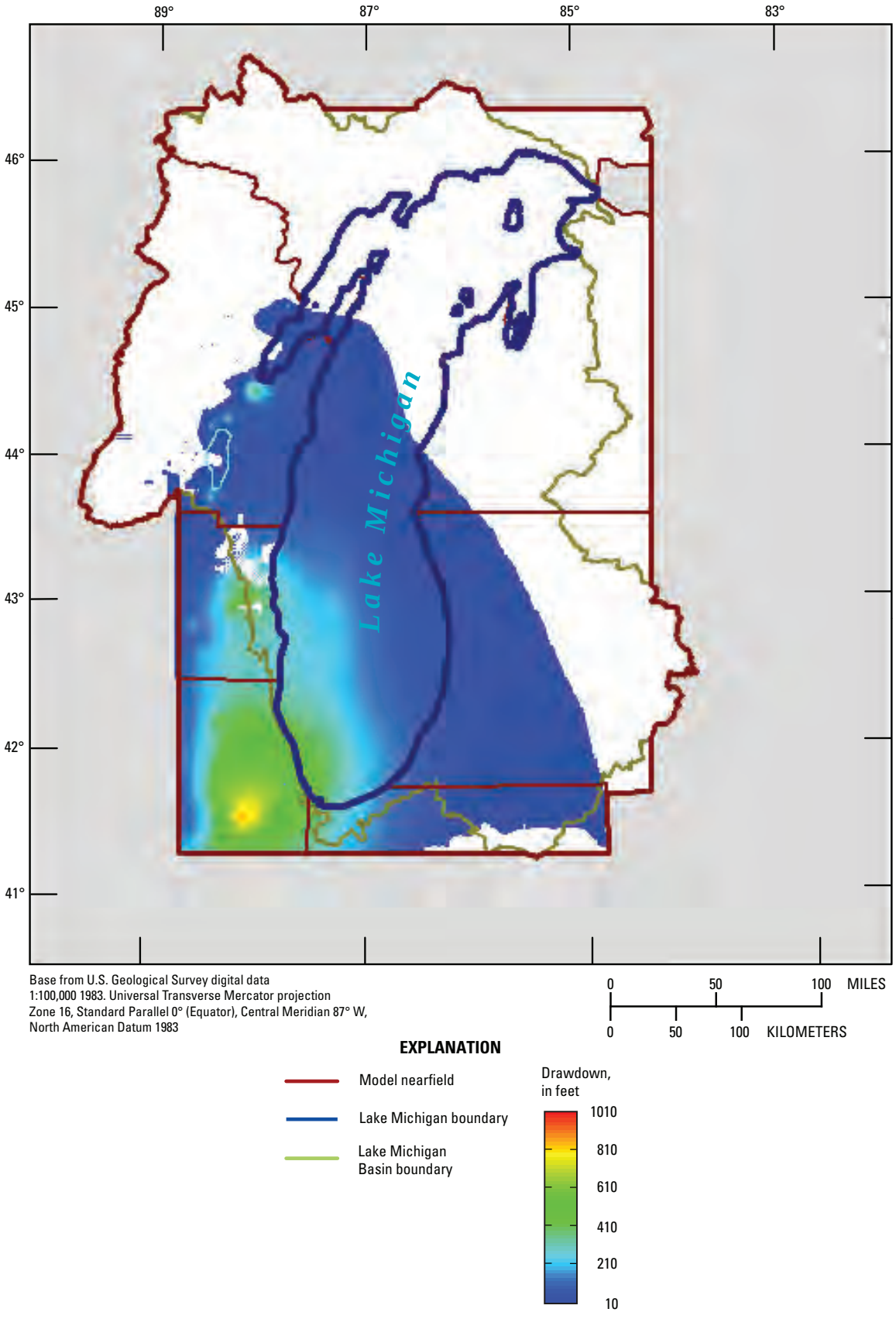

Figure 54*C*. Simulated drawdown in Ironton-Galesville aquifer, 2005.

The trends through time also can be seen by examining hydrographs of water levels at major pumping centers that draw from the MSHL and C-O aquifer systems (fig. 55). The hydrographs indicate that, for each pumping center, periods of both drawdown and recovery are evident and reflect shifting demand and changing sources of water supply. Drawdown in the MSHL system is associated with a major pumping center in the Lower Peninsula of Michigan; after 1960 water levels in this area stabilized or slightly recovered (fig. 55*B*). In the C-O system, three major pumping centers west of the lake are evident; their patterns of drawdown each evolved differently over the postdevelopment period. Pumping in NE_WI increased modestly after 1950—and drawdowns decreased after the city of Green Bay's switch to Lake Michigan surface water in 1957 (fig. 55*B*). Pumping in SE_WI increased rapidly between 1950 and 1980. Drawdowns continued to expand after 1980, but decrease in industrial pumping in the late 1990s and early 2000s slowed declines and sometimes resulted in water-level recovery. The pumping center in NE_ILL is the biggest in the model domain. Even though the wells are outside the Lake Michigan Basin, the influence of pumping continues to extend far into the basin. The maximum drawdown (on the order of 1,000 ft, as simulated for the IRGA aquifer) occurred in the early 1980s before Chicago and surrounding areas switched to Lake Michigan for water supply. By that time the drawdown areas for the C-O aquifer system in SE_WI and NE_ILL had coalesced. At the center of the area affected by drawdown in Illinois, several hundred feet of recovery relative to 1980 remained in 2005, although the rate of recovery peaked earlier than 2005 and, in some areas of NE_ILL, the trend at the end of the model simulation was again toward drawdown.

6.2 Lake Michigan Basin Water Budget

The calibrated model provides quantitative estimates of the sources and sinks in the water budget over the period 1864 through 2005. For the part of the model domain defined by the topographic boundaries of the Lake Michigan Basin, it is convenient to divide the water budget derived from the SLMB-C model into five source terms—

- recharge to the water table
- infiltration from inland surface water
- infiltration from Lake Michigan to groundwater
- release from storage due to declining water levels
- net lateral groundwater flow into the basin

and five sink terms—

- groundwater discharge to streams
- groundwater discharge to inland lakes and wetlands
- groundwater discharge directly to Lake Michigan
- gain to storage due to rising water levels
- well withdrawals

Although groundwater flows laterally both into and out of the Lake Michigan Basin, the simplified budget includes only the net flow into the basin. Similarly, it is possible for groundwater to flow inland from Lake Michigan itself, especially in the presence of pumping, so that the sink term for direct discharge to the lake is net of any inflow. Infiltration from surface water to groundwater is summed as one source term, but the discharge of groundwater to surface water is distributed among three sink terms. Finally, conditions before 1864 are simulated as steady-state conditions, so change in storage is excluded as a source or sink term and no pumping wells are active for the initial predevelopment stress period.

Most of the water-budget changes registered by the LMB model over time (fig. 56) reflect fluctuations in recharge, the major source term; and discharge to streams, the major sink term. The Lake Michigan Basin groundwater system still retains the imprint of predevelopment ("natural") conditions, despite large pumping centers and large shifts in groundwater flow patterns (see below). Withdrawals and storage changes within the basin are relatively small elements in the budget. Release from storage in the Lake Michigan Basin in 2005 (caused by reductions in recharge and by pumping) amounted to 71 Mgal/d, whereas recharge to the basin was about 16,000 Mgal/d or about 230 times that amount (fig. 57*C*). Withdrawals in the basin for 2005 amounted to 580 Mgal/d, whereas the groundwater discharge to surface-water features totaled 18,720 Mgal/d, 32 times that amount (fig. 57*D*). The model indicates that shallow and deep pumping in the Lake Michigan Basin accounted for 3.0 percent of the total discharge (19,313 Mgal/d) from the basin in 2005.

Another way to contrast the magnitude of selected fluxes in the water budget is to tabulate recharge over the Lake Michigan Basin through time and juxtapose these values with the amount of direct discharge to Lake Michigan and the amount of pumping from the basin for the same periods (table 14). Although pumping has increased over this period, it remains a small fraction of inflow from recharge. Discharge to Lake Michigan is more closely related to recharge fluctuations than to trends in pumping.

Although increased pumping over a time period acts to reduce base flow to streams, increased recharge for the same time period can counter the effect of pumping and yield a net increase in base flow. For example, comparison of sources and sinks for predevelopment (fig. 57*A, B*) to the year 2005 (fig. 57*C, D*) fails to show the regional effect of historical pumping as reduced base flow because the general increase of recharge over the same period yields a general increase of simulated base flow to streams and lakes. This increase dominates the regional water budget and masks the decreased flux to local surface-water bodies due to diversion of groundwater discharge to particular pumping centers. In light of the competing effects of time-dependent recharge and pumping, a special analysis is needed to isolate the effect of wells on the natural groundwater flow to Lake Michigan, streams, and inland lakes (see next section).

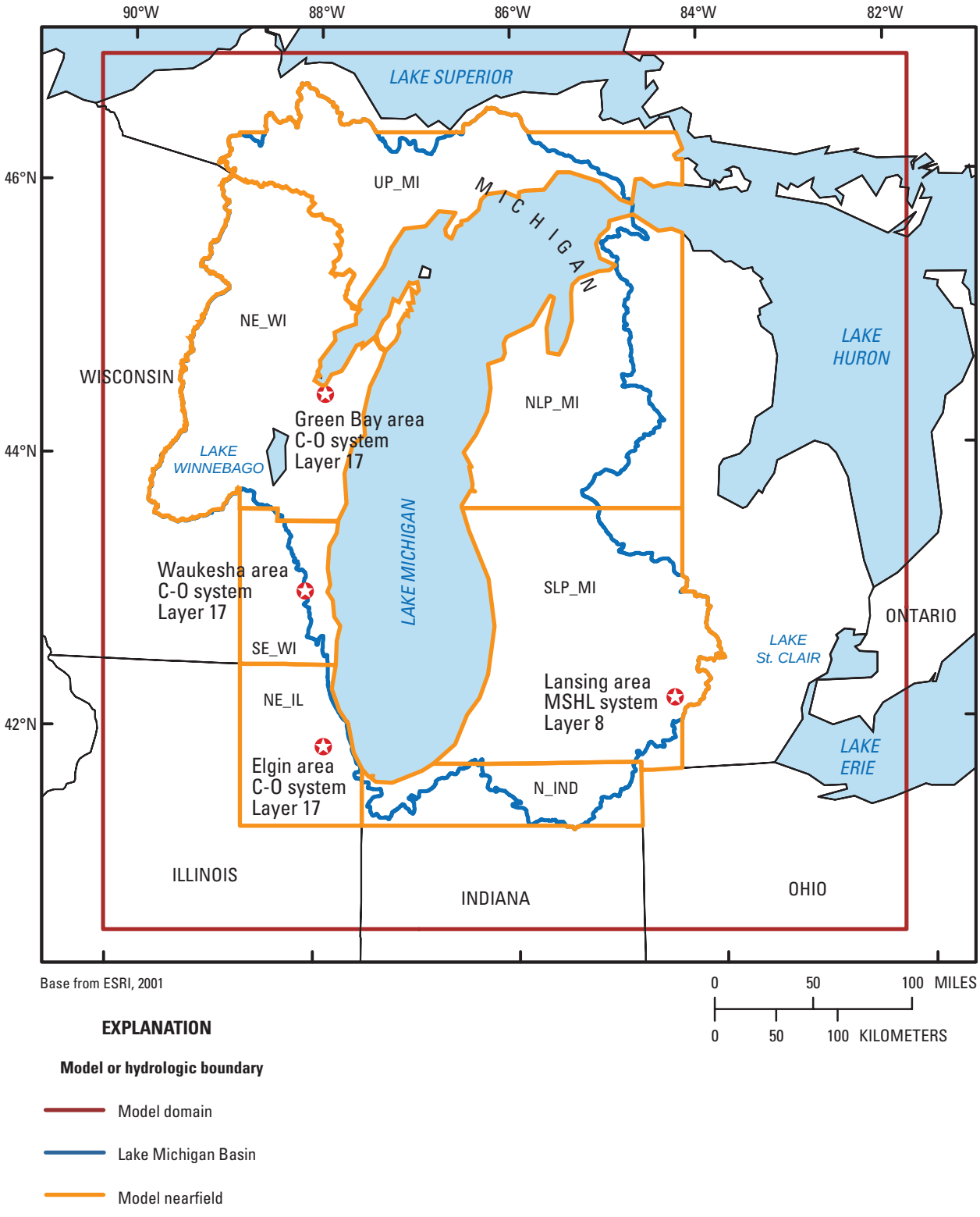

Figure 55*A*. Selected pumping centers.

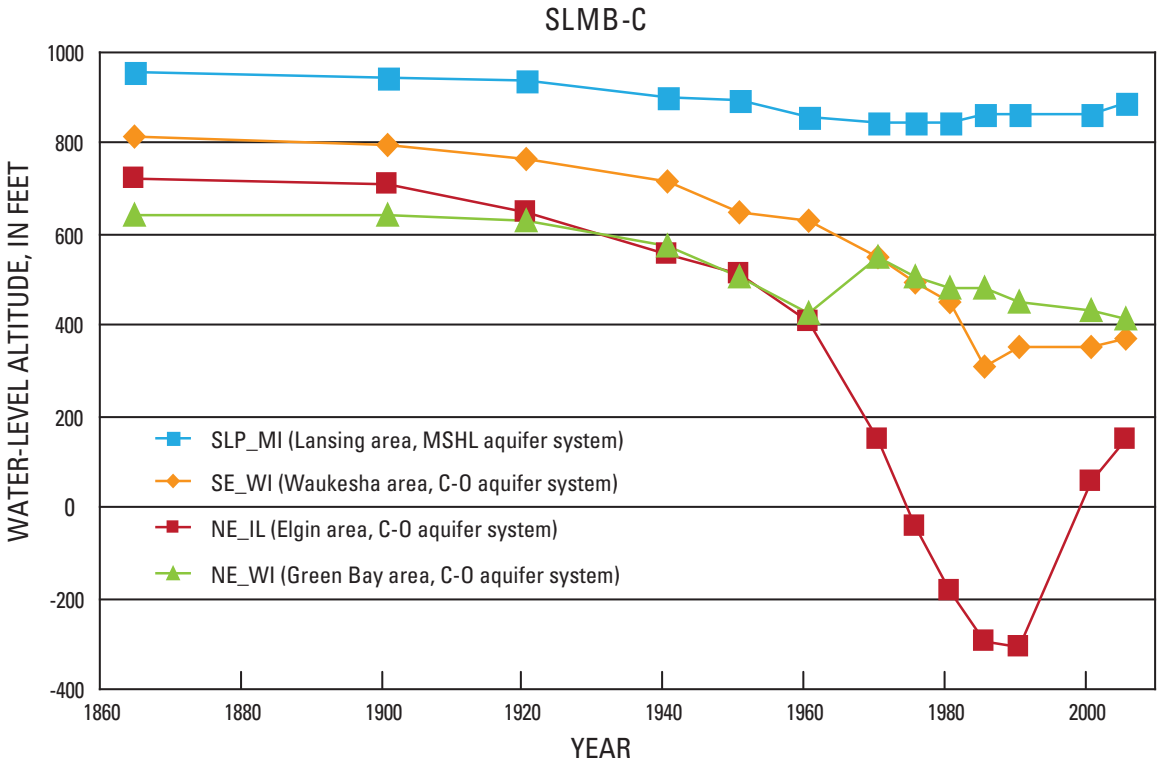

Figure 55*B*. Simulated water-level hydrographs at selected pumping centers.

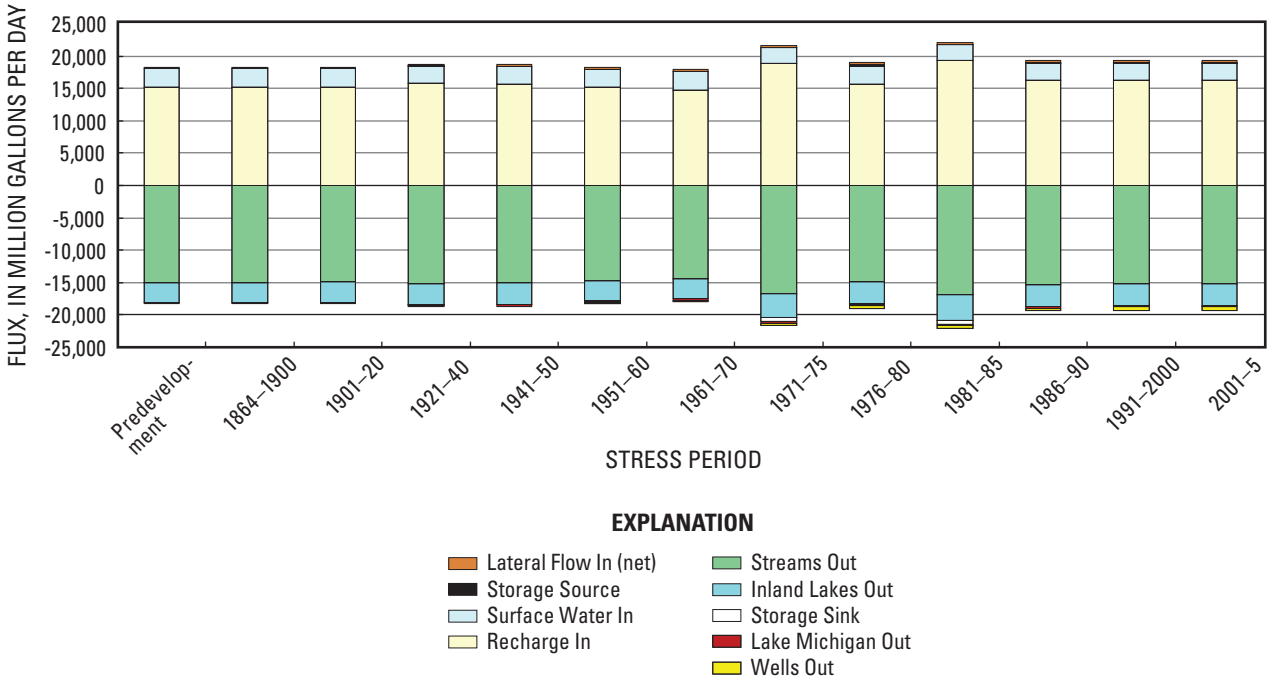

Figure 56. Simulated groundwater budget, by stress period, for Lake Michigan Basin.

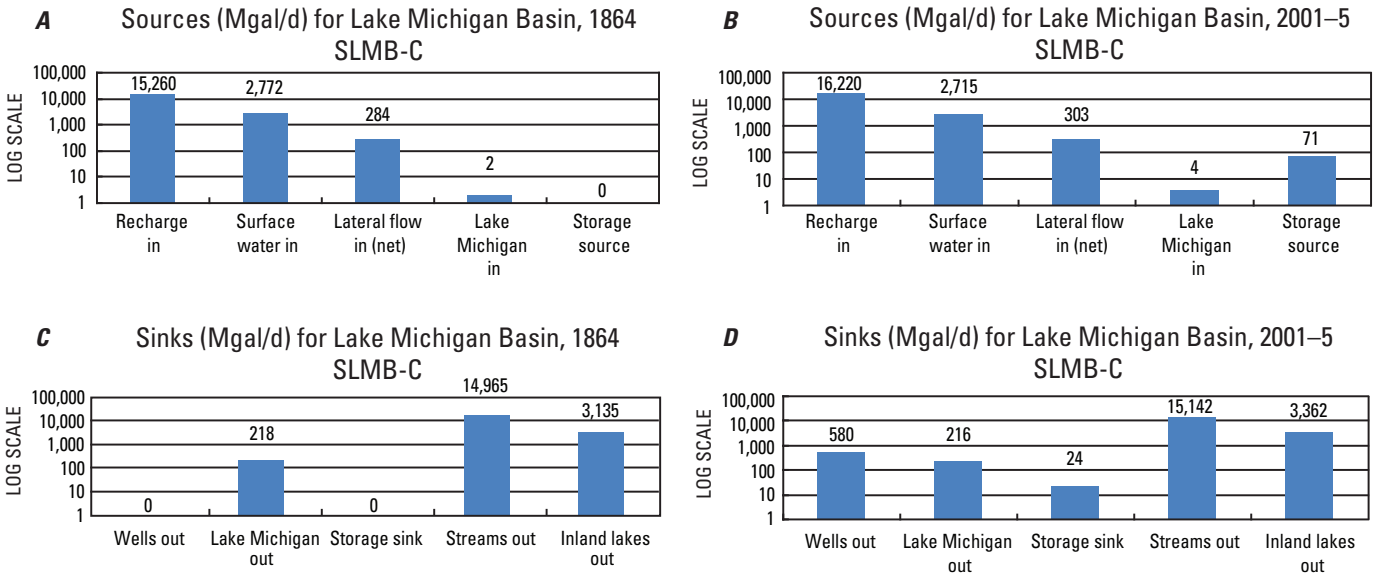

Figure 57. Simulated groundwater sources and sinks in Lake Michgan Basin for predevelopment (1864) and 2001–5 periods.

Table 14. Relative magnitude of recharge, simulated direct discharge to Lake Michigan, and withdrawals by pumping, predevelopment through 2005.

[Values correspond to the confined model, SLMB-C; Mgal/d, million gallons per day]

Stress period	Date	Recharge to Lake Michigan Basin (Mgal/d)	Direct groundwater discharge to Lake Michigan[1] (Mgal/d)	Net pumping in Lake Michigan Basin (net of injection)[2] (Mgal/d)
1	Predevelopment	15,261.15	217.90	0
2	Oct. 1864–Oct. 1900	15,261.15	217.86	8.41
3	Oct. 1900–Oct. 1920	15,261.15	217.28	19.96
4	Oct. 1920–Oct. 1940	15,769.50	223.63	55.38
5	Oct. 1940–Oct. 1950	15,687.74	222.05	118.82
6	Oct. 1950–Oct. 1960	15,131.87	220.82	187.30
7	Oct. 1960–Oct. 1970	14,781.80	219.93	272.29
8	Oct. 1970–Oct. 1975	18,807.74	223.56	317.54
9	Oct. 1975–Oct. 1980	15,639.94	221.64	368.19
10	Oct. 1980–Oct. 1985	19,349.68	224.54	423.60
11	Oct. 1985–Oct. 1990	16,199.12	221.89	435.77
12	Oct. 1990–Oct. 2000	16,221.24	215.93	576.00
13	Oct. 2000–Oct. 2005	16,221.24	215.66	569.52

[1]Lake Michigan is represented by GHB nodes in the model. The flow to the GHB nodes represents the direct discharge to the lake (that is, groundwater flow that discharges directly to the lake rather than indirectly through surface-water bodies that are tributary to the lake) .

[2]Net pumping is pumping minus injection inside the Lake Michigan topographic basin. The model simulates injection at only one cluster of locations (near Kalamazoo), where it amounts to about 10 Mgal/d for 2005.

6.3 Groundwater Flow Rates and Patterns

Simulation of changing water levels and evaluation of regional sources and sinks are two ways to analyze the status of groundwater in and around Lake Michigan. The calibrated model affords a third set of indicators through the depiction and analysis of the magnitude and direction of subsurface flow. Insight into the changing nature of the regional resource is gained by examining flow rates as a function of space and time, by mapping the changing pattern of vertical exchange between shallow and deep parts of the flow system, and by tracking the regional effect of pumping centers on flow rates and directions.

Circulation within this groundwater system is typically most vigorous in shallow unconsolidated deposits. In the model nearfield, the flow rate in the upper 100 ft of the QRNR deposits varies almost everywhere between 0.001 and 1.0 ft/d (fig. 58).[28] The rate of flow is highest where sediments are coarse and where recharge is high; for example, in parts of the northern Lower Peninsula in Michigan. The flow rate is much lower, for example, near the shoreline of Lake Michigan in Wisconsin and northeastern Illinois, areas dominated by clayey tills and fine stratified deposits. In deep bedrock units, flow rates range from 1.0 E−5 to 1.0 E−3 ft/d because the hydraulic gradients are less, and only part of the recharge to the water table reaches the deeper aquifers (fig. 59*A*–*D*). Lower flow rates, on the order of 1.0 E−6 ft/d, are simulated for the low-permeability confining units that span parts of the Wisconsin Arch and Michigan Basin.

Much information on the flow pattern can be obtained by mapping the proportion of the total subsurface flow through each aquifer system. First for consideration is the distribution of lateral flow under predevelopment conditions (blue bars in fig. 60). The pattern is very different on the east side of Lake Michigan (fig. 60*A*) as opposed to the west (fig. 60*B*). To the east, the QRNR aquifer system is the dominant conveyor of groundwater; in the N_IND subregion, for example, 92 percent of the predevelopment flow (according to the model) passes through unconsolidated deposits. Secondary in importance from the standpoint of lateral flow are the SLDV system in the NLP_MI subregion and the MSHL system in the SLP_MI subregion. To the west, the QRNR aquifer system shares flow with the SLDV and C-O systems. The simulated lateral flow in the unconsolidated deposits averages just over 50 percent of the total predevelopment flow, ranging from 39 percent in the UP_MI to 60 percent in SE_WI. The remainder is shared fairly evenly between the mostly dolomite rocks in the SLDV system and the mostly sandstone rocks in the C-O system. The introduction of pumping changes the mix. Shallow pumping increases the share in the QRNR layers for the Lower Peninsula of Michigan from an average of 61 to 72 percent of total flow. West of the lake, the redistribution is more complicated. In the UP_MI, NE_WI, and SE_WI subregions, shallow 2005 pumping increases the relative proportion of QRNR flow relative to predevelopment conditions, but in NE_ILL deep pumping routes an increased proportion of flow through bedrock units. Although the SLDV aquifer system is an important source of well withdrawals, competing withdrawals from above (QRNR system) and below (C-O system) reduce its relative share with respect to predevelopment in all four subregions west of the lake. There is a striking increase in the proportion of lateral flow through the C-O aquifer system for 2005 in SE_WI and, especially, in NE_ILL; there, despite the availability of Lake Michigan water for supply, the C-O system under the influence of pumping transmits half the total lateral flow.

Much model information that bears on how flow patterns change through time can be gleaned by comparing the vertical flow between the shallow and deep parts of the flow system before and after the installation of high-capacity wells. As defined previously in this report, the deep part of the flow system is all aquifer systems that fall below the first major confining unit at depth at any location. A map of the uppermost deep aquifer system in the model nearfield (fig. 61) indicates that the PENN and MSHL systems constitute the top of the deep part of the flow system in the center of the Michigan Basin (confined by the JURA, PEN2, and/or MICH confining units) whereas the SLDV is the uppermost system along the flanks of the Michigan Basin in the Lower Peninsula of Michigan, in northern Indiana, and under parts of Lake Michigan (beneath the DVMS confining unit). The deep flow system is restricted to the C-O aquifer under parts of Lake Michigan and over most of the model nearfield west of the lake (beneath the MAQU and SNNP confining units), whereas the entire groundwater flow system is unconfined in the northwestern corner of the nearfield because confining units are absent.

[28] In this report the term "flow rate" refers to the so-called Darcy flow, defined as the volumetric flux per unit area in the direction of flow ($ft^3/d/ft^2$ or ft/d). A related term is the "advective velocity," which equals the flow rate divided by the effective porosity of the sediments. The flow rate indicates where the amount of groundwater flow is relatively high or low, whereas the advective velocity term is used to compute traveltimes along flow paths. The "lateral flow" for a layer, unit, or aquifer system at a row/column locaton is computed as the Darcy flow moving horizontally across the right and front sides of cell faces, plus the difference between what enters and what exits vertically through the top and bottom of the cell(s).

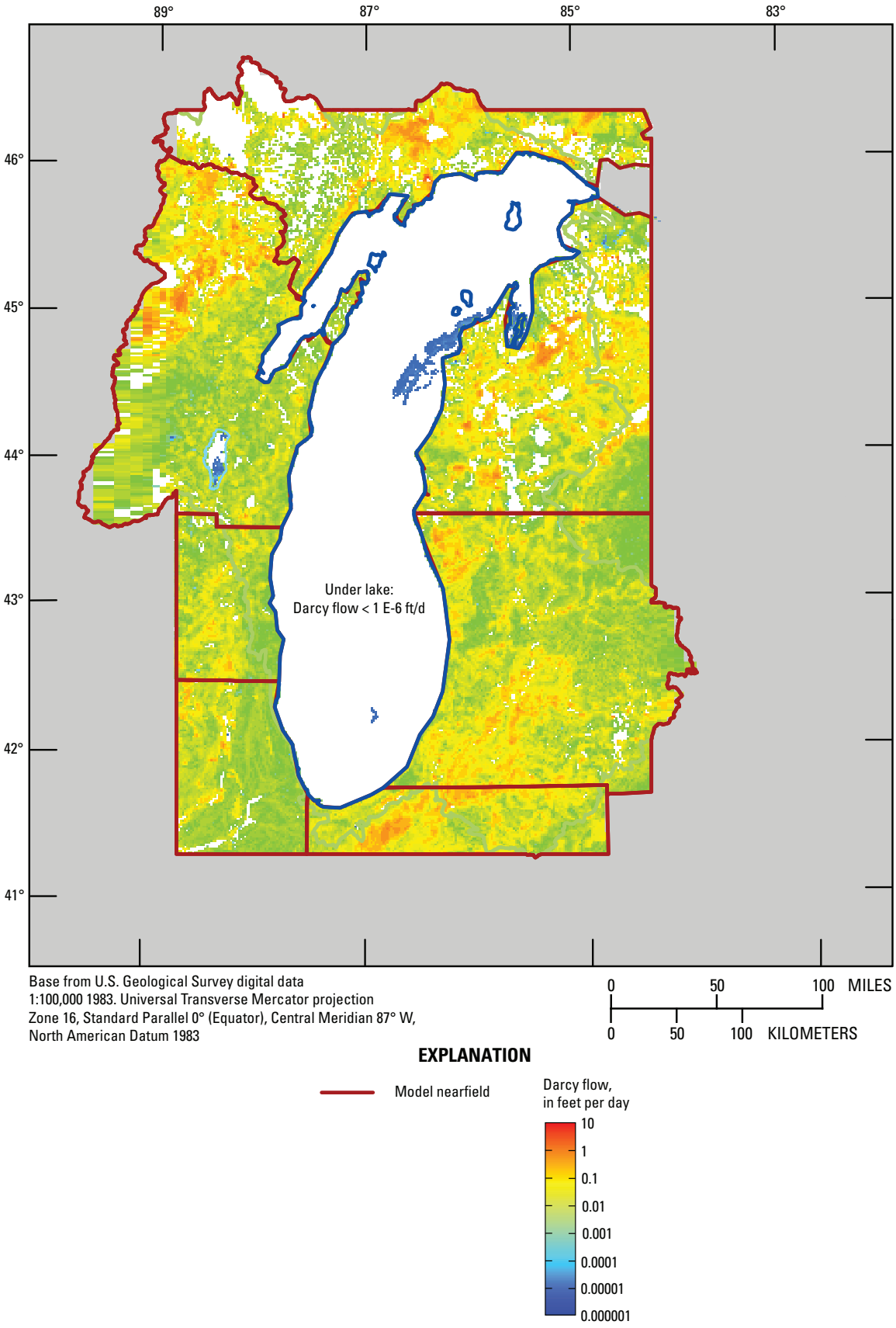

Figure 58. Simulated flow rate (Darcy flow) in model layer 1 for predevelopment conditions.

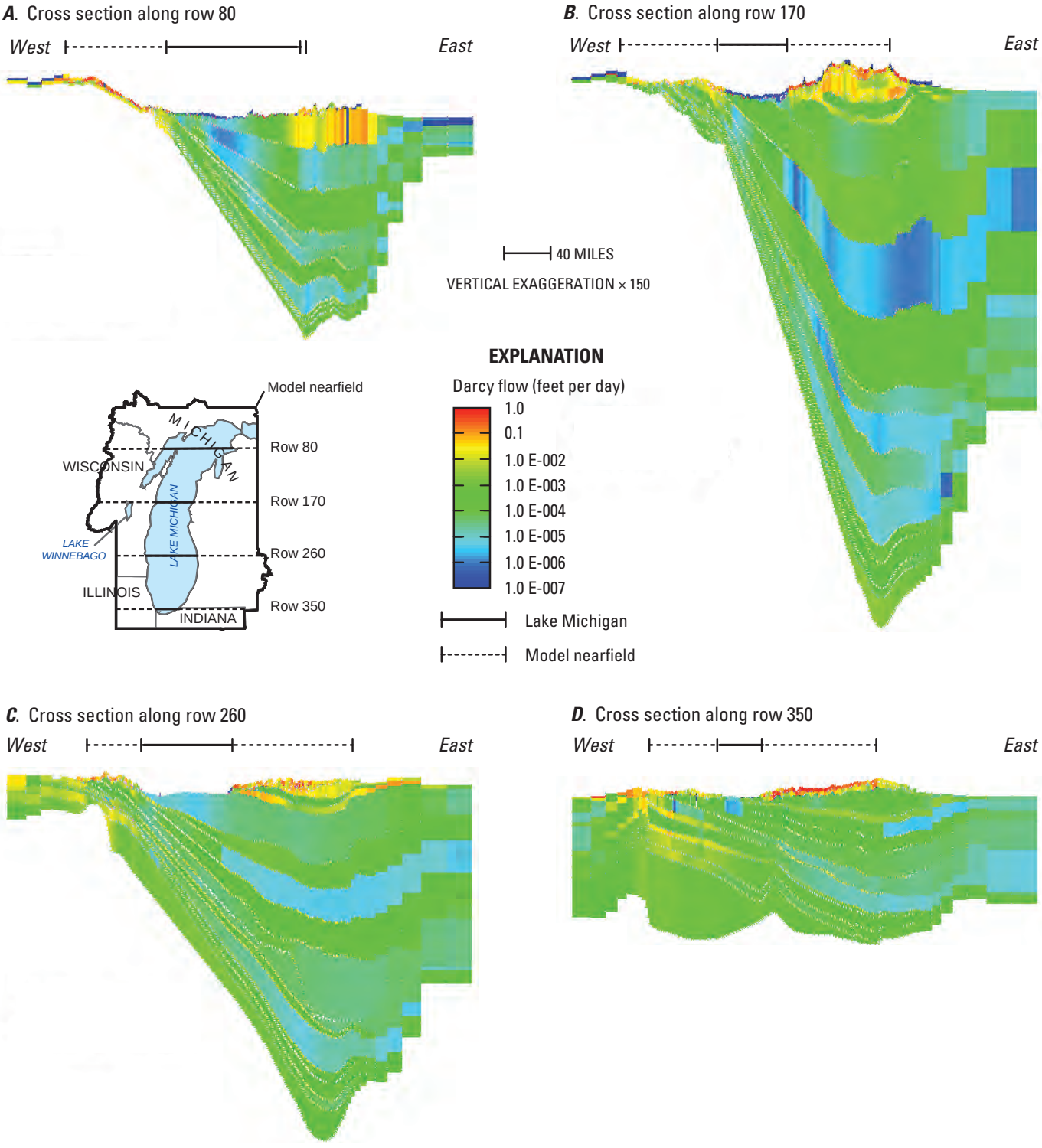

Figure 59. Simulated flow rate (Darcy flow) along selected west/east cross sections for 2005 conditions.

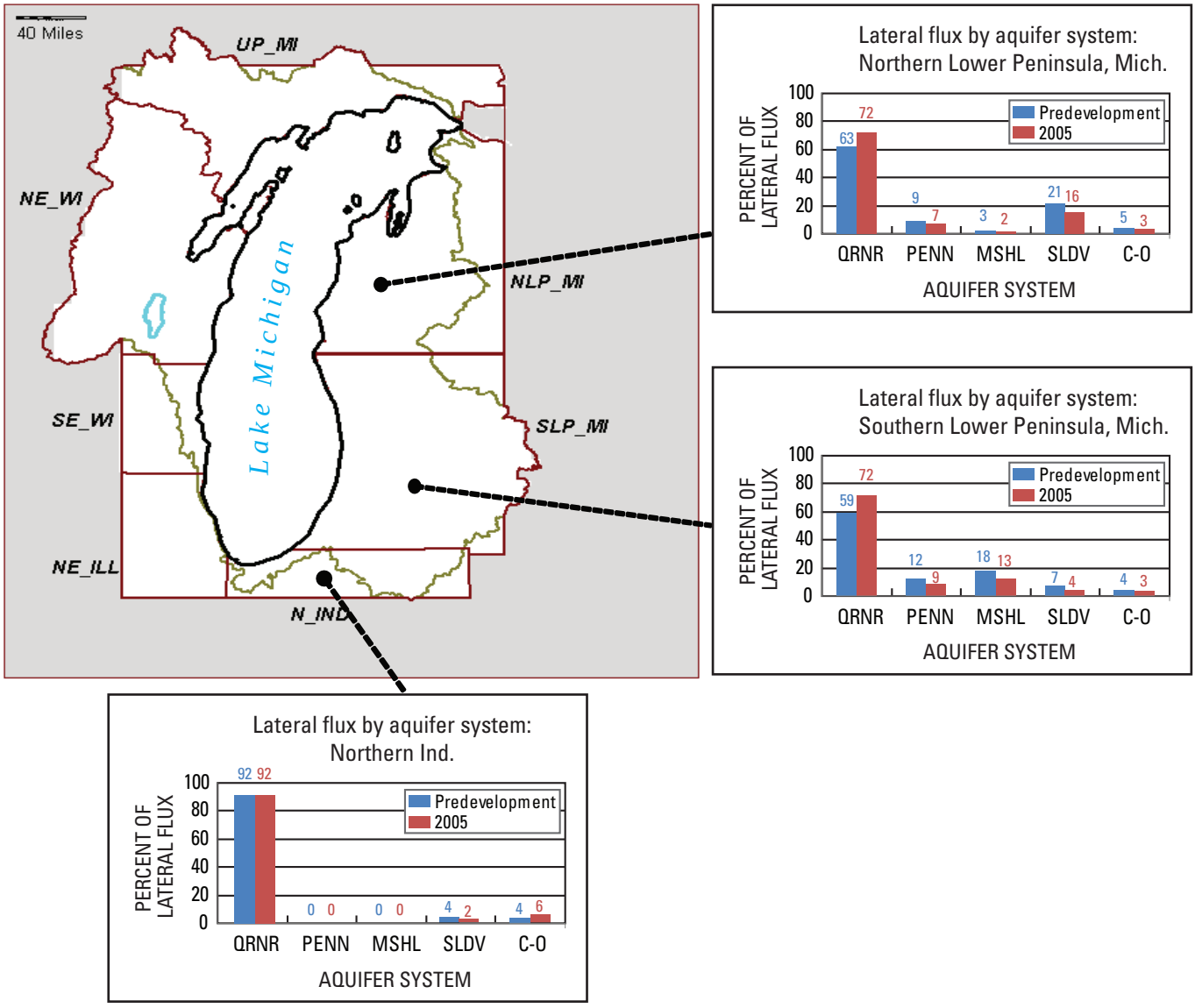

Figure 60*A*. Simulated lateral flux by aquifer system in subregions east of Lake Michigan for predevelopment and 2005 conditions.

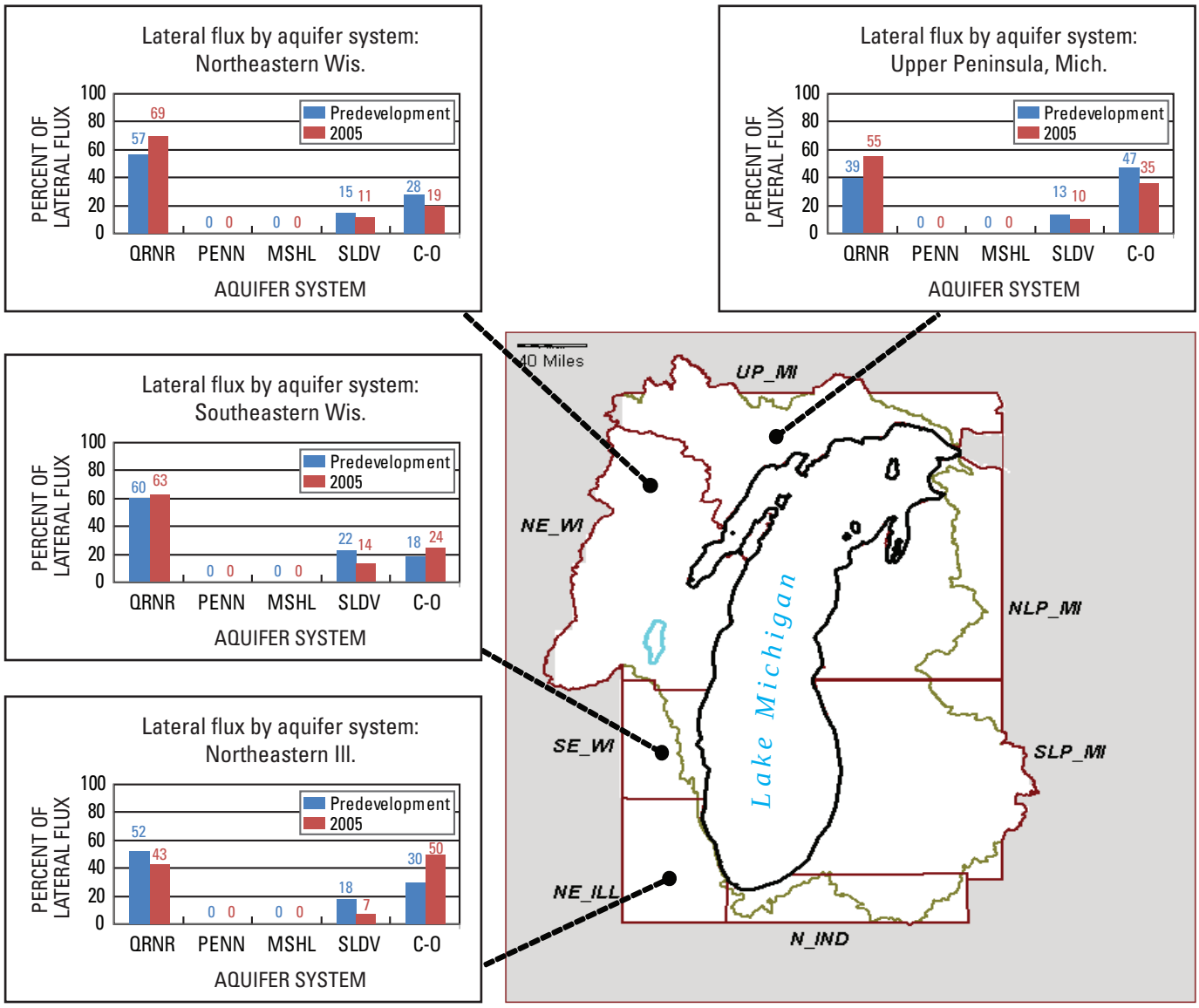

Figure 60*B*. Simulated lateral flux by aquifer system in subregions west of Lake Michigan for predevelopment and 2005 conditions.

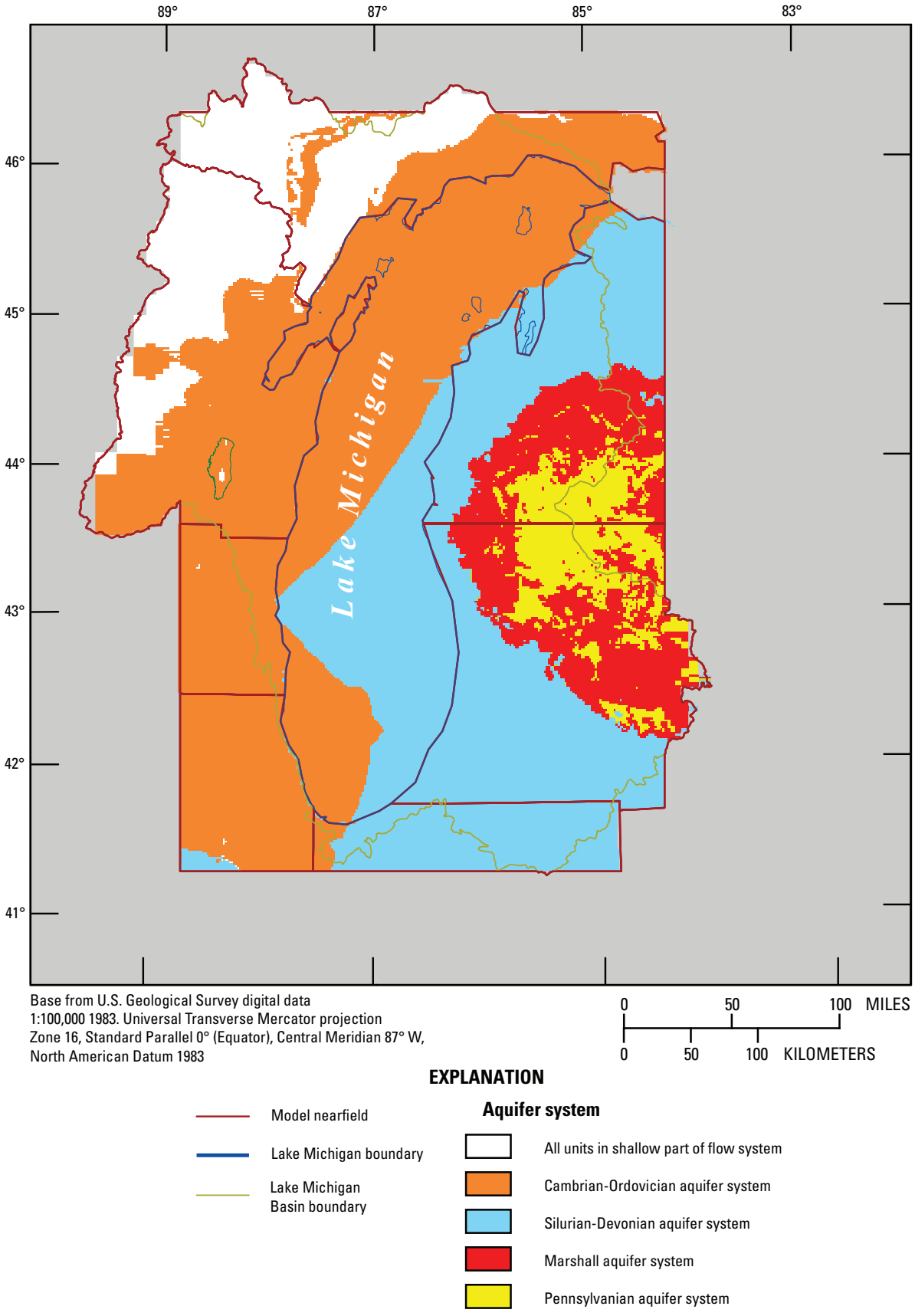

Figure 61. Uppermost aquifer system in deep part of flow system.

The downward leakage of groundwater to the deep part of the flow system under predevelopment conditions accounts for more than 10 percent of recharge in certain nearfield areas in NE_WI and NLP_MI , whereas little downward leakage occurs in broad swaths extending east from the eastern shoreline of Lake Michigan (fig. 62*A*). Flow is *upward* from the deep part to the shallow part of the flow system over large areas bordering the western shoreline of Lake Michigan (white areas in fig. 62*A*). The mixed pattern of upward and downward flow evident in the center of the Michigan Basin and also westward into Wisconsin (including parts of the model farfield not shown in fig. 62*A*) indicates that, in those areas, local circulation extends toward the bottom of the deep part of the flow system, linking recharge zones to discharge zones for the entire thickness of the groundwater system over relatively short distances.

Pumping leaves the pattern of vertical leakage to the deep part of the flow system largely unchanged east of Lake Michigan but decisively alters conditions west of the lake. Mapped conditions in 2005 (fig. 62*B*) show a large area of previously upward flow inland of the Lake Michigan western shoreline where pumping from deep wells now induces downward flow from the shallow part of the flow system to the C-O aquifer system. Over much of SE_WI and NE_ILL, the downward flow is small (on the order of 1 percent of recharge to the water table); but in the western fringe of the model nearfield (and for adjacent areas of the farfield not shown) it increases, according to the model, to well over 10 percent of available recharge. These source areas for deep pumping coincide with areas just west of the subcrop of the Maquoketa Shale where the C-O aquifer system is not confined. The model results indicate that groundwater that once flowed along regional paths to Lake Michigan now is discharged at pumping centers in the vicinity of Milwaukee and Chicago.

6.4 Sources of Water to Pumping Wells

The transfer of water from one part of the flow system to another as a consequence of pumping has implications for groundwater management; for example, source-water protection. In this subsection and the two that follow, confined model results are used to illustrate different ways the groundwater system has responded to pumping. In each case, the analysis applies *particle tracking* to model results by means of MODPATH (Pollock, 1994). This technique moves particles through the simulated flow field in order to delineate the path between sources of water (such as recharge at the water table) and sinks (such as surface water or pumping wells). The procedure also computes the time of travel along a flow path, based on the particle's advective velocity. The advective velocity is equal to the Darcy flow rate simulated by the model at a given location (the sum of the components of flow calculated as the product of hydraulic conductivity and hydraulic gradient in each coordinate direction) divided by the assumed effective porosity (dimensionless) of the sediments. For this application the effective porosity is equated with the specific yields assigned to unconsolidated deposits, carbonate-and-shale-dominated deposits, and sandstone-dominated deposits. The initial specific yields for these three types of units were 0.15, 0.005, and 0.05 respectively (see section 4). On the basis of the calibration of the unconfined version of the model for specific-yield parameter zones (see appendix 5, table A5–2, and section 7), the following values were used:

- QRNR (layers 1–3) = 0.152
- JURA, PEN1, PEN2 (layers 4–6) = 0.070
- MICH, MSHL (layers 7–8) = 0.081
- DVMS, SLDV (layers 9–12) = 0.0049
- MAQU, SNNP (layers 13–14) = 0.0044
- STPT, IRGA, PCFR, EACL, MTSM (layers 15–20) = 0.044

For steady-state conditions before 1864, the flow field is stable, and MODPATH can be applied to the simulation results. After 1864, flow-field conditions changed in response to changes in recharge and pumping. One way to reveal the dynamics of the flow system is to effectively freeze hydraulic gradients and determine particle paths that would exist if conditions corresponding to a particular timeframe were maintained indefinitely. To this end, the input to MODPATH was adjusted to show the rates and directions groundwater flow would tend under conditions that correspond to the end of the model simulation period (1991–2005).[29]

Particle tracking indicates that most recharge under 1991–2005 conditions would circulate through flow paths to surface water or pumping wells in the QRNR aquifer system (fig. 63*A*). However, some of the particles released at the water table infiltrate to bedrock aquifers and discharge to surface water and pumping wells in bedrock aquifers. Contributing areas for wells in both the QRNR and bedrock aquifer systems are delineated by plotting only the particles that terminate at pumped wells (fig. 63*B*). The resulting pattern, for 1991–2005 conditions, indicates that the contributing areas for QRNR wells dominate the areas east of Lake Michigan, with relatively small areas of leakage to PENN and MSHL wells also. West of the lake, contributing areas for SLDV and C-O wells are fairly extensive, with the contributing areas to the C-O wells generally located inland west of the Maquoketa Shale subcrop. According to the model, areas colored white in figure 63*B* are not associated with major contributing areas for wells and indicate source areas that discharge to surface-water features.

[29] To simulate particle tracking under the 1991–2005 conditions, MODPATH was given the head and flux results for the last two stress periods only. In addition, the effective porosities assigned the model were reduced by 1,000 times to speed up the flow sufficiently that the travel between sources and sinks (for example, from the water table to a deep well) is completed over the 15-year period. Subsequently, the output times of flow were multiplied by 1,000 to restore the proper times of flow (for example, if MODPATH reported a traveltime of 12 years, it was corrected to 12,000 years).

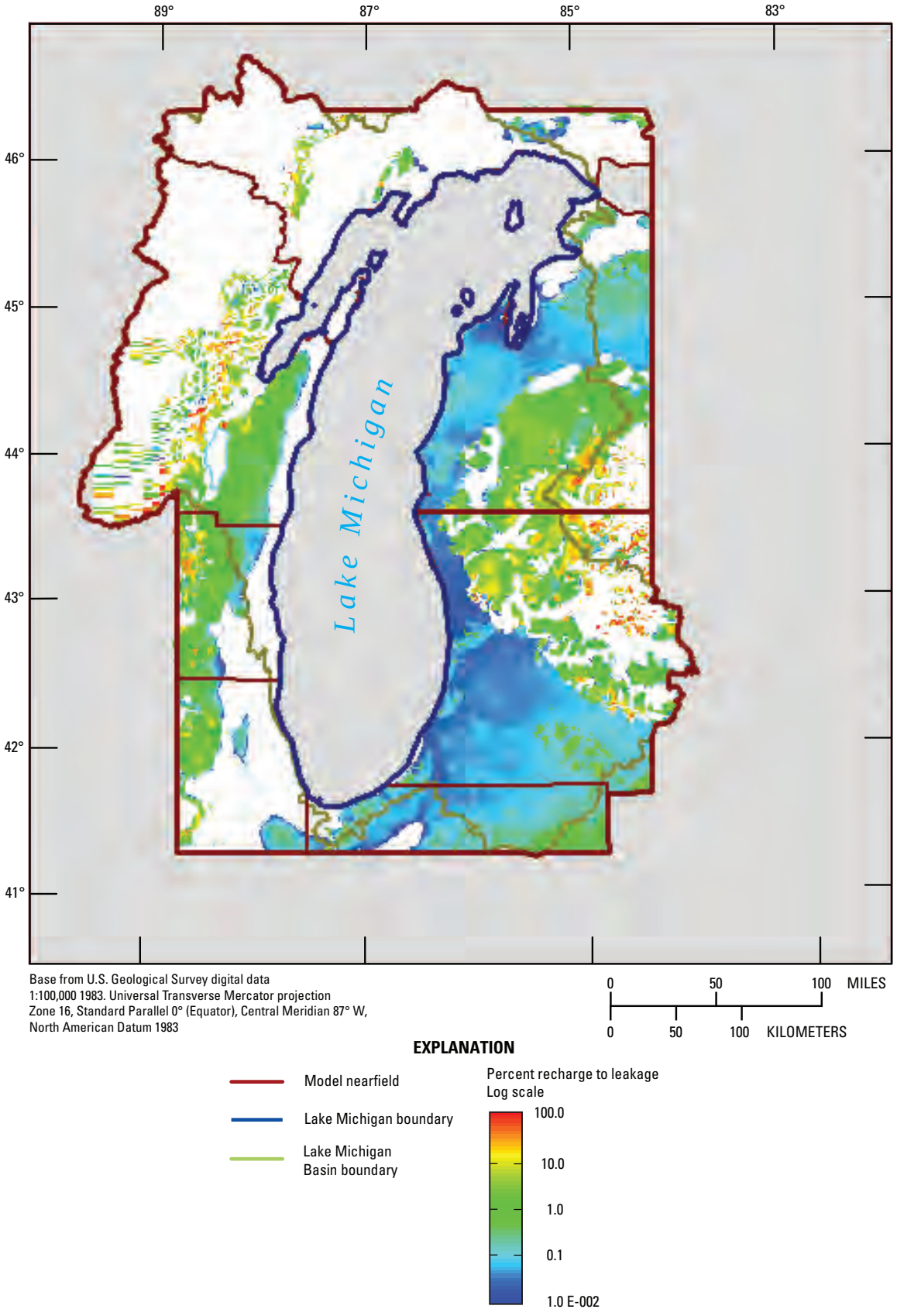

Figure 62*A*. Simulated downward leakage to uppermost aquifer system in deep part of flow system as percent of recharge: Predevelopment. (White areas represent zones of upward flow. The area of Lake Michigan is excluded because the underlying sediment does not receive groundwater recharge.)

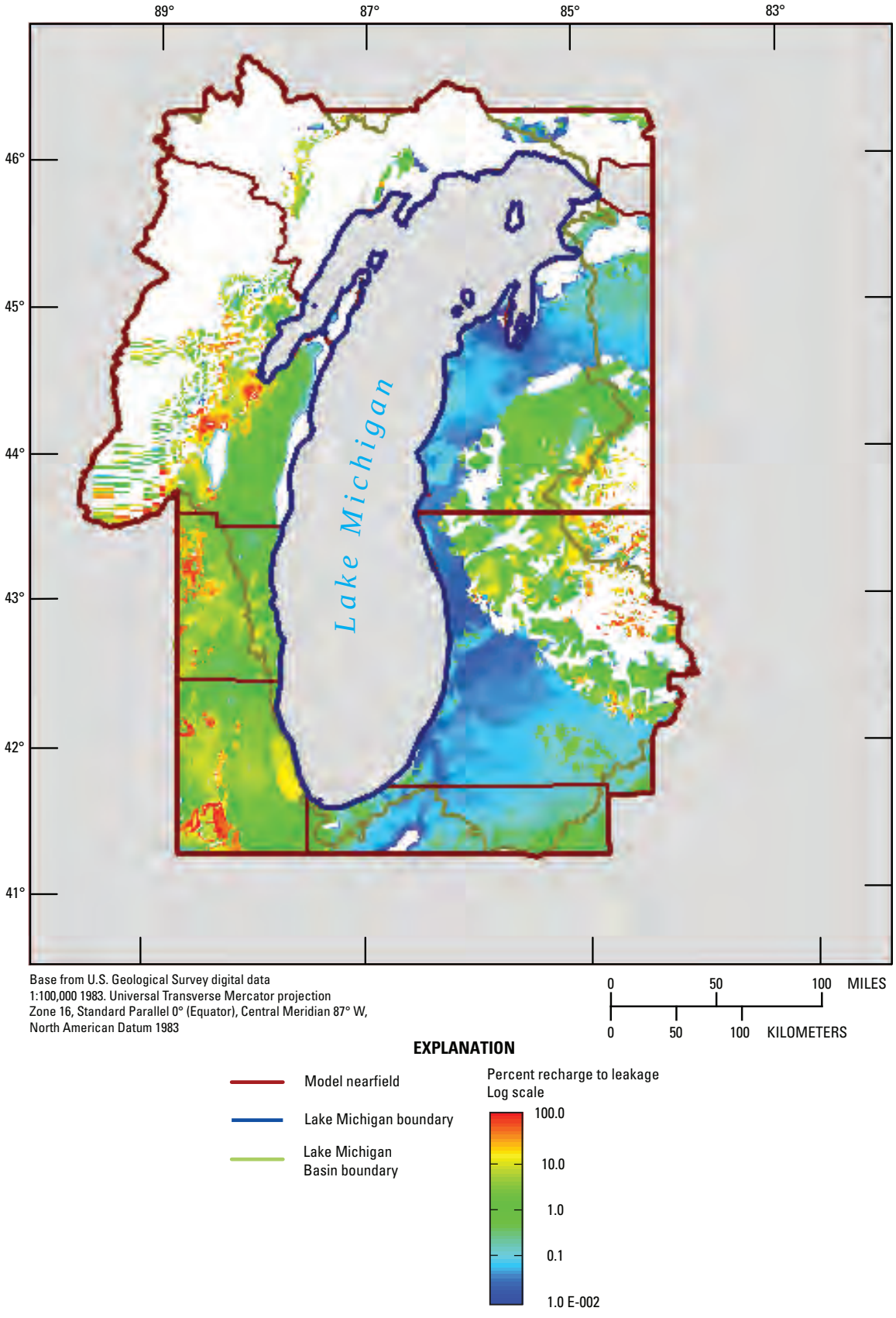

Figure 62*B*. Simulated downward leakage to uppermost aquifer system in deep part of flow system as percent of recharge: 2005. (White areas represent zones of upward flow. The area of Lake Michigan is excluded because the underlying sediment does not receive groundwater recharge.)

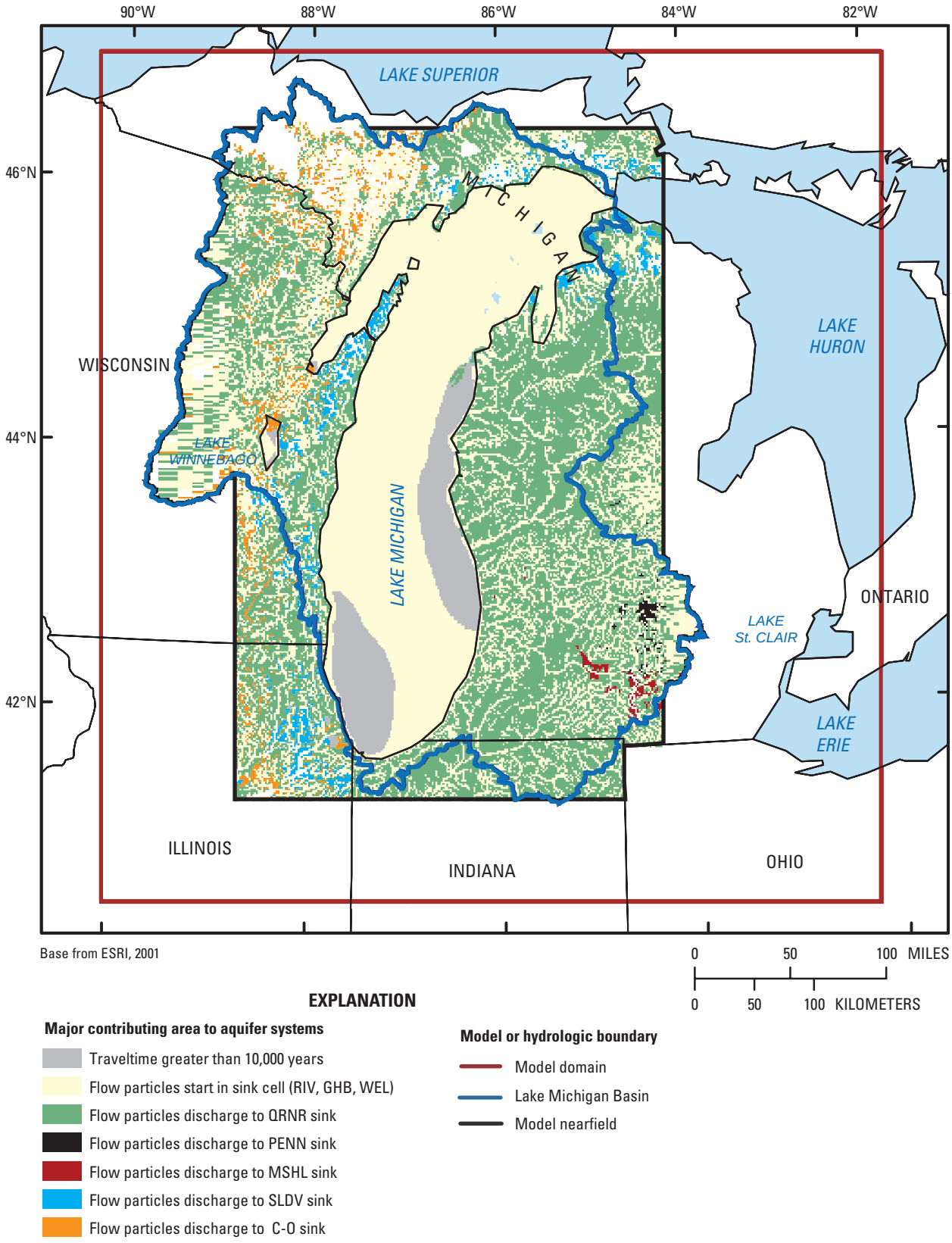

Figure 63*A*. Simulated contributing areas to aquifer-system sinks in 2005.

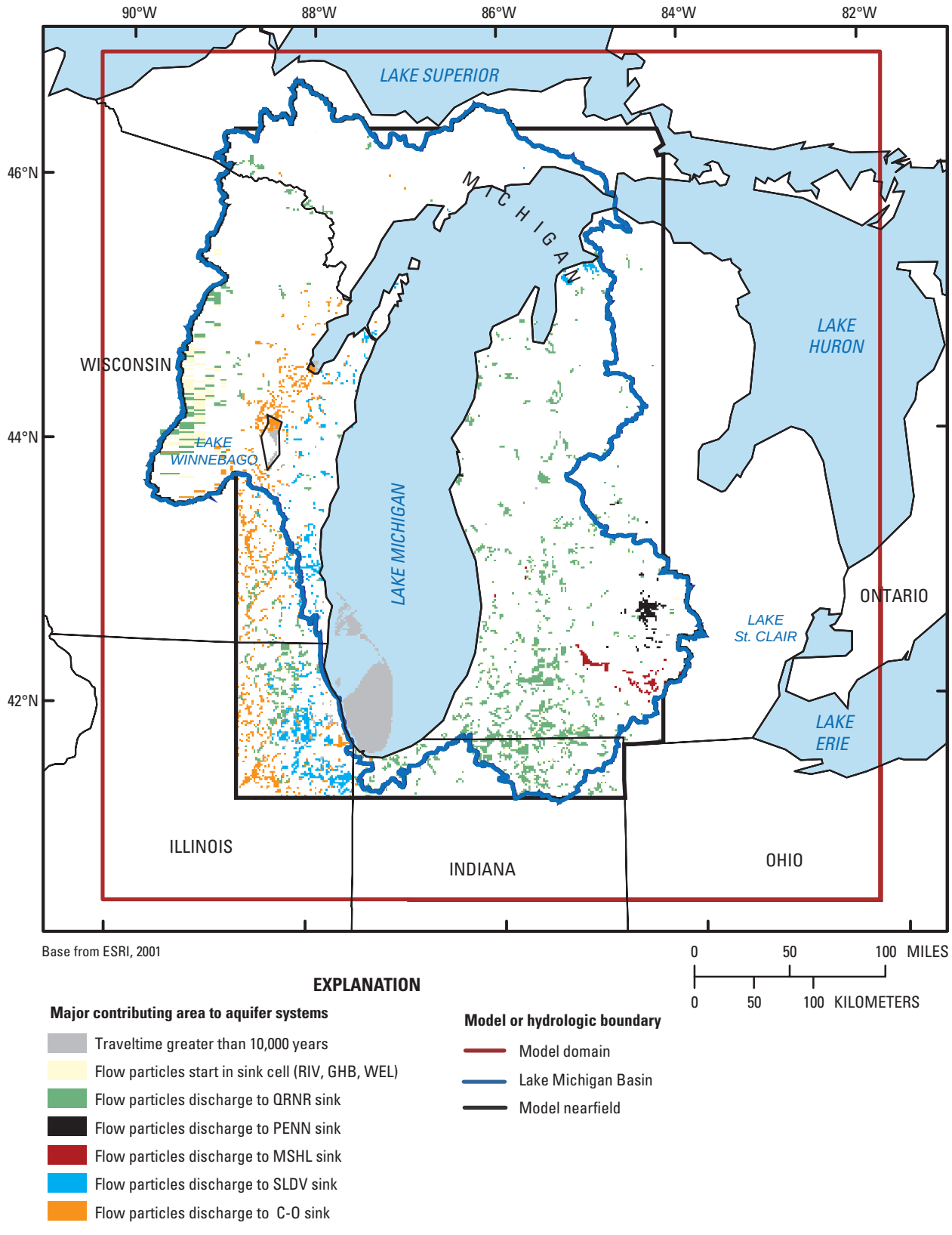

Figure 63*B*. Simulated contributing areas to pumping wells in 2005.

The simulated traveltimes to wells for 1991–2005 fixed conditions vary considerably by aquifer system. Not surprisingly, the median traveltime from the water table to pumping wells increases with the depth of the aquifer system. Circulation of recharge at the water table to wells in the QRNR and PENN systems is typically on the order of 20–30 years. It increases to a median traveltime of 60−70 years for MSHL and SLDV system wells, and then increases sharply to close to 600 years for the C-O system wells (table 15). However, the large variability around the median traveltime simulated by the model also must be recognized. Wells in all aquifer systems can withdraw relatively old water. The 95th percentile for simulated traveltimes (table 15) implies that much of the water withdrawn by C-O wells is much more than 1,000 years old. Noble gas data in conjunction with stable isotopes and ^{14}C ages of groundwater samples collected from C-O pumping wells in southeastern Wisconsin support the finding that some of the water discharged by wells is very old, dating as far back as just after the most recent glaciation, 8,000 or 9,000 years ago (Klump and others, 2008).

Table 15. Time of travel to pumping wells, by aquifer system.

[Traveltimes correspond to 1990–2005 flow conditions. Values correspond to the confined model, SLMB-C. All traveltime statistics are in years]

Aquifer system	Traveltime statistic			
	Average	Median	5th quantile	95th quantile
QRNR	59.3	21.6	2.1	235.7
PENN	174.5	24.2	9.8	389.6
MSHL	135.0	61.8	2.5	459.2
SLDV	110.4	69.7	19.1	311.3
C-O	1,361.1	577.2	44.6	5,804.5

Pumping in the Lake Michigan Basin and adjacent areas has had a profound effect on flow directions and rates, often completely transforming the natural flow pattern and substituting wells for surface-water features as regional sinks. It is instructive in this regard to contrast predevelopment flow directions and rates with 2005 conditions in the vicinity of the important pumping center in northeastern Illinois (fig. 64). Before the onset of high-capacity pumping, groundwater flow—both inland and under Lake Michigan—tended toward the lake at rates typically between 1.0 E−3 and 1.0 E−5 ft/d (fig. 64*A*). The groundwater basin in the bedrock extended far to the west of the Lake Michigan Basin topographic divide. With pumping, flow directions under the lake reversed: rather than acting as a regional sink, the lake is simulated to lose water to the groundwater system, whereas deep flow rates even in saline areas were to some extent increased (fig. 64*B*). In support of the finding that pumping has changed the flow regime in saline areas, an examination of archived data for deep bedrock aquifers in northeastern Illinois shows that, in some locations, dissolved solids in well discharge are increasing (Kelly and Meyer, 2005).

It is important to qualify the sense in which Lake Michigan is a source of water to wells under developed conditions. Although simulated gradients under the lake are reversed, the rate of flow is extremely slow, and, as shown by the gray area in figure 63*B*, pumping would have to be maintained at 2005 levels for thousands of years before any water drawn from Lake Michigan would emerge as well discharge. Although not a direct source of water to wells, parts of the lake do contribute some flow (very small in magnitude at any given location, as evidenced by the very low flow rates registered below the lake in fig. 64*B*), which replenishes water moving under the influence of reversed gradients into the areas of drawdown around pumping centers.

The ultimate sources of water pumped from wells can be quantified by comparing the relative magnitudes of sources and sinks in the simulated groundwater budget under natural conditions (without pumping) and under pumped conditions. The effect of variable recharge on the water budget can be isolated by constructing a version of the calibrated model that contains variable recharge but no pumping. The water budgets computed with this special model version can then be subtracted from the same terms from the calibrated model that contains pumping. The residuals represent the effect of pumping *alone* on the sources and sinks in the model.

For convenience, the sources of water to wells can be combined into four quantities derived from the water budget:

- Reduction in base flow to inland surface-water features combined with induced flow out of inland surface-water features to groundwater.
- Reduction in net direct discharge to Lake Michigan (reduction in direct discharge to the lake plus increased induced flow or out of the lake to groundwater).
- Lateral flow into the area of interest.
- Net release from storage.

The compilation of sources through time for the Lake Michigan Basin shows the dominant role of inland surface water as a source of water to wells pumping within the basin (table 16). The relative contribution of inland surface water increases from 86 percent of all sources for the 1940–50 period to 91 percent for the 1975–80 period, and to 94 percent for the 2001–5 period. Part of this change can be attributed to the relative shift of pumping from deep to shallow wells over time (see table 9). Shallow wells tend to draw more directly from nearby surface-water features, whereas deep wells tend to induce more lateral flow into the area of interest and, at least initially, cause rapid water-level declines that remove water from storage. The drop in the storage contribution after 1980 is attributable to reduced withdrawals in some major pumping centers resulting from a shift to a Lake Michigan water supply and from declining industrial water use.

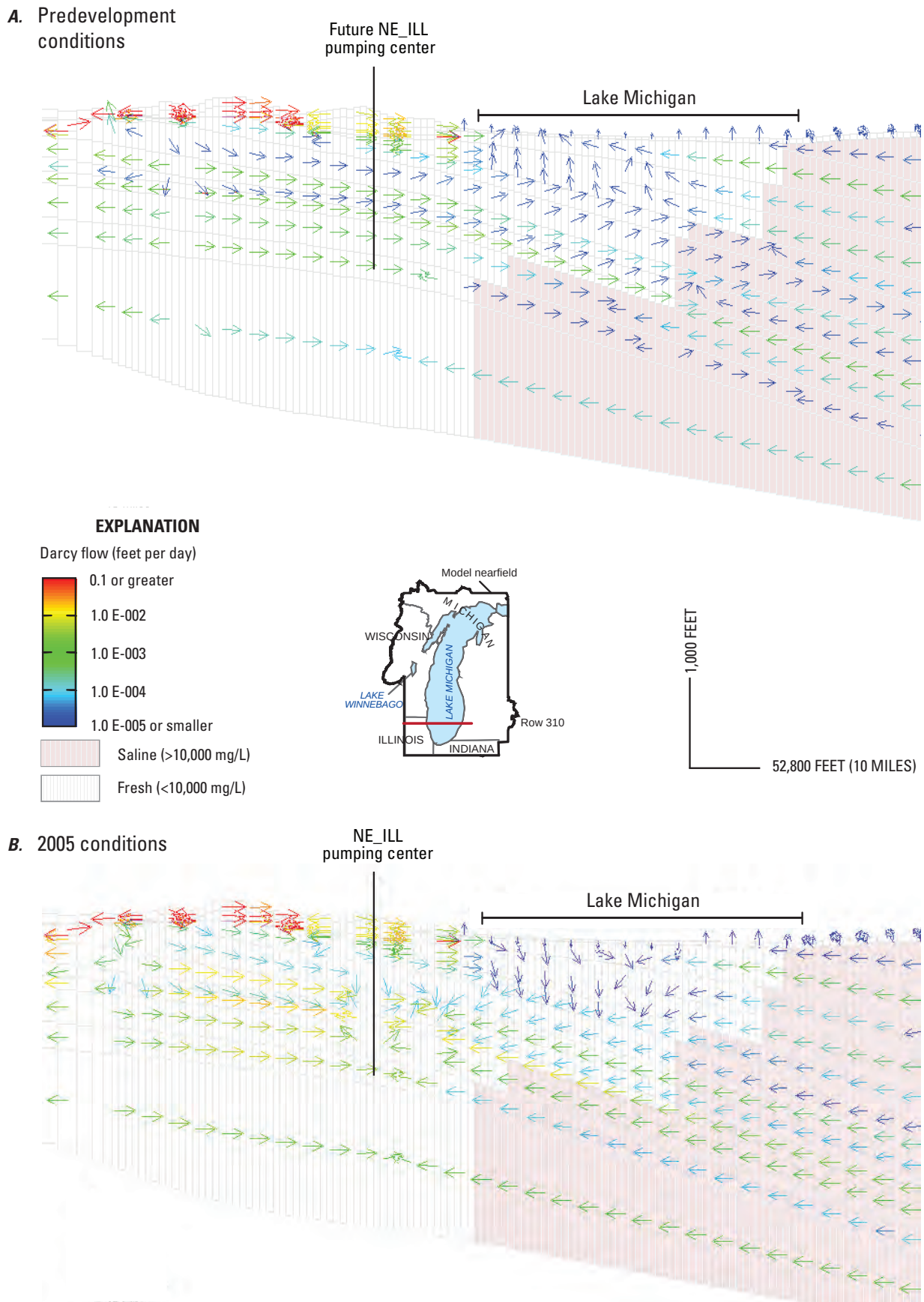

Figure 64. Simulated flow direction and magnitude along west/east cross section in NE_ILL: *A*, Predevelopment. *B*, 2005.

Table 16. Sources of water to pumping wells within Lake Michigan Basin.

[Because recharge changes between stress periods, one cannot simply use the change in direct discharge to Lake Michigan simulated by the model over time to isolate the effect of changes in pumping on flows. Instead, the effect of pumping is calculated by comparing a simulation *without* pumping to a simulation *with* pumping, and computing the difference in flows. Values correspond to the confined model, SLMB-C; Mgal/d, million gallons per day; ---, not applicable]

Stress period	Date	Source to wells from reduced base flow *to* or induced outflow *from* inland surface water (Mgal/d)	Source to wells from reduced discharge *to* or induced outflow *from* Lake Michigan (Mgal/d)	Source to wells from change in lateral flow across Lake Michigan Basin boundary[1] (Mgal/d)	Source to wells from net storage release (Mgal/d)	Total sources to wells (Mgal/d)	Well withdrawals (net of injection) (Mgal/d)	Percent discrepancy due to numerical error
1	Predevelopment	0	0	0	0	0	0	---
2	Oct. 1864–Oct. 1900	7.83	.04	−1.09	1.32	8.10	8.41	−3.58
3	Oct. 1900–Oct. 1920	17.31	.62	−3.27	5.53	20.20	19.97	1.17
4	Oct. 1920–Oct. 1940	48.32	2.53	−3.37	8.25	55.73	55.38	.63
5	Oct. 1940–Oct. 1950	102.41	4.62	−1.67	13.93	119.29	118.82	.40
6	Oct. 1950–Oct. 1960	168.18	6.80	−1.80	14.60	187.78	187.29	.26
7	Oct. 1960–Oct. 1970	250.41	7.23	−1.76	16.96	272.84	272.29	.20
8	Oct. 1970–Oct. 1975	292.42	8.08	−5.88	23.45	318.07	317.54	.17
9	Oct. 1975–Oct. 1980	336.62	9.21	−8.67	31.72	368.87	368.19	.18
10	Oct. 1980–Oct. 1985	393.08	10.18	−9.78	31.04	424.52	423.60	.22
11	Oct. 1985–Oct. 1990	404.88	11.19	−.70	20.83	436.19	435.77	.10
12	Oct. 1990–Oct. 2000	530.10	16.31	7.91	19.78	574.11	576.00	−.33
13	Oct. 2000–Oct. 2005	534.27	16.46	6.90	9.76	567.38	569.52	−.37

[1]Negative values indicate flow out of Lake Michigan Basin to wells in adjacent basins (for example, Mississippi River or Lake Huron Basins).

The relative contribution of sources of water to wells varies not only as a function of time but also as a function of the part of the Lake Michigan Basin under consideration. It is useful to contrast the sources for shallow wells and deep wells by subregion for 2005 conditions. For shallow wells in all subregions, the dominant source of water is diverted or induced flow from streams and inland lakes (fig. 65*A*). For deep wells below confining units, especially in NLP_MI, SE_WI, and NE_ILL, other sources are more important (fig. 65*B*).

The term in the water budget that reflects the effect of pumping on inland surface water can be subdivided into several components:

- Reduction of base flow to streams ("Stream Out").
- Reduction of base flow to water bodies ("Inland Lake Out").
- Increase in induced flow out of streams ("Stream In").[30]

Note that the terms, "Stream Out," "Inland Lake Out," and "Stream In" quantify sources of water to wells derived from surface-water features. Through time the most important individual source of water to wells in the Lake Michigan Basin is the reduction of base flow to streams. In 1950, 1980, and 2005, it has accounted according to the SLMB-C model for 60 percent or more of all the sources of water to pumping wells (fig. 66*A*–*C*). In the Lake Michigan Basin the chief effect of pumping is to reduce base flow to streams. However, it is also important to realize that temporal variations in recharge (see fig. 30) can cause overall base flow to increase despite increased pumping or, alternatively, to decrease more than pumping alone would provoke.

The analysis of the sources of water to wells indicates that, on balance, pumping causes lateral flow to exit the Lake Michigan Basin and flow toward wells in neighboring drainage basins for part of the postdevelopment period (resulting in negative "Outside Basin" terms in fig. 66*A*, *B*). This outflow is caused almost entirely by deep pumping in areas of SE_WI and NE_ILL, which are to the west of the Lake Michigan Basin. The dynamics of the system can be illustrated by comparing the source terms for the *Lake Michigan Basin* to the source terms for the *model nearfield* (fig. 67), which includes, but extends beyond, the basin. The lateral flow source component is inward (positive) to the model nearfield (owing to the effect of pumping centers within the nearfield but west of the Lake Michigan Basin). Moreover, the nearfield net storage contribution is larger than that for the Lake Michigan Basin. For the 1976–80 stress period, for example, the nearfield storage component amounts to 17 percent of the source of water to wells (fig. 67*B*) as opposed to only 9 percent for the Lake Michigan Basin (fig. 66*B*). This comparison shows the sensitivity of the source-of-water-to-wells analysis to the specific area referenced and points to the difference between basins defined by surface-water divides as opposed to those defined by groundwater divides. This finding is discussed further in the next subsection.

6.5 Regional Groundwater Divides

Particle tracking applied to the input and output of the calibrated LMB model can also be used to delineate the configuration of the regional Lake Michigan groundwater basin. For the objectives of this study, the extent of the regional basin is defined by the location of *divides* between areas where water discharges to sinks within the Lake Michigan Basin (that is, to inland surface water or to pumping wells within the drainage area of Lake Michigan, or to Lake Michigan itself) and areas where it discharges to sinks in surrounding basins (those, for example, within the Lake Superior, Lake Huron, Lake Erie, or Mississippi River drainages). It is important to show how the extent of the groundwater basin bounded by its regional divides varies as a function of

- the depth below the water table and
- the absence or presence of pumping.

The influence of depth is shown by mapping the extent of the Lake Michigan groundwater basin for model layers in distinct aquifer systems. The influence of pumping is shown by mapping its extent for predevelopment and for 1991–2005 conditions. Only freshwater areas are mapped to emphasize the availability of subsurface water for human use within and outside of the Lake Michigan Basin.

For all cases analyzed, it is important to contrast (1) the boundary of the regional Lake Michigan groundwater basin separating it from surrounding groundwater basins with (2) the boundary of the Lake Michigan drainage basin separating it from surrounding surface-water drainages. Whereas the outline of surface-water drainage basins is determined by land-surface *topography*, the outline of the groundwater basins is determined by the land surface over which recharge circulates to regional *groundwater sinks*, including deep pumping centers.

[30] As mentioned previously, water bodies such as lakes and wetlands are effectively treated as drains in the LMB model setup and are not permitted to lose water to the groundwater system.

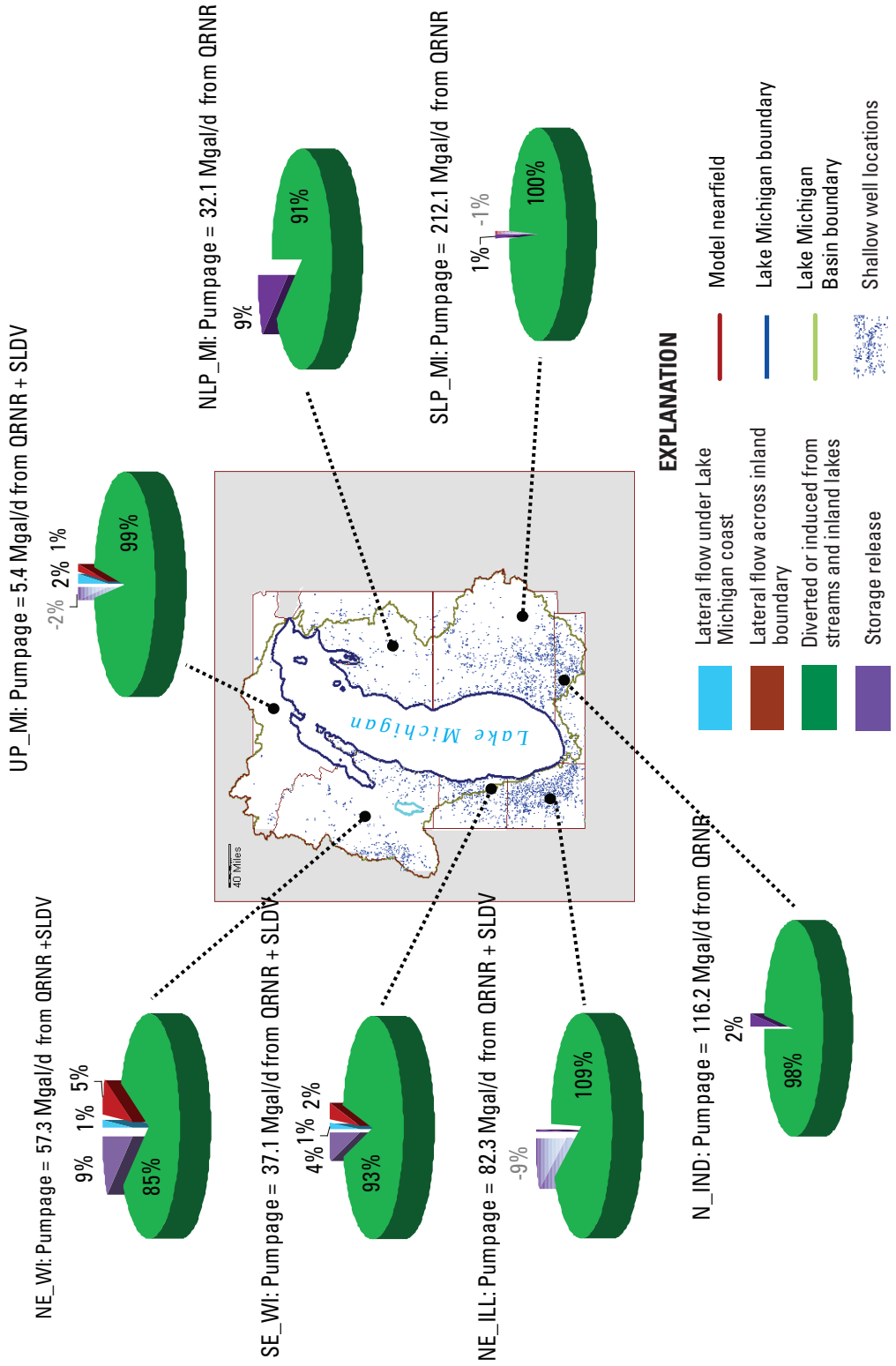

Figure 65A. Sources of water to wells by subregion in 2005: Shallow part of flow system. (Negative values (in shadow) indicate storage gain or lateral flow out of subregion. Lateral flow toward wells is distinguished as a source by whether it moves under the Lake Michigan shoreline into a subregion or whether it moves across an inland boundary into a subregion.)

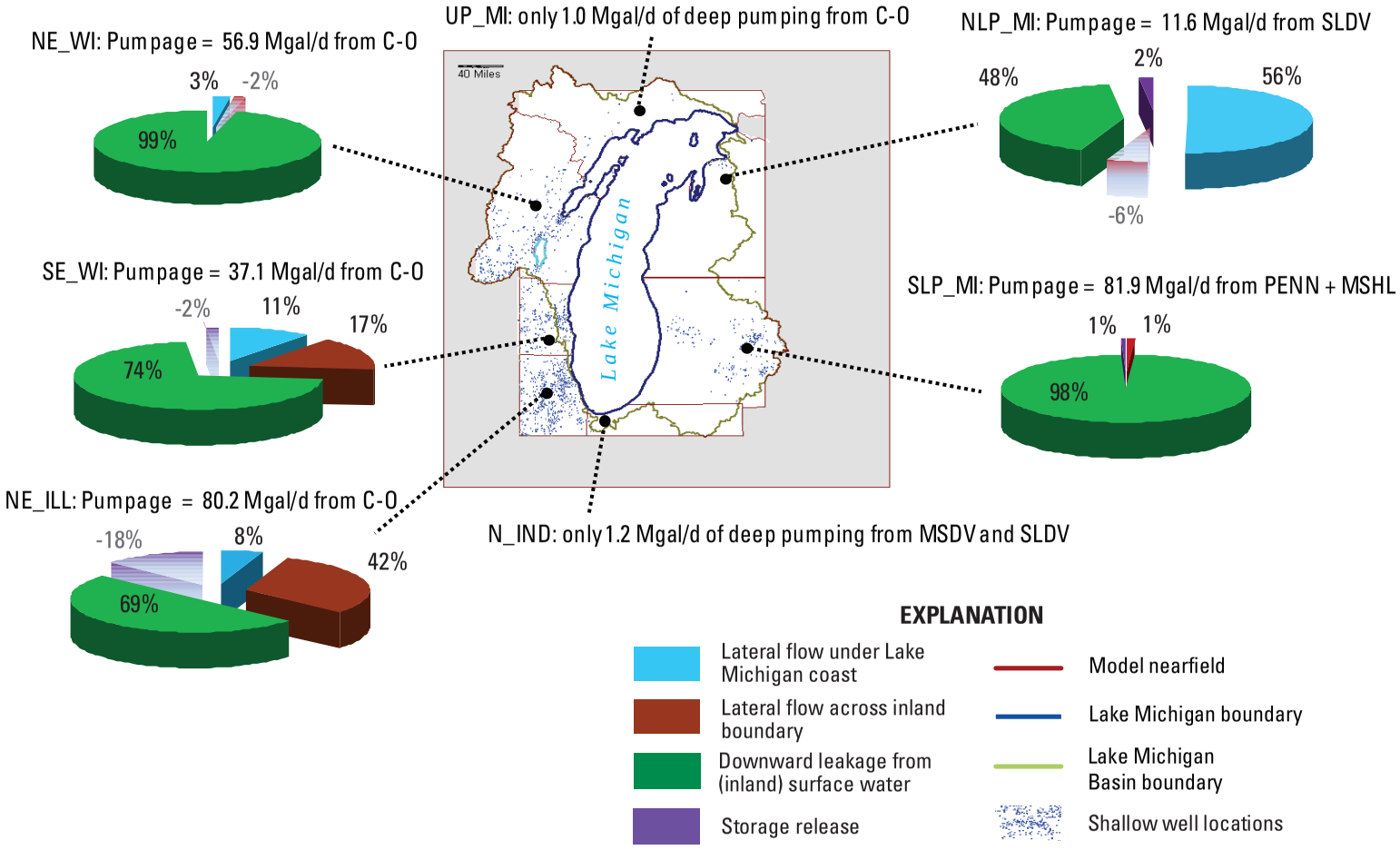

Figure 65*B*. Sources of water to wells by subregion in 2005: Deep part of flow system. (Negative values (in shadow) indicate storage gain or lateral flow out of subregion. Lateral flow toward wells is distinguished as a source by whether it moves under the Lake Michigan shoreline into a subregion or whether it moves across an inland boundary into a subregion.)

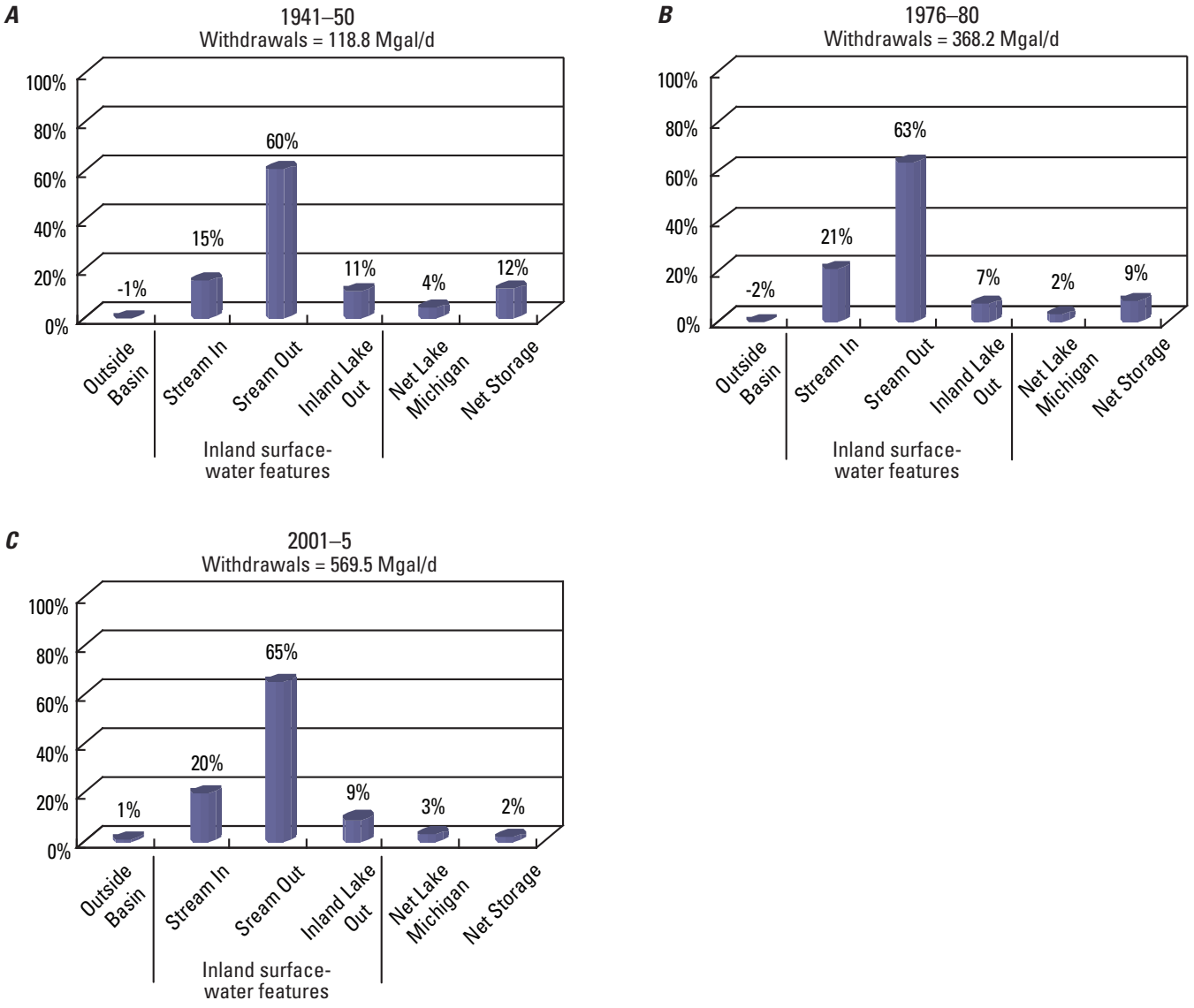

Figure 66. Sources of water to wells for Lake Michigan Basin: *A*, 1941–50. *B*, 1976–80. *C*, 2001–5. (**Outside Basin** is inflow from neighboring surface-water basins toward wells; when negative, the term represents a loss to pumping outside the Lake Michigan Basin. **Stream In** is induced flow from streams toward wells; **Stream Out** is diverted base flow from streams toward wells. **Inland Lake Out** is diverted base flow from inland lakes toward wells. **Total Lake Michigan** is diverted discharge to the lake plus induced flow from the lake toward wells. **Net Storage** is storage release around pumping wells minus storage gain around deactivated wells or injection wells.)

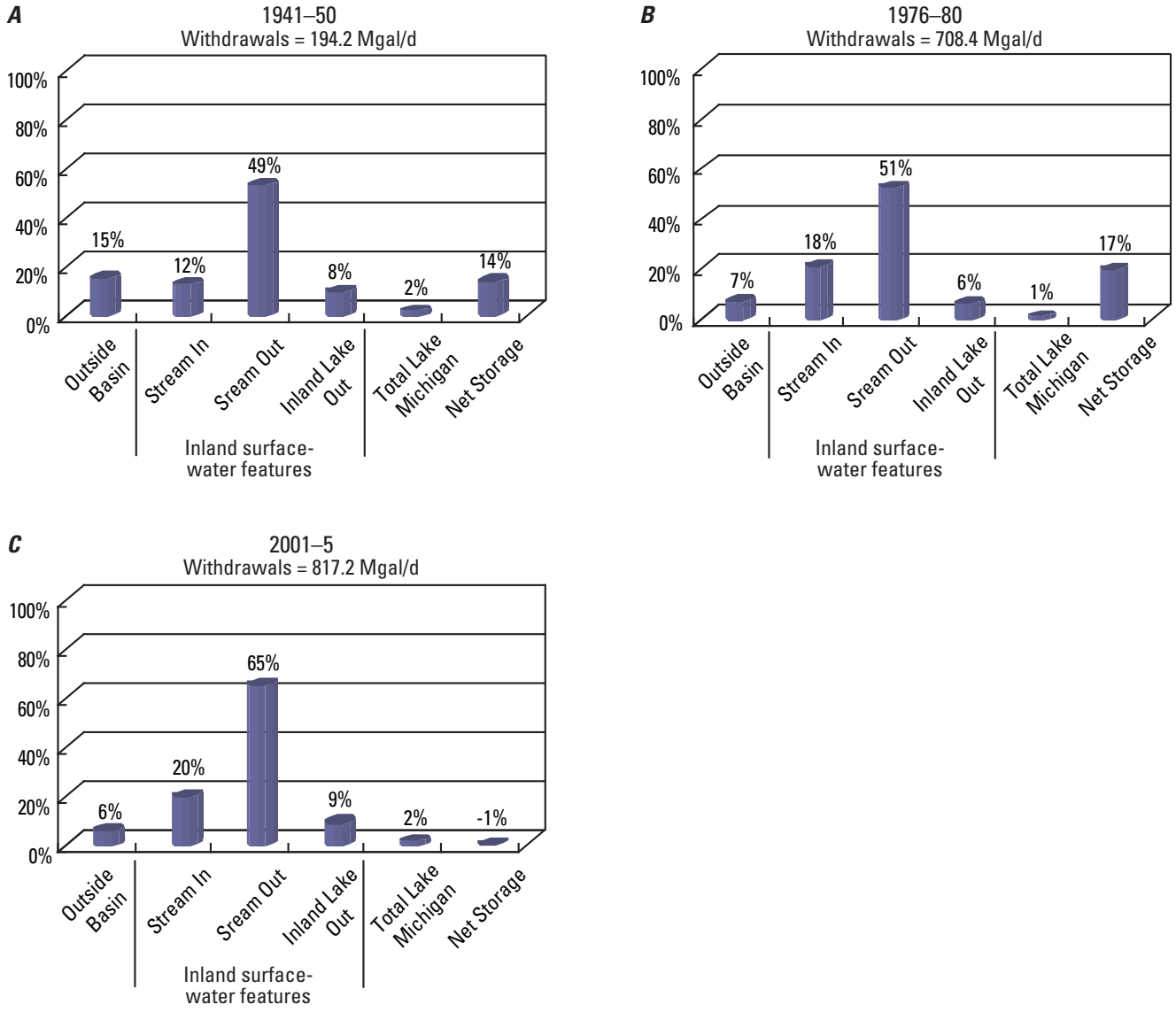

Figure 67. Sources of water to wells for model nearfield: *A*, 1941–50. *B*, 1976–80. *C*, 2001–5. (**Outside Basin** is inflow from neighboring surface-water basins toward wells; when negative, the term represents a loss to pumping outside the Lake Michigan Basin. **Stream In** is induced flow from streams toward wells; **Stream Out** is diverted base flow from streams toward wells. **Inland Lake Out** is diverted base flow from inland lakes toward wells. **Total Lake Michigan** is diverted discharge to the lake plus induced flow from the lake toward wells. **Net Storage** is storage release around pumping wells minus storage gain around deactivated wells or injection wells.)

The extent of the Lake Michigan groundwater basin simulated by the SLMB-C model for *predevelopment* conditions closely matches the extent of the Lake Michigan drainage basin for layers representative of the QRNR, PENN, and MSHL aquifer systems (figs. 68*A*–*C*). The maps indicate that groundwater flowing through these aquifer systems discharges to surface-water features within the surface-water basin. The predevelopment divides, which identify groundwater flow in the SLDV and C-O aquifer systems that discharges to surface-water features within the Lake Michigan drainage basin, do not coincide with the drainage boundaries (figs. 68*D*, *E*). The differences for the SLDV aquifer system are most marked in northern Indiana, where groundwater circulating through the dolomite in areas south of the Lake Michigan drainage area ultimately discharges to surface-water sinks to the north within the Lake Michigan drainage area. The differences for the C-O aquifer system (represented by a map of the groundwater basin in the IRGA unit, fig. 68*E*) are most marked in SE_WI and NE_ILL, where the groundwater-basin divides bulge westward into parts of the neighboring drainage basin. For both these deep aquifer systems, the lateral enlargement of the Lake Michigan groundwater-basin area at the expense of surrounding groundwater basins is fairly sizable, exceeding 20 mi.

The configuration of regional groundwater divides is more complicated after 1864 once high-capacity wells perturb the flow system. Two sets of sinks—surface-water features and pumping wells— compete for groundwater. Wells in the Lake Michigan Basin can draw water from surrounding surface-water basins, and clearly the opposite also can occur. For this reason it is useful to map the extent of the groundwater basin by means of four distinct colors that delineate areas which contribute groundwater to

- surface-water features within the Lake Michigan Basin,
- pumping wells within the Lake Michigan Basin,
- surface-water features outside the Lake Michigan Basin, and
- pumping wells outside the Lake Michigan Basin.

The combination of the first two areas constitutes the Lake Michigan groundwater basin under postdevelopment conditions. The postdevelopment period is represented by flow rates and directions simulated for the 1991–2005 model stress periods.

According to model results, pumping does not cause transfers from one regional surface-water drainage basin to another in the PENN and MSHL aquifer systems (figs. 69*B*, *C*). The groundwater-basin maps distinguish areas where flow discharges to surface water (light blue) from areas where it discharges to shallow or deep pumping wells (dark blue). For the uppermost QRNR system, cross-basin transfers occur in NE_ILL because shallow and deep wells outside of the Lake Michigan Basin are close to a drainage boundary that is almost coincident with the lakeshore (fig. 69*A*). The areas (mapped orange) under Lake Michigan contribute water to pumping wells in the Mississippi Basin. Elsewhere, areas contributing QRNR groundwater to surface-water sinks cover most of the model domain for both the Lake Michigan and surrounding drainage basins, but there are large stretches where flow generally terminates at pumping wells (for example, in NE_WI, in a zone of intensive irrigation on both sides of the boundary between the Lake Michigan and Mississippi River Basins).

For the SLDV aquifer system the contrast between groundwater divides under predevelopment conditions (fig. 68*D*) and postdevelopment conditions (fig. 69*D*) simulated by the model is particularly noticeable for the southern part of Lake Michigan. Pumping reversed the direction of much of the flow through the Silurian and Devonian units that originally discharged to the lake. Some of that flow moves from under Lake Michigan to wells in NE_ILL located in the Mississippi River drainage. The effects are even more dramatic for units in the C-O aquifer system (compare figs. 68*E* and 69*E*). The groundwater circulating under all NE_ILL and adjacent areas of Lake Michigan discharges under 1991–2005 conditions to pumping wells west of the Lake Michigan Basin. The strength of the NE_ILL deep pumping center is evident in the shift of postdevelopment groundwater divides. In SE_WI, a shift is also evident, again at the expense of the size of the Lake Michigan groundwater basin. Pumping wells in the Mississippi Basin discharge deep groundwater flow that discharged toward Lake Michigan under predevelopment conditions. The cross-basin transfers are complicated along the drainage boundaries in this area; maps for other aquifers in the C-O system (STPT, MTSM) show slightly different divides than the ones mapped for the IRGA. The simulated divide between the Lake Michigan and Mississippi River groundwater basins can vary in location by several miles depending on the C-O unit selected. Finally, it is worth noting the large effect that deep pumping has had on the location of C-O groundwater divides in parts of NE_WI.

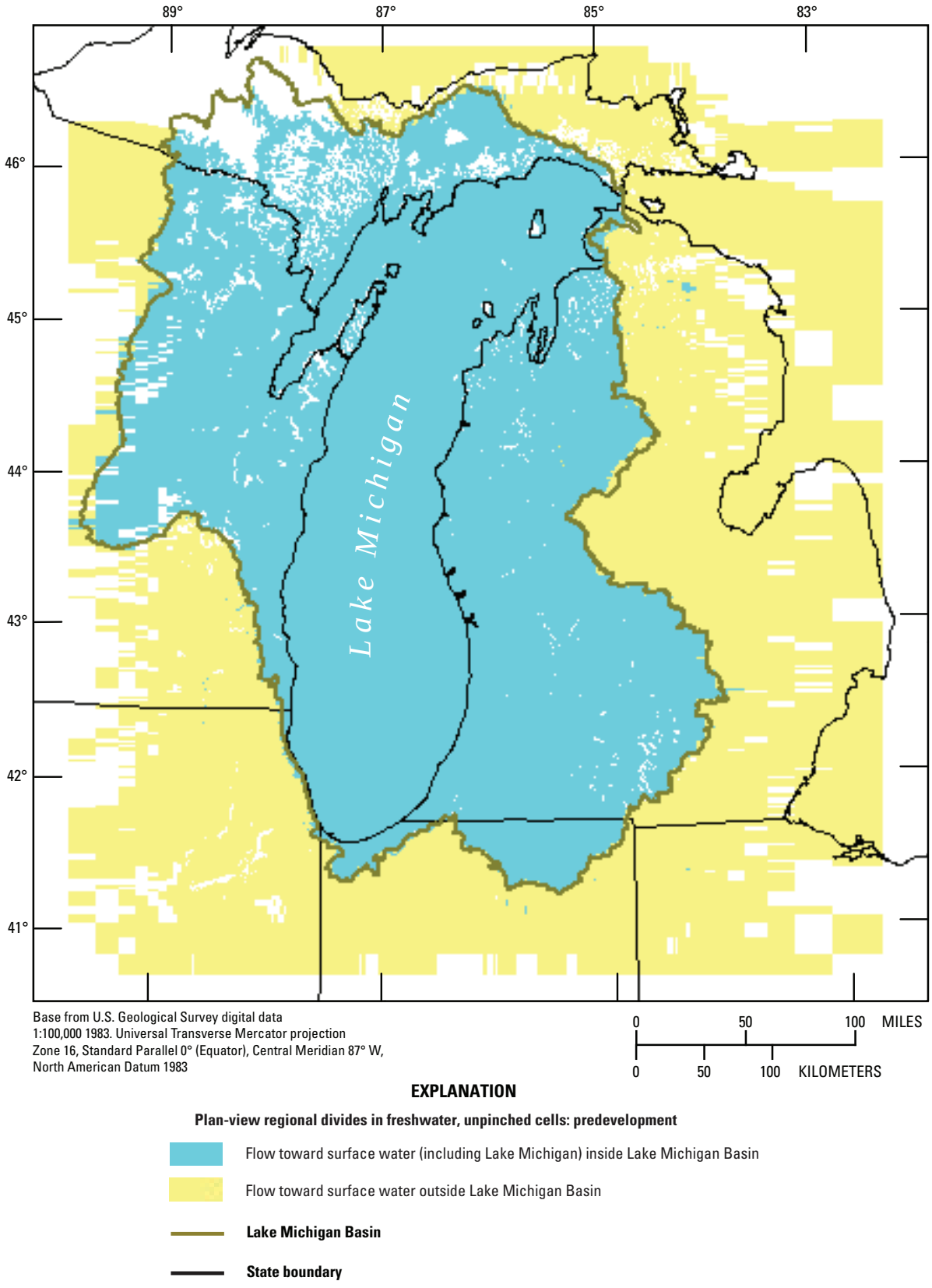

Figure 68*A*. Simulated groundwater basins, by aquifer system, for predevelopment conditions: QRNR (layer 1).

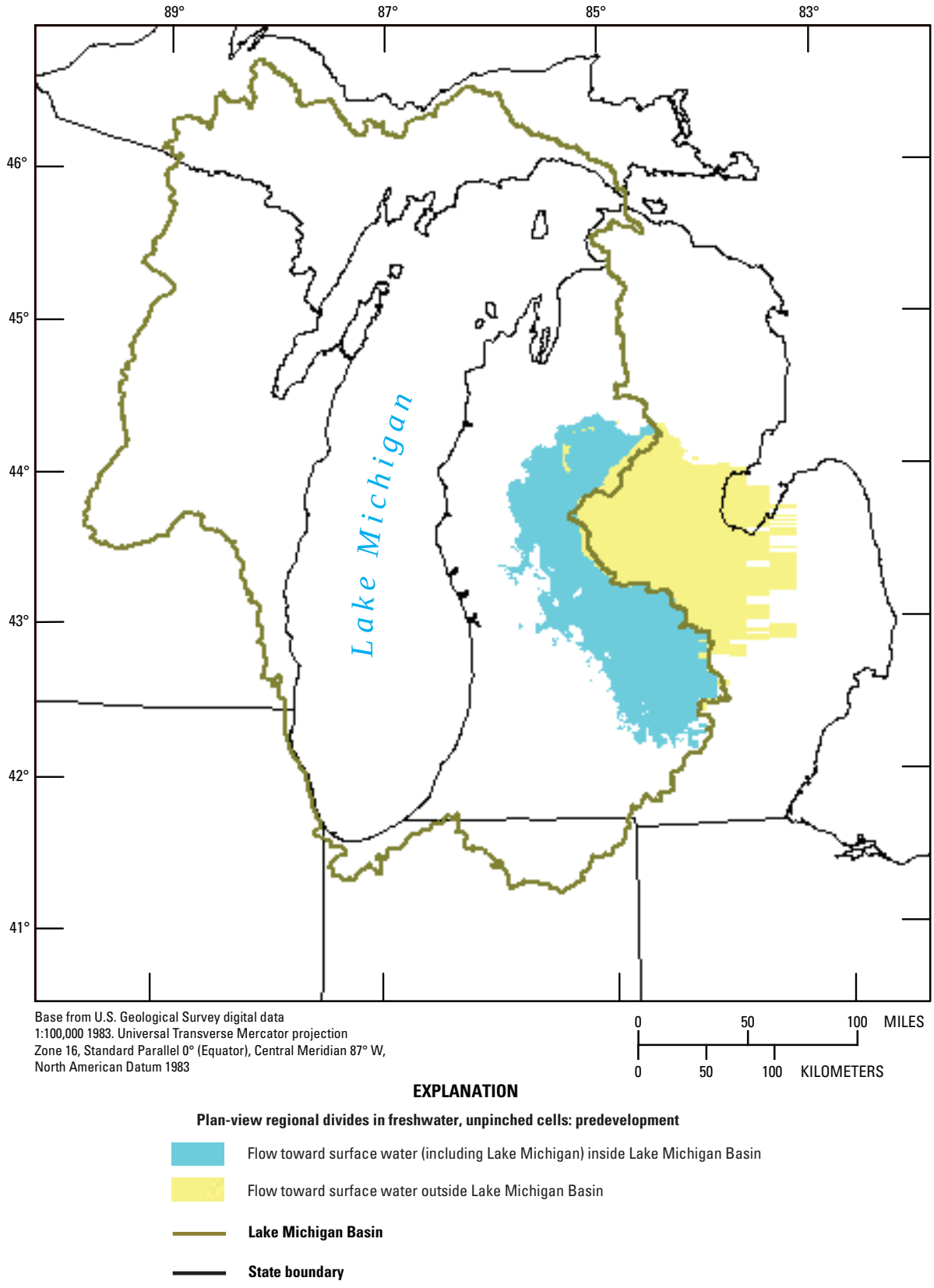

Figure 68*B*. Simulated groundwater basins, by aquifer system, for predevelopment conditions: PENN (layer 5).

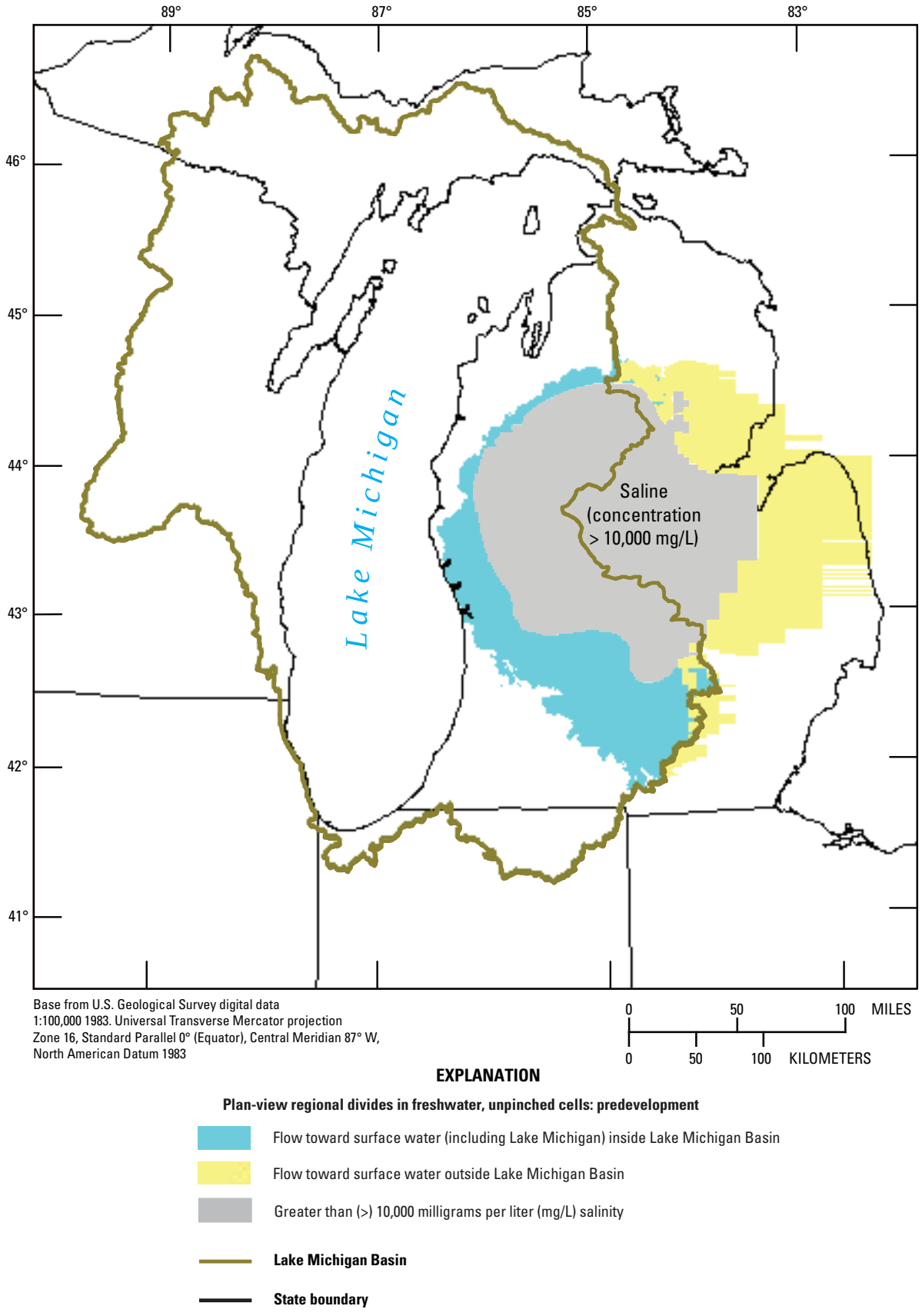

Figure 68*C*. Simulated groundwater basins, by aquifer system, for predevelopment conditions: MSHL (layer 8).

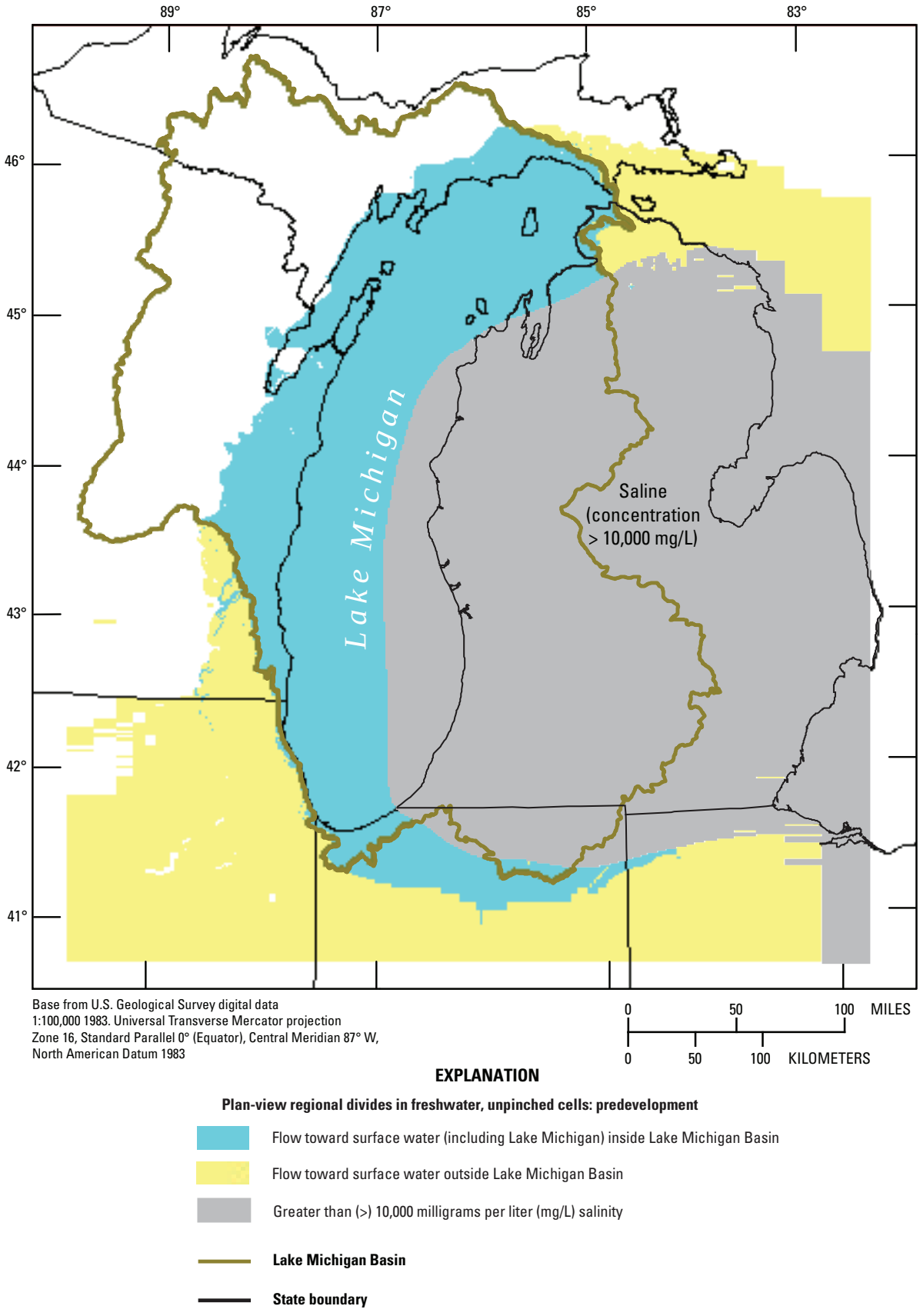

Figure 68*D*. Simulated groundwater basins, by aquifer system, for predevelopment conditions: SLDV (layer 10).

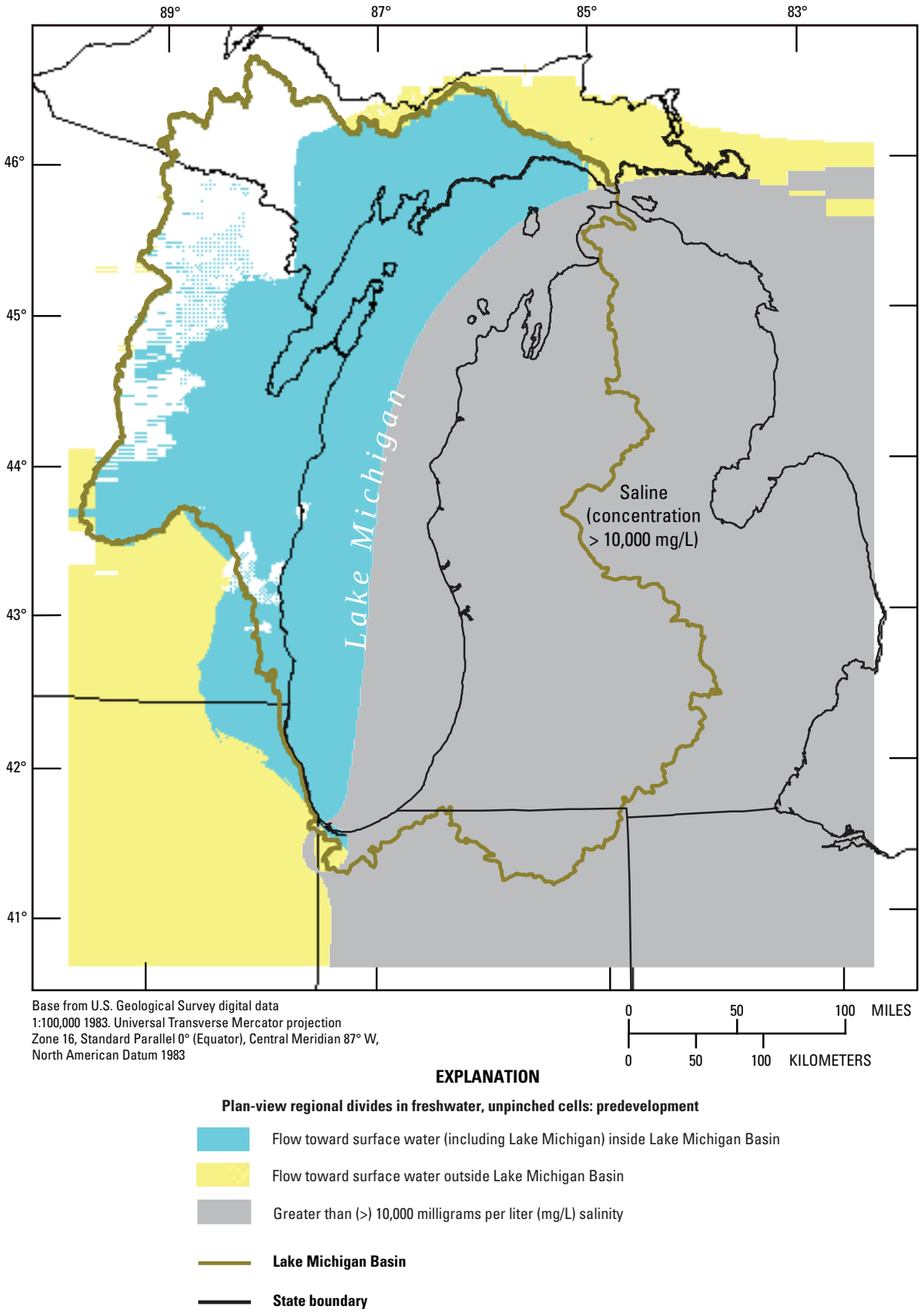

Figure 68*E*. Simulated groundwater basins, by aquifer system, for predevelopment conditions: C-O (layer 17).

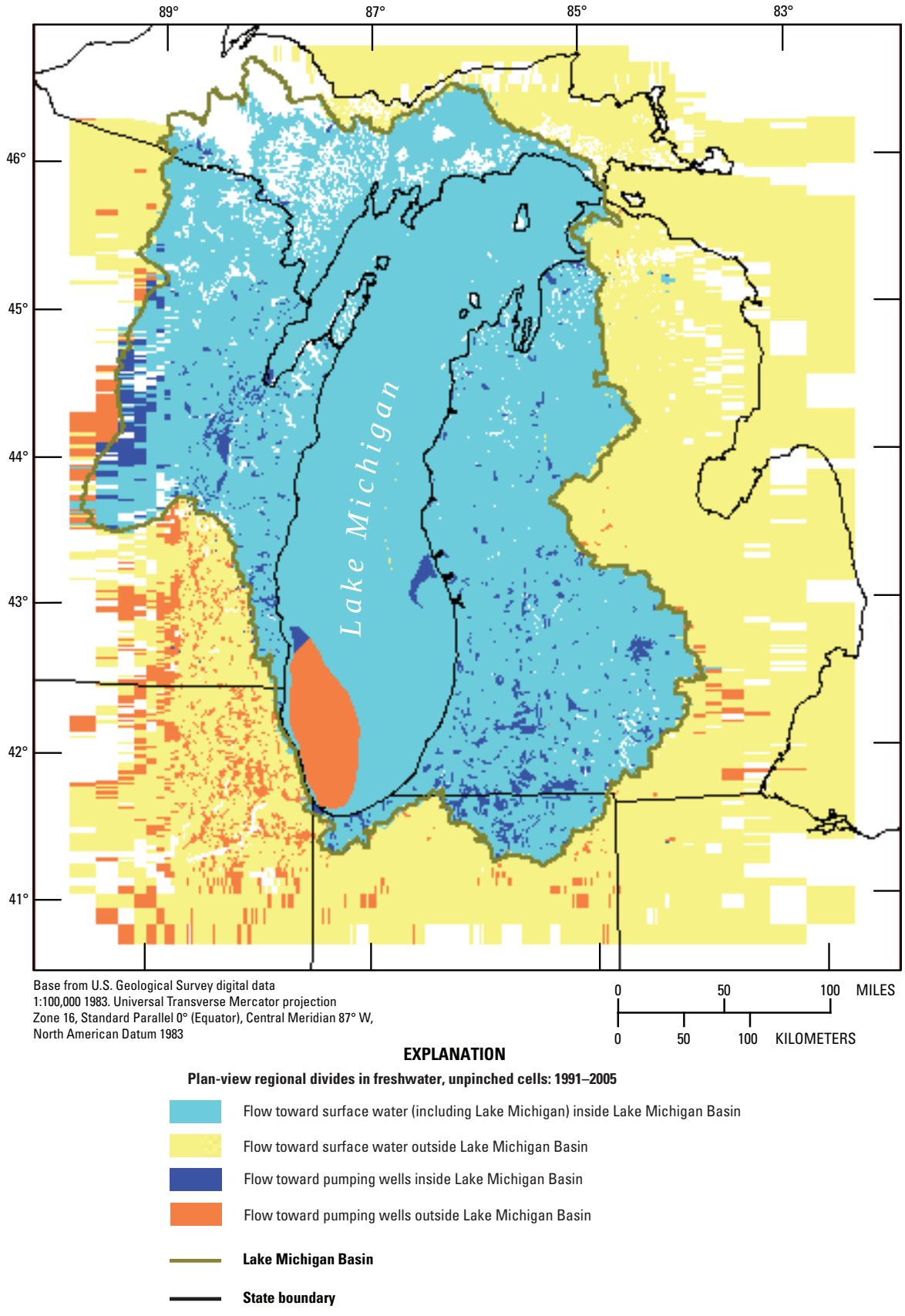

Figure 69*A*. Simulated groundwater basins, by aquifer system, for 1991–2005 conditions: QRNR (layer 1).

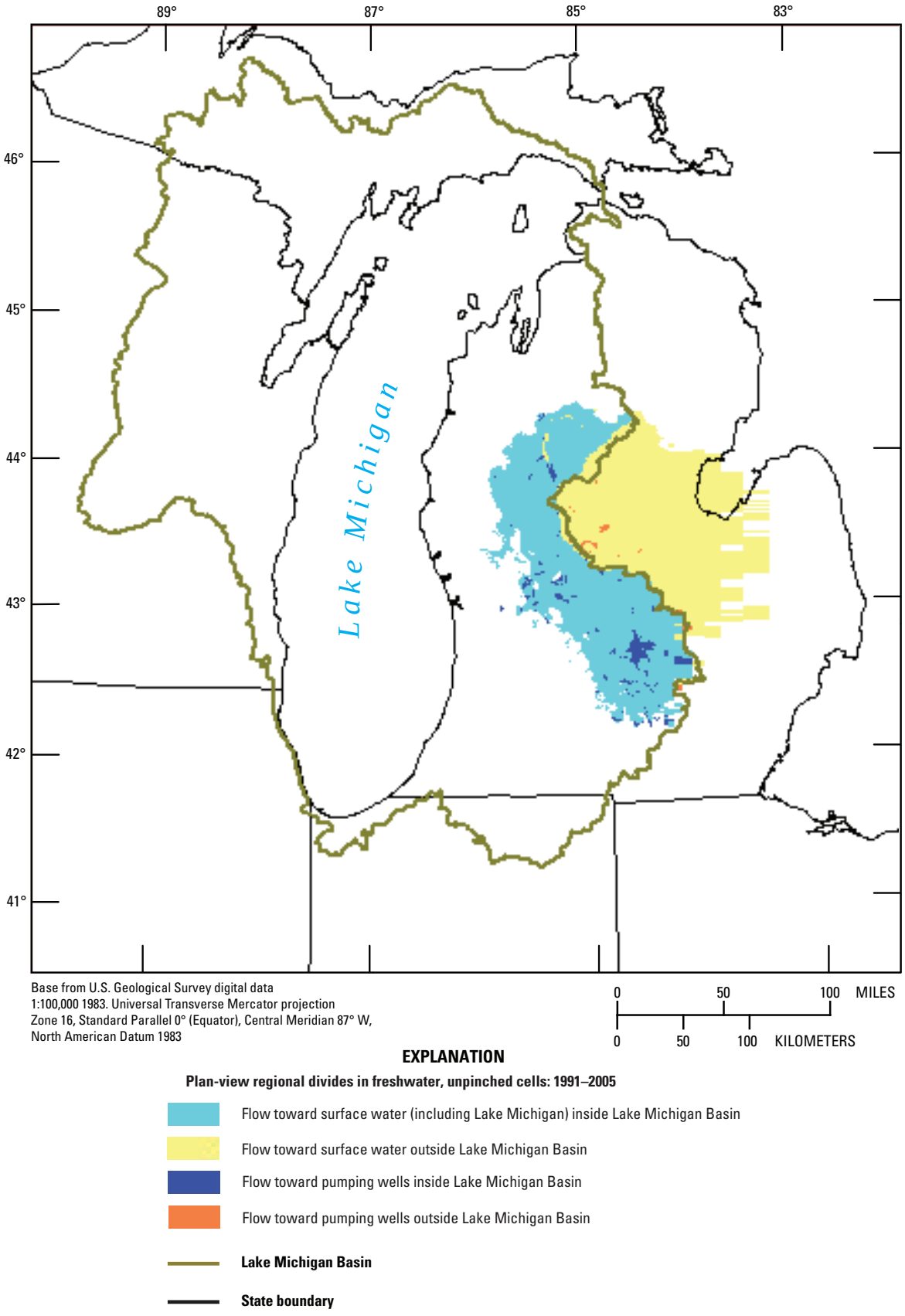

Figure 69*B*. Simulated groundwater basins, by aquifer system, for 1991–2005 conditions: PENN (layer 5).

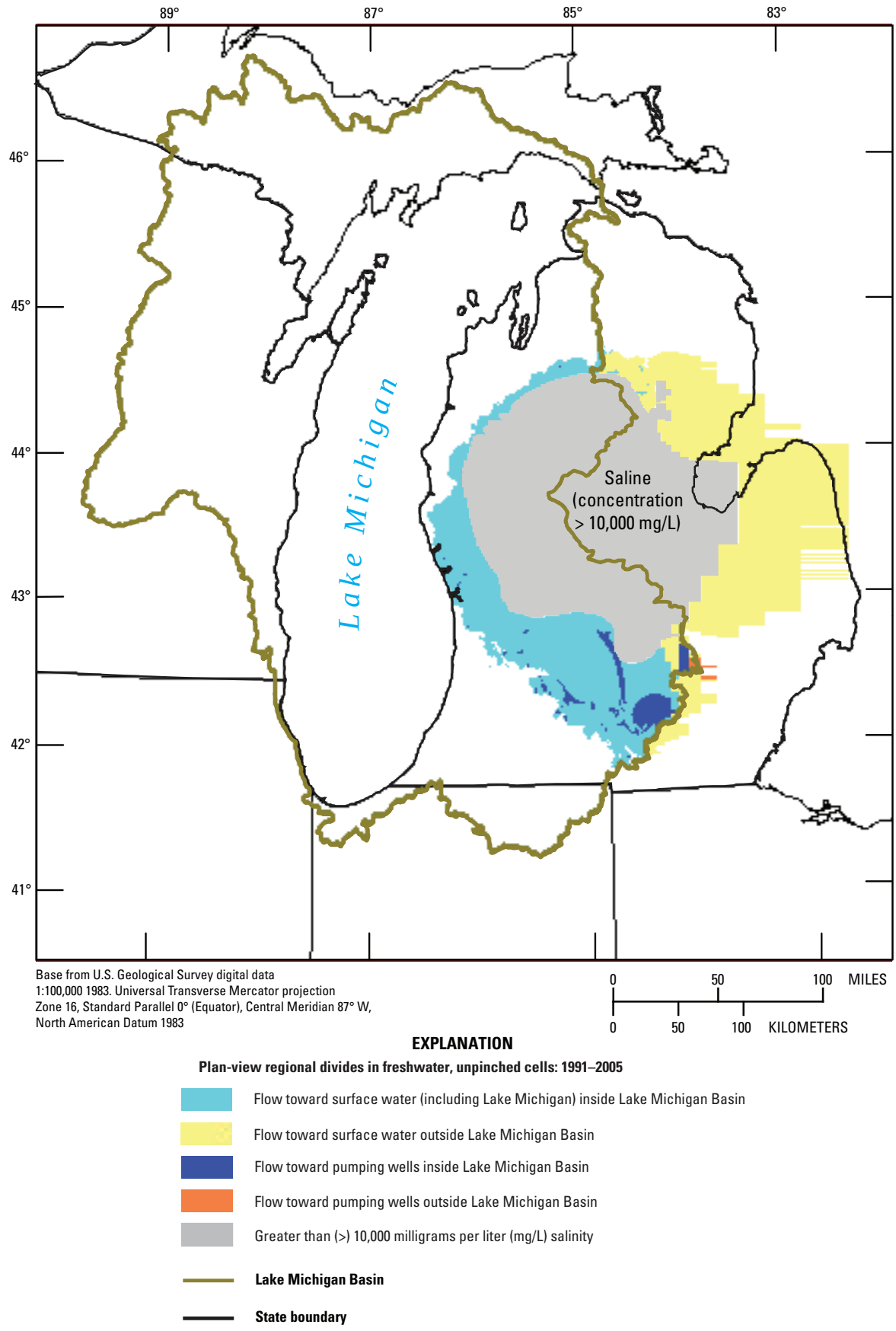

Figure 69*C*. Simulated groundwater basins, by aquifer system, for 1991–2005 conditions: MSHL (layer 8).

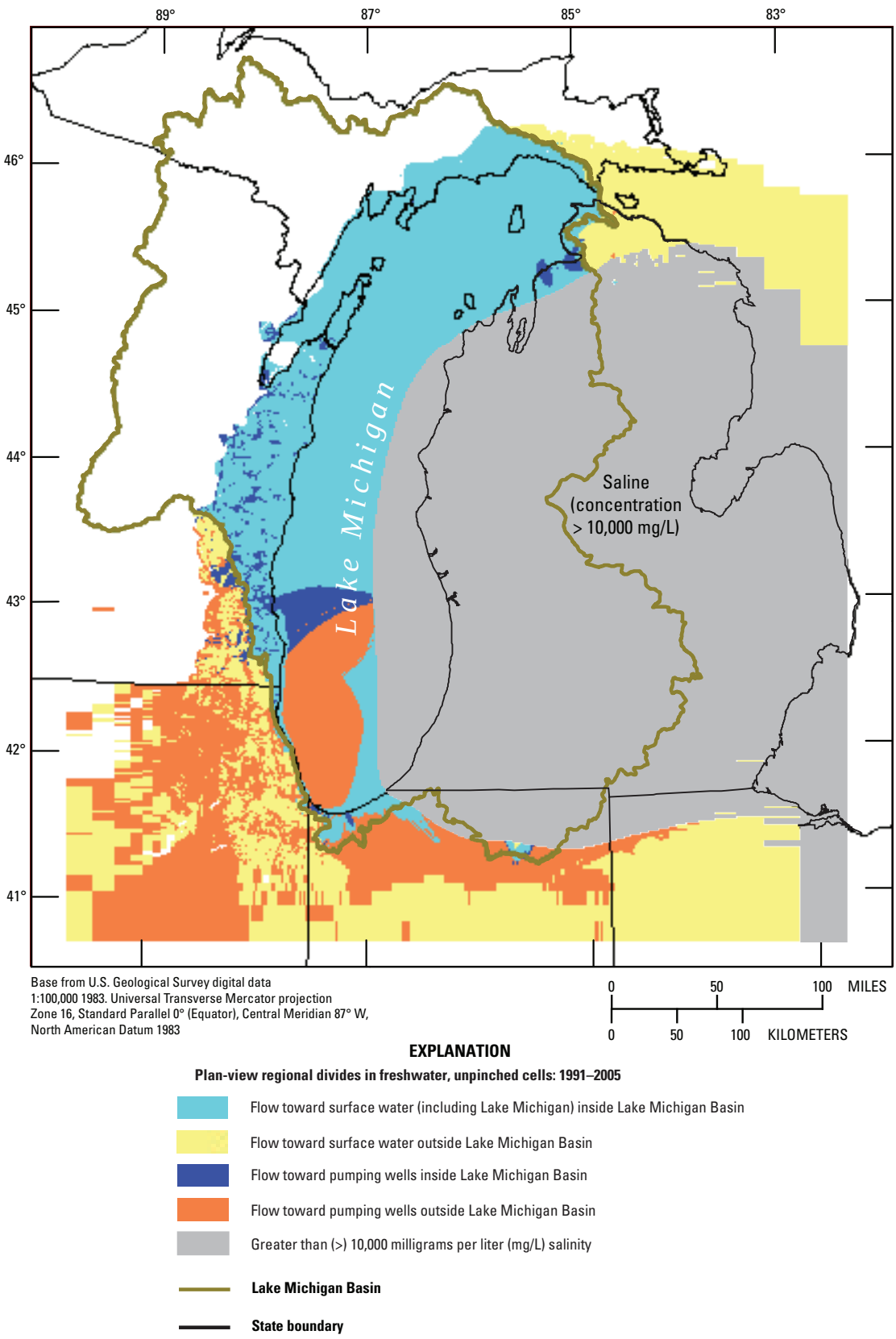

Figure 69*D*. Simulated groundwater basins, by aquifer system, for 1991–2005 conditions: SLDV (layer 10).

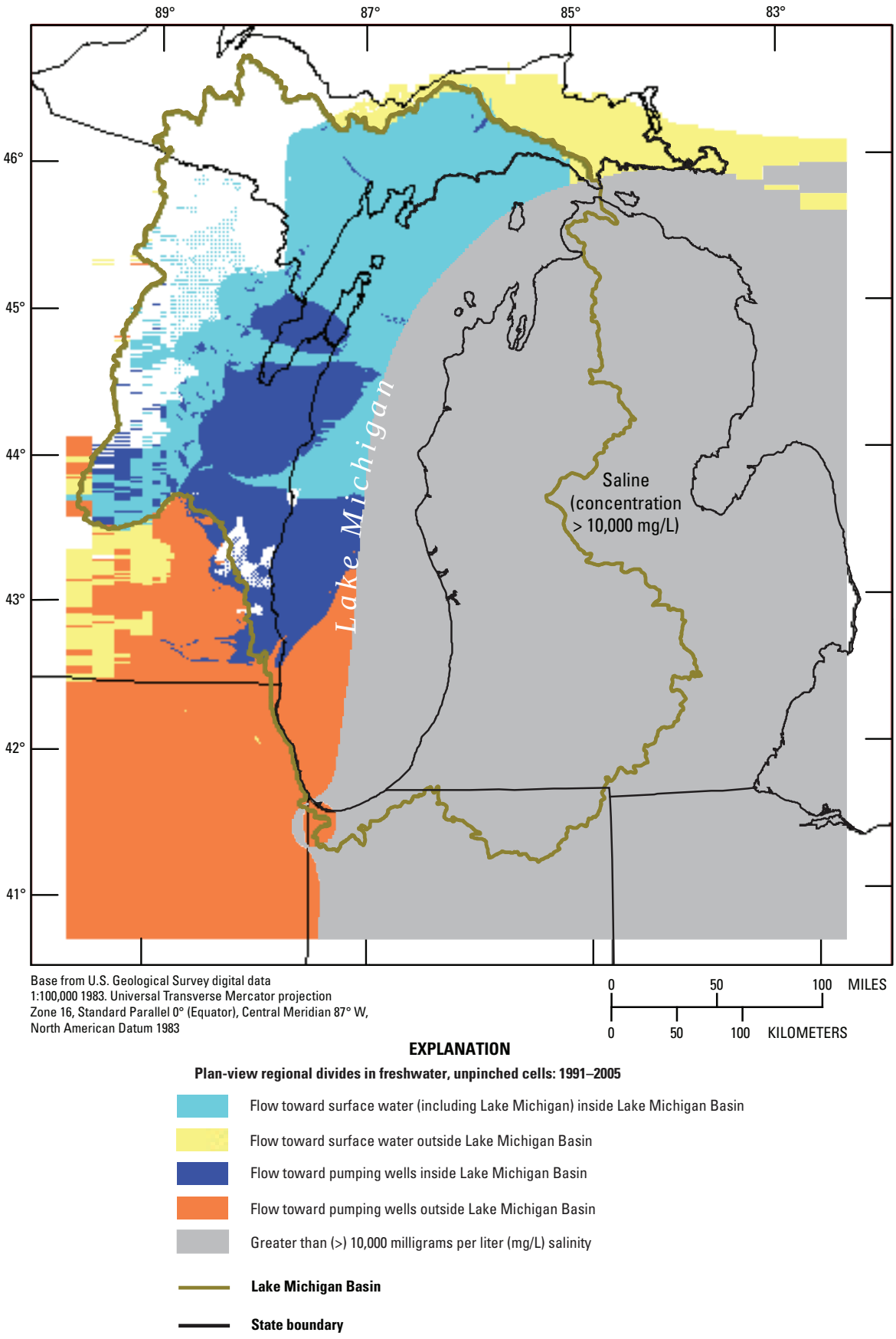

Figure 69*E*. Simulated groundwater basins, by aquifer system, for 1991–2005 conditions: C-O (layer 17).

6.6 Groundwater Interactions with Lake Michigan

A key objective of the LMB model is to provide a comprehensive account of groundwater interactions with Lake Michigan. The model encompasses the entire lake and simulates shallow and deep flow across its entire shoreline under various stress conditions. The results selected for presentation are intended to summarize the interactions between two important regional water resources, one surface and one subsurface.

A distinction is made between groundwater that enters Lake Michigan directly through the lakebed and indirectly through base flow into streams tributary to the lake. Both groundwater quantities, direct and indirect, contribute to the Lake Michigan budget. Both are influenced by climate variability and by ongoing well withdrawals.

The water-budget analysis presented earlier (fig. 57) indicates that simulated *direct discharge* of groundwater to Lake Michigan under predevelopment conditions (218 Mgal/d) is 1.2 percent of the total simulated inflow for the Lake Michigan Basin (18,318 Mgal/d). In 2005, the direct discharge (216 Mgal/d) is 1.1 percent of the total inflow (19,313 Mgal/d). The *total discharge* (*indirect and direct*) under predevelopment conditions equals the total inflow to the groundwater system because there are no other sinks for groundwater and net lateral flow to the basin is positive. By 2005, the simulated total discharge to the combined features of the Lake Michigan surface-water network (18,720 Mgal/d) captures 96.9 percent of the total groundwater inflow to the basin, whereas most of the remaining 3.1 percent of the inflow is captured by pumping.

According to the model, most of the *direct discharge* occurs near the shoreline. Under predevelopment conditions, 68 percent of the direct discharge occurs within 5,000 ft of the shoreline and 83 percent occurs within first 15,000 ft (table 17). The dropoff with distance into the lake appears to be approximately exponential (fig. 70), in agreement with theory (McBride and Pfannkuch, 1975).

Particle tracking indicates that recharge areas (source areas) of groundwater that discharges within 15,000 ft of the lakeshore extend further from the west and north lakeshores than from the east and south lakeshores (fig. 71). The pattern, although probably influenced by differences in the density of the stream network and by transmissivity of the glacial sediments, could also be partly an artifact of model-grid resolution; this possibility is explored in section 7 (“Alternative Models and Model Sensitivity”).

In parts of NE_WI, SE_WI and NE_ILL, the source areas of direct discharge to Lake Michigan for predevelopment conditions (fig. 71*A*) are somewhat wider than for 1991–2005 conditions (fig. 71*B*). The difference is due to the diversion of groundwater through pumping from shallow wells in the QRNR and SLDV aquifer systems.

Table 17. Predevelopment groundwater discharge to offshore Lake Michigan.

[Values correspond to the confined model, SLMB-C]

Area receiving discharge	Amount of discharge (million gallons per day)	Percentage of total
Total direct discharge to Lake Michigan	217.9	--
Discharge to first 5,000-foot-wide offshore ring	147.9	67.9l
Discharge to second 5,000-foot-wide offshore ring	24.9	11.4l
Discharge to third 5,000-foot-wide offshore ring	7.8	3.6l
Discharge to 15,000-foot-wide offshore ring	180.6	82.9l

Pumping from deep wells also has an effect on groundwater that, in predevelopment times, flowed from Wisconsin and Illinois eastward toward Lake Michigan through the C-O aquifer system and then discharged to the interior of the lake. To quantify the changing shallow and deep components of the system, it is helpful to characterize direct groundwater interactions with Lake Michigan not only in terms of direct discharge into nearshore areas but also by vertically integrating flow that passes under the shoreline toward the lake. The simulated rate of *shoreline discharge* varies appreciably with location; more than that, the rate and even the direction of flow changes as a function of time.

Under predevelopment conditions, flow under the shoreline ranges from less than 0.05 Mgal/d to almost 5 Mgal/d per 5,000 ft linear length (fig. 72*A*), equivalent to a range of 0.08 to 7.7 ft^3/s per mile of shoreline; the average value is 0.22 Mgal/d or 0.35 ft^3/s per mile of shoreline.

The rates simulated by the model are a complicated interplay of local-recharge, stream-density, and hydraulic-conductivity inputs. *Shoreline inflow* induced from Lake Michigan to the predevelopment groundwater system is restricted to peninsulas in the NLP_MI (fig. 72*B*). Maps of shoreline discharge to the lake and induced flow from the lake for 1980 (figs. 72*C*, *D*) show pronounced changes relative to predevelopment conditions, in large measure because of the increase in recharge computed after 1970. The average outflow rate for 1980 increased to 0.23 Mgal/d (0.36 ft^3/s) per 5,000 ft of shoreline. Development also exerted some pressure: for parts of the shore in SE_WI and NE_ILL, shallow and deep pumping caused the direction of groundwater flow to reverse from outflow toward the lake to inflow from the lake. The maps of shoreline outflow and inflow for 2005 (figs. 72*E*, *F*) show some effect on local rates from fluctuations in recharge and recovery of inland water levels with reduced deep pumping in NE_ILL; however, the average outflow rate is again 0.23 Mgal/d (0.33 ft^3/s) per 5,000 ft of shoreline.

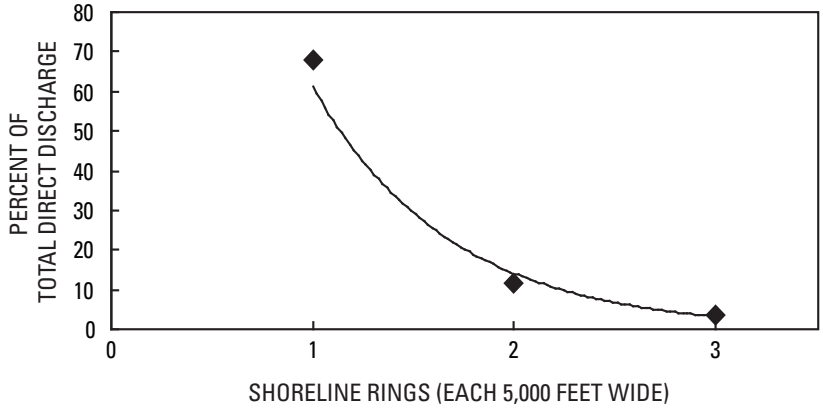

Figure 70. Percentage of total direct discharge to Lake Michigan for nearshore rings. (First nearshore ring extends 5,000 feet from shore. Second ring extends 5,000–10,000 feet from shore. Third ring extends 10,000–15,000 feet from shore. Curve is exponentially declining trendline.)

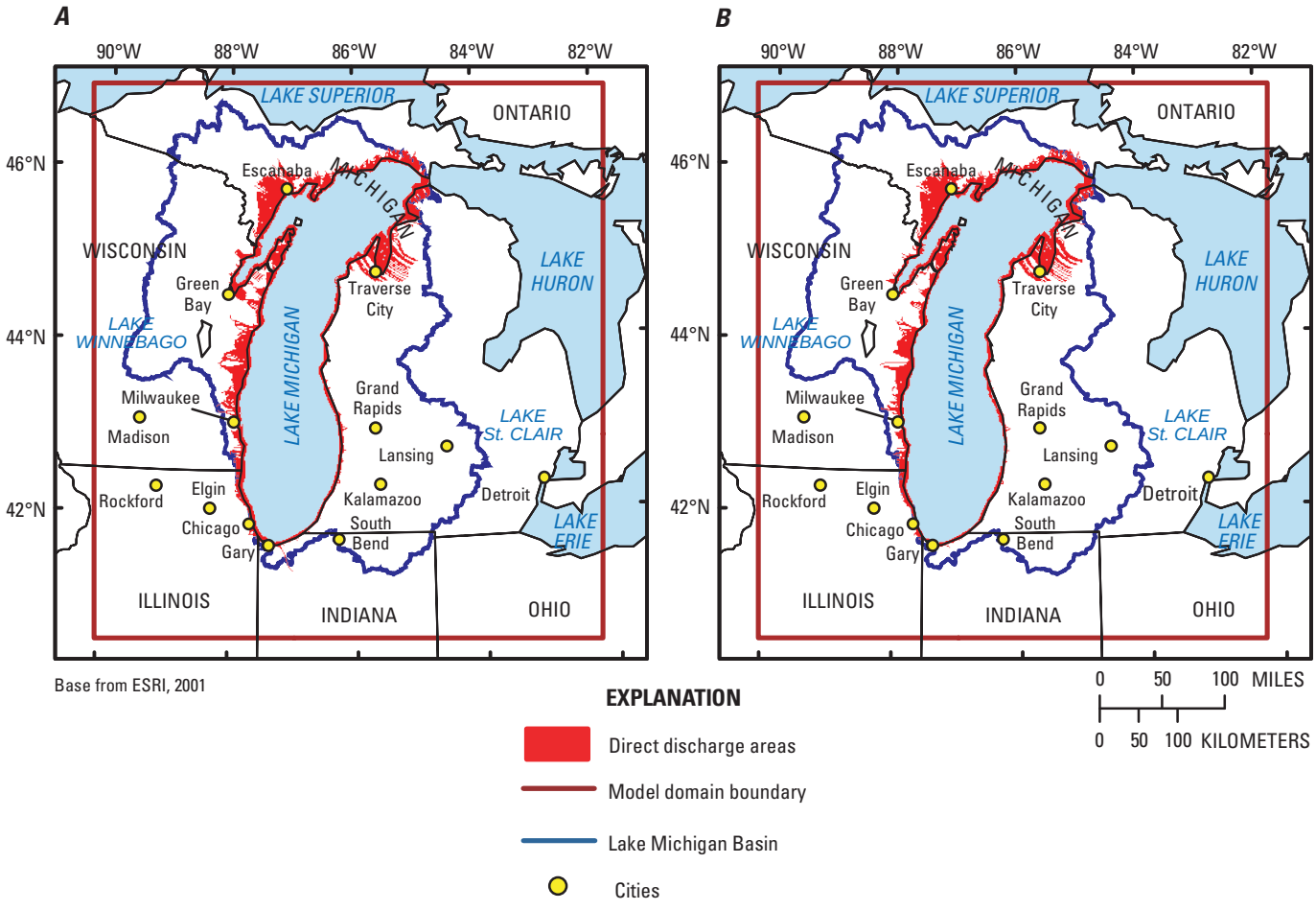

Figure 71. Simulated contributing areas for direct discharge to nearshore of Lake Michigan: *A*, Predevelopment. *B*, 1991–2005.

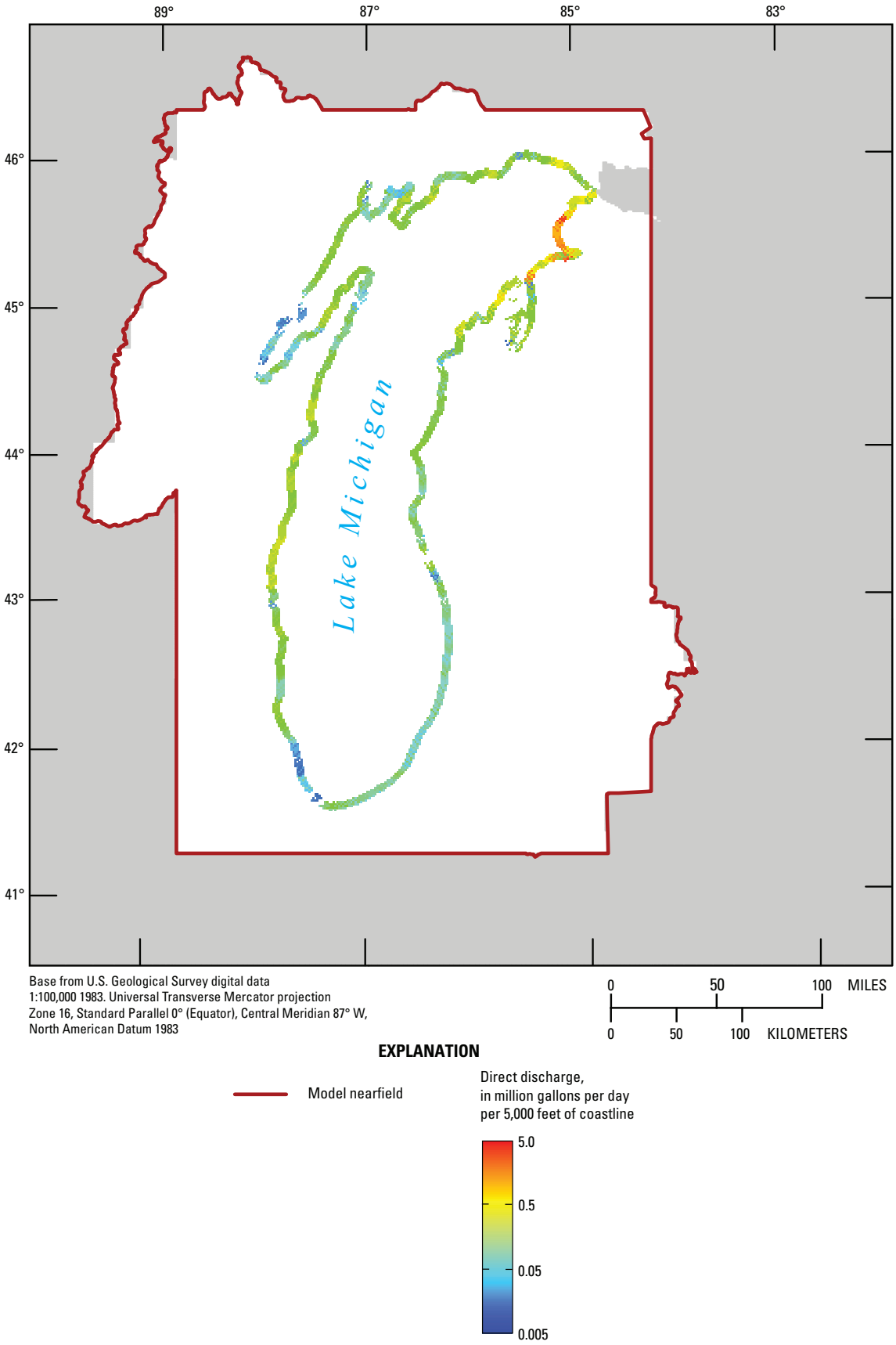

Figure 72*A*. Simulated shoreline outflow (from groundwater to Lake Michigan): Predevelopment.

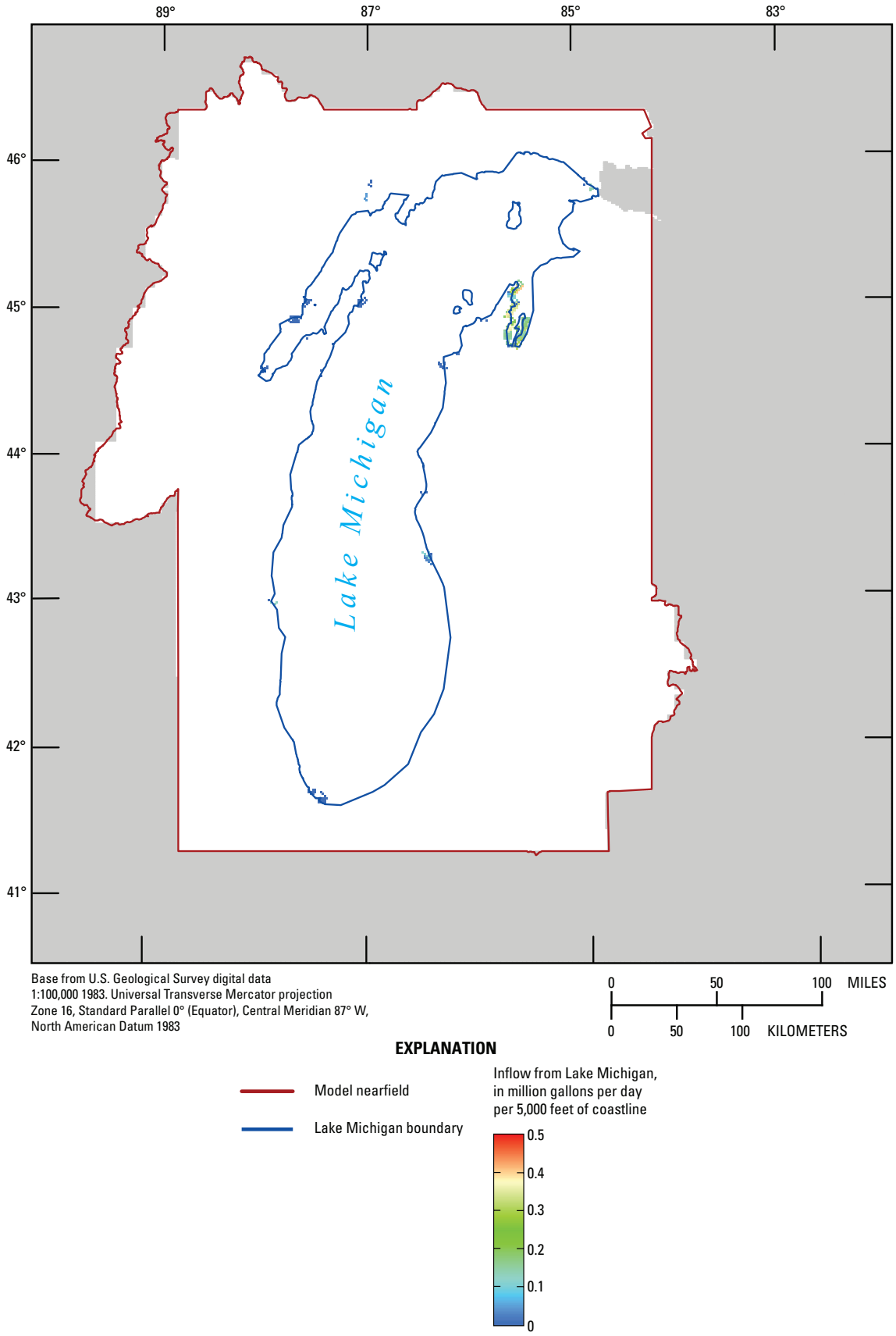

Figure 72*B*. Simulated shoreline inflow (from Lake Michigan to groundwater): Predevelopment.

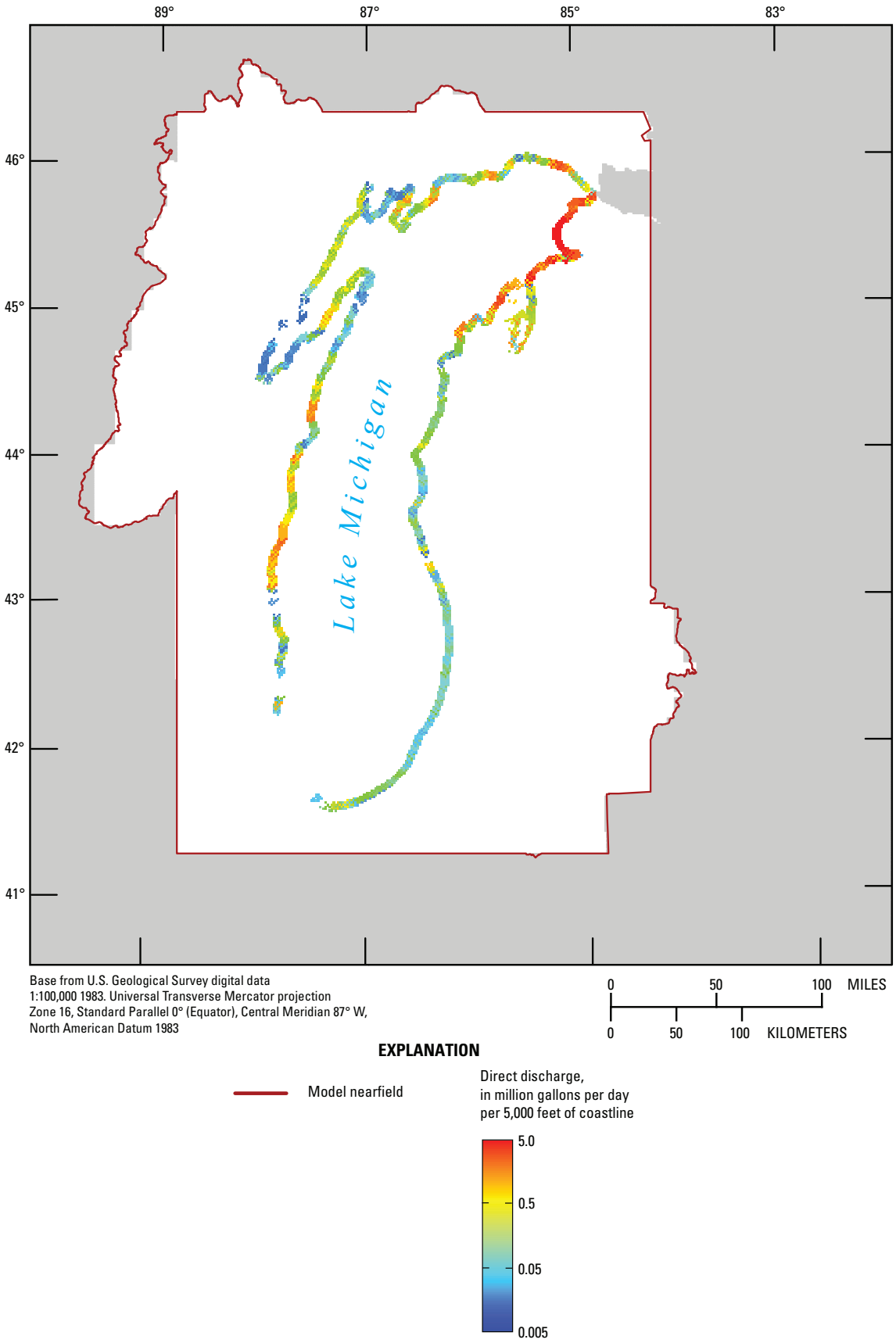

Figure 72*C*. Simulated shoreline outflow (from groundwater to Lake Michigan): 1980.

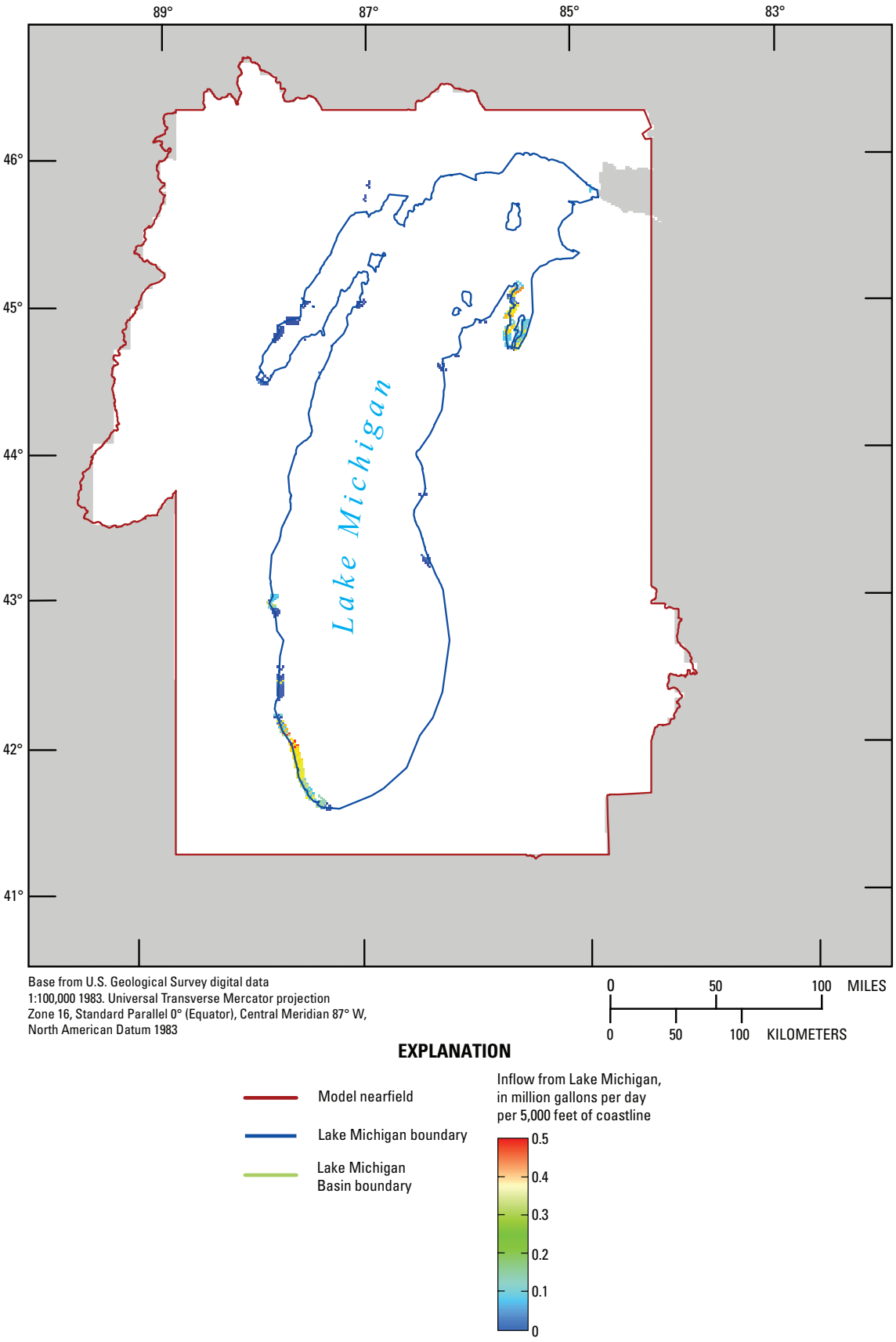

Figure 72*D*. Simulated shoreline inflow (from Lake Michigan to groundwater): 1980.

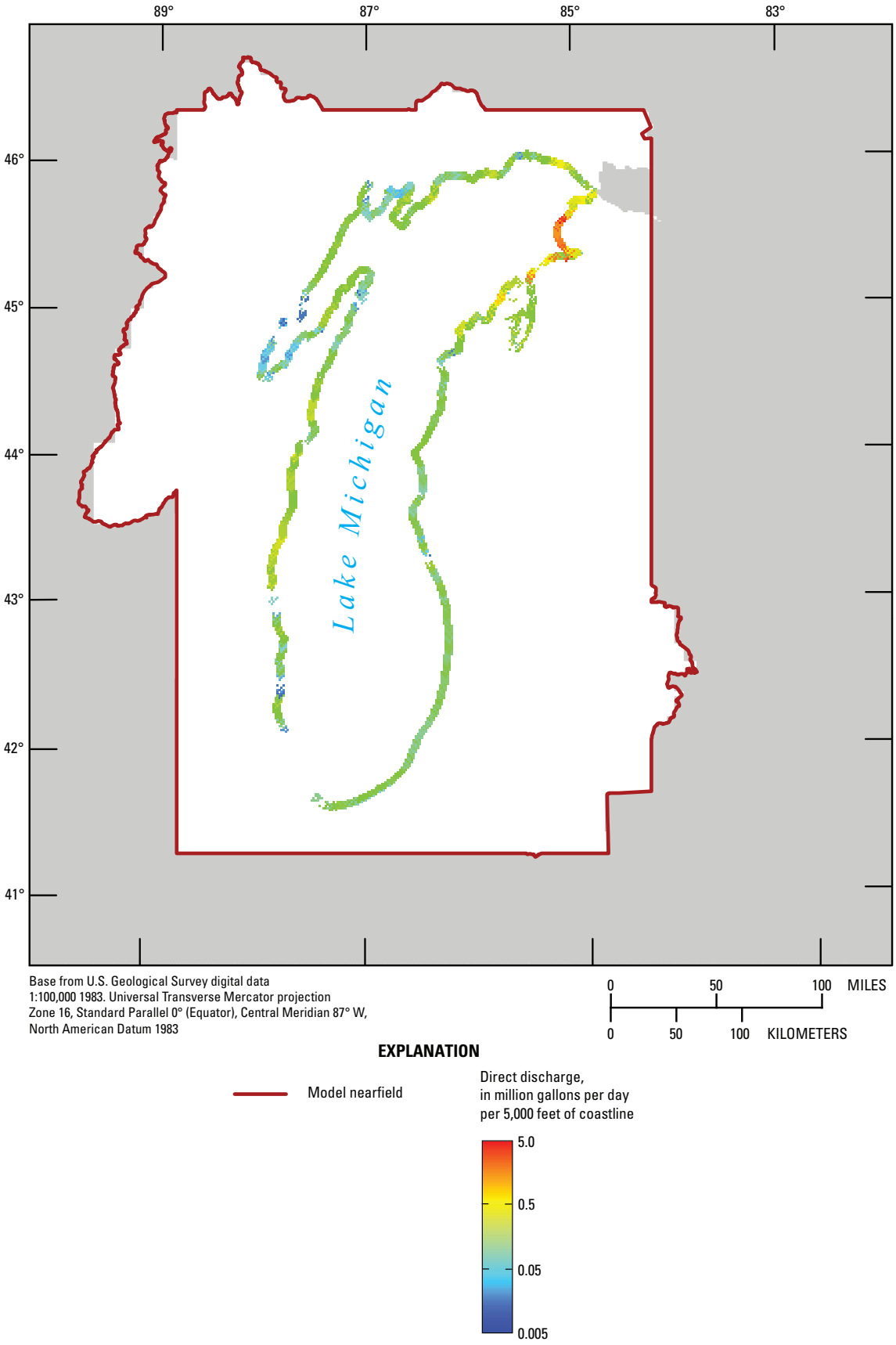

Figure 72*E*. Simulated shoreline outflow (from groundwater to Lake Michigan): 2005.

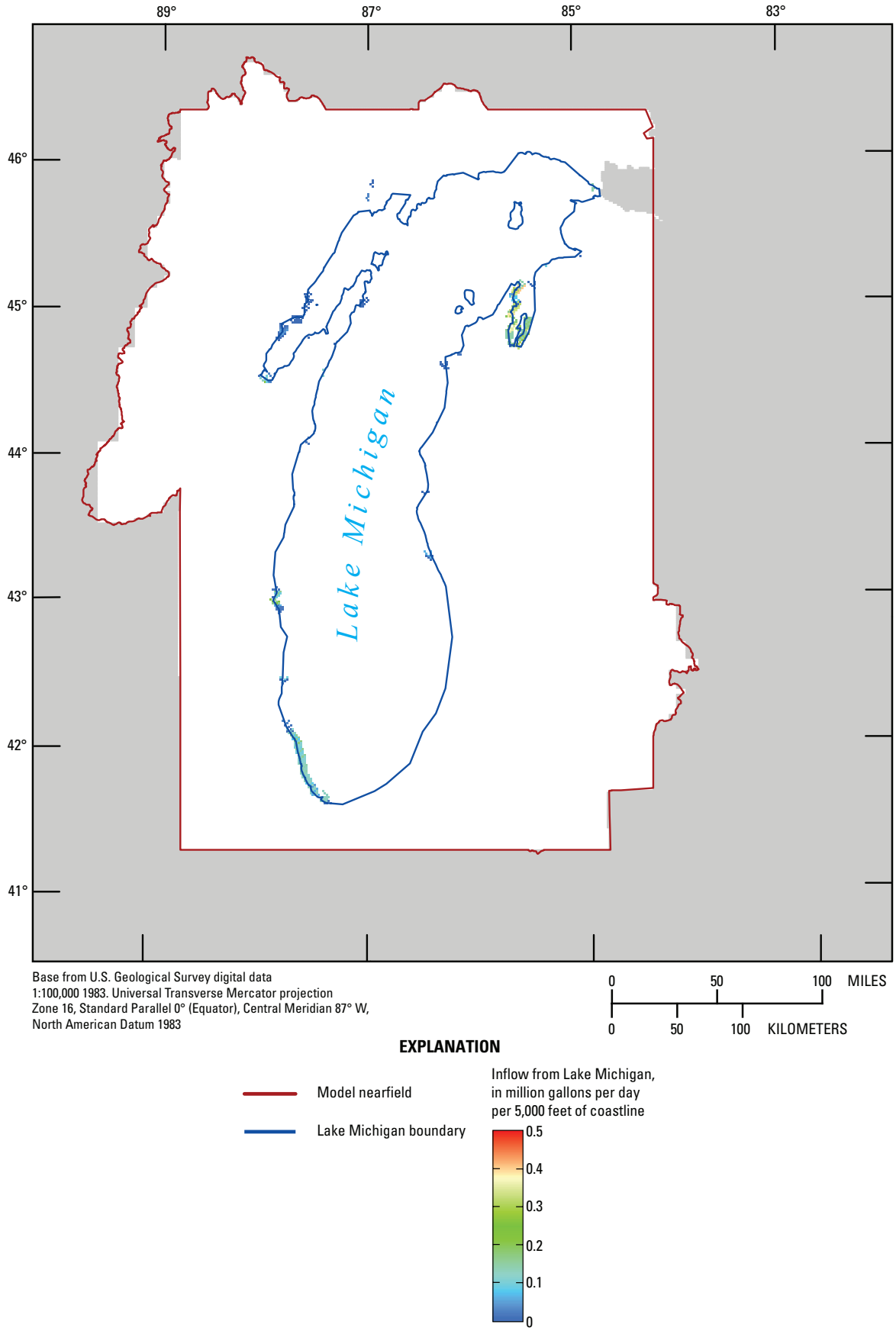

Figure 72*F*. Simulated shoreline inflow (from Lake Michigan to groundwater): 2005.

The same method employed previously to identify the sources of water to wells by comparing water budgets for natural and pumped condition was used to calculate the effect of pumping on direct discharge to the lake. Direct discharge to Lake Michigan is correlated with the trend of groundwater withdrawals from the model nearfield.[31] In 1950, the reduction in direct discharge to Lake Michigan served as a source of water pumped by wells totaling 4.1 Mgal/d, or 2.1 percent of total nearfield withdrawals (table 18). The reduction in discharge increases with time to more than 14 Mgal/d by 2005; however, the relative contribution is lower (1.8 percent of nearfield pumping in 2005) (table 18). When increased induced flow from Lake Michigan is added to the reduced discharge, the lake's relative contribution to well withdrawals becomes slightly larger (last column in table 18). All these findings are subject to an important qualification: the model does not include any return-flow component, such as wastewater-treatment plants that route pumped water after use back to Lake Michigan and possibly neighboring drainage basins. It is possible that most of the simulated reduction in direct discharge and net direct discharge to the lake is, in fact, returned, but at a different time, location, and temperature than would occur in the absence of pumping.

The contribution to pumping derived from *indirect discharge* to Lake Michigan via diverted base flow and induced flow from streams and diverted base flow from inland water bodies is much greater than the contribution attributable to net changes in *direct discharge* alone. The difference is evident when the total contribution (indirect plus direct) to pumping is calculated for the entire surface-water network, including Lake Michigan (last column of table 19). The change in the rate of groundwater interactions with the nearfield surface-water network (that is, the sum of reduced base flow and increased induced flow) accounts in the 1940 to 1985 period for about 75 to 80 percent of water flowing to nearfield wells. Subsequent to Lake Michigan diversions for water supply in NE_ILL, reduced base flow and increased induced flow account for around 90 percent or more of water flowing to nearfield wells. The percentage of nearfield pumping derived strictly from reduced direct discharge to Lake Michigan generally is between 1 and 2 percent. The remaining sources of water (storage release, lateral inflow to the nearfield) provide between 10 and 25 percent of the well discharge depending on the period.

[31] The model nearfield is used in place of the Lake Michigan Basin as the area over which to calculate the effect of pumping on groundwater interactions with Lake Michigan and also with inland surface water. This larger area is used because pumping from outside the Lake Michigan Basin (notably in SE_WI and NE_ILL) has an effect on the exchange between groundwater and the lake.

Table 18. Effect of nearfield pumping on simulated direct groundwater discharge to Lake Michigan.
[Values correspond to the confined model, SLMB-C; Mgal/d, million gallons per day]

Stress period	Date	Net pumping in model nearfield (net of injection) (Mgal/d)	Source: reduced direct discharge *to* Lake Michigan (Mgal/d)	Source: reduced direct discharge *to*, plus increased induced flow *from*, Lake Michigan (Mgal/d)
1	Predevelopment	0.00	0.00	0.00
2	Oct. 1864–Oct. 1900	16.04	.04	.04
3	Oct. 1900–Oct. 1920	56.19	.62	.62
4	Oct. 1920–Oct. 1940	114.62	2.39	2.53
5	Oct. 1940–Oct. 1950	194.16	4.14	4.62
6	Oct. 1950–Oct. 1960	280.43	5.76	6.80
7	Oct. 1960–Oct. 1970	466.98	6.59	7.23
8	Oct. 1970–Oct. 1975	617.10	6.86	8.08
9	Oct. 1975–Oct. 1980	708.37	7.51	9.21
10	Oct. 1980–Oct. 1985	769.31	8.27	10.18
11	Oct. 1985–Oct. 1990	725.49	8.94	11.19
12	Oct. 1990–Oct. 2000	821.38	14.24	16.31
13	Oct. 2000–Oct. 2005	814.37	14.37	16.46

Notes:

1. Net pumping is pumping minus injection. The model simulates injection at only one location (near Kalamazoo, Mich.), where it amounts to about 10 Mgal/d in 2005.

2. Lake Michigan is represented by GHB nodes in the model. The flow to the GHB nodes represents the *direct* discharge to the lake (that is, groundwater flow that discharges directly to the lake rather than indirectly through surface-water bodies that are tributary to the lake.)

3. Because recharge changes between stress periods, it is not possible to use the change in direct discharge to Lake Michigan simulated by the model over time to isolate the effect of changes in pumping on direct discharge. Instead, the effect of pumping is calculated by comparing a simulation *without* pumping to a simulation *with* pumping and computing the difference in the flow to the GHB nodes representing Lake Michigan.

4. Because pumping can induce flow from Lake Michigan landward (that is, out of GHB nodes), it is also possible to calculate the net direct discharge to Lake Michigan (that is, discharge minus induced flow) and the change in the net direct discharge due to pumping. Because the induced flow increases with pumping, the reduction in net direct discharge due to pumping is greater than the reduction in direct discharge.

5. It is important to note that the model does not include any return-flow component such as, for example, wastewater-treatment plants that route pumped water after use back to Lake Michigan. It is possible that most of the simulated reduction in direct discharge and net direct discharge to the lake is, in fact, returned, but at a different time, location, and temperature than under predevelopment (natural) conditions.

Table 19. Effect of nearfield pumping on total (direct plus indirect) groundwater discharge to Lake Michigan.
[Values correspond to the confined model, SLMB-C; Mgal/d, million gallons per day]

Stress period	Date	Net pumping in model nearfield (net of injection) (Mgal/d)	Source: reduced total discharge (direct and indirect) *to* nearfield surface water (Mgal/d)	Source: reduced total discharge (direct and indirect) *to*, plus increased induced flow *from*, nearfield surface water (Mgal/d)
1	Predevelopment	0.00	0.00	0.00
2	Oct. 1864–Oct. 1900	16.04	9.08	9.96
3	Oct. 1900–Oct. 1920	56.19	23.06	27.14
4	Oct. 1920–Oct. 1940	114.62	60.21	70.67
5	Oct. 1940–Oct. 1950	194.16	115.68	139.08
6	Oct. 1950–Oct. 1960	280.43	176.55	218.60
7	Oct. 1960–Oct. 1970	466.98	282.95	373.64
8	Oct. 1970–Oct. 1975	617.10	374.02	464.29
9	Oct. 1975–Oct. 1980	708.37	409.04	539.70
10	Oct. 1980–Oct. 1985	769.31	499.59	621.77
11	Oct. 1985–Oct. 1990	725.49	501.30	642.64
12	Oct. 1990–Oct. 2000	821.38	611.32	781.07
13	Oct. 2000–Oct. 2005	814.37	613.49	785.35

Explanation:

1. Net pumping is pumping minus injection inside the Lake Michigan topographic basin. The model simulates injection at only one cluster of locations (near Kalamazoo, Mich.), where it amounts to about 10 Mgal/d in 2005.

2. Lake Michigan is represented by GHB nodes in the model. Inland surface-water bodies inside the Lake Michigan Basin (streams plus lakes plus wetlands) are represented by RIV nodes. The flow to the GHB and RIV nodes represents the total discharge to the lake (that is, groundwater flow that discharges directly to the lake plus groundwater flow that discharges indirectly through surface-water bodies that are tributary to the lake). All inland surface-water bodies represented in the model inside the Lake Michigan topographic basin are considered tributary to Lake Michigan.

3. Because recharge changes between stress periods, it is not possible to simply use the change in total discharge to Lake Michigan simulated by the model over time to evaluate the effect of changes in pumping on discharges. Instead, the effect of pumping is calculated by comparing a simulation *without* pumping to a simulation *with* pumping and computing the difference in the flow to the GHB nodes representing Lake Michigan and the RIV nodes representing inland surface-water bodies.

4. Because pumping can induce flow from Lake Michigan landward and from surface-water bodes into groundwater (that is, out of GHB nodes and out of RIV nodes), it is also possible to calculate the net total discharge to Lake Michigan (that is, discharge minus induced flow) and the change in the net total discharge due to pumping. Because the induced flow increases with pumping, the reduction in net total discharge is greater than the reduction in total discharge.

5. It is important to note that the model does not include any return-flow component such as, for example, wastewater-treatment plants that route pumped water after use back to Lake Michigan. It is possible that most of the simulated reduction in direct discharge and net direct discharge to the lake is, in fact, returned, but at a different time, location, and temperature than under predevelopment (natural) conditions.

7. Alternative Conceptual Models and Model Sensitivity

Much can be learned about the dynamics of a groundwater-flow system by modifying assumptions built into a selected modeling approach. Some assumptions are linked to the conceptual model of the system, others to imposed boundary conditions and parameters, and yet others to the limitations of the solution algorithm linked to the regional grid spacing. For the groundwater-flow model of the Lake Michigan Basin, the robustness of model results was tested for the following elements of the model design:

- Alternative models—Change conceptual assumptions regarding confined versus unconfined flow, variable density, and fixed salinity concentrations.
- Input sensitivity—Change input assumptions regarding cell-by-cell variation of QRNR hydraulic conductivity, head-dependent and flux-specified farfield boundary conditions, lakebed hydraulic conductivity, and fixed stages of Lake Michigan and other Great Lakes.
- Grid-resolution sensitivity—Change assumptions regarding coarse representation of surface-water network along shoreline of Lake Michigan.

These tests are broad in scope insofar as they show the sensitivity of results not only to key parameter inputs but also to conceptual and geometric assumptions. The simulations, which sometimes involve simplifying model input and sometimes more sophisticated input, show both strengths and weaknesses of the implemented model design.

7.1 Alternative Models

The conceptual model for the calibrated, confined version of the LMB model (the "base" model) has two noteworthy assumptions:

1. Although parts of the flow system are truly unconfined, a confined version that approximates unconfined conditions by scaling inputs to take account of saturated thickness yields an adequate representation of the dynamics of the groundwater-flow system.
2. Although the distribution of salinity and fluid density gradients in the Michigan Basin is in theory subject to change in response to stresses such as pumping, the use of fixed concentration conditions in SEAWAT-2000 yields an adequate representation of the dynamics of the groundwater-flow system.

These sets of assumptions are tested with three alternative models. Each of the alternative models constructed poses advantages for certain types of applications. For this reason they, like the base SLMB-C model version, have been archived and can be distributed for later use.

7.1.1 Unconfined Version of Model

Two versions of the LMB model were calibrated: confined and unconfined. The confined model was adjusted to reflect actual unconfined conditions and employs a linearized version of the groundwater flow equation with concomittant advantages of shorter runtimes, smaller mass-balance error, fully saturated conditions, and no exclusion of pumping because of dry cells. These features facilitated the application of nonlinear regression in the parameter-estimation process. A separate calibration was done by using an unconfined model to generate a version of the LMB model capable of directly simulating unconfined conditions. Such a model version is particularly useful for simulations that focus on water availability in areas with declining saturated thickness and for construction of more finely discretized inset models within the regional model domain to simulate local interactions between shallow pumping and surface.

The unconfined version of the LMB model (SLMB-U) differs from the confined version (SLMB-C) in several ways:

- Storage in unconfined cells (all active cells in layer 1 and cells in underlying layers where the simulated water level is below the top of the cell) is proportional to specific yield rather than specific storage.
- The controlling storage variable is redefined for cells that convert from confined to unconfined—or vice versa—during the simulation.
- Transmissivity in unconfined cells varies during the simulation as a function of saturated thickness rather than remaining constant.[32]

The confined and unconfined models were subjected to the same calibration procedure, although the mass-balance error in the unconfined model was increased to provide manageable runtimes. The mass-balance error in the calibrated unconfined model is approximately twice as great as for the confined model, averaging about 0.2 percent for all time steps. The contribution of target sets to the calibration is similar for the confined and unconfined models (compare table 11*B* to table 11*A*). Both versions of the model were subjected to five regression iterations by using the same estimation techniques discussed in section 5. The model fit as reflected in the final values of the objective function differs little between the two calibrated models: 4.68 E5 confined versus 4.63 E5 unconfined. Comparison of calibration statistics for the two models (table 12) indicates that the agreement between measured and simulated targets is nearly equal, although the quality of the match is better for more target groups in the confined model.

[32] For the confined version of the LMB model, the specific storage and hydraulic conductivity are adjusted to take account of the saturated thickness in unconfined cells based on a trial simulation with initial inputs (see section 5). Also, it is worth noting that the vertical conductance term regulating vertical flow between layers is *not* a function of saturated thickness in *either* the confined or unconfined version of the LMB model.

In addition, when residuals at measured water-level targets are considered, the root mean squares error for the confined model (36.78 ft) is slightly lower than that for the unconfined version (37.57 ft).

The ranking of parameter groups by sensitivity is nearly identical in the two models (compare tables 13*A* and 13*B* and fig. 49*A*, *B*). The specific-yield parameters are relatively insensitive in the calibration of the unconfined model, and the final estimated values for specific yield nearly equal the initial values. The insensitivity of the specific-yield parameters is due to the constraints on the water-table solution imposed by the large number of RIV boundary-condition cells distributed throughout the model nearfield. Specifying a single specific-yield zone for all QRNR deposits probably also contributed to parameter insensitivity.

One way to compare the results of the unconfined model (SLMB-U) to the confined model (SLMB-C) is to inspect the parameter multipliers (appendix table A5–2). In general, the multipliers are very similar, but small differences exist for recharge, hydraulic conductivity, conductance, and storage. Two differences are worth noting:

- Slightly higher recharge in the unconfined model (multiplier on the initial value of 1.060 instead of 1.048 for the confined case).
- Slightly higher riverbed conductance terms in the unconfined model (maximum multiplier on an initial value equal to 2.3 instead of 1.5 for the confined case).

A systematic comparison of the calibration results for horizontal hydraulic conductivity involves computing the central tendency of values for the confined and unconfined models by aquifer system and by subregion (appendix 9). The biggest differences are evident for the K_h for the QRNR system, where the geometric mean is somewhat higher for the unconfined model in UP_MI, NE_WI, and SE_WI and the mean value is slightly lower in N_IND. There are small differences in the other aquifer systems, but in all instances the size of the difference between the two calibrated models is much less than the change from the initial values to calibrated values.

Two general conclusions can be drawn from the comparison of the confined and unconfined LMB models:

1. Even though more unreliable derivatives were fed to inversion routines in the unconfined as opposed to the confined case, the calibration processes produced similar calibration statistics and sensitivities for the two versions.
2. Whereas the calibrated inputs to the two models are not identical, the differences in parameter multipliers and resulting cell values generally are small.

One major difference between SLMB-U and SLMB-C is worth noting: The confined model simulation maintains all pumping input to the model, but the unconfined model loses pumping because of dry cells (where the water table falls below the bottom of a cell containing an active well, turning the cell inactive and eliminating any discharge assigned the cell). For SLMB-U, the loss amounts to about 2 percent of total net withdrawals by 2005 (21 Mgal/d of 1,095 Mgal/d) and 3 percent of 2005 net withdrawals from the Lake Michigan Basin (19 Mgal/d of 580 Mgal/d). The loss is concentrated in two nearfield subregions where withdrawals are predominantly from unconfined aquifers: the SLP_MI (more than 5 percent of pumping) and the NLP_MI (nearly 7 percent of pumping). It is possible that the exclusion of most first-order streams as internal model boundaries eliminates a source of water to wells, which contributes to overestimating drawdown in the unconfined model. It is certain that the coarse representation required by the regional scale results in misfit in some locations; in the *unconfined model*, misfits can result in dry cells and lost pumping, but in the *confined model*, misfits cannot result in lost pumping even though the simulated water level is below the cell bottom. By keeping wells in the affected cells active, the confined model provides a better account of the expected effect of known pumping on base-flow reduction and other water-budget terms, but at the possible cost of maintaining aquifer properties that are unreasonable in the vicinity of the wells.

Shifting from calibration to model results, it is instructive to compare the unconfined and confined versions of the LMB model with respect to the 2005 water budget, predevelopment heads, 2005 drawdown, and water-level hydrographs at pumping centers. Special attention is required to interpret the differences between the models when it is a question of dewatered conditions in the deep flow system.

The 2005 Lake Michigan Basin water budgets for the confined and unconfined models show identical overall patterns with small variations (fig. 73). The total recharge is slightly greater (1 percent) for SLMB-U than for SLMB-C, owing to the larger multiplier estimated for the unconfined model, whereas all the other inflow terms are slightly greater for the confined model, including storage. With respect to the outflow terms, total 2005 pumping is 3 percent lower for the unconfined model due to pumping lost from dry cells (although loss of pumping through 1990 in the unconfined model is less than 0.2 percent), whereas the distribution of discharge among surface-water features shifts slightly in favor of the inland water bodies (lakes and wetlands as opposed to streams) in the unconfined model. Direct groundwater discharge to Lake Michigan is virtually identical for the two simulations. Perhaps the most interesting difference between the model water budgets is the relative size of the storage terms. For stress periods after 1940, the average amount of storage release in the unconfined model is only two-thirds the release in the confined model; the average amount of unconfined storage gain is only about six-tenths the confined gain. It is hard to know the extent to which the smaller storage change in the unconfined case reflects smaller average fluctuations in water levels or, alternatively, smaller storage factors applied to the water-level changes.

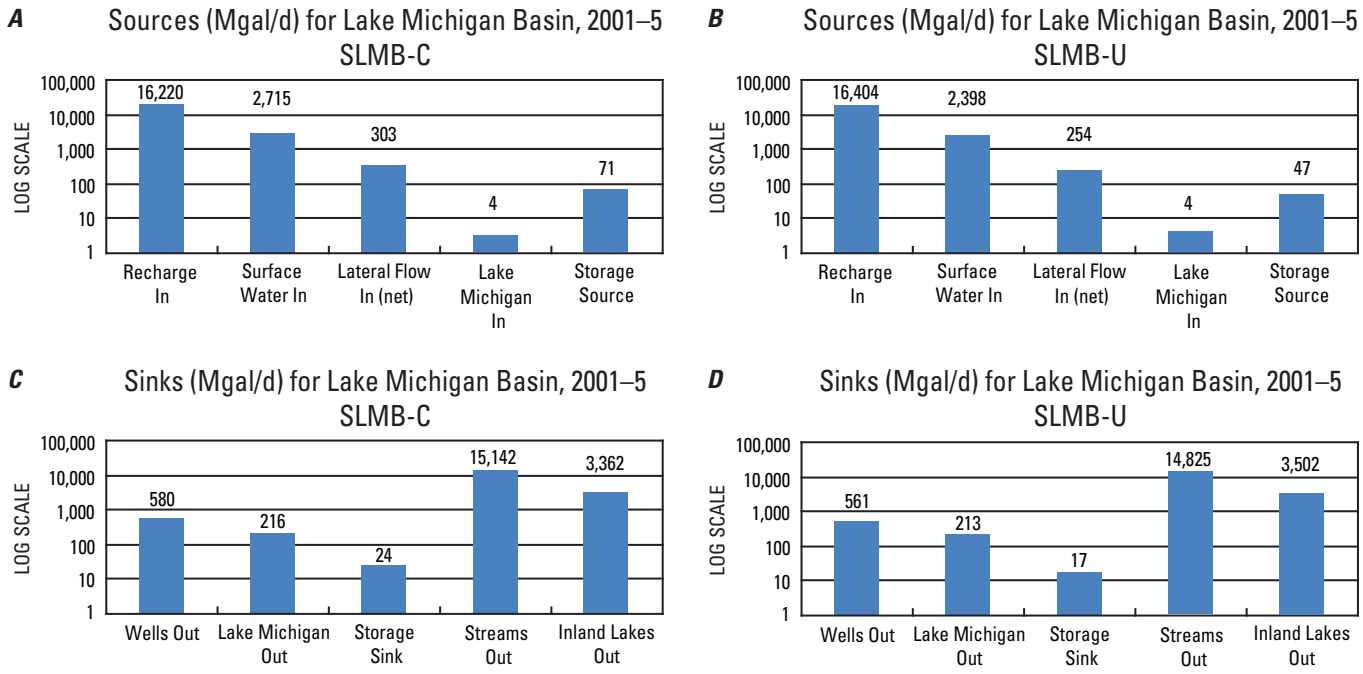

Figure 73. Simulated 2005 water budgets in Lake Michigan Basin: base model (SLMB-C) versus alternative unconfined model (SLMB-U).

Larger differences are apparent in water levels and drawdowns simulated by the two models. To facilitate the comparisons, it is convenient to tabulate by aquifer system the percentage of the model nearfield with differences greater than 20 ft (tables 20 and 21, first data column). This threshold is selected because it is roughly equal to (but less than) the Mean Absolute Error attributable to water-level residuals for the confined model calibration (25 ft). For predevelopment conditions, the unconfined model simulates a higher water table (almost 1 percent of the QRNR system) but lower water levels in some deep system (almost 2 percent of the MSHL system). There are also differences at the 20-foot threshold with respect to 2005 drawdown: the contrast is most marked in the C-O aquifer system, where drawdown in more than 3 percent of the unpinched cells in the unconfined model is lower than in the confined model. Water-level hydrographs at four selected pumping centers (locations shown in fig. 54) provide additional insight into the degree to which the two head solutions diverge. The trends appear very similar for the MSHL pumping center near Lansing, Mich., for the C-O pumping center around Green Bay, Wis., and also for the C-O pumping center in southeastern Wisconsin (compare fig. 74*A* to 74*B*). Drawdowns in northeastern Illinois simulated by the unconfined and confined models are different. Two comments are appropriate in this context. First, calibration statistics (table 12) indicate that the confined model more closely matches observed water levels, drawdown, and recovery for the C-O aquifer system in northeastern Illinois than does the unconfined model. Second, the difference in the slopes in the water-level hydrographs for the confined and unconfined models (compare fig. 74*A* to 74*B*) reflects the storage properties in the two models. In the unconfined model, storage release is small as long as the water column remains saturated because specific storage controls the release of water (equal to thickness multiplied by 1.6 E−7 ft^{-1} once the parameter multiplier of 0.636 is applied to the initial specific storage value of 2.6 E−6 ft^{-1}; see appendix 5, table A5–2). However, once a second water table emerges at depth due to dewatering at the top of the C-O aquifer system at the center of the NE_ILL pumping center, storage release is controlled by the specific yield (equal to either 4.4 E−3 or 4.4 E−2 depending on the unit where the head loss occurs). As a result, for the unconfined model, water-level declines at early times under confined (saturated) conditions are less than declines at later times under dewatered, unconfined conditions. In the confined model, a single storage coefficient, approximated as twice the geometric mean of the specific yield and the product of specific storage and thickness (see discussion of "linearization" in section 5), controls water-level declines. Therefore, the rates of decline in the confined model are less steep than in the unconfined model at early time and greater at late time (compare the NE_ILL pumping center hydrographs in fig. 74*A* and 74*B*), and water levels in the confined model are lower than in the unconfined model in the years before recovery starts in the 1980s.

Table 20. Discrepancy between alternative models and SLMB-C with respect to predevelopment water levels, by aquifer system.

20*A*. Percentage of nearfield active cells in aquifer system with predevelopment water level more than 20 feet HIGHER in alternative models relative to SLMB-C.

Aquifer system	Alternative models		
	Unconfined SLMB-U (percent)	**Uniform density MLMB-C (percent)**	**Active transport SLMB-CT3 (percent)**
QRNR	0.80	0.00	0.00
PENN	.06	.00	.00
MSHL	.04	49.50	.00
SLDV	.26	56.49	.00
C-O	.03	51.07	.00

20*B*. Percentage of nearfield active cells in aquifer system with predevelopment water level more than 20 feet LOWER in alternative models relative to SLMB-C.

Aquifer system	Alternative models		
	Unconfined SLMB-U (percent)	**Uniform density MLMB-C (percent)**	**Active transport SLMB-CT3 (percent)**
QRNR	0.03	0.00	0.00
PENN	.00	.00	.00
MSHL	1.77	.00	.00
SLDV	.32	.98	.00
C-O	.24	16.71	.00

Table 21. Discrepancy between alternative models and SLMB-C with respect to 2005 drawdown, by aquifer system.

21*A*. Percentage of nearfield active cells with 2005 drawdown more than 20 feet GREATER in alternative models relative to SLMB-C.

Aquifer system	Alternative models		
	Unconfined SLMB-U (percent)	Uniform density MLMB-C (percent)	Active transport SLMB-CT3 (percent)
QRNR	0.09	0.00	0.00
PENN	.00	.00	.00
MSHL	.00	.00	.00
SLDV	.12	.00	.05
C-O	.25	1.43	20.45

21*B*. Percentage of nearfield active cells with 2005 drawdown more than 20 feet LESS in alternative models relative to SLMB-C.

Aquifer system	Alternative models		
	Unconfined SLMB-U (percent)	Uniform density MLMB-C (percent)	Active transport SLMB-CT3 (percent)
QRNR	0.07	0.00	0.00
PENN	.00	.00	.00
MSHL	.01	.00	.00
SLDV	.32	.16	8.72
C-O	3.22	.00	.00

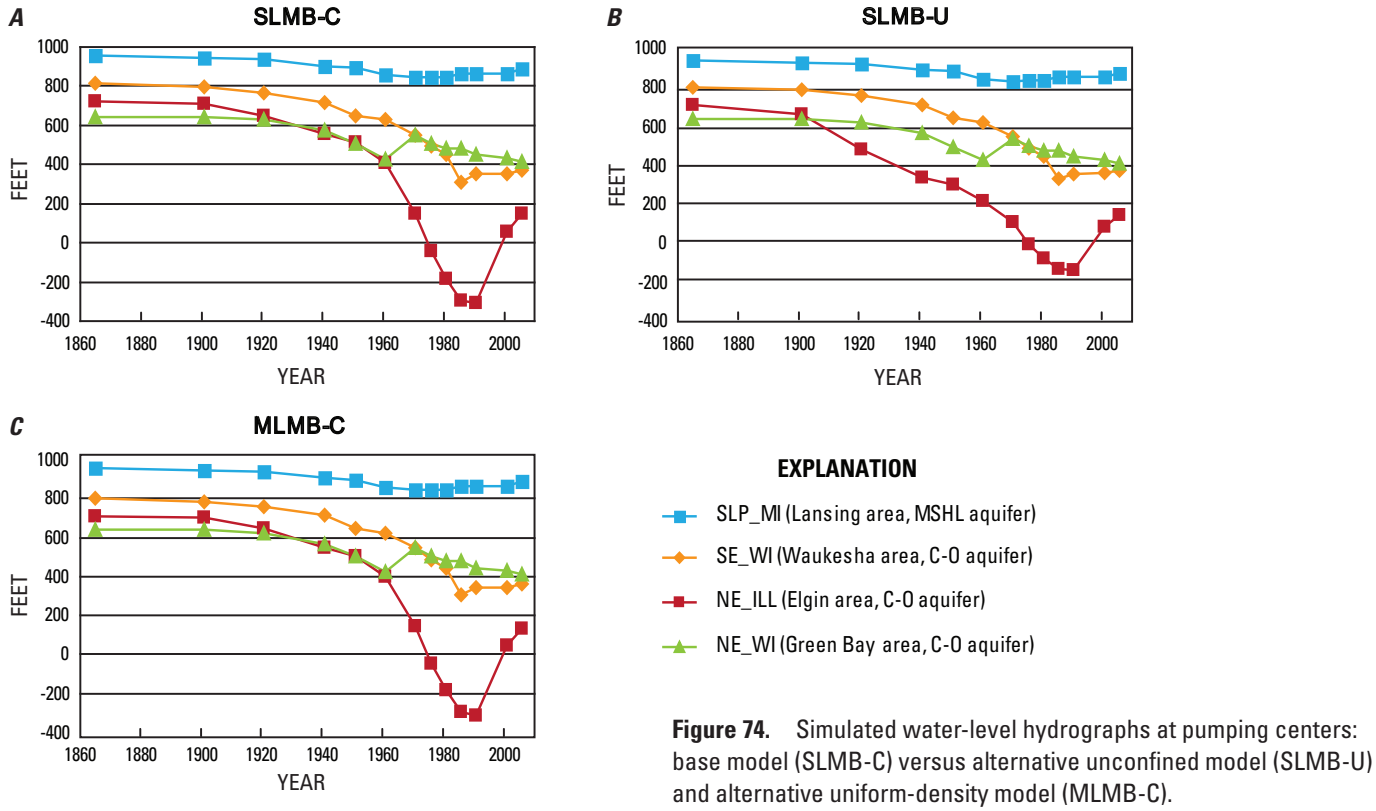

Figure 74. Simulated water-level hydrographs at pumping centers: base model (SLMB-C) versus alternative unconfined model (SLMB-U) and alternative uniform-density model (MLMB-C).

An important finding of the LMB model is that in areas close to large pumping centers with deep wells penetrating the C-O aquifer system, dewatered conditions can exist at the top of the C-O aquifer system, most commonly in the Sinnipee unit. These dewatered conditions manifest themselves in the model in one of two ways:[33] (1) All model layers contain saturated material, but the heads in the Sinnipee are below the top of that unit, implying the presence of a second water table in the dolomite. (2) The simulated head is below the bottom of the Sinnipee and the second water table is present in an underlying unit, such as the St. Peter. The first case is much more prevalent than the second, but both indicate dewatered conditions at the top of the C-O aquifer system and the existence of two saturated systems, one shallow and one deep, separated by a deep water table.

The confined and unconfined versions of the LMB model simulate dewatered areas that form after predevelopment and are attributable to deep pumping. They are found only on the west side of Lake Michigan (fig. 75). In general, the dewatered areas are larger in 2005 than in 1980, although the large dewatered area in northeastern Illinois is slightly diminished due to the switch from groundwater to Lake Michigan as a source of water supply. The agreement between the dewatered areas simulated by the confined and unconfined models is strong, suggesting that the two versions of the LMB model are generally consistent with respect to drawdown patterns and to the pattern of vertical leakage from overlying rocks to the deep C-O units. In this connection, it is worth noting that the dewatered layer for the confined version of the model (SLMB-C) is always treated as fully saturated from the standpoint of horizontal and vertical components of the groundwater flow equation whatever the head level simulated and the implied water-table condition; for the unconfined version (SLMB-U), by contrast, the transmissivity is reduced in proportion to the loss of saturated thickness in dewatered cells and, in addition, the vertical flow calculation across the cell is modified to take account of the presence of unsaturated material (McDonald and Harbaugh, 1988; Harbaugh and others, 2000). Despite these differences in the calculation routines, the results of the two model versions are very similar.

The simulated dewatering at the top of the C-O aquifer system (fig. 75) is supported by a variety of field evidence. There are four main areas where the confined and unconfined versions of the LMB model suggest that dewatering has occurred. In the vicinity of *Green Bay, Wis.*, potentiometric-surface information assembled for 2004 and 2008 indicates that water levels are drawn down to the extent that part or even all of the Sinnipee unit at the top of the C-O aquifer system is dewatered (Luczaj and Hart, 2009) in the same general area where the model simulates the presence of a deep water table for the 2005 stress period. Around *Lake Winnebago in northeastern Wisconsin*, geochemical evidence is favorable to the hypothesis that the top of the C-O aquifer system is dewatered in the same area indicated by the LMB model for 1980 and 2005. Arsenic contamination around Lake Winnebago is attributed to the oxidation of arsenic from a sulfide-bearing secondary cement horizon, which is present at the boundary between the Sinnipee rocks and the underlying unit, generally the St. Peter. Researchers have noted that the elevation of water levels in wells exerts a strong control on the release of naturally occurring arsenic to groundwater; further, they point out that in some areas where arsenic is elevated, heads have been lowered by pumping, so that the present-day levels in wells are open to the Sinnipee and St. Peter units (Gotkowitz and others, 2004). The zone of dewatering near *Waukesha, Wis.*, was noted in an earlier model centered on southeastern Wisconsin (Feinstein, Hart, and others, 2005). This finding led to the installation of nested piezometers at a location within the zone of dewatering simulated by the confined and unconfined LMB models. Water levels measured in 2004 are strong evidence that a second water table is present in the Sinnipee unit (Eaton and Bradbury, 2005). Finally, by far the largest area of simulated dewatering shown in figure 75 corresponds to the pumping centers around *Joliet in northeastern Illinois*. This finding is consistent with results obtained by a model recently constructed by the ISWS for Kane County and surrounding areas (Meyer and others, 2009). In light of these results, the ISWS has compared 2007 water levels in wells that penetrate the top units of the C-O aquifer system to the bottom elevation of the Sinnipee unit at the well locations. They conclude that the large dewatered area simulated by the models and centered on Joliet is consistent in shape and extent with the area where the water levels in the deep wells are either as much as 50 ft below the bottom of the Sinnipee unit (in a restricted zone immediately around Joliet) or at an elevation that falls within the Sinnipee (Wehrmann and others, in preparation). The simulated results of the LMB model agree with the details of this analysis insofar as they show the second water table to be in the St. Peter immediately around Joliet and in the Sinnipee in the larger surrounding area.

[33] See section 5.1 for discussion of the algorithms employed by the SEAWAT code to handle dewatered conditions in unconfined mode and in confined mode.

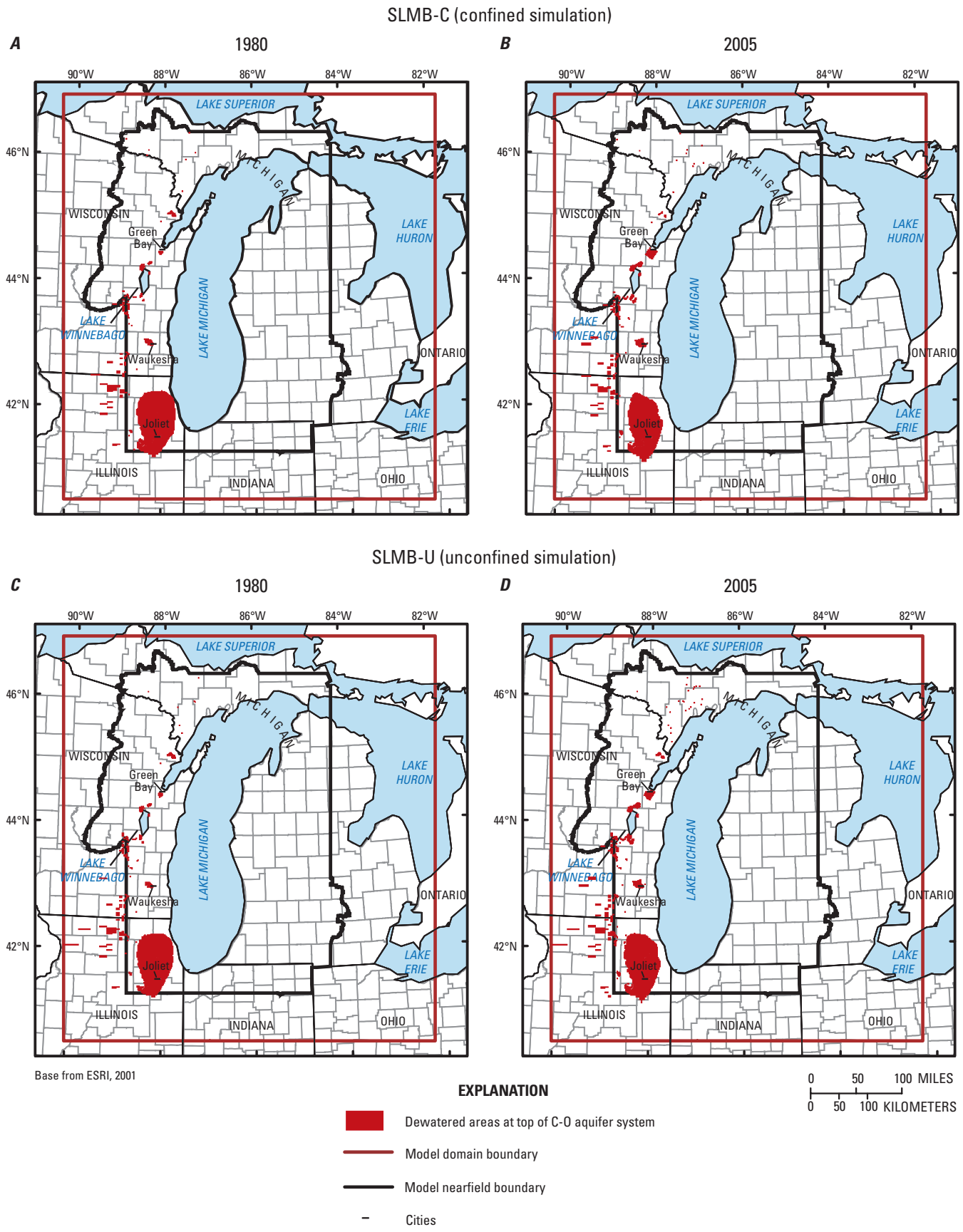

Figure 75. Simulated dewatering at top of Cambrian-Ordovician aquifer system as a result of pumping: base model versus alternative unconfined model for 1980 and 2005.

Pumping is responsible for dewatering at the top of the C-O aquifer system in both Wisconsin and Illinois, but the mechanisms that accompany this dewatering are open to speculation. Multiple water tables at the locations discussed imply that there is shallow saturated system, the top of which is defined by a water table usually in Quaternary deposits and the bottom of which is generally in the Maquoketa hydrogeologic unit. The shallow system is underlain by a deeper saturated system whose top is defined by a water table in the Sinnipee unit or possibly an underlying unit such as the St. Peter and whose bottom is below the bottom of the Mount Simon unit at the base of the sedimentary deposits. It is possible that air enters the intermediate dewatered zone between the two saturated systems by moving through boreholes that penetrate the C-O aquifer system and replaces the water withdrawn from the system. Alternatively, there may not be pathways to allow air to enter the system; in this case, the aquifer material between this second water table and the overlying system would, in fact, remain saturated but under a capillary tension that is above the air-entry pressure required to allow the largest pores to drain. Accordingly, observation wells would indicate the presence of a second, deep water table that is overlain by an intermediate zone analogous to the capillary fringe that is associated with water-table aquifers. However, because the system is not freely open to the atmosphere, the configuration and dynamics of this intermediate zone are likely complex and difficult to predict. Whatever the degree of dewatering, the model findings corroborated by field evidence suggest that pumping from the C-O aquifer system has caused deep water tables to form in the Green Bay, Lake Winnebago, Waukesha, and greater Joliet areas and that this condition occurs mostly commonly in the Sinnipee hydrogeologic unit.

7.1.2 Uniform-Density Simulation

Two alternative models have been devised to test the assumptions that (1) high levels of salinity in the Michigan Basin influence the groundwater flow field in important and detectable ways and (2) this influence can be adequately simulated by assigning fixed concentrations (and, hence, fixed density) levels to model layers in correspondence to unit-dependent maps of the saline body.

Density effects were first tested by preparing an alternative model that substitutes uniform freshwater density for spatially distributed variable density. The exact same model geometry and input used for the calibrated confined saline version of the model (SLMB-C) was applied to a confined version of the model (MLMB-C) without any recalibration. The only difference between the two simulations is that the calibrated saline version is solved with SEAWAT-2000 and the companion freshwater version is solved with MODFLOW-2000. Because SEAWAT-2000 calculations are performed in double precision, MLMB-C is solved with a double-precision version of MODFLOW-2000 to ensure consistency.

As emphasized earlier,

- model findings regarding water availability are sought principally in freshwater areas, and
- model calibration targets are restricted to freshwater areas.

Only the results for the vertical-head-difference target set shows appreciable difference for the two simulations. The statistical similarity indicates that, in freshwater areas, there is little difference between the confined model with variable density and with uniform density in freshwater areas.With respect to the global 2005 water budget for the Lake Michigan Basin, the results also are very similar (fig. 76), which is expected because recharge to the water table is the same in both simulations. The biggest difference is that the MLMB-C simulation yields a 5 percent lower rate of direct discharge to Lake Michigan than the SLMB-C simulation. Large differences are registered in the case of simulated predevelopment heads (table 20*A*, second column). For model cells containing saline water, the heads generated the uniform-density model are higher than the heads generated by a solution that accounts for salinity. The 50 percent or more of cells in the MSHL, SLDV, and C-O aquifer system with more than 20-ft discrepancies are almost all in the Michigan Basin. As far as drawdown is concerned, there is very little difference either within aquifer systems (table 21, second column) or near pumping centers (fig. 74). Closer inspection of the results for the C-O aquifer system shows that, west of Lake Michigan, the drawdown around the NE_WI, SE_WI, and NE_ILL pumping centers is on the order of 5 ft higher for the SLMB-C than the MLMB-C simulation; but east of the lake, drawdown is on the order of 5 ft less. This subtle difference can be attributed to the effect of salinity on water flowing west toward deep pumping centers from the Michigan Basin underneath Lake Michigan. The saline conditions cause more drawdown than otherwise near the pumping centers and under the west side of the lake, where freshwater can be relatively easily moved, and less drawdown than otherwise under the east side of the lake and into the Michigan Basin, where the heavier saline water resists the pull of pumping centers. In effect, the increasing salinity in the direction of the Michigan Basin acts as a kind of boundary that resists the influence of deep wells. Subtle differences also appear in the magnitude and direction of the flow fields generated by the variable- and uniform-density versions of the LMB model (table 22). For the west and east shorelines of Lake Michigan along the latitudes between the cities of Green Bay and Chicago, summation of the lateral flows by aquifer system demonstrates some discrepancies, particularly under 2005 stressed conditions. The SLMB-C simulation shows more movement through the C-O aquifer system from east to west in response to deep pumping centers than does the MLMB-C simulation. Nevertheless, the extent and boundaries of the regional groundwater basins for the freshwater part of the Lake Michigan groundwater basin in the C-O aquifer system are nearly identical for both the variable-density and uniform-density models (figs. 77*A*, *B*).

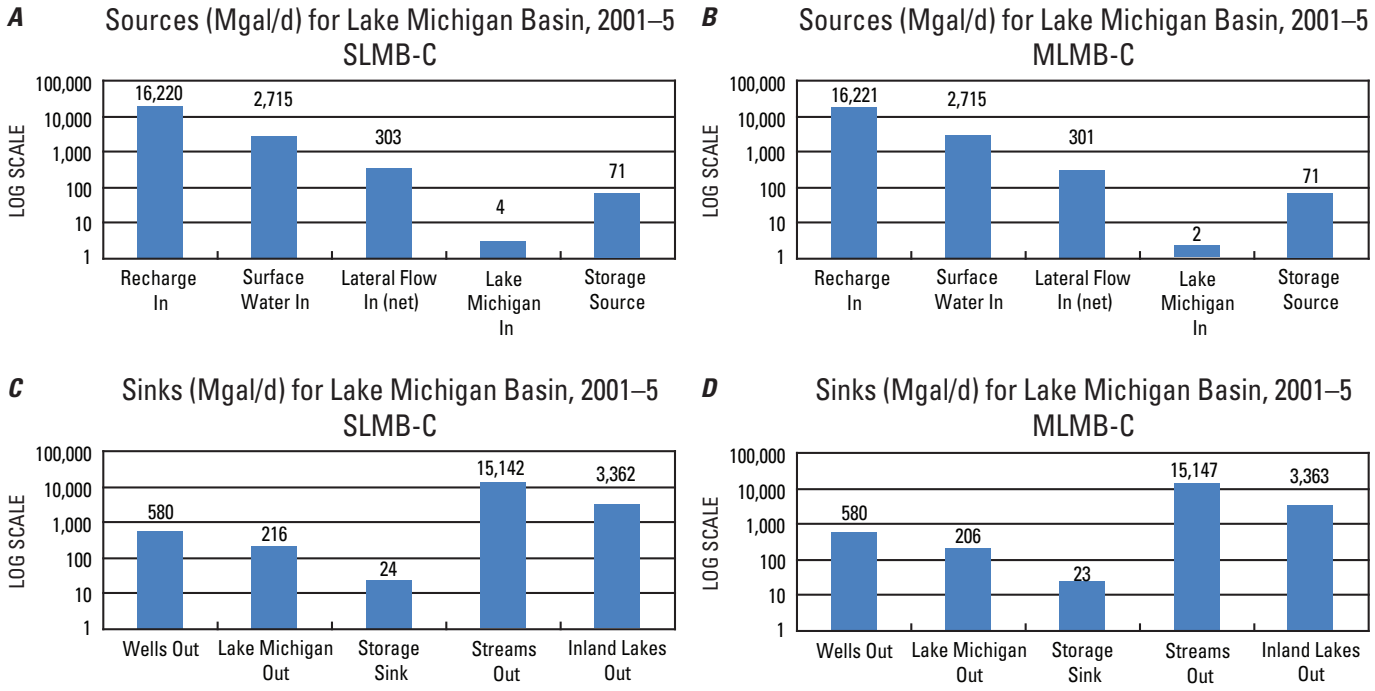

Figure 76. Simulated 2005 water budgets in Lake Michigan Basin: base model (SLMB-C) versus alternative uniform-density model (MLMB-C).

Table 22. East and west components of flow under shores of Lake Michigan between latitude of cities of Green Bay and Chicago: comparison of SEAWAT-2000 to MODFLOW-2000.

Predevelopment conditions		
SEAWAT-2000 (SLMB-C)		
Aquifer system(s) (layer interval)	**West shore net flow (Mgal/d)**	**East shore net flow (Mgal/d)**
QRNR (L1-L3)	2.2 toward lake	5.0 toward lake
PENN+MSHL+SLDV (L4-L12)	31.3 toward lake	4.5 toward lake
C-O (L13-L20)	2.6 toward lake	2.4 toward lake
TOTAL	**36.1 toward lake**	**11.9 toward lake**
MODFLOW-2000 (MLMB-C)		
Aquifer system(s) (layer interval)	**West shore net flow (Mgal/d)**	**East shore net flow (Mgal/d)**
QRNR (L1-L3)	2.1 toward lake	5.0 toward lake
PENN+MSHL+SLDV (L4-L12)	31.3 toward lake	4.6 toward lake
C-O (L13-L20)	4.5 toward lake	0.2 from lake
TOTAL	**37.9 toward lake**	**9.4 toward lake**

2005 conditions		
SEAWAT-2000 (SLMB-C)		
Aquifer system(s) (layer interval)	**West shore net flow (Mgal/d)**	**East shore net flow (Mgal/d)**
QRNR (L1-L3)	2.1 toward lake	5.1 toward lake
PENN+MSHL+SLDV (L4-L12)	30.4 toward lake	4.7 toward lake
C-O (L13-L20)	7.5 from lake	6.9 toward lake
TOTAL	**25.0 toward lake**	**16.7 toward lake**
MODFLOW-2000 (MLMB-C)		
Aquifer system(s) (layer interval)	**West shore net flow (Mgal/d)**	**East shore net flow (Mgal/d)**
QRNR (L1-L3)	2.1 toward lake	5.1 toward lake
PENN+MSHL+SLDV (L4-L12)	30.4 toward lake	4.8 toward lake
C-O (L13-L20)	5.5 from lake	4.4 toward lake
TOTAL	**27.0 toward lake**	**14.3 toward lake**

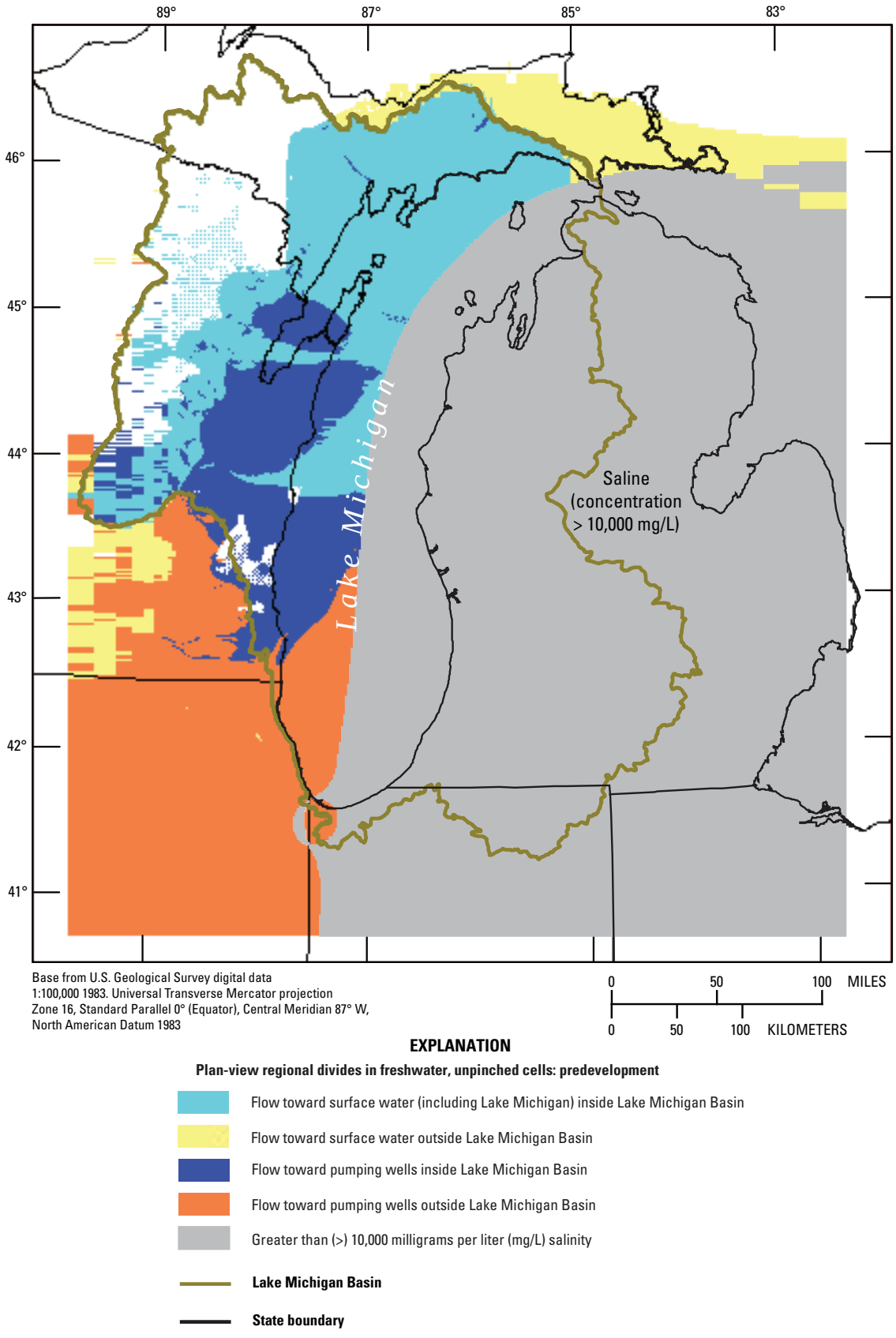

Figure 77*A*. Simulated 1991–2005 groundwater basins for C-O aquifer system: Base model.

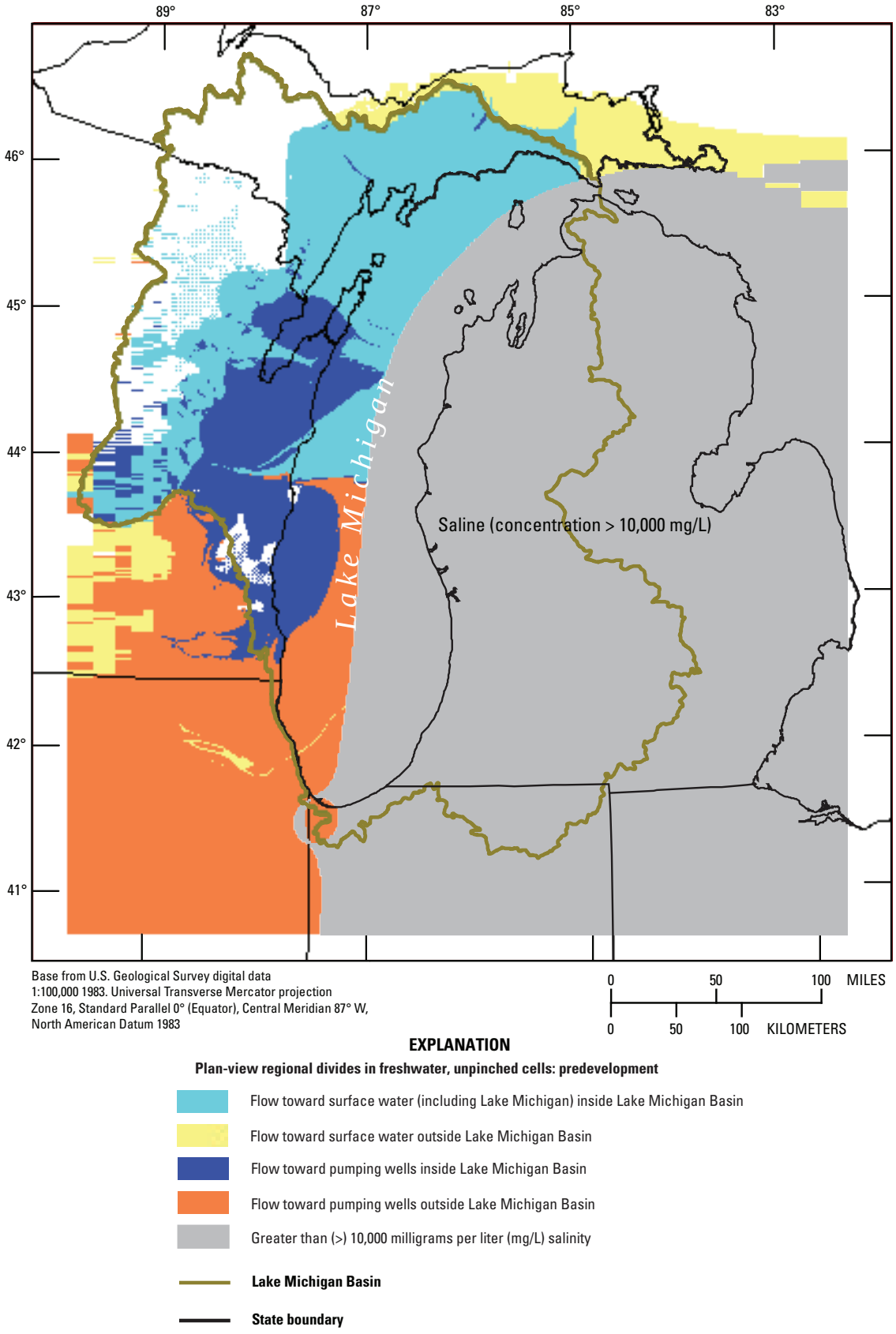

Figure 77*B*. Simulated 1991–2005 ground-water basins for C-O aquifer system: Alternative uniform-density model.

The major differences between the variable-density and uniform-density results relate to the water levels and flow dynamics simulated in the deeper units of the Michigan Basin and under Lake Michigan, where calibration targets are not available. For this reason, it could be argued that there is no basis for preferring the head and flow results of the variable-density solution except on theoretical grounds. Given (1) the extent of the highly saline body in the groundwater system underlying the Lake Michigan Basin and (2) the availability of simulation methods to account for it, a modeling strategy was adopted to consider the effects of variable density rather than neglect the phenomenon. However, comparison of the model versions suggests that, for most applications concerning water-availability issues (for example, mapping regional divides by aquifer system), the uniform-density MLMB-C model can be used in place of the variable-density SLMB-C model for regional analyses of groundwater conditions in freshwater areas.

7.1.3 Active-Transport Simulation

A second way to analyze the influence of saline conditions on the modeling process is to put more, rather than less, weight on the variable-density equation. For ease of input and, especially, to keep runtimes relatively short, the SEAWAT-2000 code was not applied to the calibrated LMB model in normal transport mode, which would permit the saline water body to move by advection and dispersion; instead, the code was executed under the assumption of fixed concentrations. In SLMB-C and SLMB-U, the distribution of spatially variable but time-constant salinities (and the resulting fixed density field) influences the flow system through its effect on hydraulic conductivity and hydraulic gradients, but the saline body itself remains stationary. This assumption can be relaxed with the addition of inputs to the model setup that take account of transport mechanisms.

To test the effect of movement of saline water on model findings, a simple transport simulation was performed for 1864 to 2005 on the basis of the already calibrated SLMB-C model with

- longitudinal, horizontal transverse, and vertical transverse dispersivity set everywhere to 10 ft, 1 ft, and 0.1 ft, respectively;
- molecular diffusion set to 1−E5 ft^2/d;
- porosity (and effective porosity) set everywhere to 0.2;
- a maximum transport time step set to 30 days; and
- an implicit finite-difference solution scheme.

The initial saline concentrations, equivalent to the fixed concentrations in SLMB-C, serve as the only source of salinity in the model. One very small change was made to the calibrated SLMB-C input: in the new model the WEL package, originally restricted to handling input for single-layer wells, also replaces the MNW package for all multilayer wells. This substitution is desirable to simplify the input of sources and sinks in the transport solution, and it is possible because the output of the calibrated SLMB-C model includes the cell-by-cell pumping rates for all stress periods as a function of the transient solution.[34] As a result, it is possible to duplicate the cell-by-cell pumping configuration of the original run with one input package for wells rather than two. However, the translation does promote a small degree of rounding error. To insure a consistent comparison between the transport solution and the fixed-concentration solution, the SLMB-C model was rerun with a single comprehensive WEL package. The corresponding transport run with the same single WEL package is called SLMB-CT3. The runtime of the latter—about 10 hours—is approximately 16 times longer than that of the former.

Mass-balance results (fig. 78), predevelopment water-level results by aquifer system (table 20, third column), 2005 drawdown results by aquifer system (table 21, third column), and hydrographs at pumping centers (fig. 79) all indicate very small differences between simulations without and with transport of saline water. Changes in DS concentration through time are small and reveal no appreciable movement of the saline water in response to pumping. However, drawdown produced from pumping centers in the C-O aquifer system is greater in simulations with transport. The increase is relatively small: the *maximum* change in 2005 between the SLMB-CF3 and SLMB-CT3 models in NE_ILL where wells are in the vicinity of saline water is 28 ft in the STPT aquifer, 23 ft in the IRGA aquifer, and 14 ft in the MTSM aquifer. These changes suggest that added density of the saline water induced to flow toward the pumping centers requires increased drawdown to withdraw groundwater at the simulated rates.

Whereas the comparisons between the fixed and variable concentration simulations demonstrate negligible cost in neglecting transport for most applications, it is conceivable that the SLMB-CT3 version of the LMB regional model might be useful for some problems. Therefore, like the SLMB-U (unconfined) and the MLMB-C (uniform density) versions, its input and output were archived, and the model made available for distribution.

[34] As mentioned earlier, the distribution of pumping between layers for MNW wells is not an input to the model but an *output* based on the total pumping prescribed for the well, aquifer conditions simulated outside the well, and the simulated circulation pattern within the well.

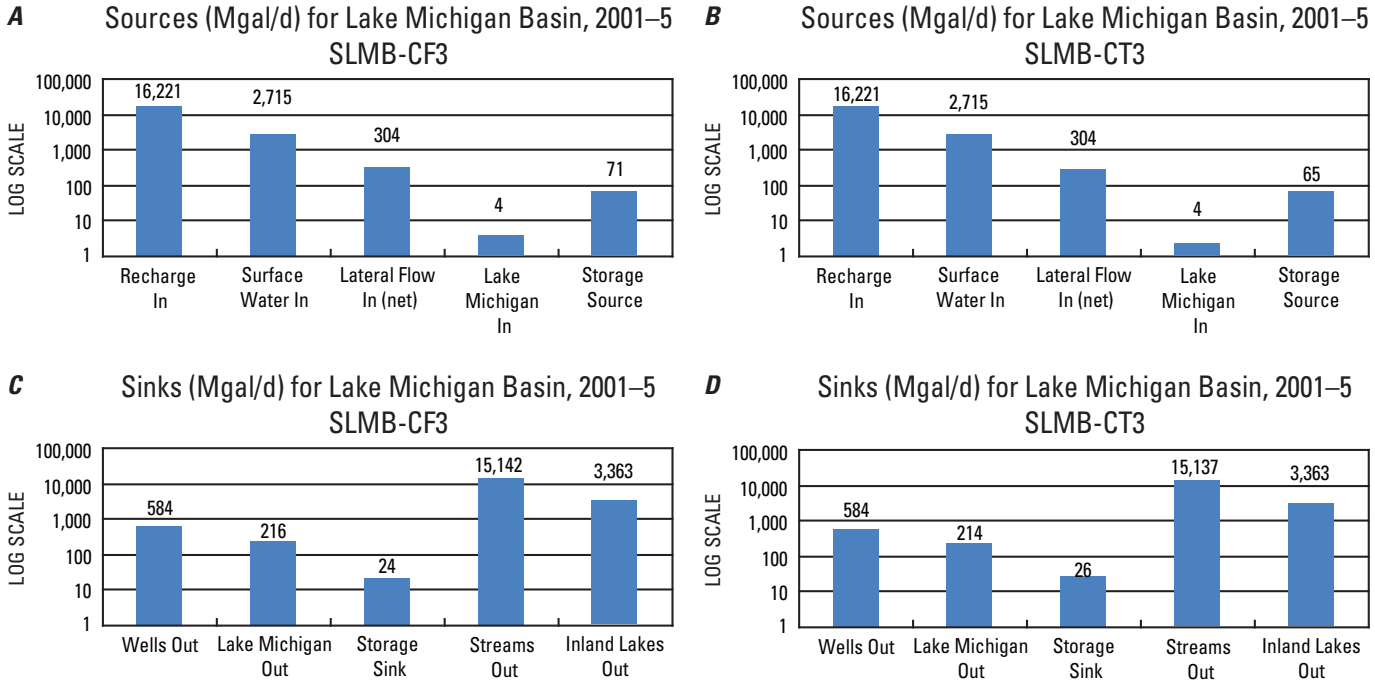

Figure 78. Simulated 2005 water budgets in Lake Michigan Basin: base model (SLMB-CF3) versus alternative active transport model (SLMB-CT3).

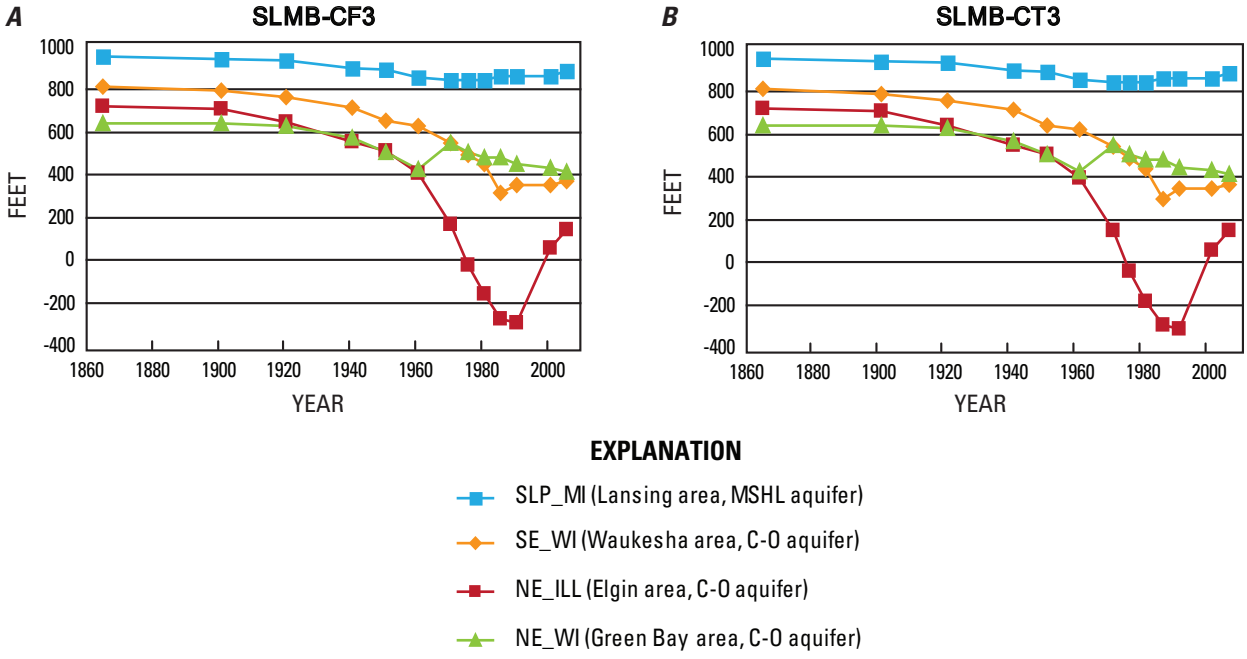

Figure 79. Simulated water-level hydrographs at pumping centers: base model (SLMB-CF3) versus alternative active transport model (SLMB-CT3).

7.2 Model Sensitivity

Model sensitivity analysis consists of modifying a single type of input in each sensitivity simulation. Selected sensitivity simulations test inputs falling into three categories: farfield boundary conditions, parameter values, and grid resolution. All the tests were done on the calibrated confined variable-density model, SLMB-C, which is considered the base model.

7.2.1 Farfield Boundary Conditions

As discussed in section 4 ("Model Construction"), the boundary conditions at the edge of the model (first or last row, first or last column) consist of two types:

- GHB (head-dependent) cells representing Great Lake stages or CHD (constant-head) cells representing surface-water stages in the highest active cell at a row/column location, with underlying cells set as no-flow boundaries at their outside edge (see figs. 26 and 27).
- WEL (constant-flow) cells representing time-dependent inflow or outflow to the bedrock across the southwestern model edge of the LMB model domain, derived from a published regional model centered on northeastern Illinois (see fig. 27).

Both conditions were modified to test sensitivity. In the first case, the lake stage and water-table values for the farfield boundary cells at the sides of the model were propagated downward as CHD cells, thereby replacing the vertical no-flow boundaries at the sides of the model with constant-head boundaries (simulation SEN1-CHD). In the second case, the time-dependent flow constituting the boundary condition in bedrock layers along the southwestern edge of the model domain were either halved (simulation SEN2-HAF) or doubled (simulation SEN3-DUB) in magnitude. The effects of the three sensitivity runs on the original SLMB-C output are presented in terms of the percentage of cells in each aquifer system that differ more than 20 ft from simulations using predevelopment heads (table 23, first three columns) and with more than 20 ft of difference with respect to 2005 drawdown conditions (table 24, first three columns). A threshold of 20 ft was selected because it is roughly the magnitude of the mean absolute error for calibrated water levels. For predevelopment water levels, the changes in excess of 20 ft, positive and negative, are concentrated in the C-O aquifer system. These discrepancies occur almost exclusively in the deep part of the Michigan Basin, which is devoid of calibration targets. Farfield boundary conditions appear to have very little effect on the drawdown distribution simulated for 2005. When the focus is on freshwater areas of the model, the effects of modifying farfield boundary conditions on both initial heads and drawdown are very small. At the selected pumping centers (see fig. 54), graphs showing the predevelopment water levels for the farfield boundary condition in sensitivity runs are similar to those showing levels for the base model, SLMB-C (fig. 80). Simulated drawdowns in 1960, 1980, and 2000 for the farfield boundary sensitivity runs are also similar to those simulated by the base model (fig. 81). For the drawdown graphs, it is interesting that the base and sensitivity runs all produce the same pattern: drawdown increases over time at the SE_WI pumping center, but the NE_ILL and SLP_MI centers both show recovery of water levels between 1980 and 2005 as a result of reductions in withdrawals, whereas the NE_WI center shows recovery between 1960 and 1980.

7.2.2 Parameter Values

Three simulations were done to test the sensitivity of model outcomes to parameter values. Clearly, a virtually unlimited number of such simulations could be devised. The ones selected bear on two important aspects of the model design: the handling of glacial heterogeneity and the treatment of groundwater exchange with Lake Michigan.

The reader may recall that the assignment of hydraulic conductivity to the inland QRNR deposits (mostly glacial in origin) in the model depends on two databases, one of which assigns glacial categories (types of tills and stratified deposits) to cells and the other of which assigns the cells a number representing coarse fraction (the proportion of sands and gravels as opposed to the proportion of silts and clays). The result is cell-by-cell variation of K_h and K_v wherever inland QRNR deposits are present in the top three model layers. The questions arise, "Given the regional scale of the model and the constraints on the solution posed by internal boundary conditions, are model results largely insensitive to the heterogeneity generated by this method, and could a simpler version of the model based on zoned input to the QRNR layers produce a similar fit to calibration targets?"

To address these questions, delineation of *K* zones was based on the extent of glacial categories in each QRNR layer (see fig. 36), and zoned values were based on the geometric means consistent with calibrated values in the SLMB-C model (see appendix 6*A*, layers 1, 2, and 3 for K_h input and appendix 6*B*, layers 1, 2, and 3 for K_v input). Apart from this change, the sensitivity simulation, called SEN4-QRN, is identical to the base SLMB-C run. In general, it produces water-level and flux results that are similar to those from the base run. For example, comparison of the residuals generated at targets by the two runs show only minor increase in the overall misfit for the run with the simplified QRNR input (the objective function increases by 2 percent), limited largely to a few target subsets. The residual differences that occur correspond mostly to differences in the simulated water-table surface. Inspection of table 23 shows that, for the sensitivity simulation, there are a fairly large number of shallow (that is, QRNR or PENN aquifer system) cells with more than 20 ft higher water levels than in the base run, owing to the simplified zonation, but an even greater number of cells with more than 20 ft lower water levels. These discrepancies are distributed throughout all subregions, but they are largest in the NLP_MI.

Table 23. Discrepancy between model-sensitivity simulations and SLMB-C with respect to predevelopment water levels, by aquifer system.

[FF, farfield; *K*, hydraulic conductivity]

23*A*. Percentage of nearfield active cells in aquifer system with predevelopment water level more than 20 feet HIGHER in model sensitivity simulations relative to SLMB-C.

Aquifer system	Model-sensitivity simulations					
	Modified FF no-flow boundaries SEN1-CHD (percent)	FF boundary fluxes halved SEN2-HAF (percent)	FF boundary fluxes doubled SEN3-DUB (percent)	Simplified *K* input to QRNR SEN4-QRN (percent)	Lake Michigan bed *K* increased by 10× SEN5-BED (percent)	Variable stage in each Great Lake SEN6-GLS (percent)
QRNR	0.00	0.00	0.00	1.65	0.00	0.00
PENN	.00	.00	.00	2.81	.00	.00
MSHL	.00	.00	.00	.08	.00	.00
SLDV	10.59	.00	.00	.04	.00	.00
C-O	51.16	.00	18.92	.06	.00	.00

23*B*. Percentage of nearfield active cells in aquifer system with predevelopment water level more than 20 feet LOWER in model sensitivity simulations relative to SLMB-C.

Aquifer system	Model-sensitivity simulations					
	Modified FF no-flow boundaries SEN1-CHD (percent)	FF boundary fluxes halved SEN2-HAF (percent)	FF boundary fluxes doubled SEN3-DUB (percent)	Simplified *K* input to QRNR SEN4-QRN (percent)	Lake Michigan bed *K* increased by 10× SEN5-BED (percent)	Variable stage in each Great Lake SEN6-GLS (percent)
QRNR	0.00	0.00	0.00	7.61	0.07	0.00
PENN	.00	.00	.00	2.74	.00	.00
MSHL	.00	.00	.00	1.92	.00	.00
SLDV	.00	.00	.00	.24	.00	.00
C-O	.00	6.84	.00	.08	.00	.00

Table 24. Discrepancy between model-sensitivity simulations and SLMB-C with respect to 2005 drawdown, by aquifer system.

[FF, farfield; *K*, hydraulic conductivity]

24*A*. Percentage of nearfield active cells in aquifer system with 2005 drawdown more than 20 feet GREATER in model sensitivity simulations relative to SLMB-C.

Aquifer system	Model-sensitivity simulations					
	Modified FF no-flow boundaries SEN1-CHD (percent)	**FF boundary fluxes halved SEN2-HAF (percent)**	**FF boundary fluxes doubled SEN3-DUB (percent)**	**Simplified *K* input to QRNR SEN4-QRN (percent)**	**Lake Michigan bed *K* increased by 10× SEN5-BED (percent)**	**Variable stage in each Great Lake SEN6-GLS (percent)**
QRNR	0.00	0.00	0.00	0.16	0.00	0.00
PENN	.00	.00	.00	.00	.00	.00
MSHL	.00	.00	.00	.01	.00	.00
SLDV	.00	.00	.00	.00	.00	.00
C-O	.00	.00	.00	.00	.00	.00

24*B*. Percentage of nearfield active cells in aquifer system with 2005 drawdown more than 20 feet LESS in model sensitivity simulations relative to SLMB-C.

Aquifer system	Model-sensitivity simulations					
	Modified FF no-flow boundaries SEN1-CHD (percent)	**FF boundary fluxes halved SEN2-HAF (percent)**	**FF boundary fluxes doubled SEN3-DUB (percent)**	**Simplified *K* input to QRNR SEN4-QRN (percent)**	**Lake Michigan bed *K* increased by 10× SEN5-BED (percent)**	**Variable stage in each Great Lake SEN6-GLS (percent)**
QRNR	0.00	0.00	0.00	0.02	0.00	0.00
PENN	.00	.00	.00	.00	.00	.00
MSHL	.00	.00	.00	.00	.00	.00
SLDV	.00	.00	.00	.00	.00	.00
C-O	.00	.00	.55	.00	.00	.00

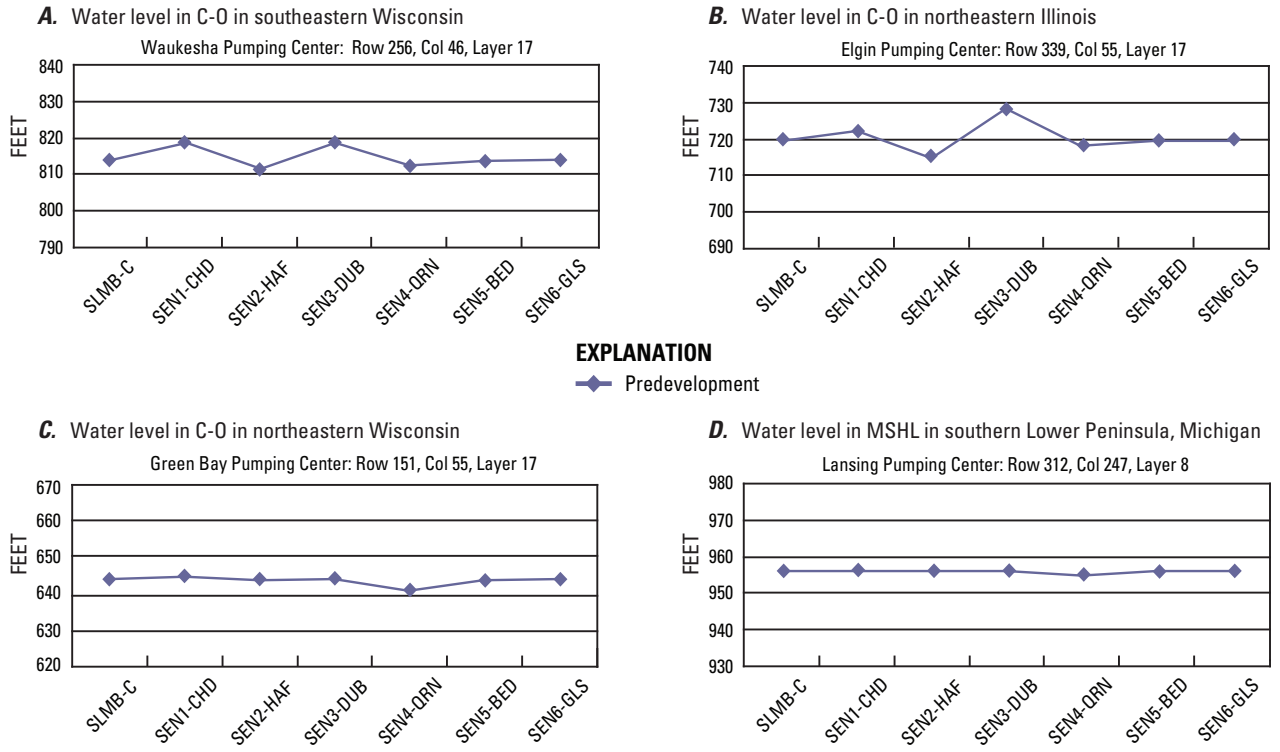

Figure 80. Comparison of simulated predevelopment water levels at selected pumping centers: base model versus sensitivity models.

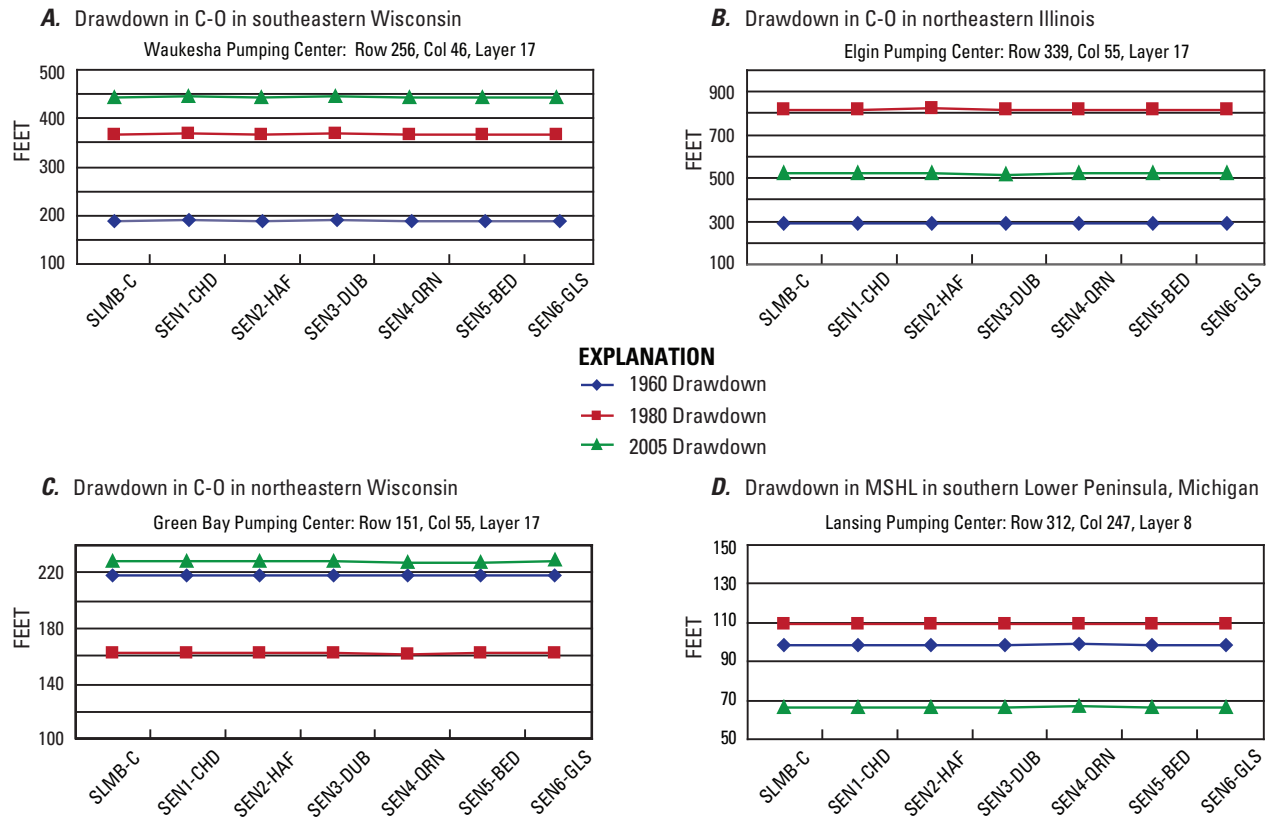

Figure 81. Comparison of simulated drawdown at selected pumping centers: base model versus sensitivity models.

Inspection of table 24 shows that drawdown results in all aquifer systems are much less affected by the simplified QRNR *K* zonation than are water levels. The effect of the simplification is extremely small at the selected pumping centers (as evident in results for SLMB-C and SEN-QNR water levels in fig. 80 and drawdown in fig. 81), which is expected because none of the centers features QRNR wells.

On the whole, it appears that the simplified *K* representation produces a water-table solution that is distinct from the solution with cell-by-cell *K* variation but simulates a very similar response to shallow pumping. The magnitude of drawdown simulated at the water table by either the base or sensitivity model is constrained by the presence of fixed head-dependent boundaries in roughly half the inland water-table cells. Although this structural element of the regional model limits the extent to which the detailed QRNR hydraulic-conductivity database is able to improve regional model results when compared to a simplified approach, the availability of the database is intended to be a product that, by itself, is a useful starting point for future studies involving the shallow groundwater-flow system in and around the Lake Michigan Basin.

Little information, either from field tests or calibration targets, is available to quantify or update the hydraulic conductivities assigned the Lake Michigan bed deposits in layers 1, 2 and 3. For this reason, a second sensitivity run, called SEN5-BED, was constructed in which the K_h and K_v of the lakebed zones were increased by 10 times with respect to the value in the base run, SLMB-C. The effect on this change is minimal on calibration target residuals, predevelopment water levels (table 23), 2005 drawdown (table 24), or conditions at pumping centers (figs. 80 and 81). In order to detect a difference, it is necessary to compare the SLMB-C and SEN5-BED water budgets. The base simulation yields a predevelopment rate of direct discharge to Lake Michigan equal to 218 Mgal/d (see fig. 57). The SEN5-BED run yields a predevelopment rate of 279 Mgal/d. The order-of-magnitude increase in *K* produces about a 30-percent increase in discharge, and this sink increases from 1.3 percent of the Lake Michigan Basin outflow budget to about 1.7 percent of the budget. Given the uncertain nature of the bed properties, an error term on the order of plus or minus 30 percent for the discharge term is not unexpected. More attention will be given in the next subsection to consideration of possible bias in the model estimate of this flux term.

The final sensitivity run, SEN6-GLS, involved time-dependent treatment of the stages assigned Lake Michigan and the farfield Great Lakes. Lake stage measurements compiled by the U.S. Army Corps of Engineers, Detroit District (2006) were averaged over stress-period intervals to modify the GHB input from the SLMB-C model. For example, the monthly excursion in the Lake Michigan/Lake Huron level recorded by the U.S. Army Corps of Engineers between 1918 and 2005 ranges from 576.04 to 582.32 ft above lake datum, with a median value of 578.86 ft. When averaged by stress-period interval, the range is from 577.52 ft in 2001–5 to 580.59 ft in 1971–75. The effect on model results of varying stage by stress period in Lake Michigan, Lake Superior, Lake Huron, Lake St. Clair and Lake Erie is extremely small (tables 23 and 24; figs. 80 and 81). Perhaps the biggest effect is on the direct discharge term to Lake Michigan. The 2001–5 rate of direct discharge to Lake Michigan changes from 216 Mgal/d in the base model to 219 Mgal/d in the sensitivity run, an increase of only 1 percent. The reason for the insensitivity of overall results to variable Great Lake stage is that most of the groundwater outflow in the model occurs not to the Great Lakes but to inland surface-water features. Owing to lack of data for the SEN6-GLS run, as for the SLMB-C run, the stages of streams and water bodies were fixed for the entire duration of the simulation; consequently, the true effect of temporal variability in surface-water levels on model results is not represented.

7.2.3 Grid Spacing

A regional finite-difference groundwater-flow model is generally characterized by a large domain discretized into a grid that is coarse relative to the density of features such as surface-water discharge zones. Among all the possible tests of the sensitivity of LMB model results to its 5,000-ft nearfield grid spacing, one was selected that centers on a key outcome of the model simulation: the rate of groundwater direct discharge to Lake Michigan. The objective was to determine how the grid resolution affects the partitioning of flow near the Lake Michigan shoreline between inland surface water (indirect discharge) and the lake (direct discharge)—that is, whether the coarse grid spacing introduces a systematic bias into the relative discharge rates simulated by the regional model.

The sensitivity analysis of discharge near the shoreline requires the use of inset models (a smaller model "inset" into the larger model, using the larger model results as boundary conditions for the smaller model) as a way of contrasting results from refined as opposed to coarse grid spacing; use of inset models in this context also demonstrates the utility of the regional model in construction of local-scale models, one of the goals of this study. Eight inset models of roughly equal area were constructed, all within the Lake Michigan Basin (fig. 82). Each nearfield subregion contains one inset model except for the NLP_MI subregion, which contains two. A telescopic mesh refinement (TMR) approach available through the Groundwater Vistas interface (Rumbaugh and Rumbaugh, 2007) allows models with refined grid resolution to be automatically constructed such that the imposed boundary conditions (CHD, RIV, and GHB) at the edges of the inset domain honor the water-level conditions simulated by the regional model. For TMR construction, the boundary heads correspond to predevelopment conditions (no pumping wells). The layering and property values specified for the inset models correspond exactly to the base regional model, SLMB-C.

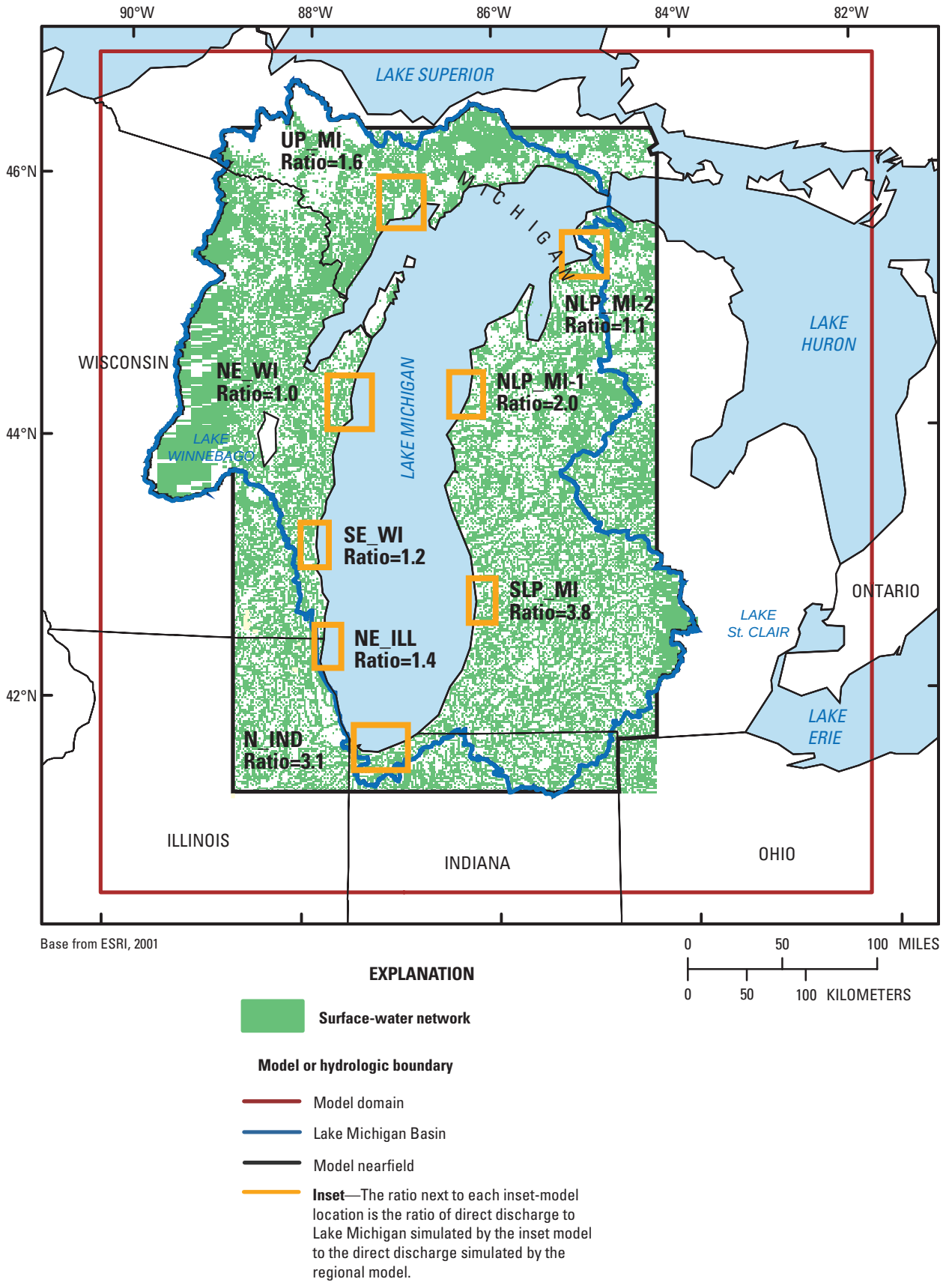

Figure 82. Locations and results for shoreline inset models.

However, the grid spacing for each inset model is smaller, producing cells 500 ft on a side with an area 1/100th the size of a regional model cell. The areal extent of the RIV cells in the inset model is the same as for the base model. (See figs. 83*A* and *B*, which contrast the grid spacing and compare the RIV cell distribution, shown in green, for the regional and inset models for the TMR in SLP_MI.) Conductance terms of the RIV cells internal to the inset domains were adjusted to ensure that the flow into and out of the inset model domain is virtually identical to the flow through the regional model for the same area. In this way, it is possible to directly compare the partitioning of a single amount of outflow between the two competing sink types, inland surface water and Lake Michigan, at two very different grid resolutions.

The assumption underlying the comparison is that the refined spacing of the inset models allows for a more accurate simulation of gradients near discharge areas, and, therefore, a more accurate account of the fate of groundwater. The theoretical basis for this understanding is discussed in appendix 2. In that discussion reference is made to a "leakage factor" symbolized by λ, which indicates the degree of grid refinement needed to accurately simulate discharge patterns around surface-water features as a function of the distribution of horizontal and vertical hydraulic conductivity and layer thicknesses (Haitjema and others, 2001). Calculation with LMB model inputs of the average value and range of values for λ around the Lake Michigan shoreline indicate that the 500-ft spacing of the inset models is generally adequate to simulate discharge without introducing numerical inaccuracies.

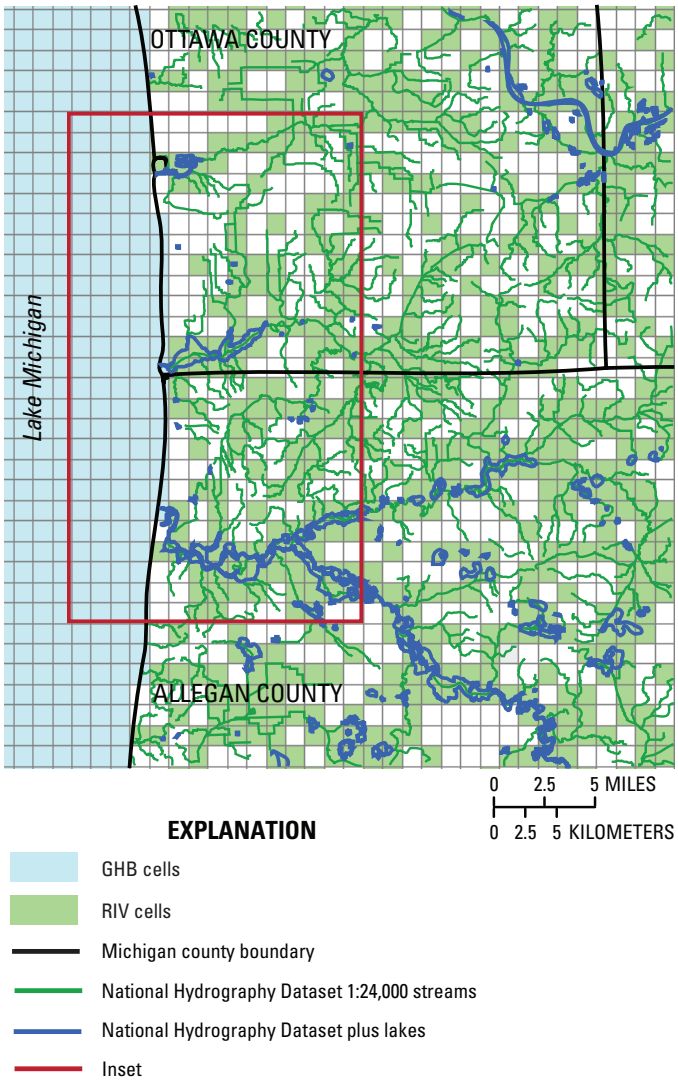

Figure 83*A*. Representation of inset area in SLP_MI: regional model.

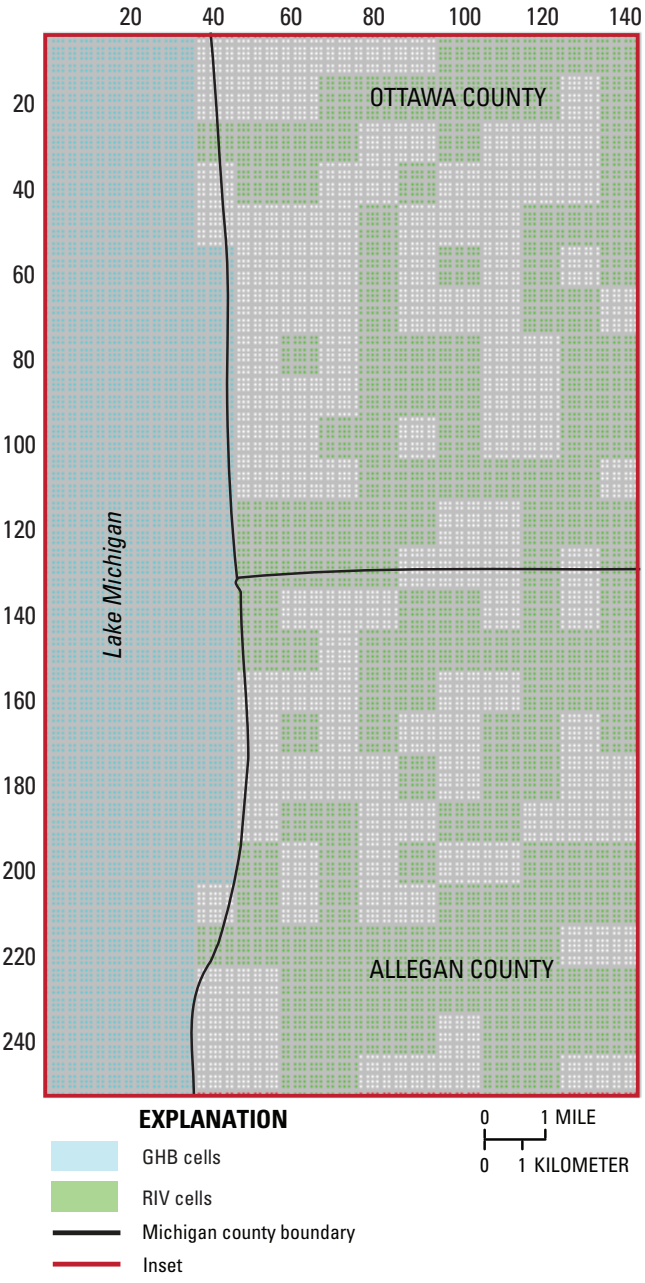

Figure 83*B*. Representation of inset area in SLP_MI: inset model with refined grid.

The results of the sensitivity analysis are presented in terms of the ratio of direct predevelopment Lake Michigan discharge simulated by the inset model relative to the regional model. A value greater than 1 indicates that the inset model yields a higher rate of discharge to the lake than does the regional model. For all eight inset areas, the ratio is greater than 1, although the value ranges from 1.02 in NE_WI to 3.81 in SLP_MI (fig. 82). The systematic discrepancy suggests that the finer resolution is needed to accurately simulate the hydraulic gradients toward Lake Michigan along its shoreline. The average ratio is 1.9; but when the total direct discharge is summed across all eight areas for the two grid resolutions, the global ratio is equal to a lower value, 1.27. This calculation suggests that the regional model, due to its coarse grid spacing, systematically underestimates the discharge to Lake Michigan by a factor on the order of 30 percent.

The coarse grid resolution of the regional model gives rise not only to inaccuracies in local gradients but also to blocky and, therefore, inaccurate representation of the elevation and geometry of surface-water features. The misrepresentation of the surface-water geometry can be compensated for by the conductance term, which incorporates the length and width of the stream segments or lake areas represented by the RIV cell. However, some distortion still arises from the grouping of multiple surface-water features in a single cell (see appendix 2). The effect of grouping multiple features was assessed by using an inset model constructed for the SLP_MI. In this case, the inland surface-water network is recast from the original blocky input (fig. 83*B*) to input that more accurately reflects the true geometry of streams and water bodies (fig. 83*C*) by matching surface-water features directly to the finer mesh. The sum of the conductance terms for each segment of surface water represented by the two sets of RIV cells is identical. This refined-grid inset model simulates greater discharge to Lake Michigan than the original inset model with a refined grid and blocky RIV input. The factor *increases* by 14 percent, changing from 3.8 to 4.3 times the regional model discharge.

The foregoing analyses suggest that bias arising from coarse grid resolution is large enough to justify a correction of the overall estimates of groundwater interactions with Lake Michigan generated by the regional LMB model. It is instructive to combine the average increase simulated by the inset models due to a refined grid alone (1.27) with the increase simulated arising from refining the surface-water network in the one case tested (1.14). If the resulting value, 1.45, is applied generally to the regional model results, it implies that

- the proportion of (predevelopment) groundwater inflow to the Lake Michigan Basin that discharges directly to Lake Michigan, rather than to competing sinks, should be increased from 1.3 percent to almost *2 percent of the overall water budget*, and
- the average rate of (predevelopment) direct groundwater discharge to Lake Michigan should be increased from the calculated value of 0.33 ft^3/s per 5,000 ft of shoreline to 0.48 ft^3/s per 5,000 ft of shoreline or, in other terms, *0.50 ft^3/s per mile of shoreline*; this corrected average rate is at the low end of the range of 0.5 to 2.0 ft^3/s per mile of shoreline estimated by Neff and Nicholas (2005).

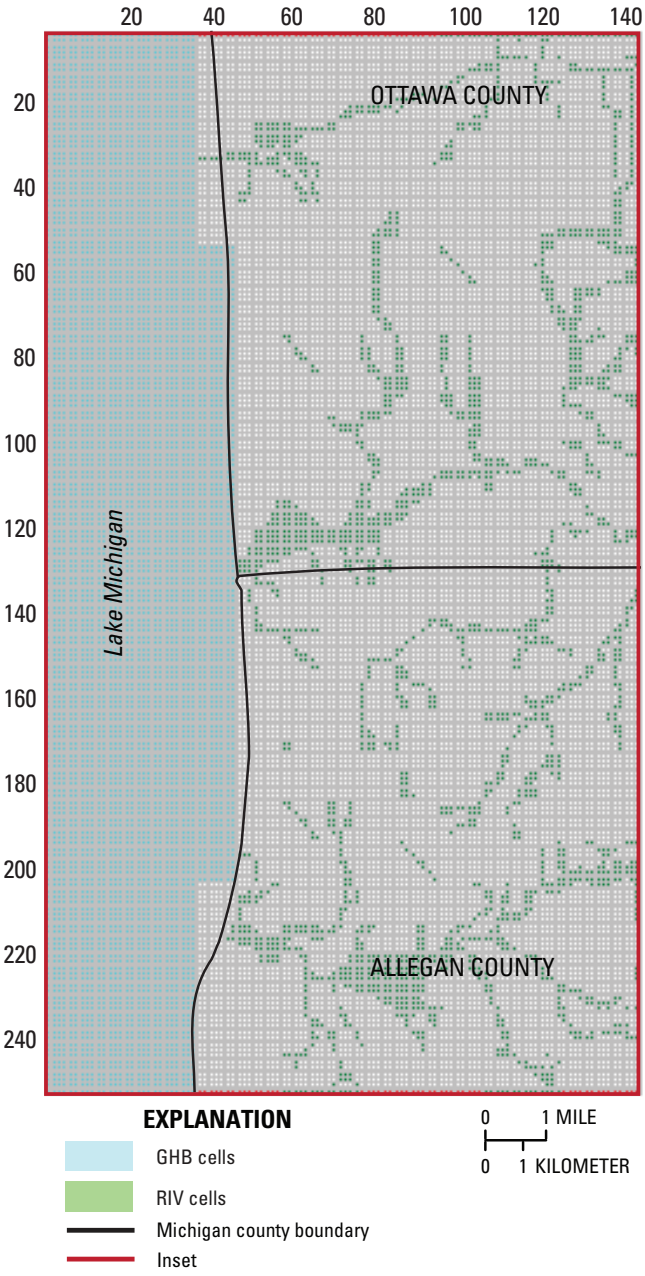

Figure 83*C*. Representation of inset area in SLP_MI: inset model with refined grid and refined surface water.

8. Model Limitations and Suggestions for Future Work

Model limitations stem from the regional scale of the study, gaps in available data, model conceptualization, and unaccounted-for processes. They are summarized below. In some cases, more detail is contained in companion reports that describe the methods and datasets used to estimate model stratigraphy and salinity (Lampe, 2009), the distribution of glacial texture (Arihood, 2009), water use (Buchwald and others, 2010), and recharge (Westenbroek and others, 2010).

Grid spacing—The 5,000-ft grid spacing in the model nearfield and the 20 layers employed to accommodate multiple aquifer systems yield a model with more than 2 million cells and approximately 100,000 cells per layer. A more finely discretized model would produce too many cells to efficiently manage with respect to input and output with the tools employed. Throughout this report, attention has been paid to the problems that arise from overlaying the dense surface-water network characteristic of the areas around the Great Lakes on the regional grid spacing. (See in particular the discussion of the conceptual model in section 3. See also the final subsection of appendix 2; there, a schematic model is presented to demonstrate that the coarse grid spacing in the regional model introduces errors in the simulated rate of exchange between groundwater and surface water, which, especially in areas of fine-grained sediments, can be on the order of 50 percent or more.) The coarse spacing restricts the magnitude of the water-table response to transient stresses, limits the value of calibration targets in the shallow flow system in estimating parameters, and distorts the partitioning of discharge among surface-water sinks. It also precludes the model from simulating flow paths shorter than 5,000 ft and limits the precision with which point features (especially pumping wells) can be located. Similarly, the large thickness of many of the bedrock layers causes pumping stresses from partially penetrating wells to sometimes be assigned too shallow or too deep.

Time stepping—Not only the spatial resolution but also the temporal resolution of the model affects the dynamics of the system and the spectrum of results. Each stress period in a MODFLOW-2000/SEAWAT-2000 simulation has its own imposed conditions, such as recharge and pumping. The conditions are updated at the beginning of a stress period and held constant for the duration of the stress period; they do not evolve continuously over the course of time. The *modeled* system responds to the stepwise changes in these conditions first through changes in water levels, which are reflected in the storage term, and then through changes in the fluxes between the groundwater system and external features, such as surface water. The rate of removal (or addition) of water from (or to) storage is highest in the first time step, immediately after the imposed stepwise changes in stresses when the rate of change of water levels is greatest, and lowest for the final time step, when water levels have had time to stabilize and external inflows and outflows have had time to adjust. Conversely, the change in flux to and from surface-water features is at its highest value for the final time step because the accumulated response to variations in pumping or recharge is greatest at the end of the stress period. All the source and sink results presented in this report correspond to the last time step in the stress period. The tabulated values for storage flux can be taken as minimum contributions for a stress period, and tabulated values for lateral flow or exchange with surface water can be taken as maximum contributions for the period.

The difference between the beginning and ending storage rates in a stress period can be large, amounting often to a reduction of more than half. For the SLMB-C simulation in the 1976–80 stress period, the storage release in the model nearfield after the first time step (60 days from the step change) is 1,926 Mgal/d, but it is only 522 Mgal/d for the last time step (2.5 to 5 years from the step change). For the 2001–5 stress period, the nearfield reduction is from 217 to 98 Mgal/d. When recharge effects are filtered from the results and only the storage fluxes associated with changes in pumping are compiled, it is possible to compare the storage contribution to wells as a function of the time step selected within a stress period. For the SLMB-C simulation in the 1976–80 period, net storage release during the first time step accounts for 26 percent of the water diverted to nearfield wells but for only 17 percent during the last time step. It is not clear which value is more representative of the overall role of storage as a source of water to wells. It is important to recognize that the results presented in figures and tables represent the low end of a range for the storage contribution and that the high end could be even 2 times greater. However, because changes in pumping are, in reality, gradual rather than stepwise, all the storage contributions simulated by the model are necessarily approximate. Because the reported changes in base flow to surface water represent maximum values for the stress period, they can be considered "conservative" estimates of the effects of pumping or recharge changes on surface-water/groundwater interactions.

Dewatering—The LMB model results are consistent with field evidence in showing that some cells at the top of the Cambrian-Ordovician aquifer system that were confined under predevelopment conditions become unconfined between 1864 and 2005. The timing of dewatering and formation of a deep water table varies from location to location. This dewatering phenomenom requires adjustments to the input of the confined version of the LMB model. For the SLMB-C simulation, the hydraulic-conductivity values of the dewatered cells are adjusted to reflect the loss of saturated thickness and yield an effective transmissivity more reflective of pumped conditions. Because MODFLOW allows only one storage parameter for a model simulated in confined mode, cells in deep aquifers that become unconfined at some time during the simulation are represented with a "compromise" value of specific storage, which is inserted for the entire simulation period and, when multiplied by cell thickness, is smaller than the specific-yield value appropriate for unconfined conditions but larger than

the storage-coefficient value appropriate for confined conditions. The methods adopted to quantify the adjusted values of hydraulic conductivity and storage parameters are discussed in section 5.1. The use of these adjusted terms introduces some error in the simulated conditions around deep pumping centers for the confined version of the LMB model. In contrast, the input to the unconfined version of the model, SLMB-U, requires no adjustments because the transmissivity is automatically a function of saturated thickness and the correct storage term is automatically selected as a function of water-level conditions. Thus, SLMB-U is not affected by the same limitations with respect to deep unconfined conditions as is SLMB-C. Comparison of their results shows that the maximum drawdown patterns for the two simulations are very similar in the areas of deep dewatering and suggests that distortions arising from the confined transmissivity and storage adjustments for SLMB-C are not large (see fig. 75). However, comparison of water-level hydrographs shows that the early drawdown history is different for the two simulations and indicates that some caution must be exercised in using the results of the confined version of the model that pertain to the rate of water-level change (see section 7.1 and fig. 74). It is also possible that the particle-tracking results discussed in section 6, particularly in relation to the contributing areas of deep Cambrian-Ordovician wells, are influenced by the assumption of fully saturated conditons implicit in the confined version of the model, which allows for vertical and horizontal flow across cells even if the simulated water level is below the cell bottom.

Data gaps—Beyond the limitations posed by the model's spatial and temporal discretization and by model assumptions, data gaps add uncertainty. Notable examples are the following:

- Zonation of subsurface properties (on the basis, for example, of scattered aquifer tests).
- Surface-water stages based on interpolation of land-surface data rather than on local stage measurements (which probably introduces a bias, given that the gridded land-surface data used to compute the stages tend to overestimate the elevation of incised channels).
- Fixed surface-water stages do not reflect variations in stage that have occurred in time as a result of wetter and drier periods.
- Absence of domestic pumping from model input (withdrawals largely but not entirely balanced by return flow through septic systems to the same shallow aquifers from which the groundwater was withdrawn).
- Absence of farfield high-capacity pumping in the farfield areas of Michigan and Indiana (an omission that probably has little effect on nearfield results because most of the missing farfield pumping is shallow and its lateral influence is buffered by surface water).
- Uneven distribution of calibration targets (for example, vertical-head-gradient targets are largely limited to the western side of Lake Michigan; even more important, although there are data against which to match the simulated rebound in NE_ILL of deep water levels after 1980, data are scarce that relate to drawdown between 1940 and 1980, making it difficult to evaluate the parameters affecting the slope of the drawdown curve).
- Uncertainty about the distribution of effective porosities (equated in this study with the distribution of calibrated specific-yield values), especially due to the effect of unknown preferential flow paths; for example, those associated with gravel beds in unconsolidated deposits or with joints and partings in bedrock units. Effective porosities are not an input to SEAWAT-2000 and therefore have no effect on simulated water-level and flux results, but they are an input to MODPATH and therefore affect particle-tracking results, notably the estimated traveltimes of flow to pumping wells.

Unrepresented processes—The modeled areas shown in this report were conceptualized in a way that was consistent with the observed data. However, alternative conceptualizations could be used to model this area. Several of these alternative conceptualizations were presented in this report, but that should not preclude other conceptualizations that fit the observed data. In particular, the fact that some processes were approximated or neglected in the conceptualization adds uncertainty to model outcomes. For example, the contribution of vertical flow through abandoned, unsealed boreholes to the downward leakage between shallow and deep aquifers is not well understood. A study of this issue as it pertains to the shallow and deep aquifers separated by the Maquoketa hydrogeologic unit in southeastern Wisconsin (Hart and others, 2008b) concluded that abandoned boreholes could potentially transmit an appreciable amount of downward leakage to the deep part of the flow system, rivaling the downward flow through the Maquoketa itself, but it is not known whether conditions around the boreholes generally allow water to readily enter or exit in order to take advantage of the open conduits. The assumption that the bedrock at the regional scale acts as an equivalent porous medium (see section 3.1, discussion of preferential flow) is a recognition that the LMB model is not capable of simulating the local effects, for example, of fractures and bedding planes on the drawdown pattern around individual wells.

The chief source of inflow to the LMB model is recharge. The soil-water-balance model (see section 4, "Model Construction") devoted to estimating the spatial and temporal distribution of recharge is a sophisticated tool, but some processes influencing the transfer of water from the surface to the water table are not considered in the way the algorithm

was applied for this study. Among the unrepresented processes are overland routing of surface runoff to account for focused recharge in low-lying areas (an effect that is probably secondary at the 5,000-ft nearfield grid spacing) and irrigation as a source of recharge (it was assumed that all but a very small proportion is consumed by evapotranspiration, which might not always be true). Other limitations affect the ability of the estimated cell-by-cell recharge distribution to be updated during the calibration process. Limitations might have been introduced by the use of partly overlapping base-flow target sets to calibrate both the SWB model and the LMB groundwater-flow model, by the routing of all the water entering surface-water features to the target locations (even from wetlands, which might lose at least part of their base flow to evapotranspiration), and by estimating only a single multiplier for recharge on the basis of conditions at the end of the model simulation and then applying that same multiplier to all earlier stress periods rather than estimating recharge independently for different periods.

Other unrepresented processes might affect the ability of the model to serve as a forecasting tool. In principle, the flux boundary in the southeastern corner of the model should be updated to reflect future flow into and out of the domain. However, sensitivity analysis suggests that the effects of neglecting variations in this flux on model results are small except in some cases for the C-O aquifer system (see section 7). Upconing of saline water around pumping centers (for example around Joliet in NE_ILL, where DS concentrations have risen in well discharge) could be simulated by running the model in transport mode, but preliminary analysis suggests that the coarse grid spacing—and, especially, the thickness of the layers—blunts the model's ability to simulate local movement of the saline body (see section 7). More generally, it must be emphasized that the LMB models (that is, both the SLMB-C and SLMB-U simulations) do not fully reflect the processes that control flow in the Michigan Basin where saline conditions are most prevalent. Variations in density are grossly estimated across the more than 10,000-ft thickness of the basin, and the influence of temperature gradients, viscosity distribution, and any lingering effect on the flow field of overpressurization due to glacial unloading (discussed, for example, by Bahr and others, 1994) are neglected. In this sense, it is probably most fitting to consider the saline body more as a boundary condition that influences conditions at the edges of the freshwater body. LMB model results simulated within the saline body—water levels and flow patterns alike—should be considered approximate.

Limited precision—Regional model results are inherently inprecise. An important example involves the simulated locations of groundwater divides. The simulated locations are uncertain because they vary with depth, they change through time, and they are very sensitivite to pumping rates as well as model inputs (such as the hydraulic-conductivity distribution) and model geometry (such as the coarse grid spacing). For all these reasons, if precise knowledge of the location of shallow or deep groundwater divides were needed for management decision-making purpose at the local scale, additional data and analysis would be needed to refine the regional results.

Most of the limitations discussed above may be considered avenues for future work. Two areas of possible future study are discussed here. The most recent version of the SEAWAT-2000 code (Langevin and others, 2008) is able to simulate temperature gradients and viscosity conditions. In principle, it could also be used to simulate overpressurization in the Michigan Basin by means of imposed areas of high head and possibly even the action of sources of salinity (for example, in the Salina Group) by means of concentration source cells. The LMB model could be used as a starting point for future models aimed at a more rigorous study of variable-density conditions in the Michigan Basin. Versions of the model with refined lateral spacing and layering might help to increase understanding of the role of pumping on movement of saline water; for example, in the MSHL aquifer system in Michigan and the C-O aquifer system in northeastern Illinois (for an example application of this type, see Lahm and Bair, 2000).

The regional model is partially designed to be a platform for inset models, which address local water-resource issues at a finer grid resolution. Two recent methodological advances have enhanced the flexibility and power of the connection between the regional model and the local refined model embedded in it. The first, called Local Grid Refinement (Mehl and Hill, 2005), allows changes in the parent regional model to influence the child local model, and the reverse is true. This advance is particularly important for maintaining proper boundary conditions for the refined inset model as stresses are added inside it or around it. For example, the gradual expansion of drawdown in the regional model due to a pumping center at some distance from the local model automatically influences conditions at the boundary and inside the local grid, something that does not occur automatically with an inset model with fixed boundary conditions. The second approach, called hybrid finite-difference/analytic-element modeling, replaces the upper layer of the MODFLOW-2000 or SEAWAT-2000 model with a gridless analytic-element layer on the basis of techniques discussed by Haitjema (1995); this substitution allows the problems associated with superimposing the surface-water network on the finite-difference grid to be largely overcome without any alteration of the original horizontal or vertical grid spacing in the layers below the top layer. The possible advantages of this approach for simultaneously simulating with enhanced accuracy shallow and deep flow conditions is the subject of ongoing research (Haitjema and others, 2010). A study area was selected within the LMB model domain—shown in figure 84—to test the new Local Grid Refinement and Hybrid methods on a single problem involving the effect of pumping near a headwater stream on low-flow surface-water discharge (Hoard, 2010).

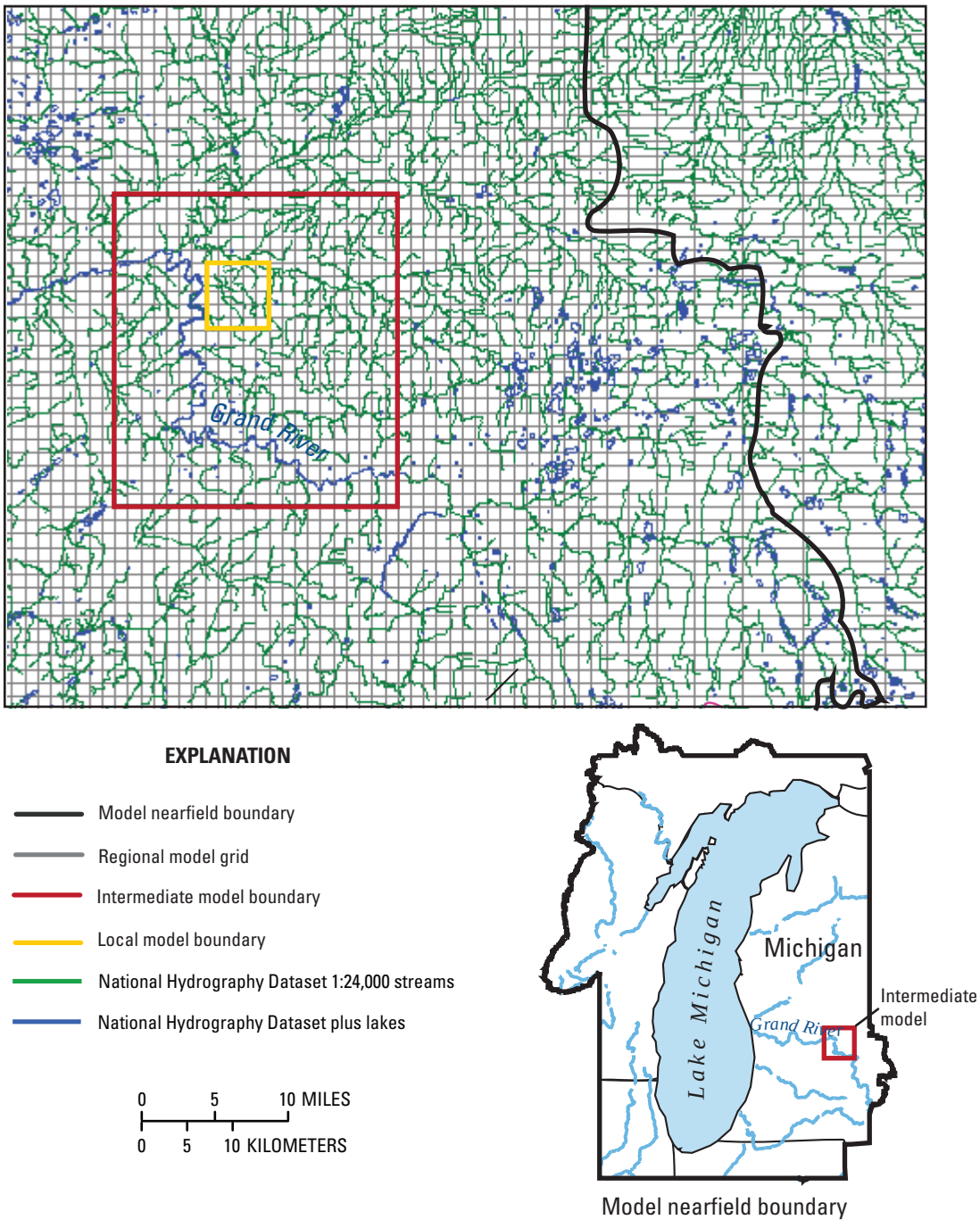

Figure 84. Demonstration area for inset models with grid refinement.

9. Summary and Conclusions

A regional groundwater-flow model of the Lake Michigan Basin and surrounding areas has been developed in support of the USGS National Assessment of Water Availability and Use—Great Lakes Basin Pilot. The transient 2-million-cell model incorporates multiple aquifers and pumping centers with drawdown that extend into deep saline waters. The 20-layer model simulates the exchange between a dense surface-water network and heterogeneous glacial deposits overlying stratified bedrock of the Wisconsin and Kankakee Arches and the Michigan Basin in the Lower and Upper Peninsulas of Michigan; eastern Wisconsin; northern Indiana; and northeastern Illinois. It provides a platform for quantifying the regional sources and sinks of groundwater (including recharge, pumping, and groundwater flow to inland surface water and to Lake Michigan—all elements of the groundwater budget that change with time) and for mapping the direction and magnitude of flows in a series of aquifers (including the source areas for wells and the locations of major groundwater divides at various depths on both sides of Lake Michigan and the migration of the divides in response to pumping).

Five datasets, which were prepared as part of the Great Lakes Basin Pilot to serve as the foundation for model development, are described in separate reports:

- a three-dimensional hydrogeologic representation of aquifers and confining units above the Precambrian basement, with a maximum thickness of 15,000 ft in the middle of the Michigan Basin (Lampe, 2009);
- maps of the coarse fraction of unconsolidated material at depth intervals of 0–100 ft, 100–300 ft, and greater than 300 ft, overlaid on existing interpretations of glacial categories (Arihood, 2009);
- location, depth, and pumping rates of high-capacity public-supply, industrial, and irrigation wells from the early 20th century through 2005 (Buchwald and others, 2010), a compilation that documents generally upward trends in withdrawals and some shifts between deep and shallow pumping;
- maps of recharge derived from a soil-water-balance model that reveals trends in the spatial and temporal distribution of inflow to the water table (Westenbroek and others, 2010); and
- maps of salinity in hydrogeologic units that show the three-dimensional boundary between fresh and saline water, as well as the distribution of high concentrations of dissolved solids in the Michigan Basin (Lampe, 2009).

These datasets, along with boundary conditions linked to outlying Great Lakes (see section 4), hydrologic coverages delineating the surface-water network (see appendix 2), and hydrogeologic information relating primarily to hydraulic conductivity (see appendix 4) provided the input required by the SEAWAT-2000 model to simulate groundwater flow before pumping (steady-state simulation) and after development (transient simulation with 12 stress periods extending from 1864 to 2005). The simulation uses a form of the groundwater-flow equation that takes account of variable density (Langevin and others, 2003). Two versions of the model were calibrated: one for confined conditions (SLMB-C) and one for unconfined conditions (SLMB-U). Multiple target sets developed from observations of head and base flow and inversion methods using the suite of PEST computer programs (Doherty, 2008a, b; Doherty and others, in press) guided the adjustment of initial inputs. Comparison of updated parameter values, calibration statistics, and parameter sensitivities demonstrated that SLMB-C and SLMB-U produced solutions similar in most respects.

The output of the calibrated confined model was selected for detailed presentation largely for reasons of numerical stability during inversion and no loss of pumping to dry cells as a result of drawdown. The simulated results, organized laterally into seven subregions and vertically into five aquifer systems, included maps, cross sections, and tables of

- regional predevelopment water-table and head conditions at depth in bedrock units;
- changes in water levels (drawdown and recovery) over time, by aquifer system;
- changes in the magnitude and direction of shallow and deep flow; and
- water budgets that quantify regional sources (such as recharge and storage release) and sinks (such as base flow to streams and discharge to wells) through time.

Analysis of the results by means of particle tracking revealed

- sources of water to shallow and deep wells by subregion;
- the changing configuration of the divides that delineate the Lake Michigan groundwater basin and the postdevelopment groundwater basins around pumping centers; and
- the distribution of direct and indirect discharge of groundwater to Lake Michigan and the modifying effects of pumping on the distribution.

The multiple perspectives provided by the model output portray a regional groundwater-flow system that, over time, has largely maintained its natural predevelopment configuration but locally has been strongly affected by well withdrawals. The quantity of rainfall in the Lake Michigan Basin and adjacent areas supports a dense surface-water network and recharge rates consistent with generally shallow water tables and a flow system generally dominated by shallow circulation. At the regional scale, pumping has not caused appreciable disruption of the shallow flow system; however, pumping has resulted in decreases in base flow to streams and in direct discharge to Lake Michigan. Comparison of inset models

constructed along the Lake Michigan coastline suggests that the regional model, because of its coarse grid spacing and coarse representation of surface water, underestimates the direct discharge by about 48 percent. When the bias is corrected, the results indicate that about 2 percent of total groundwater flow is directly discharged to the lake at a rate of about 0.5 ft^3/s per mile of shoreline.

Well withdrawals have caused reversals in regional flow patterns around pumping centers in deep, confined aquifers (most noticeably in the Cambrian-Ordovician aquifer system on the west side of Lake Michigan near the cities of Green Bay and Milwaukee in eastern Wisconsin, and around Chicago in northeastern Illinois), as well as in some shallow bedrock aquifers (for example, in the Marshall aquifer near Lansing, Mich.). The shifts in flow have been accompanied by large drawdowns with consequent local decrease in storage (moderated in some areas by metropolitan water-supply projects that substituted Lake Michigan water for groundwater supplies). On the west side of Lake Michigan, well withdrawals have caused a complete reconfiguration of the deep divides. Before the advent of pumping, the deep Lake Michigan groundwater basin boundaries extended to the west of the Lake Michigan surface-water basin boundary, in some places by tens of miles. Over time, the pumping centers have replaced Lake Michigan as the regional sink for the deep part of the flow system.

The regional model results provide a broad picture of the status of the groundwater resource and how it has responded to pumping. However, there are limitations imposed by the relatively coarse grid spacing. Laterally, the finite-difference cells are 5,000 ft on a side in the Lake Michigan Basin and in adjoining areas. At this resolution, the simulation of the water-table response to pumping is severely constrained by the necessity of including enough of the surface-water system in model cells to provide outlets for recharge and, thereby, to avoid spurious simulated water-level mounding. The mounding that occurs when discharge points are neglected can be offset by increasing hydraulic conductivity; but, as discussed in section 3, this fix distorts the K_h and K_v fields relative to field conditions. In order to avoid distorting the hydraulic conductivity input, more than half the water-table cells in the Lake Michigan Basin model contain surface-water features, each of which is represented by a boundary condition with a fixed stage. The stage tends to "staple" the water-table solution because there is generally a small gradient between the average groundwater head solved for the cell and the surface-water level assigned to the cell. The regional model by itself cannot overcome this limitation; however, in conjunction with techniques for inset models, it can lay the foundation for any number of applications designed to address local management problems related to optimizing water supply and maintaining ecologic flows. Two promising new techniques—Local Grid Refinement in MODFLOW-2005 and Hybrid Analytic- Element/Finite- Difference Modeling—could allow enhanced versions of the regional model to simulate groundwater/surface-water interactions in the presence of pumping at the necessary level of refinement while still maintaining the regional pattern of flow needed to properly simulate water availability. Research aimed at demonstrating these two methods in a setting characterized by pumping near headwater streams is part of the Great Lakes Basin Pilot project (see Haitjema and others, 2010; and Hoard, 2010).

The construction of alternative versions of the regional model reveals important *in*sensitivities with respect to model design. One is related to variable density. Whereas the specification of salinity dramatically affects groundwater conditions in the deep Michigan Basin and even though the simulated drawdown around pumping centers extends into the highly saline waters, model results indicate that variable density can be neglected with only very small effect on the range of simulated results in *freshwater* areas under either predevelopment or stressed postdevelopment conditions. Relaxing the assumption that saline concentrations are fixed through time also has little effect on model output. A second finding of insensitivity is related to the level of detail appropriate for the values assigned to the hydraulic conductivity of unconsolidated sediments. The availability of geologic descriptions from hundreds of thousands of driller logs for household wells permitted cell-by-cell mapping of hydraulic conductivity in the top three model layers. When this distribution is zoned more broadly on the basis of glacial categories alone (that is, on the basis of material types such as clayey till and coarse outwash), the model results give rise to a somewhat modified water-table solution, but the agreement to calibration targets is only weakly compromised, and the findings are very similar to the more detailed model with respect to the regional drawdown response and the regional water budget.

In summary, the results of this modeling effort have yielded

- improved estimates of the various components of the water budget for the region,
- improved estimates of the various hydraulic properties of the geologic units in the region, and
- a better understanding of the groundwater flow throughout the region.

The regional model is also intended to support the framework pilot study of water availability and use at the scale of the entire Great Lakes Basin. To that end, an ongoing effort has been undertaken to distill the model findings using a series of *sustainability indicators*. These are intended to reveal overall patterns in the status of the water resource in terms of the human effect on natural groundwater flows and on groundwater/surface-water interactions. Ongoing work includes application of the regional model in *forecasting* mode to shed light on the effects of possible future levels of pumping on the groundwater system, and the model is being used to test hypotheses regarding the effect of *climate variability and change* on water availability. These aspects, along with a demonstration of the procedures for embedding models and sample results related to ecologic flows, are discussed in detail in a USGS Professional Paper on the comprehensive findings of the Great Lakes Basin Pilot Project (Reeves, in press).

10. References

Allen, W.B., 1977, Flowing wells in Michigan, 1974: Michigan Geological Survey Water Information Series Report 2, 27 p.

Allen, W.B., and Waller, R.M., 1975, Great Lakes Basin framework study—Appendix 3, Geology and ground water: Ann Arbor, Mich., Great Lakes Basin Commission, 152 p.

Anderson, M.P., and Woessner, W.W., 1992, Applied groundwater modeling—Simulation of flow and advective transport: San Diego, Academic Press, 381 p.

Apple, B.A., and Reeves, H.W., 2007, Summary of hydrogeologic conditions by county for the State of Michigan: U.S. Geological Survey Open-File Report 2007–1236, 79 p.

Arihood, L.D., 2009, Processing, analysis, and general evaluation of well-driller logs for estimating hydrogeologic parameters of the glacial sediments in a ground-water flow model of the Lake Michigan Basin: U.S. Geological Survey Scientific Investigations Report 2008–5184, 26 p.

Arihood, L.D., and Basch, M.E., 1994, Geohydrology and simulated ground-water flow in an irrigated area of northwestern Indiana: U.S. Geological Survey Water-Resources Investigations Report 92–4046, 38 p.

Arihood, L.D., and Cohen, D.A., 1998, Geohydrology and simulated ground-water flow in northwestern Elkhart County, Indiana: U.S. Geological Survey Water-Resources Investigations Report 97–4204, 47 p.

Arnold, J.G., Muttiah, R.S., and Allen, P.M., 2000, Regional estimation of base flow and groundwater recharge in the Upper Mississippi river basin: Journal of Hydrology, v. 227, no. 1, p. 21–40.

Arnold, T.L., and Friedel, M.J., 2000, Effects of land use on recharge potential of surficial and shallow bedrock aquifers in the upper Illinois River Basin: U.S. Geological Survey Water-Resources Investigations Report 00–4027, 18 p. (Also available at *http://il.water.usgs.gov/nawqa/uirb/pubs/reports/WRIR_00-4027.pdf.*)

Arvin, D.V., and Spaeth, Ralph, 1996, Trends in Indiana's water use, 1986–96: Indiana Department of Natural Resources, Division of Water, Special Report 1, 19 p.

Avery, C.F., 1995, Reversal in declining ground-water levels in the Chicago area: U.S. Geological Survey Fact Sheet FS–222–95, 2 p.

Ayers, J.C. [n.d.], Surficial bottom sediments of Lake Michigan: Ann Arbor, Mich., Great Lakes Environmental Research Laboratory, unpub. preliminary data document, p. 247–253.

Ayers, J.C., and Chandler, D.C., 1967, Studies on the environment and eutrophication of Lake Michigan: Ann Arbor, Mich., University of Michigan, Great Lakes Research Division, Final Report of U.S. Public Health Service Grant WP–00311, Special Report 30, p. 228–246.

Bahr, J.M., Moline, G.R., and Nadon, G., 1994, Anomalous pressures in the deep Michigan Basin, *in* Ortoleva, P., ed., Basin compartments and seals: American Association of Petroleum Geologists Memoir 61, p. 153–165.

Bailey, Z.C., Greeman, T.K., and Crompton, E.J., 1985, Hydrologic effects of ground- and surface-water withdrawals in the Howe area, Lagrange County, Indiana: U.S. Geological Survey Water-Resources Investigations Report 85–4163, 130 p.

Balding, G.O., 1991, Changes in chloride concentration in water from municipal wells that tap aquifers in rocks of Cambrian and Ordovician age in northeastern Illinois, 1915–84: U.S. Geological Survey Water-Resources Investigations Report 90–4116, 52 p.

Baltusis, M.A., Quigley, M.F., and Mandle, R.J., 1992, Municipal ground-water development and withdrawals in the central Lower Peninsula of Michigan, 1870–1987: U.S. Geological Survey Open-File Report 91–215, 89 p.

Barton, G.J., Mandle, R.J., and Baltusis, M.A., Jr., 1996, Predevelopment freshwater heads for the glaciofluvial, Saginaw, and Marshall aquifers in the Michigan Basin: U.S. Geological Survey Open-File Report 95–319, 15 p.

Bartošová, Alena; McConkey, Sally; Lin, Yu-Feng; and Walker, Douglas, 2004, Using NHD to estimate stream geometry characteristics for MODFLOW, *in* Geographic Information Systems and Water Resources III, American Water Resources Association Spring Specialty Conference, Nashville, Tenn., May 17–19, 2004: 7 p.

Bassett, J.L., and Hasenmueller, N.R., 1980, Map of Indiana showing structure on top of the Maquoketa Group (Ordovician): Indiana Department of Natural Resources, Geological Survey, METC/EGSP Series No. 812, 1 pl.

Batten, W.G., 1987, Water resources of Langlade County, Wisconsin: Wisconsin Geological and Natural History Survey Information Circular 58, 28 p.

Batten, W.G., 2004, Preliminary Paleozoic geologic map of Fond du Lac County, Wisconsin: Wisconsin Geological and Natural History Survey Open-File Report 2004–23, scale 1:100,000, 1 pl.

Batten, W.G., and Bradbury, K.R., 1996, Regional groundwater flow system between the Wolf and Fox Rivers near Green Bay, Wisconsin: Wisconsin Geological and Natural History Survey Information Circular 75, 28 p.

Batten, W.G., and Conlon, T.D., 1993, Hydrogeology of glacial deposits in a preglacial bedrock valley, Waukesha County, Wisconsin: U.S. Geological Survey Water-Resources Investigations Report 92–4077, 15 p.

Batten W.G., Yeskis , D.J., and Dunning C.P., 1999, Hydrologic properties of the Ordovician Sinnipee Group at test well BN–483, Better Brite Superfund Site, DePere, Wisconsin: U.S. Geological Survey Water-Resources Investigations Report 99–4199, 19 p.

Baxter, G.P., and Wallace C.C., 1916, Changes in volume upon solution in water of halogen salts of alkali metals, II: American Chemical Society Journal, v. 38, no. 1, p. 70–104.

Bayless, E.R., and Arihood L.D., 1996, Hydrogeology and simulated ground-water flow through the unconsolidated aquifers of northeastern St. Joseph County, Indiana: U.S. Geological Survey Water-Resources Investigations Report 95–4225, 47 p.

Bayless, E.R., Westjohn, D.B., and Watson, L.R., 1995, Use of surface and borehole geophysics to delineate the glacial-drift stratigraphy of northeastern St. Joseph County, Indiana: U.S. Geological Survey Water-Resources Investigations Report 95–4041, 42 p.

Becker, L.E., Hreha, A.J., and Dawson, T.A., 1978, Pre-Knox (Cambrian) stratigraphy in Indiana: Bloomington, Ind., Indiana Department of Natural Resources, Geological Survey Bulletin 57, 72 p.

Bedell, D.J., 1982, Municipal water withdrawals in Michigan: Michigan Department of Natural Resources, Water Management Division, 43 p.

Bennett, G.D., Kontis, A.L., and Larson, S.P., 1982, Representation of multiaquifer well effects in three-dimensional ground-water flow simulation: Ground Water, v. 20, no. 3, p. 334–341.

Bond, D.C., 1972, Hydrodynamics in deep aquifers of the Illinois basin: Illinois State Geological Survey Circular 470, 51 p.

Bradbury, K.R., 1982, Hydrogeological relationships between Green Bay of Lake Michigan and onshore aquifers of Door County, Wisconsin: University of Wisconsin-Madison, Ph.D. dissertation, 287 p.

Bradbury, K.R., Hart, D.J., and Feinstein, D.T, 2007, Where is the deep groundwater divide in southeastern Wisconsin?: American Water Resources Association, Wisconsin Section, Program and Abstracts 2007, p. 61.

Bradbury, K.R., and Muldoon, M.A., 1990, Hydraulic conductivity determinations in unlithified glacial and fluvial materials, *in* Nielsen, D.M., and Johnson, A.I., eds., Ground water and vadose zone monitoring: Philadelphia, American Society for Testing and Materials, ASTM STP 1053, p. 138–151.

Bradbury, K.R., and Muldoon, M.A., 1994, Effects of fracture density and anisotropy on wellhead protection area delination in fractured-rock aquifers: Applied Hydrogeology, v. 2, no. 3, p. 17–23.

Bradbury, K.R., and Rayne, T.W., 2009, Shallow groundwater sustainability analysis demonstration for the SEWRPC region: A report to the Southeastern Wisconsin Regional Planning Commision, Technical Report Number 48, 39 p.

Braschayko, S.M., 2005, The Waukesha Fault and its relationship to the Michigan Basin—A literature compilation: Wisconsin Geological and Natural History Survey Open-File Report 2005–05, 60 p.

Brenden, T.O., Clark, R.D., Jr., Cooper, A.R., Seelbach, P.W., Wang, L., Aichele, S.S., Bissell, E.G., and Stewart, J.S., 2006, A GIS Framework for collecting, managing, and analyzing multi-scale landscape variables across large regions for river conservation and management, *in* Hughes, R.M., Wang, L., and Seelbach, P.W., eds., Influence of landscapes on stream habitats and biological assemblages: Bethesda, Md., American Fisheries Society Special Publication 48, p. 49–74.

Bricker, D.M., Milstein, R.L., and Reszka, C.R., Jr., 1983, Selected studies of Cambro-Ordovician sediments within the Michigan Basin: Michigan Geological Survey Report of Investigation 26, 54 p.

Brown, T.A., Dunning, C.P., and Sharpe, J.B., 2000, Altitude, depth, and thickness of the Galena-Platteville bedrock unit in the subcrop area of Illinois and Wisconsin: U.S. Geological Survey Water-Resources Investigations Report 97–4054–C, 3 map sheets.

Buchwald, C.A., 2009, Water use in Wisconsin, 2005: U.S. Geological Survey Open-File Report 2009–1076, 76 p.

Buchwald, C.A., Luukkonen, C.L., and Rachol, C.M., 2010, Estimation of groundwater use for a groundwater-flow model of the Lake Michigan Basin and adjacent areas, 1864–2005: U.S. Geological Survey Scientific Investigations Report 2010–5068, 120 p.

Bugliosi, E.F., 1999, The Midwestern Basins and Arches regional aquifer system in parts of Indiana, Ohio, Michigan, and Illinois—Summary: U.S. Geological Survey Professional Paper 1423–A, 46 p.

Bunner, D.W., 1993, Bedrock-surface altitude in the Midwestern Basins and Arches region of Indiana, Ohio, Michigan, and Illinois: U.S. Geological Survey Water-Resources Investigations Report 93–4050, map sheet, scale 1:1,000,000.

Burch, S.L., 1991, The new Chicago model—A reassessment of the impacts of Lake Michigan allocations on the Cambrian-Ordovician aquifer system in Northeastern Illinois: Champaign, Ill., Illinois State Water Survey Research Report 119, 52 p.

Burch, S.L., 2002, A comparison of potentiometric surfaces for the Cambrian-Ordovician aquifers of Northeastern Illinois, 1995 and 2000: Champaign, Ill., Illinois State Water Survey Data/Case Study 2002–02, 63 p.

Buschbach, T.C., 1964, Cambrian and Ordovician strata of Northeastern Illinois: Urbana, Ill., Illinois State Geological Survey Report of Investigation 218, 90 p.

Calver, A., 2001, Riverbed permeabilities—Information from pooled data: Ground Water, v. 39, no. 4, p. 546–553.

Capps, S.R., 1910, The underground waters of north-central Indiana: U.S. Geological Survey Water-Supply Paper 254, 279 p.

Carlson, D.A., 2000, Dependence of conductivities and anisotropies on geologic properties within the near-surface aquifer in Milwaukee, Wisconsin: University of Wisconsin-Milwaukee, unpublished Ph.D. dissertation (Geosciences), 768 p.

Casey, G.D., 1992, Hydrogeology of the basal confining unit of the carbonate aquifer system in the Midwestern Basins and Arches region of Indiana, Ohio, Michigan, and Illinois: U.S. Geological Survey Open-File Report 92–489, scale 1:1,000,000, 2 sheets.

Casey, G.D., 1994, Hydrogeology of the Silurian and Devonian carbonate-rock aquifer in the Midwestern Basins and Arches region, Indiana, Ohio, Michigan, and Illinois: U.S. Geological Open-File Report 93–663, scale 1:1,000,000, 2 sheets.

Casey, G.D., 1997, Hydrogeologic framework of the Midwestern Basins and Arches region in parts of Indiana, Ohio, Michigan, and Illinois: U.S. Geological Survey Professional Paper 1423–B, 46 p., 2 pl.

Chamberlin, T.C., 1877, Geology of eastern Wisconsin, *in* Geology of Wisconsin: Wisconsin Geological and Natural History Survey, v. 2, pt. 2, p. 93–405.

Cherkauer, D.S., 1999, Controls on the spatial distribution of ground-water recharge in Washington County, Wisconsin: Unpublished final report to UWS Ground-Water Research Program Project, 45 p.

Cherkauer, D.S., 2001, Distribution of ground-water recharge in southeastern Wisconsin: Unpublished final report to Source Water Protection Program, Wisconsin Department of Natural Resources, 31 p.

Cherkauer, D.S., 2004, Quantifying ground water recharge at multiple scales using PRMS and GIS: Ground Water, v. 42, no. 1, p. 97–110.

Cherkauer, D.S., 2007, Simulating the role of domestic wells in the ground-water system of southeastern Wisconsin: Abstract, Annual meeting of Wisconsin section of the American Water Resources Association.

Cherkauer, D.S., and Hensel, B.R., 1986, Groundwater flow into Lake Michigan from Wisconsin: Journal of Hydrology, v. 84, no. 3/4, p. 261–271.

Cherkauer, D.S., Taylor, R.W., and Anderson, M.P., 1990, Final report on measurement of the interaction between Lake Michigan and the ground water of Wisconsin: University of Wisconsin-Milwaukee, unpub. report, 92 p.

Cherkauer, D.S., Taylor, R.W., and Bradbury, K.R., 1987, Relation of lake bed leakance to geoelectric properties: Ground Water, v. 25, no. 2, p. 135–140.

Clayton, L., 2001, Pleistocene geology of Waukesha County, Wisconsin: Wisconsin Geological and Natural History Survey Bulletin 99, 33 p.

Colgan, P.M., and Principato, S., 1998, Distribution of glacial landforms and sediments in Wisconsin, and the Upper Peninsula of Michigan—An application of GIS to glacial geology: Poster for the North Central Geological Socitey of America regional meeting in Columbus, Ohio, accessed at *http://www.casdn.neu.edu/~geology/ department/staff/colgan/poster/POSTER.htm.*

Conlon, T.D., 1998, Hydrogeology and simulation of groundwater flow in the sandstone aquifer, northeastern Wisconsin: U.S. Geological Survey Water-Resources Investigations Report 97–4096, 60 p.

Coon, W.F., and Sheets, R.A., 2006, Estimate of groundwater storage in the Great Lakes Basin, United States, 2006: U.S. Geological Survey Scientific Investigations Report 2006–5180, 19 p.

Cornett, C.L., Crowley, S.L., McGowan, R.M., Blumer, S.P., and Reeves, H.W., 2006, Summary of recovered historical ground-water-level data for Michigan, 1934–2005: U.S. Geological Survey Open-File Report 2006–1057, 369 p.

Council of Great Lakes Governors, 2001, The Great Lakes charter annex: A supplementary agreement to the Great Lakes charter, accessed April 14, 2008, at *http://www.cglg.org/projects/water/docs/GreatLakesCharterAnnex.pdf.*

Council of Great Lakes Governors, 2005a, Great Lakes-St. Lawrence River Basin Sustainable Water Resources Agreement, accessed April 15, 2008, at *http://www.cglg.org/projects/water/docs/12-13-05/Great_Lakes-St_Lawrence_River_Basin_Sustainability_Water_Resources_Agreement.pdf.*

Council of Great Lakes Governors, 2005b, Great Lakes-St. Lawrence River Basin Water Resources Compact, accessed April 14, 2008, at *http://www.cglg.org/projects/water/docs/12-13-05/Great_Lakes-St_Lawrence_River_Basin_Water_Resources_Compact.pdf.*

Council of Great Lakes Governors, 2008, February 28 letter to U.S. Congress members, accessed April 11, 2008, at *http://www.cglg.org/projects/priorities/docs/FY09LettertoCongress22508.pdf.*

Craig, K.D., 1989, Determination of ground-water discharge into Green Bay and Lake Michigan Door Peninsula, Wisconsin: University of Wisconsin-Milwaukee, M.S. thesis, 162 p.

Crompton, E.J., Peters, J.G., Miller, R.L., Stewart, J.A., Banaszak, K.J., and Shedlock, R.J., 1986, Review of the hydrologic data-collection network in the St. Joseph River basin, Indiana: U.S. Geological Survey Water-Resources Investigations Report 86–4157, 51 p.

Devaul, R.W., 1975a, Probable yields of wells in the sandstone aquifer, Wisconsin: Wisconsin Geological and Natural History Survey map, scale 1:500,000, 1 sheet.

Devaul, R.W., 1975b, Probable yields of wells in the Niagara aquifer, Wisconsin: Wisconsin Geological and Natural History Survey map, scale 1:500,000, 1 sheet.

Devaul, R.W., 1975c, Probable yields of wells in the sand-and-gravel aquifer, Wisconsin: Wisconsin Geological and Natural History Survey map, scale 1:500,000, 1 sheet.

Doherty, John, 2003, Ground water model calibration using pilot points and regularization: Ground Water, v. 41, no. 2, p. 170–177.

Doherty, John, 2008a, PEST, Model Independent Parameter Estimation—User manual (5th ed.): Brisbane, Australia, Watermark Numerical Computing, accessed October 1, 2009, at *http://www.pesthomepage.org/Downloads.php.*

Doherty, John, 2008b, PEST, Model Independent Parameter Estimation—Addendum to user manual (5th ed.): Brisbane, Australia, Watermark Numerical Computing, accessed October 1, 2009, at *http://www.pesthomepage.org/Downloads.php.*

Doherty, John, Fienen, M.N., and Hunt, R.J., in press, Approaches to highly parameterized inversion—Pilot-point theory, guidelines, and research directions: U.S.Geological Survey Scientific Investigations Report 2010–5168.

Doherty, John, and Hunt, R.J., in press, Approaches to highly parameterized inversion—A guide to groundwater model calibration using PEST: U.S. Geological Survey Scientific Investigations Report 2010–5169.

Drescher, W.J., 1953, Ground-water conditions in artesian aquifers in Brown County, Wisconsin: U.S. Geological Survey Water-Supply Paper 1190, 49 p.

Dripps, W.R., 2003, The spatial and temporal variability of ground-water recharge within the Trout Lake basin of northern Wisconsin: University of Wisconsin-Madison, unpublished Ph.D. dissertation (Geology and Geophysics), 231 p.

Dripps, W.R., Anderson, M.P., and Potter, K.W., 2001, Temporal and spatial variability of natural ground-water recharge: Madison, Wis., University of Wisconsin Water Resources Institute, Groundwater Research Report WRI GRR 01–07, 24 p., accessed August 2006 at *http:/didgital.library.wisc.edu/1711.dl/EcoNatRes.WRIGRR01-07.*

Dripps, W.R., and Bradbury, K.R., 2007, A simple daily soil-water balance model for estimating the spatial and temporal distribution of ground-water recharge in temporate humid areas: Hydrogeology Journal, v. 15, no. 3, p.433–444.

Duan, Q., Gupta, V.K., and Sorooshian, S., 1993, A shuffled complex evolution approach for effective and efficient global minimization: Journal of Optimization Theory and Applications, v. 76, no. 3, p. 501–521.

Duan, Qingyun; Sorooshian, Soroosh; and Gupta, Vijai, 1992, Effective and efficient global optimization for conceptual rainfall-runoff models: Water Resources Research, v. 28, no. 4, p. 1015–1031.

Dunning, C.P., Feinstein, D.T., Hunt, R.J., and Krohelski, J.T., 2004, Simulation of ground-water flow, surface-water flow, and a deep sewer tunnel system in the Menonminee Valley, Milwaukee, Wisconsin: U.S. Geological Survey Scientific Investigations Report 2004–5031, 40 p.

Eadie, B.J., and Lozano, Stephen, 1999, Grain size distribution of the surface sediments collected during the Lake Michigan mass balance and environmental mapping and and assessment programs: National Oceanic and Atmospheric Administration, NOAA Technical Memorandum ERL GLERL–111, 42 p.

Eaton, T.T., 2002, Fracture heterogeneity and hydrogeology of the Maquoketa aquitard, southeastern Wisconsin: University of Wisconsin-Madison, unpublished Ph.D. dissertation (Geology and Geophysics), 211 p.

Eaton, T.T., Bradbury, K.R., and Evans, T.J.,1999, Characterization of the hydrostratigraphy of the deep sandstone aquifer in southeastern Wisconsin—Final report to the Wisconsin Deptartment of Natural Resources: Wisconsin Geological and Natural History Survey Open-File Report 1999–02, 30 p.

Eberts, S.M., 2000, Ground-water levels and ground-water discharge, glacial-deposits and carbonate-bedrock regional aquifer system, Midwestern Basins and Arches region: U.S. Geological Survey Hydrologic Investigations Atlas HA–725, scale 1:1,000,000, 2 sheets.

Eberts, S.M., and George, L.L., 2000, Regional ground-water flow and geochemistry in the Midwest Basins and Arches aquifer system in parts of Indiana, Ohio, Michigan, and Illinois: U.S. Geological Survey Professional Paper 1423–C, 103 p.

Ellefson, B.R., Fan, C.H., and Ripley, J.L.,1997, Water use in Wisconsin, 1995: U.S. Geological Survey Open-File Report 97–356,1 pl.

Ellefson, B.R., Mueller, C.D., and Buchwald, C.A., 2002, Water use in Wisconsin, 2000: U.S. Geological Survey Open File Report 2002–356, 1 sheet.

Ellefson, B.R., Sabin, T.J., and Krohelski, J.T., 1993, Water use in Wisconsin, 1990: USGS Open-File Report 93–118, 1 sheet.

Emrich, G.H., 1966, Ironton and Galesville (Cambrian) sandstones in Illinois and adjacent areas: Illinois State Geological Survey Circular 403, 55 p.

Emrich, G.H., and Bergstrom, R.E., 1962, Des Plaines Disturbance, northeastern Illinois: Geological Society of America Bulletin, v. 73, p. 959–968.

Environmental Modeling Systems, Inc. (EMS-I), 2000, Groundwater modeling system on line: Documentation available at *http://www.ems-i.com/gmshelp/gmsv40help.htm.*

Feinstein, D.T., and Anderson, M.P., 1987, Recharge to and potential for contamination of an aquifer system in northeastern Wisconsin: University of Wisconsin-Madison, Water Resources Center Technical Report 87–01, 112 p.

Feinstein, Daniel; Dunning, Charles; Hunt, R.J.; and Krohelski, Jim, 2003, Stepwise use of GFLOW and MODFLOW to determine relative importance of shallow and deep receptors: Ground Water, v. 41, no. 2, p. 190–199.

Feinstein, D.T., Eaton, T.T., Hart, D., Krohelski, J.T., and Bradbury, K.R., 2005, Regional aquifer model for southeastern Wisconsin; Report 1—Data collection, conceptual model development, numerical model construction, and model calibration: Southeastern Wisconsin Regional Planning Commission, Technical Report 41a, 81 p.

Feinstein, Daniel; Haitjema, Henk; and Hunt, Randall, 2006, Towards more accurate leakage and conjunctive use simulations—A coupled GFLOW-MODFLOW application: Conference proceedings for MODFLOW and More 2006, v. 1, p. 109–113.

Feinstein, D.T., Hart, D.J., Krohelski, J.T., Eaton, T.T., and Bradbury, K.R., 2005, Regional aquifer model for southeastern Wisconsin; Report 2—Model results and interpretation: Southeastern Wisconsin Regional Planning Commission, Technical Report 41b, 63 p.

Feinstein, Daniel; Hunt, Randall; and Reeves, Howard, 2008, Calibrating a big model—Strategies and limitations: Conference Proceedings for MODFLOW and More 2008, 5 p.

Feinstein, Daniel; Saad, David; Hart, D.; and Zeiler, K., 2003, Reconciling recharge and discharge in a regional flow model: Conference Proceedings for MODFLOW and More 2003, September 2003, v. 1, p. 351–355.

Fenelon, J.M., Bobay, K.E., and others, 1994, Hydrogeologic atlas of aquifers in Indiana: U.S. Geological Survey Water-Resources Investigations Report 92–4142, 197 p.

Fenelon, J.M., and Watson, L.R., 1992, Geohydrology and water quality of the Calumet aquifer, in the vicinity of the Grand Calumet River/Indiana Harbor Canal, northwestern Indiana: U.S. Geological Survey Water-Resources Investigations Report 92–4115, 151 p.

Fennemann, N.M., and Johnson, D.W., 1946, Physiographic divisions of the conterminous U.S.: U.S. Geological Survey, 1:7,000,000-scale map and polygon coverage.

Fienen, M.N., Muffels, C.J., and Hunt, R.J., 2009, Methods note—On constraining pilot point calibration with regularization in PEST: Ground Water, v. 47, no. 6, DOI: 10.1111/j.1745-6584.2009.00579.x, p. 835–844.

Fleck, W.B., and McDonald, M.G., 1978, Three-dimensional finite-difference model of ground-water system underlying the Muskegon County wastewater disposal system, Michigan: U.S. Geological Survey Journal of Research, v. 6, no. 3, p. 307–318.

Foley, F.C., Walton, W.C., and Drescher, W.J., 1953, Groundwater conditions in the Milwaukee-Waukesha Area, Wisconsin: U.S. Geological Survey Water-Supply Paper 1229, 96 p.

Fowler, K.K., and Arihood, L.D., 1998, Geohydrology and quality of ground water in unconsolidated aquifers near South Bend, Indiana: U.S. Geological Survey Water-Resources Investigations Report 98–4139, 3 sheets.

Fowler, K.K., and Wilson, J.T., 1996, Low-flow characteristics of Indiana streams: U.S. Geological Survey Water-Resources Investigations Report 96–4128, 313 p.

Fullerton, D.S., Bush, C.A., and Pennell, J.N., 2003, Map of surficial deposits and materials in the eastern and central United States (east of 102° west longitude): U.S. Geological Survey Geologic Investigations Series I–2789, 46 p.

Gebert, W.A., Radloff, M.J., Considine, E.J., and Kennedy, J.L., 2007, Use of streamflow data to estimate base flow/ground-water recharge for Wisconsin: Journal of the American Water Resources Association, v. 43, no. 1, p. 220–236, accessed January 24, 2008, at *http://www3.interscience.wiley.com/cgi-bin/fulltext/118544614/PDFSTART.*

Ging, P.B., Long, D.T., and Lee, R.W., 1996, Selected geochemical characteristics of ground water from the Marshall aquifer in the central Lower Peninsula of Michigan: U.S. Geological Survey Water-Resources Investigations Report 94–4220, 19 p.

Gotkowitz, M.B., Schreiber, M.E., and Simo, J.A., 2004, Effects of water use on arsenic release to well water in a confined aquifer: Ground Water, v. 42, no. 4, p. 568–576.

Government of Canada and U.S. Environmental Protection Agency, 1995, The Great Lakes—An environmental atlas and resource book: EPA 905–B–95–001, 46 p.

Grannemann, N.G., Hunt, R.J., Nicholas, J.R., Reilly, T.E., and Winter, T.C., 2000, The importance of ground water in the Great Lakes Region: U.S. Geological Survey Water-Resources Investigations Report 00–4008, 13 p.

Grannemann, N.G., and Reeves, H.W., 2005, Great Lakes basin water availability and use—A study of the National Assessment of Water Availability and Use Program: U.S. Geological Survey Fact Sheet 2005–3113, 4 p.

Grannemann, N.G., and Weaver, T.L., 1999, An annotated bibliography of selected references on the estimated rates of direct ground-water discharge to the Great Lakes: U.S. Geological Survey Water-Resources Investigations Report 98–4039, 24 p.

Gray, H.H., 2003, Bedrock topography contours, Indiana: Indiana Geological Survey, 1:500,000, line shapefile, accessed April 4, 2008, at *http://igs.indiana.edu/arcims/statewide/download.html.*

Green, J.H., and Hutchinson, R.D., 1965, Ground-water pumpage and water-level changes in the Milwaukee-Waukesha Area, Wisconsin, 1950–61: U.S. Geological Survey Water-Supply Paper 1809–I, 19 p.

Guo, Weixing, and Langevin, C.D., 2002, User's guide to SEAWAT—A computer program for simulation of three-dimensional variable-density ground-water flow: U.S. Geological Survey Techniques of Water-Resources Investigations, book 6, chap. A7, 77 p.

Gupta, Neeraj, 1993, Geologic and fluid-density controls on the hydrodynamics of the Mt. Simon Sandstone and overlying geologic units in Ohio and surrounding states: Columbus, Ohio State University, unpublished Ph.D. dissertation, 266 p.

Gupta, Neeraj, and Bair, E.S., 1997, Variable-density flow in the midcontinent basins and arches region of the United States: Water Resources Research, v. 33, no. 8, p. 1785–1802.

Gutschick, R.C., and Sandberg, C.A., 1991, Late Devonian history of Michigan Basin, *in* Catacosinos, P.A., and Daniels, P.A., eds., Early sedimentary evolution of the Michigan basin: Boulder, Colo., Geological Society of America Special Paper 256, p. 181–202.

Haitjema, H.M., 1995, Analytic element modeling of groundwater flow: San Diego, Acadmeic Press, 394 p.

Haitjema, Henk; Feinstein, Daniel; Hunt, Randy; and Gusyev, Maksym, 2010, A hybrid finite difference and analytic element model for detailed surface-ground water modeling on a regional scale: Ground Water, doi: 10.1111/j.1745-6584.2009.00672.x, 11 p.

Haitjema, Henk; Kelson, Vic; and de Lange, Wim, 2001, Selecting MODFLOW cells sizes for accurate flow fields: Ground Water, v. 39, no. 6, p. 931–938.

Halford, K.J., and Hanson, R.T., 2002, MODFLOW-2000—User guide for the drawdown-limited, Multi-Node Well (MNW) package for the U.S. Geological Survey's modular three-dimensional ground-water flow model, Versions MODFLOW-96 and MODFLOW-2000: U.S. Geological Survey Open-File Report 02–293, 33 p.

Hansen, Nikolaus; Müller, S.D.; and Koumoutsakos, Petros, 2003, Reducing the time complexity of the derandomized evolution strategy with covariance matrix adaptation (CMA-ES): Evolutionary Computation, v. 11, no. 1, p. 1–18.

Hansen, Nikolaus, and Ostermeier, Andreas, 2001, Completely derandomized self-adaptation in evolution strategies: Evolutionary Computation, v. 9, no. 2, p. 159–195.

Harbaugh, A.W., Banta, E.R., and McDonald, M.C., 2000, MODFLOW-2000, the U.S. Geological Survey modular ground-water model—User guide to modularization processes and the ground-water flow process: U.S. Geological Survey Open-File Report 00–92, 121 p.

Hart, David; Bradbury, Ken; Feinstein, Daniel; and Tikoff, Basil, 2008, Mechanisms of groundwater flow across the Maquoketa Formation: Wisconsin Geological Survey Open-File Report 2008–03, 47 p.

Hart, D.J., Scoephoester, P.R., and Bradbury, K.R., 2008, Groundwater recharge in southeastern Wisconsin estimated by a GIS-based water-balance model: Southeastern Wisconsin Regional Planning Commission Technical Report 47, 23 p.

Hensel, B.R., 1992, Natural recharge of groundwater in Illinois: Champaign, Ill., Illinois State Geological Survey Environmental Geology Notes 143, 33 p.

Hill, M.C., and Tiedeman, C.R., 2007, Effective groundwater model calibration—with analysis of data, sensitivities, prediction, and uncertainty: Hoboken, N.J., John Wiley and Sons, 455 p.

Hoaglund, J.R., 1996, Recharge to discharge groundwater travel times in the Michigan Basin and the effect of glacial ice loading: East Lansing, Mich., Michigan State University, Department of Geological Sciences, Ph.D. dissertation, 275 p.

Hoaglund, J.R., 2004, Analysis of modern and Pleistocene hydrologic exchange between Saginaw Bay (Lake Huron) and Saginaw Lowland area: Geological Society of America Bulletin, v. 116, no. 1/2, p. 3–15.

Hoagland, J.R., Huffman, G.C., and Grannemann, N.G., 2002a, Simulation of ground water flow in the glaciofluvial, Saginaw, Parma-Bayport, and Marshall aquifers, central Lower Peninsula of Michigan: U.S. Geological Survey Open-File Report 2000–504 [no pagination].

Hoaglund, J.R., Huffman, G.C., and Grannemann, N.G., 2002b, Michigan basin regional ground water flow discharge to three Great Lakes: Ground Water, v. 40, no. 4, p. 390–406.

Hoard, C.J., 2010, Implementation of local grid refinement in MODFLOW for the Lake Michigan Basin regional groundwater flow model: U.S. Geological Survey Scientific Investigations Report 2010–5117, 25 p.

Hodgkins, G.A., Dudley, R.W., and Aichele, S.S., 2007, Historical changes in precipitation and streamflow in the U.S. Great Lakes Basin, 1915–2004: U.S. Geological Survey Scientific Investigations Report 2007–5118, 31 p.

Holmstrom, B.K., 1978, Low-flow characteristics of streams in the Rock-Fox River Basin, Wisconsin: U.S. Geological Survey Water Resources Investigations 78–85, 98 p.

Holtschlag, D.J., 1997, A generalized estimate of ground-water-recharge rates in the Lower Peninsula of Michigan: U.S. Geological Survey Water-Supply Paper 2437, 37 p.

Holtschlag, D.J., Luukkonen, C.L., and Nicholas, J.R., 1996, Simulation of ground-water flow in the Saginaw aquifer, Clinton, Eaton, and Ingham Counties, Michigan: U.S. Geological Survey Open-File Report 96–174, 49 p.

Holtschlag, D.J., and Nicholas, J.R., 1998, Indirect groundwater discharge to the Great Lakes: U.S. Geological Survey Open-File Report 98–579, 25 p.

Hunt, R.J., Doherty, John, and Tonkin, M.J., 2007, Are models too simple?—Arguments for increased parameterization: Ground Water, v. 45, no. 3, p. 254–262, doi:10.1111/j.1745-6584.2007.00316.x.

Hutchinson, R.D., 1970, Water resources of Racine and Kenosha Counties, southeastern Wisconsin: U.S. Geological Survey Water-Supply Paper 1878, 63 p.

Indiana Department of Natural Resources, 1987, Water resource availability in the St. Joseph River Basin, Indiana: State of Indiana Water Resource Assessment 87–1, 137 p.

Indiana Department of Natural Resources, 1990, Water resource availability in the Kankakee River Basin, Indiana: State of Indiana Water Resource Assessment 90–3, 247 p.

Indiana Department of Natural Resources, 1994, Water resource availability in the Lake Michigan Region, Indiana: State of Indiana Water Resource Assessment 94–4, 257 p.

Indiana Department of Natural Resources, 1996, Water resource availability in the Maumee River Basin, Indiana: State of Indiana Water Resource Assessment 96–5, 235 p.

Indiana Department of Natural Resources, Division of Water, 1980, The Indiana water resource, availability, uses, and needs: Indiana Department of Natural Resources, Governor's Water Resources Study Commission, 508 p.

Indiana Department of Natural Resources, Division of Water, 2002, Water Well Record Database: Water Rights and Use Section, accessed July 22, 2008, at *http://www.in.gov/dnr/water/3595.htm.*

Jansen, J.R., 1995, Ground water exploration by the combined use of fracture trace analysis and azimuthal resistivity in the Silurian dolomite aquifer of eastern Wisconsin: University of Wisconsin-Milwaukee, unpublished Ph.D. dissertation (Geosciences), 558 p.

Kammerer, P.A., 1995, Ground-water flow and quality in Wisconsin's shallow aquifer system: U.S. Geological Survey Water-Resources Investigations Report 90–4171, 42 p.

Kammerer, P.A., Trotta, L.C., Krabbenhoft, D.P., and Lidwin, R.A., 1998, Geology, ground-water flow, and dissolved-solids concentrations in ground water along hydrogeologic sections through Wisconsin aquifers—Hydrogeologic sections, ground-water province II: U.S. Geological Survey Hydrologic Investigations Atlas HA–731, sheet 3 (of 4).

Kay, R.T., 2002, Estimated water withdrawals, water use, and water consumption in Illinois, Indiana, Iowa, Kentucky, Michigan, Missouri, and Wisconsin, 1950–95: U.S. Geological Survey Water-Resources Investigations Report 01–4116, 29 p.

Kay, R.T., Arihood, L.D., Arnold, T.L., and Fowler, K.K., 2006, Hydrogeology, water use, and simulated groundwater flow and availability in Campton Township, Kane County, Illinois: U.S. Geological Survey Scientific Investigations Report 2006–5076, 99 p.

Kay, R.T., Duwelius, R.F., Brown, T.A., Micke, F.A., and Witt-Smith, C.A., 1996, Geohydrology, water levels and directions of flow, and occurrence of light-nonaqueous-phase liquids on ground water in northwestern Indiana and the Lake Calumet area of northeastern Illinois: U.S. Geological Survey Water-Resources Investigations Report 95–4253, 84 p.

Kay, R.T., Mills, P.C., Dunning, C.P., Yeskis, D.J., Ursic, J.R., and Vendl, Mark, 2004, A cross-site comparison of methods used for hydrogeologic characterization of the Galena-Platteville aquifer in Illinois and Wisconsin, with examples from selected Superfund sites: U.S. Geological Survey Scientific Investigations Report 2004–5136, 241 p.

Kelly, W.R., and Meyer, S., 2005, Temporal changes in deep bedrock groundwater quality in northeastern Illinois: Champaign, Ill., Illinois State Water Survey, Contract Report 2005–05, 40 p.

Klump, Stephan, Grundl, Tim, Purtschert, Roland, and Kipfer, Rolf, 2008, Groundwater and climate dynamics derived from noble gas, ^{14}C, and stable isotope data: Geology, v. 35, no. 5, p. 395–398.

Knoerle, Bender, Stone & Associates, Inc., 1977, Des Plaines River system tunnels and shafts of the tunnel and reservoir plan, Part II Geotechnical Report: Prepared for The Metropolitan Sanitary District of Greater Chicago.

Knowles, D.B., 1964, Ground-water conditions in the Green Bay area, Wisconsin, 1950–60: U.S. Geological Survey Water-Supply Paper 1669–J, 37 p.

Knowles, D.B., Dreher, F.C., and Whetstone, G.W., 1964, Water resources of the Green Bay area, Wisconsin: U.S. Geological Survey Water-Supply Paper 1499–G, 67 p.

Kolata, D.R., Buschbach, T.C., and Treworgy, J.D., 1978, The Sandwich Fault Zone of northern Illinois: Urbana, Ill., Illinois State Geological Survey Circular 505, 26 p.

Kolata, D.R., and Graese, A.M., 1983, Lithostratigraphy and depositional environments of the Maquoketa Group (Ordovician) in northern Illinois: Illinois State Geological Survey Circular 528, 49 p.

Kontis, A.L., and Mandle, R.J., 1980, Data-base system for northern Midwest regional aquifer-system analysis: U.S. Geological Survey Water-Resources Investigations Report 80–104, 23 p.

Kontis, A.L., and Mandle, R.J., 1988, Modifications of a three-dimensional ground-water flow model to account for variable water density and effects of multiaquifer wells: U.S. Geological Survey Water-Resources Investigations Report 87–4265, 78 p.

Krohelski, J.T., 1986, Hydrogeology and ground-water use and quality, Brown County, Wisconsin: Wisconsin Geological and Natural History Survey Information Circular 57, 42 p.

Krohelski, J.T., Bradbury, K.R., Hunt, R.J., and Swanson, S.K., 2000, Numerical simulation of groundwater flow in Dane County, Wisconsin: Wisconsin Geological and Natural History Survey Bulletin 98, 31 p.

Krohelski, J.T., Ellefson, B.R., and Storlie, C.A., 1987, Estimated use of ground water for irrigation in Wisconsin, 1984: U.S. Geological Survey Water-Resources Investigations Report 86–4079, 12 p.

Lahm, T.D., and Bair, E.S., 2000, Regional depressurization and its impact on the sustainability of freshwater resources in an extensive midcontinent variable-density aquifer: Water Resources Research, v. 36, no. 11, p. 3167–3177.

Lampe, D.C., 2009, Hydrogeologic framework of bedrock units and initial salinity distribution for a simulation of ground-water-flow for the Lake Michigan Basin: U.S. Geological Survey Scientific Investigations Report 2009–5060, 49 p.

Langevin, C.D., Shoemaker, W.B., and Guo, Weixing, 2003, MODFLOW-2000, the U.S. Geological Survey modular ground-water model—Documentation of the SEAWAT-2000 version with the Variable-Density Flow Process (VDF) and the Integrated MT3DMS Transport Process (IMT): U.S. Geological Survey Open-File Report 03–426, 43 p.

Langevin, C.D., Thorne, D.T., Jr., Dausman, A.M., Sukop, M.C., and Guo, Weixing, 2007, SEAWAT Version 4—A computer program for simulation of multi-species solute and heat transport: U.S. Geological Survey Techniques and Methods, book 6, chap. A22, 39 p.

Lapham, W.W., 1981, Ground-water resources of the White River Basin, Madison County, Indiana: U.S. Geological Survey Water-Resources Investigations 81–35, 112 p.

Lawrence, C.L., and Ellefson, B.R., 1982, Water use in Wisconsin, 1979: U.S. Geological Survey Open-File Report 82–444, p. 11–17.

Lawrence, C.L., Ellefson, B.R., and Cotter, R.D., 1984, Public-supply pumpage in Wisconsin, by aquifer: U.S. Geological Survey Open File Report 83–931, p. 10–40.

LeRoux, E.F., 1957, Geology and ground-water resources of Outagamie County, Wisconsin: U.S. Geological Survey Water-Supply Paper 1421, 57 p.

Leverett, Frank, and Taylor, F.B., 1915, The Pleistocene of Indiana and Michigan and history of the Great Lakes: U.S. Geological Survey Monograph 53, 529 p.

Lindgren, H.A, Peters, J.G., Cohen, D.A., and Crompton, E.J., 1985, Hydrologic effects of ground- and surface-water withdrawals in the Milford area, Elkhart and Kosciusko Counties, Indiana: U.S. Geological Survey Water-Resources Investigation Report 85–4166, 75 p.

Lineback, J.A., Gross, D.L., and Meyer, R.P., 1972, Geologic cross sections derived from seismic profiles and sediment cores from southern Lake Michigan: Illinois State Geological Survey Environmental Geology Note 54, 43 p.

Lineback, J.A., Gross, D.L., Meyer, R.P., and Unger, W.L., 1971, High-resolution seismic profiles and gravity cores of sediments in southern Lake Michigan: Illinois State Geological Survey Environmental Geology Note 47, 31 p.

Lloyd, O.B., and Lyke, W.L., 1995, Ground-water atlas of the United States—Segment 10, Illinois, Indiana, Kentucky, Ohio, and Tennessee: U.S. Geological Survey Hydrologic Investigations Atlas 730–K, 30 p.

Luukonen, C.L., Blumer, S.P., Weaver, T.L., and Jean, Julie, 2004, Simulation of the ground-water-flow system in the Kalamazoo County Area, Michigan: U.S. Geological Survey Scientific Investigations Report 2004–5054, 65 p.

Magnuson, J.J., Krohelski, J.T., Kunkel, K.E., and Robertson, D.M., 2003, Wisconsin's waters and climate—Historical changes and possible futures: Transactions of the Wisconsin Academy of Sciences, Arts, and Letters, v. 90, p. 23–36.

Mandle, R.J., and Kontis, A.L., 1992, Simulation of regional ground-water flow in the Cambrian-Ordovician aquifer system in the northern Midwest, United States: U.S. Geological Survey Professional Paper 1405–C, 97 p.

Mandle, R.J., and Westjohn, D.B., 1989, Geohydrologic framework and ground-water flow in the Michigan Basin, *in* Swain, L.A., and Johnson, A.I., eds., Regional aquifer systems of the United States—Aquifers of the Midwestern area: American Water Resources Association Monograph Series, no. 13, p. 83–109.

Mason, R.R., and Yorke, T.H., 1997, Streamflow information for the Nation: U.S. Geological Survey Fact Sheet FS–006–97, 4 p.

McBride, M.S., and Pfannkuch, H.O., 1975, The distribution of seepage within lakebeds: U.S. Geological Survey Journal of Research, v. 3, no. 5, p. 505–512.

McDonald, M.G., and Harbaugh, A.W., 1983, A modular three-dimensional finite-difference ground-water flow model: US. Geological Survey Open-File Report 83–875, 528 p.

McDonald, M.G., and Harbaugh, A.W., 1988, A modular three-dimensional finite-difference ground-water flow model: U.S. Geological Survey Techniques of Water-Resources Investigations, book 6, chap. A1, 576 p.

Mehl, S.W., and Hill, M.C., 2005, MODFLOW-2005, the U.S. Geological Survey Modular Ground-water Model—Documentation of shared node Local Grid Refinement (LGR) and the Boundary Flow and Head (BFH) package: U.S. Geological Survey Techniques and Methods 6–A12, 68 p.

Meisburger, E.P., Williams, S.J., and Prins, D.A., 1979, Sand resources of Lake Michigan: Fort Belvoir, Va., U.S. Army Corps of Engineers, Coastal Engineering Research Center, Miscellaneous Report 79–3, 61 p.

Meissner, B.D., Long, D.T., and Lee, R.W., 1996, Selected geochemical characteristics of ground water from the Saginaw aquifer in the central Lower Peninsula of Michigan: U.S. Geological Survey Water-Resources Investigations Report 93–4220, 19 p.

Meyer, S.C., Lin, Y.-F., Roadcap, G.S., and Walker, D.D., 2009, Kane County water resources investigations—Simulation of groundwater flow in Kane County and northeastern Illinois: Illinois State Water Survey Contract Report 2009–07, 425 p.

Michigan Department of Environmental Quality, 1987, Bedrock geology, 1:63,360 polygon shapefile available at *http://www.mcgi.state.mi.us/mgdl/?rel=thext&action=thmname&cid=2&cat=Bedrock+Geology.*

Michigan Department of Environmental Quality, 2005a, Groundwater Mapping Project, accessed January 20, 2009, at *http://gwmap.rsgis.msu.edu/*.

Michigan Department of Environmental Quality, 2005b, State of Michigan, Public Act 148, Groundwater Inventory and Map (GWIM) Project, executive summary: 31 p.

Michigan Department of Environmental Quality, 2006, State of Michigan, Public Act 148, Groundwater Inventory and Map (GWIM) Project, technical report: 257 p., accessed February 3, 2008, at *http://gwmap.rsgis.msu.edu/Technical_Report.pdf.*

Michigan Department of Environmental Quality, 2008, WellLogic, Statewide Ground Water Database (SGWD): Department of Environmental Quality (continuously updated), last accessed March 28, 2008, at *http://www.mcgi.state.mi.us/mgdl?rel=thext&action=thmname&cid=2&cat=Drinking+Water+Wells.*

Michigan Department of Environmental Quality, Water Bureau, 2006a, Water withdrawals for agricultural irrigation in Michigan, 2006: 12 p.

Michigan Department of Environmental Quality, Water Bureau, 2006b, Water withdrawals for golf course irrigation in Michigan, 2006: 10 p.

Michigan Department of Environmental Quality, Water Bureau, 2006c, Water withdrawals for major water uses in Michigan, 2004: 13 p.

Michigan Department of Environmental Quality, Water Bureau, 2006d, Water withdrawals for public water supply in Michigan, 2006: 10 p.

Michigan Department of Environmental Quality, Water Bureau, 2006e, Water withdrawals for self-supplied industrial manufacturing in Michigan, 2006: 11 p.

Michigan Department of Public Health, 1943, Public water supplies in Michigan: Engineering Bulletin no. 12, sec. 1.

Mikulic, D.G., Sargent, M.L., Norby, R.D., and Kolata, D.R., 1985, Silurian geology of the Des Plaines River valley, northeastern Illinois: Illinois State Geological Survey Guidebook 17, 56 p.

Morris, D.A., and Johnson, A.I., 1967, Summary of hydrologic and physical properties of rock and soil materials as analyzed by the hydrologic laboratory of the U.S. Geological Survey, 1948–1960: U.S. Geological Survey Water Supply Paper 1839–D, 42 p.

Mueller, S.D., 1992, Three-dimensional digital simulation of the ground-water contribution to Lake Michigan from the Silurian aquifer of southeastern Wisconsin: University of Wisconsin-Milaukee, unpublished M.S. thesis, 231 p.

Muldoon, M.A., Simo, J.A., and Bradbury, K.R., 2001, Correlation of hydraulic conductivity with stratigraphy in a fractured-dolomite aquifer, northeastern Wisconsin, USA: Hydrogeology Journal, v. 9, no. 6, p. 570–583.

Nadon, G.C., Simo, J.A., Dott, R.H., Jr., and Byers, C.W., 2000, High-resolution sequence stratigraphic analysis of the St. Peter Sandstone and Glenwood Formation (Middle Ordovician), Michigan Basin, U.S.A.: American Association of Petroleum Geologists Bulletin, v. 84, p. 975–996.

National Geophysical Data Center, 1998, GEODAS gridded data format, accessed April 2008 at *http://www.ngdc.noaa.gov/mgg/gdas/gd_designagrid.html?dbase=grdglb.*

National Oceanic and Atmospheric Administration, 2005, Lake Michigan geomorphology, accessed August 8, 2006, at *http://www.ngdc.noaa.gov/mgg/greatlakes/lakemich_cdrom/html/geomorph.htm.*

Nauta, Robert, 1987, A three-dimensional groundwater flow model of the Silurian dolomite aquifer of Door County, Wisconsin: University of Wisconsin-Madison, unpublished M.S. thesis, 105 p.

Neff, B.P., Day, S.M., Piggott, A.R., and Fuller, L.M., 2005, Base flow in the Great Lakes Basin: U.S. Geological Survey Scientific Investigations Report 2005–5217, 23 p.

Neff, B.P., and Nicolas, J.R., 2005, Uncertainty in the Great Lakes water balance: U.S. Geological Survey Scientific Investigations Report 2004–5100, 42 p.

Neff, B.P., Piggott, A.R.,and Sheets, R.A., 2005, Estimation of shallow ground-water recharge in the Great Lakes Basin: U.S. Geological Survey 2005–5284, 20 p.

Newport, T.G., 1962, Geology and ground-water resources of Fond du Lac County, Wisconsin: U.S. Geological Survey Water-Supply Paper 1604, 52 p.

Nicholas, J.R., Sherrill, M.G., and Young, H.L., 1987, Hydrogeology of the Cambrian-Ordovician aquifer system at a test well in northeastern Illinois: U.S. Geological Survey Water-Resources Investigations/Open-File Report 84–4165, 30 p.

Ohio Division of Geological Survey, 2005, Bedrock topography of Ohio, BG–3: CD-ROM.

Olcott, P.G., 1966, Geology and ground-water resources of Winnebago County, Wisconsin: U.S. Geological Survey Water-Supply Paper 1814, 61 p.

Olcott, P.G., 1992, Groundwater atlas of the United States, Segment 9—Iowa, Michigan, Minnesota, and Wisconsin: U.S. Geological Survey Hydrologic Investigations Atlas 730–J, 31 p.

Passero, R.N., Straw, W.T., and Schmaltz, L.J., 1981, Hydrogeologic atlas of Michigan: Kalamazoo, Mich.,Western Michigan University, Department of Geology, 35 pl.

Poeter, E.P., and Hill, M.C., 1997, Inverse models—A necessary next step in ground-water modeling: Ground Water, v. 35, no. 2, p. 250–260.

Pollock, D.W., 1994, User's guide for MODPATH/MODPATH-PLOT, Version 3: U.S. Geological Survey Open-File Report 94–464 [variously paged].

Prickett, T.A., 1967, Designing pumped well characteristics into electric analog models: Ground Water, v. 5, no. 4, p. 38–46.

Prickett, T.A., and Lonnquist, C.G., 1971, Selected digital computer techniques for groundwater resources evaluation: Urbana, Ill., Illinois State Water Survey Bulletin 55, 62 p.

PRISM Group, 2008, Temperature and precipitation data, accessed June 2008 at *http://www.prismclimate.org.*

Rayne, T.W., Bradbury, K.R., and Mickelson, D.M., 1996, Variability of hydraulic conductivity in uniform sandy till, Dane County, Wisconsin: Wisconsin Geological and Natural History Survey Information Circular 74, 19 p.

Reeves, H.W., in press, Water availability and use pilot—Multiscale assessment in the U.S. Great Lakes Basin: U.S. Geological Survey Professional Paper 1778.

Reeves, H.W., Wright, K.V., and Nicholas, J.R., 2004, Hydrogeology and simulation of regional ground-water-level declines in Monroe County, Michigan: U.S. Geological Survey Water-Resources Investigation Report 03–4312, 72 p.

Remote Sensing and Geographic Information Science, 2006, Groundwater mapping project: Groundwater Inventory and Mapping Database available online at *http://gwmap.rsgis.msu.edu/*.

Rodenbeck, S.A., 1988, Merging Pleistocene lithostratigraphy with geotechnical and hydrogeologic data—Examples from eastern Wisconsin: University of Wisconsin-Madison, unpublished M.S. thesis, 286 p.

Rosenshein, J.S., 1963, Recharge rates of principal aquifers in Lake County, Indiana: Ground Water, v. 1, no. 4, p. 13–20.

Rovey, C.W., II, 1990, Stratigraphy and sedimentology of Silurian and Devonian Carbonates, eastern Wisconsin, with implications for ground-water discharge into Lake Michigan: University of Wisconsin-Milwaukee, unpublished Ph.D. dissertation (Geosciences), 427 p.

Rumbaugh, J.O., and Rumbaugh, D.B., 2004, 2007, Groundwater Vistas, version 5: Reinholds, Pa., Environmental Simulations, Inc., 375 p.

Rupp, J.A., 1991, Structure and isopach maps of the Paleozoic rocks of Indiana: Bloomington, Ind., Indiana Department of Natural Resources, Geological Survey, Special Report 48, 106 p.

Rutledge, A.T., 1998, Computer programs for describing the recession of ground-water discharge and for estimating mean ground-water recharge and discharge from streamflow data—Update: U.S. Geological Survey Water-Resources Investigations Report 98–4148, 43 p.

Ryling, R.W., 1961, A preliminary study of the distribution of saline water in the bedrock aquifers of eastern Wisconsin: Wisconsin Geological and Natural History Survey Information Circular 5, 23 p.

Sasman, R.T., 1965, Ground-water pumpage in northeastern Illinois through 1962: Illinois State Water Survey Report of Investigation 50, 31 p.

Schicht, R.J., Adams, J.R., and Stall, J.B., 1976, Water resources availability, quality, and cost in northeastern Illinois: Illinois State Water Survey Report of Investigation 83, 90 p.

Schnoebelen, D.J., Bugliosi, E.F., Hanover, R.H., and Rupp, J.A., 1998, Approximate location of the 10,000-milligram-per-liter dissolved-solids boundary in the Silurian and Devonian carbonate rock aquifer, southwestern and northern Indiana: U.S. Geological Survey Water-Resources Investigations Report 95–4071, 12 p.

Schnoebelen, D.J., Bugliosi, E.F., and Krothe, N.C., 1995, Deliniation of a saline ground-water boundary from borehole geophysical data: Ground Water, v. 33, no. 6, p. 965–976.

Sellinger, C.E., 1995, Groundwater flux into a portion of eastern Lake Michigan: Journal of Great Lakes Research, v. 21, p. 53–63.

Seybold, C.A., Grossman, R.B., and Pierce, F.J., 2003, On-site assessment of use-dependent soil properties in Michigan: Communications in Soil Science and Plant Analysis, v. 34, no. 5–6, p. 765–780.

Shaffer, K.H., and Runkle, D.L., 2007, Consumptive water-use coefficients for the Great Lakes Basin and climatically similar areas: U.S. Geological Survey Scientific Investigations Report 2007–5197, 191 p.

Shaver, R.H.; Ault, C.H.; Burger, A.M.; Carr, D.D.; Droste, J.B.; Eggert, D.L.; Gray, H.H.; Harper, Denver; Hasenmueller, N.R.; Hasenmueller, W.A.; Horowitz, A.S; Hutchison, H.C.; Keith, B.D.; Keller, S.J.; Patton, J.B.; Rexroad, C.B.; and Wier, C.E., 1986, Compendium of Paleozoic rock-unit stratigraphy in Indiana—A revision: Indiana Department of Natural Resources, Geological Survey, Bulletin 59, 229 p.

Sheets, R.A., Dumouchelle, D.H., and Feinstein, D.T., 2005, Ground-water modeling of pumping effects near regional ground-water divides and river/aquifer systems—Results and implications of numerical experiments: U.S. Geological Survey Scientific Investigations Report 2005–5141, 31 p.

Sheets, R.A., and Simonson, L.A., 2006, Compilation of regional ground-water divides for principal aquifers corresponding to the Great Lakes Basin, United States: U.S. Geological Survey Scientific Investigations Report 2006–5102, 23 p.

Simpkins, W.W., 1989, Genesis and spatial distribution of variability in the lithostratigraphic, geotechnical, hydrogeological and geochemical properties of the Oak Creek Formation in southeastern Wisconsin: University of Wisconsin-Madison, unpublished Ph.D. dissertation (Geology and Geophysics), 394 p.

Singh, K.P., and Ramamurthy, G.S., 1993, 7-day, 10-year low flows of streams in northeastern Illinois: Illinois State Water Survey Contract Report CR–545, rev. 2003.

Soller, D.R., 1998, Map showing the thickness and character of Quaternary sediments in the glaciated United States east of the Rocky Mountains, northern Great Lakes states and central Mississippi Valley states, the Great Lakes, and southern Ontario; U.S. Geological Survey Miscellaneous Investigations Series, Map I–1970–B.

Soller, D.R., and Packard, P.H., 1998, Digital representation of a map showing the thickness and character of Quaternary sediments in the glaciated United States east of the Rocky Mountains: U.S. Geological Digital Data Series DDS–38.

Solley, W.B., Pierce, R.R., and Perlman, H.A., 1998, Estimated use of water in the United States in 1995: U.S. Geological Survey Circular 1200, 71 p.

Sonnenfeld, P., and Al-Aasm, I., 1991, The Salina evaporites in the Michigan Basin, *in* Catacosinos, P.A., and Daniels, P.A., Jr., eds., Early sedimentary evolution of the Michigan Basin: Geological Society of America Special Paper 256, p. 139–153.

Southeastern Wisconsin Regional Planning Commission and Wisconsin Geological and Natural History Survey, 2002, Groundwater resources of southeastern Wisconsin: Southeastern Wisconsin Regional Planning Commission Technical Report 37, 203 p.

Spitz, Karlheinz, and Moreno, Joanna, 1996, A practical guide to groundwater flow and solute transport modeling: New York, John Wiley and Sons, 426 p.

Stallman, R.W., and Klaer, F.H., Jr., 1950, Ground-water resources of Noble County, Indiana: Indiana Department of Conservation, Division of Water Resources, Bulletin 5, 91 p., 5 pl.

Stocks, D.L., 1998, Hydrostratigraphy of the Ordovician Sinnipee Group dolomites, eastern Wisconsin: University of Wisconsin-Madison, unpublished M.S. thesis (Geology and Geophysics), 192 p.

Suter, M., Bergstrom, R.E., Smith, H.F., Emrich, G.H., Walton, W.C., and Larson, T.E., 1959, Preliminary report on the ground-water resources of the Chicago Region, Illinois: Illinois State Water Survey and Illinois State Geological Survey Cooperative Ground-Water Report 1, 89 p.

Swezey, C.S., 2008, Regional stratigraphy and petroleum systems of the Michigan Basin, North America: U.S. Geological Survey Scientific Investigations Map 2978.

Thornthwaite, C.W., and Mather, J.R., 1955, The water balance: Centerton, N.J., Laboratory of Climatology, Publications in Climatology, v. 8, no. 1, p. 1–104.

Tikhonov, A.N., 1963a, Solution of incorrectly formulated problems and the regularization method: Soviet Mathematics—Doklady, v. 4, p. 1035–1038.

Tikhonov, A.N., 1963b, Regularization of incorrectly posed problems: Soviet Mathematics—Doklady, v. 4, p. 1624–1627.

Tonkin, M.J., and Doherty, John, 2005, A hybrid regularized inversion methodology for highly parameterized models: Water Resources Research, v. 41, W10412, doi:10.1029/2005WR003995.

Topper, Ralf, 2007, Memorandum to South Plattte River Basin Roundtable—Consumptive/non-consumptive water use by residences using individual sewage disposal systems: Colorado Department of Natural Resources, 3 p.

Trescott, P.C. 1975, Documentation of finite-difference model for simulation of three-dimensional ground-water flow: U.S. Geological Survey Open-File Report 75–438, 32 p.

Tescott, P.C., and Larson, S.P., 1976, Documentation of finite-difference model for simulation of three-dimensional ground-water flow—Supplement to Open-File Report 75–438: U.S. Geological Survey Open-File Report 76–59, 21 p.

U.S. Army Corps of Engineers, Detroit District, 2006, Historic Great Lakes levels, accessed May 30, 2008, at *http://www.lre.usace.army.mil/greatlakes/hh/greatlakeswaterlevels/historicdata/greatlakeshydrographs/*.

U.S. Census Bureau, 2006, County boundaries: U.S. Census Bureau database, accessed April 2008 at *http://gis.glin.net/ogc/services.php#mi_county_boundaries_2000.*

U.S. Congress, 2008, Great Lakes-St. Lawrence River Basin Water Resources Compact: U.S. Congress, 110th, Public Law 110–342, 122 STAT. 3739, [26] p., accessed February 2, 2009, at *http://frwebgate.access.gpo.gov/cgi-bin/getdoc.cgi?dbname=110_cong_public_laws&docid=f:publ342.110.pdf.*

U.S. Department of Agriculture, 1986, Urban hydrology for small watersheds: Soil Conservation Service, Engineering Division, Technical Release 55, 164 p.

U.S. Department of Agriculture–Natual Resources Conservation Service, 2006, Digital general soil map of U.S.: Fort Worth, Tex., accessed January 2007 at *http://SoilDataMart.nrcs.usda.gov.*

U.S. Geological Survey, 2000a, U.S. GeoData digital elevation models: U.S. Geological Survey Fact Sheet 040–00, accessed January 2007 at *http://erg.usgs.gov/isb/pubs/factsheets/fs04000.html.*

U.S. Geological Survey, 2000b, National Land Cover Dataset: U.S. Geological Survey Fact Sheet 108–00, accessed January 2007 at *http://erg.usgs.gov/isb/pubs/factsheet/fs10800.html.*

U.S. Geological Survey, 2001, National Elevation Dataset (NED) 30-meter Digital Elevation Models (DEMs): National Mapping Division, accessed November 8, 2002, at *http://gisdata.usgs.net/NED.*

U.S. Geological Survey, 2001a, National Hydrography Dataset, accessed November 29, 2001, at *http://nhd.usgs.gov/data.html.*

U.S. Geological Survey, 2001b, National Elevation Dataset, accessed November 29, 2001, at *http://edcnts12.cr.usgs.gov/ned/default.htm.*

U.S. Geological Survey, 2003, National Atlas of the United States of America—Principal aquifers: scale 1:2,500,000, accessed May 2005 at *http://www.nationalatlas.gov/index.html.*

U.S. Geological Survey, 2005a, National Hydrography Dataset, accessed September 21, 2005, at *http://nhd.usgs.gov/*.

U.S. Geological Survey, 2005b, National Elevation Dataset, accessed September 21, 2005, at *http://ned.usgs.gov/*.

U.S. Geological Survey, National Water Information System (NWIS), 2002, accessed January 10, 2002, at *http://waterdata.usgs.gov/nwis/*.

Visocky, A.P., 1993, Water-level trends and pumpage in the deep bedrock aquifers in the Chicago region, 1985–1991: Illinois State Water Survey Circular 177, 43 p.

Visocky, A.P., 1997, Water level trends and pumpage in the deep bedrock aquifers in the Chicago Region, 1991–1995: Illinois State Water Survey Circular 182, 45 p.

Visocky, A.P., Sherrill, M.G., and Cartwright, Keros, 1985, Geology, hydrology, and water quality of the Cambrian and Ordovician Systems in northern Illinois: Illinois State Geological Survey and Illinois State Water Survey Cooperative Groundwater Report 10, 136 p.

Wahrer, M.A., Long, D.T., and Lee, R.W., 1996, Selected geochemical characteristics of ground water from the Glaciofluvial aquifer in the central Lower Peninsula of Michigan: U.S. Geological Survey Water-Resources Investigations Report 94–4017, 21 p.

Walker, D.D., Meyer, S.C., and Winstanley, D., 2003, Uncertainty of estimates of groundwater yield for the Cambrian-Ordovician Aquifer in northeastern Illinois, *in* Mishra, S., ed., Groundwater Quality Modeling and Management Under Uncertainty—Proceedings of the Probabilistic Approaches & Groundwater Modeling Symposium held during the World Water and Environmental Resources Congress, Philadelphia, Pa., June 24–26, 2003: Reston, Va., American Society of Civil Engineers, p. 273–283.

Walton, W.C., 1960, Leaky artesian aquifer conditions in Illinois: Illinois State Water Survey Report of Investigation 39, 27 p.

Walton, W.C., 1964, Future water-level declines in deep sandstone wells in Chicago region: Illinois State Water Survey Reprint 36, 8 p.

Walton, W.C., 1965, Ground-water recharge and runoff in Illinois: Illinois State Water Survey Report of Investigation 48, 55 p.

Walton, W.C., and Csallany, S.C., 1962, Yields of deep sandstone wells in northern Illinois: Illinois State Water Survey Report of Investigation 43, 473 p.

Webb, E.K., 1989, Estimating groundwater discharge to Lake Michigan using a three-dimensional groundwater flow model, along a portion of the shoreline from Door County to Port Washington, Wisconsin: University of Wisconsin-Madison, unpublished M.S. thesis (Geology and Geophysics), 227 p.

Weidman, Samuel, and Schultz, A.R., 1915, The underground and surface water supplies of Wisconsin: Wisconsin Geological and Natural History Survey Bulletin 35, 664 p.

Weist, W.G., Jr., 1978, Summary appraisals of the Nation's ground-water resources—Great Lakes region: U.S. Geological Survey Professional Paper 813–J, 29 p.

Westenbroek, S.M., Kelson, V.A., Dripps, W.R., Hunt, R.J., and Bradbury, K.R., 2010, SWB—A modified Thornthwaite-Mather Soil-Water-Balance code for estimating ground-water recharge: U.S. Geological Survey Techniques and Methods 6–A31, 59 p.

Western Michigan University, Department of Geology, 1981, Hydrogeologic atlas of Michigan: Prepared for U.S. Environmental Protection Agency, Underground Injection Control Program, 35 pl.

Westjohn, D.B., and Weaver, T.L., 1996a, Hydrogeologic framework of Pennsylvanian and Late Mississippian rocks in the central Lower Peninsula of Michigan: U.S. Geological Survey Water-Resources Investigations Report 94–4107, 44 p.

Westjohn, D.B., and Weaver, T.L., 1996b, Hydrogeologic framework of Mississippian rocks in the central Lower Peninsula of Michigan: U.S. Geological Survey Water-Resources Investigations Report 94–4246, 46 p.

Westjohn, D.B., and Weaver, T.L., 1996c, Configuration of freshwater/saline-water interface and geologic controls on distribution of freshwater in a regional aquifer system, central Lower Peninsula of Michigan: U.S. Geological Survey Water-Resources Investigations Report 94–4242, 44 p.

Westjohn, D.B., and Weaver, T.L., 1998, Hydrogeologic framework of the Michigan Basin regional aquifer system, central Lower Peninsula of Michigan: U.S. Geological Survey Professional Paper 1418, 47 p.

Westjohn, D.B., Weaver, T.L., and Zacharias, K.E, 1994, Hydrogeology of Pleistocene glacial deposits and Jurassic "red beds" in the central Lower Peninsula of Michigan: U.S. Geological Survey Water-Resources Investigations Report 93–4152, 14 p.

Wickstrom, L.H., Gray, J.D., and Stieglitz, R.D., 1992, Stratigraphy, structure, and production history of the Trenton Limestone (Ordovician) and adjacent strata in northwestern Ohio: Ohio Division of Geological Survey Report of Investigations 143, 78 p., 1 pl.

Wisconsin Department of Natural Resources, 1997, Status of groundwater quantity in Wisconsin: PUBL–DG–043–97, available at *http://www.dnr.state.wi.us/org/water/dwg/gcc/gw-quantity.pdf*.

Wisconsin Department of Natural Resources, 2006, Water well data—Wisconsin well construction reports plus other related files: Wisconsin Bureau of Drinking Water & Groundwater, created December 6, 2005, CD-ROM.

Wisconsin Geological and Natural History Survey, 2004, wiscLITH—A digital lithologic and stratigraphic database of Wisconsin geology: Wisconsin Geological and Natural History Survey Open-File Report 2003–05, 39 p.

Wold, R.J., and Hutchinson, D.R., 1979, Lake Michigan geological and geophysical data sources: U.S. Geological Survey Miscellaneous Field Studies Map MF–1095, 6 maps on 3 sheets.

Yager, R.M., Kappel, W.M., and Plummer, L.N., 2007, Origin of halite brine in the Onondaga Trough near Syracuse, New York State, USA—Modeling geochemistry and variable-density flow: Hydrogeology Journal, v. 15, no. 7, p. 1321–1339.

Young, H.L., 1976, Digital-computer model of the sandstone aquifer in southeastern Wisconsin: Southeastern Wisconsin Regional Planning Commission Technical Report 16, 42 p.

Young, H.L., 1992, Summary of ground-water hydrology of the Cambrian-Ordovician aquifer system in the Northern Midwest, United States: U.S. Geological Survey Professional Paper 1405–A, 55 p.

Young, H.L., Mackenzie, A.J., and Mandle, R.J., 1989, Simulation of ground-water flow in the Cambrian-Ordovician aquifer system in the Chicago-Milwaukee area of the Northern Midwest, *in* Swain, L.A., and Johnson, A.I., eds., Regional aquifer systems of the United States—Aquifers of the Midwestern Area: American Water Resources Association Monograph Series, no. 13, p. 39–72.

Zeizel, A.J., Walton, W.C., Sasman, R.T., and Prickett, T.A., 1962, Ground-water resources of DuPage County, Illinois: Illinois State Water Survey and Illinois State Geological Survey Cooperative Ground-Water Report 2, 103 p.

Zheng, Chunmiao, and Wang, P.P., 1999, MT3DMS—A modular three-dimensional multi-species transport model for simulation of advection, dispersion and chemical reactions of contaminants in groundwater systems—Documentation and user's guide—Contract report SERDP-99-1: Vicksburg, Miss., U.S. Army Engineer Research and Development Center, 169 p. (Available at *http://hydro.geo.ua.edu.*)